PATRÍCIA CASTRO BELTING

“VAPOR LIQUID PHASE EQUILIBRIUM IN THE VEGETABLE OIL INDUSTRY”

“EQUILÍBRIO LÍQUIDO VAPOR NA INDÚSTRIA DE ÓLEOS VEGETAIS”

CAMPINAS

2013

UNIVERSIDADE ESTADUAL DE CAMPINAS

Faculdade de Engenharia de Alimentos

PATRÍCIA CASTRO BELTING

"VAPOR LIQUID PHASE EQUILIBRIUM IN THE VEGETABLE OIL INDUSTRY"

"EQUILÍBRIO LÍQUIDO VAPOR NA INDÚSTRIA DE ÓLEOS VEGETAIS"

Thesis presented to the Faculty of Food Engineering of the University of Campinas in partial fulfillment of the requirements for the degree of Doctor in the area of Food Engineering.

Tese apresentada à Faculdade de Engenharia de Alimentos da Universidade Estadual de Campinas como parte dos requisitos exigidos para a obtenção do título de Doutora na área de Engenharia de Alimentos.

Supervisor / *Orientador*: Prof. Dr. Antonio José de Almeida Meireles

Co-Supervisors / *Coorientadores*: Profa. Dra. Roberta Ceriani
Prof. Dr. Osvaldo Chiavone-Filho
Prof. Dr. Jürgen Gmehling
Dr. Jürgen Rarey

ESTE EXEMPLAR CORRESPONDE À VERSÃO FINAL DA TESE DEFENDIDA PELA ALUNA PATRÍCIA CASTRO BELTING, E ORIENTADA PELO PROF. DR. ANTONIO JOSÉ DE ALMEIDA MEIRELLES

_____

CAMPINAS
2013

Ficha Catalográfica
Universidade Estadual de Campinas
Biblioteca da Faculdade de Engenharia de Alimentos
Claudia Aparecida Romano de Souza - CRB8/5816

Belting, Patrícia Castro, 1977-
F419v Vapor liquid phase equilibrium in the vegetable oil industry / Patrícia Castro Belting -- Campinas, SP: [s.n.], 2013.

Orientador: Antonio José de Almeida Meirellles
Coorientadores: Roberta Ceriani, Osvaldo Chiavone-Filho, Jürgen Gmehling e Jürgen Rarey.
Tese (doutorado) - Universidade Estadual de Campinas, Faculdade de Engenharia de Alimentos.

1. Equilíbrio líquido-vapor. 2. Termodinâmica. 3. Óleos e gorduras. 4. Ácidos graxos. I. Meirelles, Antonio José de Almeida. II. Ceriani, Roberta. III. Chiavone-Filho, Osvaldo. IV. Gmehling, Jürgen. V. Rarey, Jürgen. VI. Universidade Estadual de Campinas. Faculdade de Engenharia de Alimentos. VII. Título.

Informações para Biblioteca Digital

Título em outro idioma: Equilíbrio líquido vapor na indústria de óleos vegetais
Palavras-chave em inglês:
Vapor-liquid equilibrium
Thermodynamic
Fats and oils
Fatty acids
Área de concentração: Engenharia de Alimentos
Titulação: Doutora em Engenharia de Alimentos
Banca examinadora:
Antonio José de Almeida Meirellles [Orientador]
Erika Cristina Cren
Jorge Andrey Wilhelms Gut
Luiza Helena Meller da Silva
Martín Aznar
Data da defesa: 24-10-2013
Programa de Pós Graduação: Engenharia de Alimentos

BANCA EXAMINADORA

_____

Prof. Dr. Antonio José de Almeida Meirelles - FEA / UNICAMP
(Orientador)

_____

Profa. Dra. Erika Cristina Cren - Escola de Engenharia / UFMG
(Membro Titular)

_____

Prof. Dr. Jorge Andrey Wilhemls Gut - Escola Politécnica / USP
(Membro Titular)

_____

Profa. Dra. Luiza Helena Meller da Silva - Instituto de Tecnologia / UFPA
(Membro Titular)

_____

Prof. Dr. Martín Aznar - FEQ / UNICAMP
(Membro Titular)

_____

Prof. Dr. Charlles Rubber de Almeida Abreu - Escola de Química / UFRJ
(Suplente)

_____

Profa. Dra. Lireny Aparecida Guaraldo Gonçalves - FEA / UNICAMP
(Suplente)

_____

Profa. Dra. Maria Alvina Krähenbühl - FEQ / UNICAMP
(Suplente)

ABSTRACT

Thermodynamic properties are useful for the reliable design, optimization and modelling of thermal separation processes as well as for the selection of solvents used in extraction processes. They are also required for the development of new thermodynamic models and for the adjustment of reliable model parameters. In order to improve the thermodynamic properties data bank of fatty compounds, the systematic determination of activity coefficients at infinite dilution (γ^{∞}), excess enthalpies (H^E) and vapor-liquid equilibria (VLE) data of systems containing fatty acids and vegetable oils was performed. The first part of this work presents γ^{∞} data for several organic solutes dissolved in saturated and unsaturated fatty acids measured by gas-liquid chromatography at temperatures from 303.13 K to 368.19 K and the comparison to available literature data. Different trends for polar and non-polar compounds could be identified both in the series of fatty acids and as function of temperature. It appears that both the presence and the number of *cis* double bonds in the fatty acid alkyl chain have influence on the solvent-solute interactions and hence on the values of γ^{∞}. The second part of this work deals with measurements performed on systems with refined vegetable oils. Soybean, sunflower and rapeseed oils were submitted to measures of γ^{∞}, H^E, and VLE. The measurements of γ^{∞} for n-hexane, methanol and ethanol dissolved in these vegetable oils were determined by gas stripping method (dilutor technique) in the temperature range of 313.15 K to 353.15 K. The experimental data were compared with the results of the group contribution methods original UNIFAC and modified UNIFAC (Dortmund) and an extension of the latter method to triacylglycerols was proposed. The H^E data were measured for eleven mixtures

containing solvents (organic and water) and the prior mentioned vegetable oils in the temperature range from 298.15 K to 383.15 K. All systems investigated showed deviation from the ideal behavior and their experimental H^E data are mostly positive. Isothermal VLE data have been measured for methanol, ethanol, and n-hexane with the same vegetable oils at 348.15 K and 373.15 K using a computer-driven static apparatus. For mixtures with n-hexane it was observed a negative deviation from Raoult's law and a homogeneous behavior, while mixtures with alcohols had a positive deviation from ideal behavior and, in some cases, with miscibility gap. The experimental VLE data were satisfactorily represented by the UNIQUAC model, while the mod. UNIFAC (Dortmund) method and its proposed extension for triacylglicerols were capable of predicting the experimental data only in a qualitative way. Finally, isobaric VLE data were measured for mixtures of ethanol with refined soybean oil at 101.3 kPa and for n-hexane and cottonseed oil at 41.3 kPa using a modified Othmer-type ebulliometer. The results of the UNIQUAC correlation also showed good agreement with the experimental results. This work resulted in a total of 1829 new data that will expand the available fatty compounds data base, allowing a more accurate description of the real behavior of fatty systems.

Keywords: Vapor-liquid equilibrium; Thermodynamic; Fats and oils; Fatty acids.

RESUMO

Propriedades termodinâmicas são úteis para a realização de projetos confiáveis, otimização e modelagem de processos que envolvam separação térmica e para a seleção de solventes usados em processos de extração. Tais propriedades são também necessárias no desenvolvimento de novos modelos termodinâmicos e no ajuste de parâmetros de modelos preditivos. Este trabalho de tese teve como objetivo principal ampliar o banco de dados de propriedades termodinâmicas para compostos graxos através da determinação sistemática do coeficiente de atividade à diluição infinita (γ^{∞}), entalpia de excesso (H^E) e dados de equilíbrio líquido-vapor (ELV) de sistemas contendo ácidos graxos e óleos vegetais. A primeira parte deste trabalho apresenta os dados de γ^{∞} para vários solutos orgânicos diluídos em ácidos graxos saturados e insaturados, medidos pelo método de cromatografia gás-líquido na faixa de temperatura entre 303,13 K e 368,19 K. Através dos resultados obtidos, puderam ser identificadas diferentes tendências para compostos polares e não polares, tanto na série de ácidos graxos como também em relação à temperatura. Foi verificado que tanto a presença quanto o número de insaturações na cadeia carbônica do ácido graxo têm influência nas interações solvente-soluto e, consequentemente, nos valores de γ^{∞}. A segunda parte deste trabalho tratou de medidas realizadas em sistemas contendo óleos vegetais refinados. Os óleos de soja, girassol e canola foram submetidos a determinações de γ^{∞}, H^E e ELV. As medidas de γ^{∞} para n-hexano, metanol e etanol diluídos nos óleos vegetais foram determinadas pela técnica do Dilutor na faixa de temperatura entre 313,15 K e 353,15 K. Os dados experimentais obtidos foram comparados com os resultados gerados pelos métodos UNIFAC original e modificado (Dortmund) e

para este último modelo, foi proposta uma extensão para os triacilgliceróis. Os dados de H^E foram medidos para 11 misturas contendo solventes e os óleos vegetais relacionados anteriormente na faixa de temperatura de 298,15 K a 383,15 K. Todos os sistemas investigados apresentaram desvio em relação ao comportamento ideal e os valores de H^E apresentaram-se, na maioria, positivos. Dados isotérmicos de ELV foram medidos para misturas entre os mesmos óleos vegetais e metanol, etanol e n-hexano a 348,15 K e 373,15 K através de um método estático. Para misturas com n-hexano, foi observado desvio negativo da lei de Raoult e um comportamento homogêneo, enquanto que as misturas com álcool apresentaram desvio positivo da idealidade e imiscibilidade. Os dados experimentais de ELV foram representados satisfatoriamente pelo modelo UNIQUAC, enquanto que os modelos UNIFAC modificado (Dortmund) e sua extensão proposta para triacilgliceróis foram capazes de predizer os sistemas apenas de forma qualitativa. Finalmente, dados isobáricos de ELV foram medidos para misturas com etanol + óleo de soja a 101,3 kPa e n-hexano + óleo de algodão a 41,3 kPa utilizando o ebuliômetro de Othmer modificado. Os resultados da correlação UNIQUAC também apresentaram boa concordância com os dados experimentais. Este trabalho resultou em um total de 1829 novos dados que irão expandir o banco de dados disponível para compostos graxos, permitindo uma descrição mais precisa do comportamento real de sistemas contendo tais substâncias.

Palavras-chave: Equilíbrio líquido-vapor; Termodinâmica; Óleos e gorduras; Ácidos graxos.

SUMÁRIO

DEDICATÓRIA

Dedico este trabalho ao meu querido esposo Wolfgang, pelo amor e apoio incondicional. Ao meu filho Aurélio, que torna a minha vida mais feliz e aos meus pais Olívia e Juarez, pelo exemplo de vida e incentivo em todos os momentos.

AGRADECIMENTOS

Agradeço a Deus, pela minha existência, pela minha família, pelas oportunidades e pela capacidade de aproveitá-las.

Agradeço ao meu amado esposo Wolfgang, pelo carinho, atenção, paciência, motivação e apoio durante todo o período de doutorado.

Agradeço aos meus queridos pais Juarez e Olívia, pelo suporte constante e pela indissolúvel confiança em meu potencial e ao meu irmão Juarez que, mesmo a distância, apoiou-me e encorajou-me na realização desta pesquisa.

Agradeço aos meus sogros Josef e Agnes, pelo encorajamento, apoio e compreensão, especialmente na fase final deste trabalho.

Agradeço de forma especial ao Prof. Dr. Antonio José de Almeida Meirelles, "Prof. Tonzé", que em 2009 aceitou orientar o meu doutoramento, pela proposta do tema, pela liberdade de trabalho concedida, pela prontidão nos momentos decisivos e pelas discussões construtivas que contribuiram para o sucesso deste trabalho.

Agradeço aos meus coorientadores: Profa. Dra. Roberta Ceriani, Prof. Dr. Osvaldo Chiavone-Filho, Prof. Dr. Jürgen Gmehling, e o Dr. Jürgen Rarey, pelo importante suporte, apoio e supervisão, e pelas ideias e opiniões produtivas.

Agradeço aos colegas de trabalho Syllos (FOTEQ), Rainer e Helmut (IRAC), pela disponibilidade, pela paciência, pelo companheirismo e por, em muitas ocasiões, facilitarem a minha vida.

Agradeço aos membros das bancas de qualificação e de defesa, pela atenção e tempo dispensados na correção do trabalho escrito e pelas valiosas sugestões.

Agradeço à UNICAMP, à UFRN e à *Carl von Ossietzky Universität Oldenburg,* pela infraestrutura concedida.

Agradeço aos antigos e atuais membros do grupo de trabalho do ExTrAE (Laboratório de Extração, Termodinâmica Aplicada e Equilíbrio), FOTEQ (Laboratório de Fotoquímica e Equilíbrio de Fases) e do IRAC (*Institut für Reine und Angewandte Chemie*), pela cooperação e pelo amigável ambiente de trabalho.

Agradeço aos colegas da Engenharia Química e do laboratório de Bioquímica e à querida professora Hélia, pelo acolhimento, pelos cafezinhos, pelas partidas de vôlei e pelos bons momentos de descontração.

Agradeço ao CNPq (Conselho Nacional de Desenvolvimento Científico e Tecnológico) e ao DAAD (*Deutscher Akademischer Autausch Dienst*), pela concessão da bolsa e apoio financeiro a este projeto de pesquisa.

Não poderia deixar de agradecer aos meus queridos amigos Haroldo Kawaguti e Michelle Abreu, que sem a sua ajuda jamais teria conseguido concluir este trabalho.

Enfim, agradeço a todos que de diferentes formas contribuíram na elaboração deste trabalho: família, parentes, amigos e colegas pelo companheirismo, pela atenção e pela confiança dispensados.

"Queremos ter certezas e não dúvidas, resultados e não experiências, mas nem mesmo percebemos que as certezas só podem surgir através das dúvidas e os resultados somente através das experiências. "

Carl Gustav Jung

LISTA DE ILUSTRAÇÕES

LISTA DE TABELAS

CAPÍTULO 1: INTRODUÇÃO GERAL

Nos últimos anos, os óleos vegetais e outros compostos graxos, tais como ácidos graxos, ésteres de ácidos graxos, glicerol, acilgliceróis parciais e triacilgliceróis, têm desempenhado um papel cada vez mais importante na indústria e no mercado mundial. Além da importância destes compostos na dieta humana, devido ao seu valor nutricional e ao valor nutracêutico de alguns compostos minoritários normalmente dissolvidos nessas misturas graxas, o interesse nesses compostos tem aumentado principalmente pelo fato de serem considerados uma possível fonte de combustível renovável, como o biodiesel.

Nos processos industriais que envolvem compostos graxos é possível identificar diversas etapas de separação, para as quais propriedades termofísicas e dados de equilíbrio de fases são de grande importância para o dimensionamento e operação de equipamentos, especialmente porque esses processos frequentemente envolvem misturas multicomponentes. Dentre eles podem ser destacados: a separação e recuperação do solvente de extração de óleos vegetais (MILLIGAN e TANDY, 1974; WILLIAMS, 2005; DEMARCO, 2009), a destilação de ácidos graxos (XU et al., 2002), o fracionamento de álcoois graxos, a produção e purificação de acilgliceróis parciais (XU et al., 1998; XU, SKANDS e ADLER-NISSEN, 2001; XU et al., 2002) e o refino físico de óleos vegetais, em especial as etapas de desacidificação (PINA e MEIRELLES, 2000; RODRIGUES, ONOYAMA e MEIRELLES, 2006; GONÇALVES, PESSÔA FILHO e MEIRELLES, 2007) e desodorização (MATTIL, 1964; HÉNON et al., 1999; DE GREYT e KELLENS, 2005). Podem ser ainda mencionados os processos de purificação na indústria de biodiesel

(ésteres e glicerol) e a recuperação do excesso de álcool utilizado no processo de transesterificação (MA e HANNA, 1999; MEHER, SAGAR e NAIK, 2006; MARCHETTI, MIGUEL e ERRAZU, 2007).

Apesar da grande importância industrial dos compostos graxos e sua aplicação na geração de diversos produtos, dados experimentais de propriedades termofísicas e de equilíbrio de fases destes compostos puros são escassos na literatura. Até mesmo dados de misturas, como os óleos vegetais, apresentam-se em número limitado. Deve-se ressaltar que tais compostos com elevado grau de pureza são extremamente caros, tornando muitas vezes inviável, do ponto de vista econômico, a determinação de propriedades de compostos puros ou de misturas simples destes compostos. Já sistemas multicomponentes, como os óleos vegetais, são misturas complexas de difícil caracterização e sua composição exata varia de acordo com a fonte. Com o intuito de preencher essa lacuna, procurando obter uma maior quantidade de dados experimentais confiáveis e desenvolver modelos preditivos para estimar propriedades de compostos graxos que auxiliem na otimização e simulação de processos industriais, grupos de pesquisas em todo o mundo têm conduzido diversos trabalhos com esses compostos.

Esta tese de doutorado é parte do intenso trabalho de medição de propriedades físicas e termodinâmicas de compostos graxos que vem sendo desenvolvido no decorrer dos últimos anos pelo Laboratório de Extração, Termodinâmica Aplicada e Equilíbrio (ExTrAE – UNICAMP). O grupo de pesquisa do ExTrAE tem acumulado larga experiência na medição de dados de equilíbrio de fases líquido-líquido (ANTONIASSI, ESTEVES e MEIRELLES, 1998; CHIYODA et al., 2010; FOLLEGATTI-ROMERO et al., 2010;

SILVA et al., 2010; SILVA et al., 2011; BASSO, MEIRELLES e BATISTA, 2012; FOLLEGATTI-ROMERO, OLIVEIRA, BATISTA, COUTINHO, et al., 2012; FOLLEGATTI-ROMERO, OLIVEIRA, BATISTA, BATISTA, et al., 2012; ANSOLIN et al., 2013; BASSO et al., 2013), sólido-líquido (COSTA, BOROS, et al., 2010; COSTA, ROLEMBERG, et al., 2010; CARARETO et al., 2011; COSTA, BOROS, COUTINHO, et al., 2011; COSTA, BOROS, SOUZA, et al., 2011; COSTA et al., 2012; ROBUSTILLO et al., 2013) e, mais recentemente, líquido-vapor (FALLEIRO, MEIRELLES e KRÄHENBÜHL, 2010; AKISAWA SILVA, L. Y. et al., 2011; CARARETO et al., 2012), na determinação de propriedades como viscosidade, densidade, solubilidade e pressão de vapor (GONÇALVES et al., 2007; CERIANI et al., 2008; SANAIOTTI et al., 2010; AKISAWA SILVA, L. Y. et al., 2011; FALLEIRO et al., 2012; BASSO, MEIRELLES e BATISTA, 2013) de sistemas envolvendo compostos graxos, na modelagem e simulação de etapas do processamento de óleos vegetais (CERIANI e MEIRELLES, 2004c; b; 2005; CERIANI e MEIRELLES, 2006; CERIANI e MEIRELLES, 2007; CERIANI, COSTA e MEIRELLES, 2008; CERIANI, MEIRELLES e GANI, 2010; CUEVAS et al., 2010; SAMPAIO et al., 2011), assim como no desenvolvimento de modelos de predição de propriedades destes compostos (CERIANI e MEIRELLES, 2004a; CERIANI et al., 2007; GONÇALVES et al., 2007).

A parte experimental dessa tese foi desenvolvida em colaboração com os grupos de pesquisa do FOTEQ (Laboratório de Fotoquímica e Equilíbrio de Fases) da UFRN (Universidade Federal do Rio Grande do Norte) e do IRAC (*Institut für Reine und*

Angewandte Chemie ou Instituto de Química Pura e Aplicada) da Universidade de Oldenburg, na Alemanha.

O objetivo principal desse trabalho de doutorado foi determinar, modelar e avaliar propriedades termodinâmicas e dados de equilíbrio de fases de sistemas contendo componentes graxos e diversos solventes, sendo alguns destes solventes de interesse direto para aplicação em processos industriais e outros relevantes para um melhor entendimento termodinâmico das misturas de interesse industrial. Espera-se que os dados experimentais medidos neste trabalho sejam no futuro utilizados na revisão e extensão de modelos de contribuição de grupos, como o método UNIFAC (*UNIversal Functional Activity Coefficient*) modificado (Dortmund), e para o ajuste de parâmetros dos modelos moleculares confiáveis que possam ser utilizados na simulação e otimização de processos de extração e separação na industrialização de compostos graxos (óleos vegetais, acilgliceróis parciais, ácidos graxos, álcoois graxos, entre outros), assim como do biodiesel. Neste contexto, os seguintes objetivos específicos podem ser destacados:

- Determinação de coeficientes de atividade à diluição infinita de diversos solutos em ácidos graxos saturados e insaturados e óleos vegetais;

- Determinação da entalpia de excesso de misturas envolvendo óleos vegetais e solventes orgânicos;

- Determinação experimental do equilíbrio de fases líquído-vapor de sistemas com óleo vegetal e solventes orgânicos;

- Realização da modelagem termodinâmica dos dados experimentais utilizando o modelo molecular UNIQUAC (*UNIversal QUAsi-Chemical*) e a predição através de modelos de contribuição de grupos UNIFAC original e UNIFAC modificado (Dortmund);

- Investigação do efeito da estrutura molecular e caracterísitcas químicas dos compostos graxos e dos solutos sobre o coeficiente de atividade à diluição infinita e sobre as propriedades de excesso;

- Avaliação da aplicação, desempenho, precisão e confiabilidade de diferentes métodos para a determinação de coeficientes de atividade à diluição infinita e dados de equilíbrio líquido-vapor em sistemas contendo compostos graxos.

A presente tese de doutorado está organizada em 9 capítulos e anexos, os quais correspondem à Introdução Geral (Capítulo 1), à Revisão Bibliográfica (Capítulo 2) e aos artigos científicos publicados e submetidos durante o período de doutoramento (Capítulo 3 a 8), os quais apresentam separadamente as metodologias utilizadas, os dados medidos, as discussões realizadas e as conclusões obtidas para cada um dos temas tratados e, por fim, as Considerações Finais e Conclusões Gerais da tese (Capítulo 9). O detalhamento das metodologias utilizadas neste trabalho e os dados não publicados estão apresentados na forma de anexos.

A Tabela 1.1 apresenta, de forma resumida, as informações a respeito dos dados medidos, reagentes utilizados e metodologia adotada neste trabalho de doutorado, sendo que a última coluna da tabela indica o capítulo ou anexo correspondente da tese.

Tabela 1.1: Resumo das determinações experimentais realizadas.

Componente graxo	N° de reagentes de mistura	Dado Medido	Intervalo de temperatura ou Pressão	Metodologia utilizada	Quantidade de dados	Capítulo
Ác. cáprico	1 (etanol)	ELV[(1)]	75°C e 100°C	Método estático	19	Anexo VI
	21 [a]	γ^{∞}[(2)]	40,09 °C a 80,15 °C	GLC[(5)]	94	3
	6 [b]	γ^{∞}	39,98 °C a 80,15 °C	Dilutor Technique	25	5
Ác. láurico	21 [a]	γ^{∞}	55,67 °C a 84,95 °C	GLC	103	3
Ác. mirístico	21 [a]	γ^{∞}	65,12 °C a 85,18 °C	GLC	109	3
Ác. palmítico	21 [a]	γ^{∞}	67,02 °C a 85,17 °C	GLC	68	3
Ác. esteárico	21 [a]	γ^{∞}	76,23 °C a 95,04 °C	GLC	81	4
Ác. oléico	21 [a]	γ^{∞}	65,21 °C a 85,13 °C	GLC	69	4
Ác. linoléico	20 [c]	γ^{∞}	65,13 °C a 85,18 °C	GLC	74	4
Ác. linolênico	14 [d]	γ^{∞}	29,95 °C a 50,11 °C	GLC	42	4
óleo de soja	3 (metanol, etanol e n-hexano)	γ^{∞}	40 °C a 80 °C	Dilutor Technique	15	5
	4 [e]	H^{E}[(3)]	25 °C, 80 °C, 110 °C	Calorimetria de fluxo isotérmico	99	6
	3 (metanol, etanol e n-hexano)	ELV	75 °C e 100 °C	Método estático	194	7
	1 (etanol)	ELV	80 kPa e 101,3 kPa	Método dinâmico (ebuliometria)	31 32	8 Anexo VIII
	(etanol + n-heptano)	ρ[(4)]	20 °C a 80 °C 25°C	Densimetria	7 41	5 Anexo IX
óleo de girassol	2 (etanol e n-heptano)	ρ	25 °C	Densimetria	42	Anexo VII
	3 (metanol, etanol e n-hexano)	γ^{∞}	40 °C a 80 °C	Dilutor Technique	15	5
	4 [e]	H^{E}	80 °C e 110 °C	Calorimetria de fluxo isotérmico	88	6

Continuação da Tabela 1.1.

óleo de girassol	3 (metanol, etanol e n-hexano)	ELV		75 °C e 100 °C	Método estático	180	7
			ρ	20 °C a 80 °C	Densimetria	7	5
óleo de canola	3 (metanol, etanol e n-hexano)		γ^{∞}	40 °C a 80 °C	Dilutor	15	5
	3[f]		H^E	80 °C e 110 °C	Calorimetria de fluxo isotérmico	71	6
	3 (metanol, etanol e n-hexano)	ELV		75 °C e 100 °C	Método estático	156	7
			ρ	20 °C a 80 °C	Densimetria	7	5
óleo de coco	1 (etanol)	ELV		80 kPa e 101,3 kPa	Método dinâmico (ebuliometria)	28 + 37	Anexo VIII
	2 (etanol e n-heptano)		ρ	25 °C	Densimetria	42	Anexo IX
óleo de algodão	1 (n-hexano)	ELV		41,3 kPa	Método dinâmico (ebuliometria)	27	8
	1 (hexano)		ρ	25 °C	Densimetria	11	8
Total						**1829**	

[a] n-Hexano, n-Heptano, Isooctano, 1-Hexeno, Tolueno, Ciclohexano, Etilbenzeno, Metanol, Etanol, 1-Propanol, 1-Butanol, 2-Propanol, 2-Butanol, Clorofórmio, Tricloroetileno, Clorobenzeno, 1,2-Dicloroetano, Clorobenzil, Etilacetato, Acetona, Anisole;

[b] Acetona, Metanol, Etanol, n-Hexano, Ciclohexano, Tolueno;

[c] n-Hexano, n-Heptano, Isooctano, 1-Hexeno, Tolueno, Ciclohexano, Etilbenzeno, Metanol, Etanol, 1-Propanol, 1-Butanol, 2-Propanol, 2-Butanol, Clorofórmio, Clorobenzeno, 1,2-Dicloroetano, Clorobenzil, Etilacetato, Acetona, Anisole; d Metanol, Etanol, 2-Propanol, Água, n-Hexano;

[d] n-Hexano, n-Heptano, Isooctano, 1-Hexeno, Tolueno, Ciclohexano, Metanol, Etanol, 1-Propanol, 2-Propanol, Clorofórmio, 1,2-Dicloroetano, Etilacetato, Acetona;

[e] Metanol, Etanol, 2-Propanol, n-Hexano

[f] Metanol, Etanol, n-Hexano

(1) ELV = Equilíbrio Líquido Vapor, (2) γ^{∞}= Coeficiente de atividade à diluição infinita, (3) H^E= entalpia de excesso, (4) ρ = densidade, (5) GLC = cromatografia gás-líquido.

Como se observa pela Tabela 1.1, o Capítulo 3 apresenta dados de coeficientes de atividade à diluição infinita, γ^{∞}, em ácidos graxos saturados, permitindo discutir os efeitos da cadeia carbônica dos ácidos graxos e do tipo de soluto sobre o comportamento termodinâmico deste tipo de sistema. O Capítulo 4 apresenta dados similares para ácidos graxos insaturados, os principais tipos de ácidos graxos encontrados nas estruturas químicas dos triacilgliceróis. Neste capítulo verificou-se a influência das insaturações na cadeia carbônica sobre as interações solvente-soluto de sistemas graxos, completando assim informações relevantes para um melhor entendimento dos comportamentos destes sistemas.

Os Capítulos 5, 6 e 7 trazem artigos referentes ao estudo sistemático das propriedades termofísicas (coeficiente de atividade à diluição infinita, γ^{∞}, e entalpia de excesso, H^{E}) e do equilíbrio de fases líquido-vapor (ELV) de misturas contendo óleos de soja, girassol e canola refinados.

O Capítulo 5 traz os dados experimentais de coeficiente de atividade à diluição infinita em óleos vegetais refinados. A técnica do Dilutor (método do gás de arraste inerte) foi utilizada neste trabalho possibilitando a determinação de γ^{∞} de sistemas compostos por misturas multicomponentes. Neste trabalho foi ainda realizada a validação do uso da técnica do dilutor para compostos graxos, comparando os dados de γ^{∞} do ácido cáprico com os medidos pelo método GLC (cromatografia gás-líquido). Adicionalmente realizou-se a comparação dos dados experimentais de γ^{∞} com os resultados obtidos pelos métodos de contribuição de grupos UNIFAC original e UNIFAC modificado (Dortmund) e foi proposta uma extensão deste último método para a molécula de triacilglicerol.

Os mesmos óleos foram utilizados na determinação da entalpia de excesso. O Capítulo 6 traz o artigo com os resultados experimentais de H^E obtidos nas misturas dos óleos vegetais com solventes orgânicos e a comparação com dados disponíveis na literatura. Neste trabalho, os sistemas estudados também foram comparados em termos de interação molecular.

Os capítulos 7 e 8 encerram os objetivos previstos para esse trabalho de tese, pois apresentam os artigos com os dados de equilíbrio de fases líquido-vapor (ELV) de sistemas compostos por óleos vegetais refinados e solventes.

O artigo apresentado no Capítulo 7 traz dados isotérmicos de ELV (*P*-*x*) obtidos a partir de um método estático, a correlação destes dados realizada pelo modelo UNIQUAC e predições realizadas pelo modelo UNIFAC modificado (Dortmund). Em ambas modelagens os óleos vegetais foram considerados como pseudocomponentes.

O artigo apresentado no Capítulo 8 contém dados isobáricos de ELV (*PTxy*) obtidos por ebuliometria (método dinâmico); foi realizada a correlação dos dados pelo método UNIQUAC considerando o óleo vegetal um pseudocomponente e a predição por diferentes versões do método UNIFAC, considerando o óleo um sistema multicomponente.

O Capítulo 9 (Considerações Finais e Conclusões Gerais) trata das considerações finais deste trabalho de tese, ressalta os principais resultados e conclusões obtidos em cada um dos artigos apresentados e apresenta algumas sugestões para trabalhos futuros.

CAPÍTULO 2: REVISÃO BIBLIOGRÁFICA

Óleos e gorduras são lipídeos encontrados naturalmente em tecidos vegetais ou animais (BOCKISCH, 1998; O'BRIEN, 2000b; a). As gorduras são substâncias que se apresentam sólidas à temperatura ambiente, já os óleos são líquidos (WAN, 2000). Os lipídeos possuem baixíssima solubilidade em água, isto é, somente sob condições extremas de temperatura (> 250 °C) e pressão (> 2 MPa), a água é moderadamente solúvel na fase oleosa (GERVAJIO, 2005; GUPTA, 2005; SCRIMGEOUR, 2005). Em relação ao aspecto nutricional, os lipídeos possuem alto valor calórico, cerca de 9 $kcal \cdot g^{-1}$, além da presença de vitaminas, ácidos graxos essenciais e compostos antioxidantes (WAN, 2000).

Os óleos e gorduras constituem misturas complexas de diversos triacilgliceróis (TAGs) e sua composição exata depende da fonte do lípideo (semente, castanha, fruto ou tecido) e da região onde foram produzidos (GUNSTONE, 2005). O triacilglicerol (TAG) é um éster formado por uma molécula de glicerol e três moléculas de ácidos graxos que podem ser saturados ou insaturados (SWERN, 1964; BOCKISCH, 1998; WAN, 2000); portanto, constitui uma molécula de cadeia longa, ligeiramente polar e com elevada massa molecular (na ordem de 850 $g \cdot mol^{-1}$) (DE LA FUENTE B. et al., 1997). Aproximadamente 5 % da composição dos óleos e gorduras brutos é constituída de: ácidos graxos livres, acilgliceróis parciais (mono-; di- ou triacilgliceróis), fosfatídeos (gomas), esteróis, cera e compostos minoritários como: umidade, tocoferóis e tocotrianóis pigmentos (como carotenos e clorofilas), vitaminas, metais (principalmente: ferro, cobre, cálcio e

magnésio), produtos de reações de oxidação (como peróxidos), entre outros (O'BRIEN, 1998; 2000a; WAN, 2000; GUNSTONE, 2005).

Os ácidos graxos são ácidos carboxílicos alifáticos saturados ou insaturados com cadeia carbônica entre C_6 e C_{24}. O ácido graxo livre é qualquer ácido graxo não ligado a uma molécula de glicerol (BROCKMANN, DEMMERING e KREUTZER, 1987). O teor de ácidos graxos livres é um bom indicativo de qualidade dos óleos bruto e refinado, e seu valor determina o tratamento necessário para neutralizar a sua acidez (O'BRIEN, 1998). No Brasil, o teor de ácidos graxos livres de óleos e gorduras comestíveis deve ser reduzido a um valor inferior a 0,3 % em massa, expresso em ácido oléico (BRASIL, 1969).

Os fosfatídeos são álcoois poli-hídricos esterificados a ácidos graxos e ácido fosfórico, combinado com um componente nitrogenado. Os dois tipos de fosfatídeos mais comuns em óleos vegetais são: lecitina e cefalina (O'BRIEN, 1998).

Os esteróis são os principais constituintes da matéria insaponificável dos óleos vegetais, são compostos sem cor, termicamente estáveis e relativamente inertes. As altas temperaturas do refino físico e da desodorização são capazes de removê-los de forma efetiva (BOCKISCH, 1998; O'BRIEN, 1998).

Alguns dos componentes presentes naturalmente nos óleos e gorduras brutos afetam a estabilidade do produto final em termos de cor, sabor e odor e podem gerar problemas durante o processamento, como a formação de espuma e fumaça (O'BRIEN, 1998; 2000b). Por isso, frequentemente, os óleos e gorduras são submetidos a várias etapas de purificação, chamadas de refinamento. Após o refino, a composição final do óleo em TAG é superior a 98 % em massa (WAN, 2000; DE GREYT e KELLENS, 2005). Deve-se ressaltar, porém,

que nem todos os componentes minoritários presentes no óleo são indesejáveis. Os tocoferóis, por exemplo, tem ação antioxidante e os ácidos graxos poli-insaturados são considerados essenciais ao organismo; por isso a presença de ambos no óleo é altamente desejável (O'BRIEN, 1998). No entanto, dependendo da intensidade do processamento de refino, em especial processos que envolvem tratamento térmico, como a desodorização, a perda de tocoferóis pode variar entre 30 e 60 % (MATTIL, 1964). Além disso, podem ocorrer também reações de isomerização de ácidos graxos poli-insaturados (HÉNON et al., 1999).

2.2. Óleos Vegetais

Os óleos vegetais são considerados fontes naturais renováveis, já que a produção agrícola das plantas de origem excede a demanda da população (O'BRIEN, 2000b). Os óleos de soja (produzido principalmente nos Estados Unidos, Brasil, Argentina e China), de palma (Malásia e Indonésia), de canola (China, União Europeia, Índia e Canadá) e de girassol (Rússia, União Europeia e Argentina) dominam a produção e exportação mundial (GUNSTONE, 2005) e por isso são tratados como "*commodities*" (BURKE, 2005; GUNSTONE, 2005).

O uso dos óleos vegetais na indústria de alimentos está bem estabelecido. No entanto, existem outras várias indústrias que também utilizam esse produto como matéria prima. Dentre elas podem ser destacadas a indústria de sabão, detergente e surfactantes (BURKE, 2005; LYNN JR., 2005; SCRIMGEOUR, 2005), de lubrificantes (ERHAN, 2005), de polímeros (NARINE e KONG, 2005), as indústrias farmacêuticas e de

cosméticos (HERNANDEZ, 2005), de tintas e vernizes (LIN, 2005), e de produtos têxteis (KRONICK e KAMATH, 2005). Mais recentemente, os óleos vegetais tem assumido um importante papel na indústria química e oleoquímica devido ao fato de serem a principal matéria prima na produção do biodiesel, um combustível renovável alternativo aos combustíveis fósseis (MA e HANNA, 1999; ENCINAR et al., 2002; MARCHETTI, MIGUEL e ERRAZU, 2007; BAROUTIAN et al., 2008).

2.2.1. Processamento do óleo vegetal

2.2.1.1. Extração do óleo vegetal por solvente

Com os objetivos de maximizar o rendimento e permitir a obtenção de um produto lipídico de boa qualidade, os óleos vegetais são normalmente submetidos a alguma forma de processamento cuja primeira etapa é a separação ou extração do óleo. Este é então submetido a vários procedimentos que podem incluir reações químicas e separações físicas (O'BRIEN, 2000a).

A extração do óleo dos materiais da planta original é normalmente feita por prensagem mecânica ou pela extração por solvente, ou pela combinação deles (que apresenta maior rendimento). Na prensagem mecânica, a quantidade de óleo recuperado é menor que pela extração com solvente; além disso, com o intuito de melhorar o rendimento do processo, a prensagem mecânica pode fazer uso de altas temperaturas, causando danos ao óleo extraído. A utilização de solventes promove uma extração mais completa do óleo sob menores temperaturas (O'BRIEN, 2000b; KEMPER, 2005; DEMARCO, 2009).

A extração por solvente é a etapa de obtenção do óleo bruto a partir de sementes de oleaginosas previamente tratadas mediante preparação adequada. Existem várias operações unitárias utilizadas em cada uma das etapas de extração, mas sem dúvida, as mais importantes estão relacionadas à transferência de massa (DEMARCO, 2009). Esta operação depende das características químicas do solvente, do tempo e do tipo de contato entre o solvente e o material a extrair e da temperatura do processo. Além disso, propriedades do óleo como: índice de refração, densidade, índice de saponificação e teor de ácidos graxos livres afetam a escolha do tipo de solvente a ser utilizado no processo de extração (BERA et al., 2006).

Na transferência do óleo desde a base sólida até a miscela (nome dado à mistura de solvente e óleo), operam mecanismos distintos: o material a ser extraído se põe em contato com o solvente, este inunda os poros intracelulares e dissolve o óleo formando a miscela, cuja composição é estabelecida pelo equilíbrio existente entre o óleo dissolvido no solvente e aquele retido na fase sólida. O óleo se difunde até o exterior da partícula através desta miscela e, posteriormente, é transportado até a saída do leito do extrator. Tão importante quanto a difusão do óleo no interior do sólido é o arraste do óleo até sua superfície (DEMARCO, 2009).

O tipo de contato é um fator muito relevante na eficiência desta operação. Os extratores comerciais disponíveis trabalham quase exclusivamente segundo os métodos básicos de contato para dissolver o óleo no solvente: a imersão e a percolação. Atualmente, na indústria de óleos, os extratores do tipo percoladores são os mais utilizados. O processo de extração se dá por uma série de etapas que geralmente operam com um escoamento em

contracorrente. Para alcançar uma boa eficiência na operação, não se deve produzir misturas entre as miscelas das distintas etapas (JOHNSON, 2000; DEMARCO, 2009).

O tempo de contato entre o solvente e o material a extrair durante a operação de extração é um fator importante para a eficiência do processo, independentemente do tipo de extrator utilizado. Em linhas gerais, quanto maior o tempo de extração, melhor será o desempenho da planta no seu conjunto, embora, para certos tipos de sementes, à medida que se aumenta o tempo de extração, ocorre também a retirada de certas substâncias indesejáveis (DEMARCO, 2009).

Logo que a fração de óleo é extraída pelo solvente da fração de farelo ou torta (matriz vegetal com teor reduzido de óleo), ambas correntes do processo terminam com alto conteúdo de solvente. O solvente da fração de óleo deve ser eliminado a níveis residuais muito baixos, utilizando a evaporação de múltiplo efeito e o *stripping* (FORNARI, BOTTINI e BRIGNOLE, 1994); estes processos constituem a destilação da miscela (PARAÍSO, ANDRADE e ZEMP, 2005). O solvente da fração de farelo é mais difícil de ser eliminado, geralmente se retira através de um processo de aquecimento em contracorrente em um equipamento denominado dessolventizador tostador (DEMARCO, 2009).

A destilação da miscela é um conjunto de operações que visa separar o solvente do óleo bruto. As operações principais presentes na destilação da miscela são: a evaporação e a dessorção com aplicação direta do vapor d'água superaquecido (*stripping*) (PARAÍSO, 2001).

A partir da miscela obtêm-se dois compostos distintos: solvente e óleo. O teor residual de solvente no óleo vegetal deve ser da ordem de alguns $mg \cdot kg^{-1}$ (ppm). De acordo com o órgão americano *Food and Drug Administration* (FDA) o resíduo de n-hexano em óleos e gorduras não pode ser superior a 25 $mg \cdot kg^{-1}$, já na União Européia esse limite é ainda mais restrito sendo aceito no máximo 1 mg de n-hexano por kg de óleo ou gordura comestível (EUROPEAN UNION, 2009; FDA, 2011). Por esta razão, o conhecimento preciso do equilíbrio líquido-vapor (ELV) da mistura óleo vegetal e solvente é imprescindível para o projeto e operação do processo de separação (FORNARI, BOTTINI e BRIGNOLE, 1994).

Os processos de destilação da miscela e recuperação do solvente se iniciam na saída do extrator, de onde a miscela é encaminhada à primeira etapa de evaporação a vácuo (economizadores). Nesta etapa, é evaporado cerca de 90 a 95% do solvente (DEMARCO, 2009). A miscela concentrada em óleo é então destinada à coluna de destilação ou *stripping*, onde entra em contato com vapor injetado em contracorrente e que remove o solvente até os níveis exigidos pela legislação (ANVISA, 2005). A coluna opera a pressões de 559 a 711 mmHg (WILLIAMS e HRON, 1996). O conteúdo final de solvente no óleo dependerá da temperatura, do vácuo e da quantidade de vapor injetado no *stripper* (evaporador de filme). O óleo obtido é finalmente encaminhado às etapas de refino (DEMARCO, 2009).

2.2.1.2. Solventes utilizados na extração de óleos vegetais

O solvente geralmente empregado para a extração de óleos vegetais comestíveis de sementes oleaginosas é uma fração de petróleo rica em n-hexano (C_6H_{14}) (FORNARI, BOTTINI e BRIGNOLE, 1994). Tendo em vista as suas características de flamabilidade e impacto ambiental, algumas questões a respeito da segurança do uso dessa mistura rica em n-hexano têm sido levantadas (SCHWARZBACH, 1997; BERA et al., 2006). Apesar da busca por solventes alternativos ser antiga, até o presente momento, nenhuma alternativa economicamente viável foi encontrada (ANDERSON, 1996).

A presença de solvente residual no óleo vegetal refinado, em quantidades superiores ao estabelecido pela legislação, é nociva à saúde. Por ser mais denso que o ar, foi comprovado que a liberação do vapor do solvente n-hexano constitui um perigo ao meio ambiente, contribuindo com a poluição atmosférica, colocando em risco a saúde dos operadores e das comunidades próximas à unidade processadora (LUSAS, WATKINS e KOSEOGLU, 1991; SCHWARZBACH, 1997).

Schwarzbach (1997) estima que, para cada tonelada de grão processado, cerca de 2 L de solvente são perdidos para o meio ambiente, por isso o processo de extração de óleos vegetais é considerado muito poluente pelos órgãos de proteção ambiental. Hron, Koltun e Graci (1982) relataram que, em uma estimativa modesta, a quantidade de n-hexano perdido no processo de extração do óleo corresponde a cerca de 0,15 % do peso de grão processado. Por essa razão, vários autores (HRON, KOLTUN e GRACI, 1982; RITTNER, 1992; ANDERSON, 1996; SCHWARZBACH, 1997) reiteram a necessidade de desenvolver processos alternativos, porém rentáveis, para a extração do óleo vegetal.

A busca de alternativas para substituição do solvente n-hexano na extração de óleos vegetais tem como meta reduzir a dependência tecnológica em relação aos derivados de petróleo, além da preservação do meio ambiente e do homem, tendo em vista a alta toxicidade do n-hexano (HRON, KOLTUN e GRACI, 1982; RITTNER, 1992). Outros solventes como o álcool etílico e álcool isopropílico tem sido recomendados para extração de óleos vegetais .

Em 1982, Hron, Koltun e Graci fizeram uma revisão dos potenciais solventes renováveis que poderiam ser utilizados para substituir o n-hexano; neste estudo, os autores avaliaram as diferentes alternativas para a extração de óleos vegetais e, entre outros métodos, consideraram a extração com álcool uma alternativa viável. O interesse em usar álcool etílico como solvente para extração de óleo é antigo; Rao et al., em 1955, avaliaram a solubilidade de diferentes tipos de óleos vegetais em etanol em diferentes temperaturas e a influência da pressão.

O uso do álcool etílico para substituir o n-hexano apresenta boas perspectivas comerciais, uma vez que o etanol pode ser obtido a partir de diferentes fontes vegetais, a preços competitivos; além disso, o etanol não é tóxico e, embora também inflamável, é menos perigoso que o n-hexano. A obtenção de álcool etílico a partir da cana de açúcar coloca o Brasil em uma posição privilegiada na eliminação do uso de derivados de petróleo no processamento de oleaginosas (RITTNER, 1992). Várias outras pesquisas (RAO et al., 1955; HRON, KOLTUN e GRACI, 1982; HRON e KOLTUN, 1984; REGITANO-D'ARCE, 1985; 1991; RITTNER, 1992; FREITAS, MONTEIRO e LAGO, 2000; BERA et al., 2006; FREITAS e LAGO, 2007) têm demonstrado resultados satisfatórios no uso do

etanol como solvente na extração de óleos vegetais. No entanto, estudos que abordam a etapa de recuperação deste solvente são praticamente inexistentes.

2.2.1.3. Refino de óleos vegetais

Refino é um termo genérico dado às etapas de purificação dos óleos vegetais brutos. O objetivo é remover as impurezas presentes nos óleos, com o menor dano possível aos triacilgliceróis, tocoferóis e outros compostos, cuja presença no óleo é desejável. Dentre as principais impurezas a serem removidas estão ácidos graxos livres, fosfatídeos, pigmentos e traços de metais, que podem ocasionar desde a formação de espuma e fumaça no processamento do óleo, até a precipitação de materiais sólidos durante as operações de aquecimento. Já a presença de carotenóides e tocoferóis, substâncias nutricionalmente importantes que também melhoram a estabilidade oxidativa do óleo, é altamente desejável em todos os óleos e gorduras (TRUJILLO-QUIJANO, 1997).

O refino pode ser realizado por dois sistemas: químico ou físico. Os dois sistemas utilizam processos muito similares. A maior diferença se encontra no método usado para a remoção dos ácidos graxos livres (desacidificação) (O'BRIEN, 2000b). Esta é a etapa mais importante do processo de purificação de óleos, principalmente devido ao rendimento de óleo neutro, que tem um efeito significativo no custo global final do processo (TANDY e MCPHERSON, 1984; PETRAUSKAITÈ, DE GREYT e KELLENS, 2000).

O refino químico é o método convencional de remoção de impurezas não glicerídicas de óleo comestível e consiste nas seguintes etapas: degomagem, neutralização com hidróxido de sódio, clarificação e desodorização. A qualidade do óleo obtido é boa e o

processo possui grande flexibilidade, podendo ser utilizado para diferentes tipos de óleos. No entanto, apresenta alguns inconvenientes como: a produção de sabões e o risco de formação de emulsões durante o processo de neutralização, grandes perdas de óleo neutro quando o óleo bruto apresenta grande teor de ácidos graxos livres (superior a 3,0%); e maior quantidade de efluentes formados durante o processo (O'BRIEN, 2000b). Antoniassi, Esteves e Meirelles (1998) reportam perdas de até 14% em refinarias brasileiras, para óleos com 4% de acidez.

O refino físico, também conhecido como desacidificação por destilação (CERIANI e MEIRELLES, 2006), consiste na remoção de ácidos graxos livres do óleo por destilação com injeção direta de vapor d'água sob vácuo (*stripping*). O refino físico deve ser realizado após a remoção dos fosfatídeos por degomagem e antes do processo de clarificação do óleo. As maiores vantagens deste processo são: a não formação de sabões, o baixo custo e a necessidade de poucos processos para a operação e manutenção. O refino físico é recomendado para óleos contendo alto teor de ácidos graxos livres e baixo conteúdo de fosfatídeos, como: os óleos de coco, palma, palmiste e arroz (O'BRIEN, 2000b).

O processo de desodorização tem como objetivo eliminar odores indesejáveis dos óleos vegetais (MATTIL, 1964). A desodorização é realizada através de um processo semelhante ao utilizado no refino físico, a destilação a vapor ou *stripping*, isto é, aplicação de altas temperaturas sob baixíssimas pressões no óleo. Essas condições extremas de processamento podem resultar em alterações indesejáveis afetando a qualidade do produto final (MAZA, ORMSBEE e STRECKER, 1992; PETRAUSKAITÈ, DE GREYT e KELLENS, 2000). Apesar da destilação a vapor visar atingir apenas os compostos

indesejáveis, uma perda simultânea de componentes desejáveis do óleo (por exemplo, triacilgliceróis e antioxidantes naturais) é inevitável (MAZA, ORMSBEE e STRECKER, 1992).

Ao final do processo de refino, os óleos contém pelo menos 98% de triacilgliceróis, o restante é composto por diacilgliceróis (< 0,5%), ácidos graxos livres (<0,1%), esteróis (<0,3%), tocoferóis (< 0,1%) e traços de fosfolipídios e pigmentos (WAN, 2000).

2.3. Biodiesel

Biodiesel constitui em uma mistura de ésteres de alquila de ácidos graxos que tem propriedades semelhantes ao diesel de petróleo, podendo ser utilizado puro ou misturado em todas as proporções ao diesel de petróleo em motores diesel convencionais (MA e HANNA, 1999).

Devido ao aumento contínuo nos preços do petróleo, aos escassos recursos de energias fósseis e às preocupações ambientais que visam limitar o uso de combustíveis derivados do petróleo (MA e HANNA, 1999; MARCHETTI, MIGUEL e ERRAZU, 2007), a busca por combustíveis alternativos tem se tornado o principal tema para diversos grupos de pesquisa. Entretanto, os combustíveis alternativos para motores diesel devem ser tecnicamente viáveis, economicamente competitivos, ambientalmente aceitáveis e facilmente disponíveis (SRIVASTAVA e PRASAD, 2000). Do ponto de vista dessas exigências, o biodiesel é visto como um combustível alternativo promissor e viável, já que pode ser produzido a partir de triacilgliceróis (TAGs) e seus derivados, cujas fontes principais são óleos vegetais e gorduras animais (MA e HANNA, 1999; SRIVASTAVA e

PRASAD, 2000; MARCHETTI, MIGUEL e ERRAZU, 2007; BAROUTIAN et al., 2008). Os óleos vegetais, em especial, estão amplamente disponíveis a partir de diversas fontes consideradas renováveis (SRIVASTAVA e PRASAD, 2000; ENCINAR et al., 2002). Dessa forma, o biodiesel pode ser considerado uma fonte de energia sustentável, renovável, biodegradável e menos tóxica (MA e HANNA, 1999; MARCHETTI, MIGUEL e ERRAZU, 2007; BAROUTIAN et al., 2008).

O biodiesel apresenta as seguintes vantagens em relação ao diesel de petróleo: produz menos fumaça e partículas durante a combustão, possui maiores índices de cetano, produz menores emissões de monóxido de carbono e hidrocarbonetos, é biodegradável e não tóxico, e favorece a lubrificação do motor, mesmo para diesel com baixo teor de enxofre. Por outro lado, apresenta desafios técnicos como a baixa volatilidade, elevados pontos de fluidez e de núvem, elevada temperatura de entupimento de filtro a frio, elevadas emissões de óxido nitroso (NO_x) e combustão incompleta (MA e HANNA, 1999; SRIVASTAVA e PRASAD, 2000; ENCINAR et al., 2002; ENCINAR, GONZÁLEZ e RODRIGUEZ-REINARES, 2007).

O método mais comum de produção de biodiesel é através da reação de transesterificação. Este processo envolve a combinação de qualquer óleo ou gordura, com álcool e um catalisador (MA e HANNA, 1999; ENCINAR et al., 2002; ENCINAR, GONZÁLEZ e RODRIGUEZ-REINARES, 2007; BAROUTIAN et al., 2008).

A transesterificação consiste na sequência de três reações reversíveis consecutivas. A primeira etapa consiste na conversão do TAG em diacilglicerol (DAG), em seguida ocorre a conversão de DAG em monoacilglicerol (MAG) e, finalmente, de MAG em

glicerol (glicerina), produzindo uma molécula de éster a cada etapa. Pela estequiometria da reação, são requeridos três moles de álcool para cada mol de TAG, mas na prática uma proporção maior (6:1) é utilizada para deslocar o equilíbrio no sentido de maior produção de éster (MA e HANNA, 1999; ENCINAR et al., 2002; ENCINAR, GONZÁLEZ e RODRIGUEZ-REINARES, 2007).

Os álcoois que podem ser utilizados na reação de transesterificação são os de cadeia curta como: metanol, etanol, propanol, butanol e álcool amílico; a opção por algum deles deve ser baseada no seu custo e desempenho. Em geral, o metanol e o etanol são os mais frequentemente empregados. Em outros países, o metanol é o álcool que apresenta menor custo e, portanto, mais utilizado. No Brasil, o etanol é preferível devido à sua grande disponibilidade e por alcançar total independência a partir de álcoois à base de petróleo, já que o etanol é um derivado de produto agrícola. Além disso, é renovável e biologicamente menos agressivo ao meio ambiente e apresenta melhores propriedades como solvente, isto é, possui um maior poder de dissolução dos óleos e, assim, a etanólise possui menor limitação na transferência de massa. No entanto, a formação de emulsão estável com o óleo faz com que a recuperação do éster seja bastante dificultada (ENCINAR, GONZÁLEZ e RODRIGUEZ-REINARES, 2007; BAROUTIAN et al., 2008).

Uma instalação típica de produção e purificação de biodiesel contém três seções principais de processamento: uma unidade de transesterificação, uma seção de purificação de biodiesel e uma seção de recuperação de glicerol (HAAS et al., 2006). Os passos de purificação da reação de transesterificação são extremamente importantes, a fim de fornecer combustível com os níveis de qualidade exigidos pelas normas vigentes (OLIVEIRA et al.,

2010). Outro ponto importante para a viabilidade do processo de produção do biodiesel é a recuperação e reutilização do álcool presente em excesso.

2.4. Termodinâmica do Equilíbrio de Fases

O equilíbrio de fases termodinâmico constitui um tema de especial interesse na química, na engenharia química (PRAUSNITZ, LICHTENTHALER e GOMES DE AZEVEDO, 1999) e também na engenharia de alimentos, já que muitas operações unitárias presentes nos processos industriais dessas áreas consistem no contato de fases, como por exemplo: a extração, a adsorção, a destilação, a lixiviação e a absorção.

O equilíbrio de fases visa estabelecer as relações entre várias propriedades do sistema; entre elas podem ser destacadas: a temperatura, a pressão e a composição do sistema, que permanecerão constantes quando duas ou mais fases atingirem o estado de equilíbrio, no qual toda tendência a mudanças cessa (PRAUSNITZ, LICHTENTHALER e GOMES DE AZEVEDO, 1999). Assim, o equilíbrio termodinâmico de um sistema fechado e heterogêneo entre duas fases (α e β) existe se as seguintes condições forem atendidas (PRAUSNITZ, LICHTENTHALER e GOMES DE AZEVEDO, 1999; SANDLER, 1999; SMITH, VAN NESS e ABBOTT, 2000; GMEHLING et al., 2012):

$$T^{\alpha} = T^{\beta} \tag{2.1}$$

$$P^{\alpha} = P^{\beta} \tag{2.2}$$

$$\mu_i^{\alpha} = \mu_i^{\beta} \tag{2.3}$$

Isto é, além do equilíbrio térmico e mecânico, o equilíbrio de fases exige que o potencial químico de cada componente i em todas as fases sejam iguais. O potencial químico do componente i é igual à energia de Gibbs parcial molar, como indicado na equação 2.4 (PRAUSNITZ, LICHTENTHALER e GOMES DE AZEVEDO, 1999; GMEHLING et al., 2012).

$$\mu_i^{\alpha} = \left(\frac{\partial n_T g}{\partial n_i}\right)_{T,P,n_{j\neq i}} = \bar{g}_i^{\alpha} \tag{2.4}$$

onde: μ_i^{α} é o potencial químico do componente i; g e $\bar{g}_i^{\alpha}$. são a energia de Gibbs e energia de Gibbs parcial molar do componente i, repectivamente; e n_i é o número de moles do componente i.

Considerando que a energia de Gibbs das fases (α e β) também pode ser expressa em termos de fugacidade (equação 2.5) (GMEHLING et al., 2012), pode ser aplicado ao equilíbrio de fases o critério de isofugacidade de Lewis, expresso pela equação 2.6.

$$\bar{g}_i^{\alpha}(T,P,z_i) = g_i^{\alpha}(T,P^0) + RTln\frac{f_i^{\alpha}(T,P,z_i)}{f_i^{0\alpha}(T,P^0)} \tag{2.5}$$

onde: T e P são a temperatura e a pressão do sistema, respectivamente; z_i é a fração molar do componente i; P^0 é a pressão no estado padrão (referência arbitrária); f_i^{α} é a fugacidade do componente i na fase α; e $f_i^{0\alpha}$ é a fugacidade no estado padrão (referência arbitrária) do componente i na fase α.

$$f_i^{\alpha}(T,P,z_i^{\alpha}) = f_i^{\beta}\left(T,P,z_i^{\beta}\right) \tag{2.6}$$

onde: f_i^{α} e f_i^{β} são as fugacidades do componente i nas fases α e β, respectivamente.

Para o cálculo do equilíbrio de fases, os dois critérios apresentados nas equações 2.3 e 2.6 são válidos. No entanto, do ponto de vista prático, isto é, para a aplicação da termodinâmica na resolução de problemas físicos, o uso da fugacidade é mais conveniente e a equação 2.6 é a mais utilizada (PRAUSNITZ, LICHTENTHALER e GOMES DE AZEVEDO, 1999). Considerando misturas em que os seus componentes não possuem forte associação entre si e que não se encontram a alta pressão, pode-se considerar que tal sistema possui comportamento ideal e a fugacidade do componente i passa a ser igual à pressão parcial do componente na mistura e, no caso de compostos puros, igual à pressão de vapor.

A relação da fugacidade com quantidades mensuráveis pode ser obtida a partir da introdução de parâmetros auxiliares como o coeficiente de atividade, γ_i, e o coeficiente de fugacidade, φ_i. Utilizando essas variáveis auxiliares, a fugacidade, f_i, pode ser relacionada à fração molar de cada fase, z_i, a partir das equações 2.7 e 2.8.

$$\gamma_i \equiv \frac{f_i}{z_i f_i^{\,0}} \tag{2.7}$$

$$\varphi_i \equiv \frac{f_i}{z_i P}\,. \tag{2.8}$$

onde f_i^0é a fugacidade do componente i no estado padrão e P é a pressão total do sistema.

2.4.1. Equilíbrio de fases líquido-vapor

No equilíbrio líquido-vapor (ELV), a temperatura, pressão e fugacidades dos componentes das fases líquida e vapor são iguais (PRAUSNITZ, LICHTENTHALER e

GOMES DE AZEVEDO, 1999; SANDLER, 1999; SMITH, VAN NESS e ABBOTT, 2000; POLING, PRAUSNITZ e O'CONNELL, 2001; GMEHLING et al., 2012), conforme apresentado na equação 2.9.

$$f_i^L = f_i^V \tag{2.9}$$

Utilizando as diferentes definições para as fugacidades (equações 2.7 e 2.8), podem ser usadas duas abordagens para a descrição do ELV, sendo elas (GMEHLING et al., 2012):

- abordagem $\varphi - \varphi$:

$$x_i \varphi_i^L = y_i \varphi_i^V \tag{2.10}$$

- abordagem $\gamma - \varphi$:

$$x_i \gamma_i f_i^0 = y_i \varphi_i^V P \tag{2.11}$$

Pela abordagem $\varphi - \varphi$, os coeficientes de fugacidade das fases líquida (φ_i^L) e vapor (φ_i^V) descrevem o desvio do sistema em relação ao comportamento de gás ideal e de mistura ideal e podem ser calculados com o auxílio das equações de estado e regras de misturas adequadas. Já pela abordagem $\gamma - \varphi$, além do coeficiente de atividade, γ_i, um valor para a fugacidade padrão, f_i^0, é requerido. No caso de ELV, normalmente utiliza-se a fugacidade do componente líquido puro à temperatura e pressão do sistema como fugacidade padrão (GMEHLING et al., 2012).

Embora as equações de estado sejam muito atrativas para os cálculos de ELV, pela abordagem $\varphi - \varphi$, são necessárias, além da própria equação de estado, regras de misturas

que descrevam o comportamento não somente da fase vapor, mas também da fase líquida com a requerida precisão. Apesar do progresso alcançado nos últimos 20 anos, até o momento não existem equações de estado e regras de misturas que possam ser aplicadas de forma bem sucedida em qualquer tipo de sistema numa ampla faixa de temperatura e pressão e para componentes puros e misturas. Então para os cálculos do ELV, a abordagem $\gamma - \varphi$ é a mais frequentemente utilizada (GMEHLING et al., 2012).

Rigorosamente, o equilíbrio de fases líquido-vapor (ELV) pela abordagem $\gamma - \varphi$ é definido pela equação 2.12:

$$x_i \gamma_i \varphi_i^S P_i^S exp\left[\frac{v_i^L (P - P_i^S)}{RT}\right] = y_i \varphi_i^V P \qquad (2.12)$$

onde P e T são a pressão e temperatura do sistema; x_i e y_i são as frações molares do componente i nas fases líquido e vapor, respectivamente; γ_i o coeficiente de atividade como função de x_i e T; P_i^S é a pressão de saturação do composto em função da temperatura do sistema; R é a constante dos gases; v_i^L é o volume molar do composto i como líquido; φ_i^S é o coeficiente de fugacidade do composto i na saturação; φ_i^V é o coeficiente de fugacidade do composto i na fase vapor nas condições de temperatura e pressão consideradas; e $exp\left[\frac{v_i^L (P - P_i^S)}{RT}\right]$ é o fator de Poynting (Poy_i).

O fator de Poynting (Poy_i) constitui uma correção da fugacidade em relação à do líquido puro. Se a diferença de pressão $P - P_i^S$ não é muito grande, o valor de Poy_i é aproximadamente 1.

O coeficiente de fugacidade da fase vapor pode ser calculado através da equação virial truncada no segundo termo (equação 2.13), ou qualquer outra equação de estado (PRAUSNITZ, LICHTENTHALER e GOMES DE AZEVEDO, 1999; GMEHLING et al., 2012). A equação 2.13 apresenta a equação virial para um sistema multicomponente.

$$ln\varphi_i^V = \left[2\sum_j y_j B_{ij} - B\right]\frac{P}{RT} \tag{2.13}$$

O segundo coeficiente virial, B, é definido pela Equação 2.14:

$$B = \sum_i^n \sum_j^n y_i y_j B_{ij} \tag{2.14}$$

onde n é o número de componentes da mistura multicomponente; y_i e y_j são as frações molares da fase vapor dos compostos i e j, respectivamente e B_{ij} é o segundo coeficiente da equação virial cruzado. Para o cálculo de φ_i^s, substitui-se, na equação anterior, P por P_i^s (pressão de saturação do componente puro na temperatura do sistema) e se escreve como componente puro.

Uma forma de estimar o segundo coeficiente da equação virial é através da correlação empírica proposta por Pitzer e Curl Jr. (1957) e modificada por Tsonopoulos (1974) apresentadas na sequência de equações: 2.15 a 2.23 ou pelas correlações do DIPPR (*Design Institute for Physical Properties*) (DIPPR, [2005, 2008, 2009, 2010]) cujos parâmetros podem obtidos no DDB (*Dortmund Data Bank*) (DDB, 2011).

Para compostos apolares, o cálculo do segundo coeficiente virial é realizado pela equação (2.15):

$$\frac{BP_c}{RT_c} = \mathcal{F}^{(0)} + \omega\mathcal{F}^{(1)} \tag{2.15}$$

onde: ω é o fator acêntrico, P_c e T_c são a pressão e temperatura crítica do composto e $\mathcal{F}^{(0)}$ e $\mathcal{F}^{(1)}$ são funções da temperatura definida pelas seguintes equações:

$$\mathcal{F}^{(0)} = 0{,}1445 - \frac{0{,}330}{T_R} - \frac{0{,}1385}{T_R^2} - \frac{0{,}0121}{T_R^3} - \frac{0{,}000607}{T_R^8} \tag{2.16}$$

$$\mathcal{F}^{(1)} = 0{,}0637 + \frac{0{,}331}{T_R^2} - \frac{0{,}423}{T_R^3} - \frac{0{,}008}{T_R^8} \tag{2.17}$$

sendo:

$$T_R = \frac{T}{T_C} \tag{2.18}$$

Para compostos polares, o segundo coeficiente virial pode ser calculado pela seguinte equação:

$$\frac{BP_c}{RT_c} = \mathcal{F}^{(0)} + \omega\mathcal{F}^{(1)} + \mathcal{F}^{(2)} \tag{2.19}$$

onde:

$$\mathcal{F}^{(2)} = \frac{a}{T_R^6} - \frac{b}{T_R^8} \tag{2.20}$$

Os parâmetros a e b foram correlacionados de acordo com a classe de composto.

O segundo coeficiente da equação virial cruzado pode ser calculado pelas equações acima usando as seguintes regras de mistura para ω, P_c e T_c:

$$\omega_{ij} = \frac{\omega_i + \omega_j}{2} \tag{2.21}$$

$$P_{cij} = \frac{4T_{cij}\left(\frac{P_{ci}V_{ci}}{T_{ci}} + \frac{P_{cj}V_{cj}}{T_{cj}}\right)}{\left(V_{ci}^{1/3} + V_{cj}^{1/3}\right)} \tag{2.22}$$

$$T_{cij} = (1 - k_{ij})\sqrt{(T_{ci}T_{cj})} \quad (2.23)$$

A não idealidade do equilíbrio líquido-vapor (ELV) é descrita essencialmente pelos coeficientes de atividade da fase líquida, os quais são função da temperatura e especialmente da composição (GMEHLING e ONKEN, 1979; GMEHLING et al., 2012).

O coeficiente de atividade é definido pela Equação 2.24 (FREDENSLUND, GMEHLING e RASMUSSEN, 1977; PRAUSNITZ, LICHTENTHALER e GOMES DE AZEVEDO, 1999; SANDLER, 1999; SMITH, VAN NESS e ABBOTT, 2000; POLING, PRAUSNITZ e O'CONNELL, 2001; GMEHLING et al., 2012):

$$ln\gamma_i = \frac{1}{R.T}\left(\frac{\partial n_T g^E}{\partial n_i}\right)_{T,P,n_{j\neq i}} = \frac{\bar{g}_i^E}{RT} \quad (2.24)$$

Então para o cálculo dos coeficientes de atividade na fase líquida, γ_i, torna-se necessário o uso de modelos que descrevam a energia de Gibbs molar de excesso em todo o intervalo de concentração do sistema. Assim, modelos termodinâmicos adequados são utilizados para descrever coeficientes de atividade e para a seleção de solventes e do processo.

2.5. Modelos Termodinâmicos

A uma temperatura fixa, a energia de Gibbs de excesso (g^E) de uma mistura depende da sua composição e, em uma extensão menor, da pressão. A pressões moderadas, bem abaixo das condições críticas (para o ELV, $P < 20$ bar, são consideradas pressões moderadas), o efeito da pressão pode ser desprezado (PRAUSNITZ, LICHTENTHALER e GOMES DE AZEVEDO, 1999).

As abordagens utilizadas para descrever a energia livre de Gibbs molar de excesso podem ser classificadas como modelos de moleculares como: os modelos de Wilson (WILSON, 1964) NRTL - *NonRandom, Two-Liquid* (RENON e PRAUSNITZ, 1968) e UNIQUAC – *Universal Quasi-Chemical equation* (ABRAMS e PRAUSNITZ, 1975) e os métodos de contribuição de grupos, como as diferentes versões do modelo UNIFAC - *UNIquac Functional group Activity Coefficients* (FREDENSLUND, JONES e PRAUSNITZ, 1975; FREDENSLUND, GMEHLING e RASMUSSEN, 1977; LARSEN, RASMUSSEN e FREDENSLUND, 1987b; WEIDLICH e GMEHLING, 1987; GMEHLING, LI e SCHILLER, 1993) e o modelo ASOG– *Analytical Solutions of Groups* (KOJIMA e TOCHIGI, 1979). Esses modelos permitem o cálculo do comportamento real de sistemas multicomponentes. Diferentes informações são necessárias para o cálculo do γ_i pelos modelos de moleculares e pelos métodos de contribuição de grupos. Os modelos de moleculares baseiam-se nas interações binárias entre as moléculas envolvidas na mistura de acordo com o conceito de composição local introduzido por Wilson (1964), enquanto que os métodos de contribuição de grupos assumem que a mistura não consiste de moléculas mas sim de grupos funcionais, assim, as propriedades da mistura podem ser representadas pela soma das contribuições individuais de cada um dos grupos funcionais que a compõe (FREDENSLUND, JONES e PRAUSNITZ, 1975; FREDENSLUND, GMEHLING e RASMUSSEN, 1977; PRAUSNITZ, LICHTENTHALER e GOMES DE AZEVEDO, 1999; POLING, PRAUSNITZ e O'CONNELL, 2001; GMEHLING et al., 2012).

A principal vantagem dos métodos de contribuição de grupos em relação aos modelos moleculares é a possibilidade de representar uma ampla gama de sistemas

tecnologicamente interessantes com um número relativamente pequeno de parâmetros. Isto é resultado do fato desses métodos utilizarem um número muito menor de possíveis grupos funcionais, em comparação com o número de moléculas individuais.

2.5.1. Modelos moleculares

2.5.1.1. Equação de Wilson

Em 1964, Wilson introduziu o conceito de fração molar local, em que o desvio da concentração macroscópica é levado em consideração com o auxílio das energias de interação entre os diferentes compostos, utilizando os fatores de Boltzmann. Dessa forma, baseada em considerações moleculares, a equação de Wilson para o cálculo da energia de Gibbs de excesso pode ser escrita da seguinte forma para sistemas binários:

$$\frac{g^E}{RT} = -x_1 ln(x_1 + \Lambda_{12} x_2) - x_2 ln(x_2 + \Lambda_{21} x_1) \tag{2.25}$$

Os coeficientes de atividade derivados desta equação são calculados pelas seguintes expressões:

$$ln\gamma_1 = -ln(x_1 + \Lambda_{12} x_2) + x_2 \left(\frac{\Lambda_{12}}{x_1 + \Lambda_{12} x_2} - \frac{\Lambda_{21}}{\Lambda_{21} x_1 + x_2} \right) \tag{2.26}$$

$$ln\gamma_2 = -ln(x_2 + \Lambda_{21} x_1) - x_1 \left(\frac{\Lambda_{12}}{x_1 + \Lambda_{12} x_2} - \frac{\Lambda_{21}}{\Lambda_{21} x_1 + x_2} \right) \tag{2.27}$$

Os parâmetros ajustáveis da equação de Wilson, Λ_{12} e Λ_{21}, estão relacionados aos volumes molares dos componentes puros e às diferenças de energia característica pelas seguintes expressões:

$$\Lambda_{12} \equiv \frac{v_2}{v_1} exp\left(-\frac{\lambda_{12}-\lambda_{11}}{RT}\right) \quad (2.28)$$

$$\Lambda_{21} \equiv \frac{v_1}{v_2} exp\left(-\frac{\lambda_{21}-\lambda_{22}}{RT}\right) \quad (2.29)$$

onde v_i é o volume molar líquido do componente puro i e λ é a energia de interação entre as moléculas designadas nos subíndices.

A grande vantagem da equação de Wilson é que apenas parâmetros binários são requeridos para o cálculo do comportamento real de sistemas multicomponente. No entanto, a equação de Wilson apresenta a desvantagem de, ao contrário de outros modelos moleculares, não poder ser aplicada para o cálculo de equilíbrio de fases líquido-líquido (ELL), isto é, para sistemas com miscibilidade parcial (PRAUSNITZ, LICHTENTHALER e GOMES DE AZEVEDO, 1999; GMEHLING et al., 2012). Além disso, as equações 2.26 e 2.27 não podem ser aplicadas, assim como as equações de van Laar, para sistema cujo gráfico $ln\gamma_i$ versus x exibem máximo ou mínimo.

2.5.1.2. Equação NRTL (NonRandom, Two-Liquid)

Assim como a equação de Wilson, o modelo NRTL (RENON e PRAUSNITZ, 1968) também é baseado no conceito de composição local e permite a predição dos coeficientes de atividade de sistemas multicomponentes usando apenas parâmetros binários. Diferentemente da equação de Wilson, a equação NRTL pode ser utilizada para o cálculo de ELL.

A equação NRTL para energia de Gibbs de excesso é a seguinte:

$$\frac{g^E}{RT} = x_1 x_2 \left(\frac{\tau_{21} G_{21}}{x_1 + x_2 G_{21}} + \frac{\tau_{12} G_{12}}{x_2 + x_1 G_{12}} \right) \tag{2.30}$$

onde:

$$\tau_{12} = \frac{g_{12} - g_{22}}{RT} \text{ e } \tau_{21} = \frac{g_{21} - g_{11}}{RT} \tag{2.31}$$

$$G_{12} = exp(-\alpha_{12} \tau_{12}) \text{ e } G_{21} = exp(-\alpha_{12} \tau_{21}) \tag{2.32}$$

g_{12} é um parâmetro energético característico da interação $i - j$. O parâmetro α_{12} está relacionado à não aleatoriedade na mistura: quando $\alpha_{12} = 0$ a mistura é completamente aleatória e o modelo NRTL se reduz ao modelo de Margules. A equação NRTL contém três parâmetros de ajuste, mas a redução de dados experimentais de um grande número de sistemas binários indicou que α_{12} varia de 0,20 a 0,47. Dessa forma, quando os dados experimentais são escassos o valor deste parâmetro é ajustado arbitrariamente.

Os coeficientes de atividade são obtidos pelas equações 2.33 e 2.34.

$$ln\gamma_1 = x_2^2 \left[\tau_{21} \left(\frac{G_{21}}{x_1 + G_{21} x_2} \right)^2 + \frac{\tau_{12} G_{12}}{(G_{12} x_1 + x_2)^2} \right] \tag{2.33}$$

$$ln\gamma_2 = x_1^2 \left[\tau_{12} \left(\frac{G_{12}}{x_2 + G_{12} x_1} \right)^2 + \frac{\tau_{21} G_{21}}{(G_{21} x_1 + x_1)^2} \right] \tag{2.34}$$

O uso do modelo NRTL é especialmente vantajoso para misturas fortemente não ideais e especialmente para aquelas que apresentam miscibilidade parcial (PRAUSNITZ, LICHTENTHALER e GOMES DE AZEVEDO, 1999).

2.5.1.3. Modelo UNIQUAC (UNIversal QUAsi-Chemical)

Abrams e Prausnitz (1975) derivaram uma equação que estende a teoria quasi-química para misturas não aleatórias de Guggenheim para soluções contendo moléculas de diferentes tamanhos, é a chamada teoria quasi-química universal ou UNIQUAC. O cálculo do coeficiente de atividade pela equação UNIQUAC consiste de duas partes: a combinatorial e a residual. A parte combinatorial tenta descrever a contribuição entrópica dominante e é determinada somente pela composição e pelos tamanhos e formas das moléculas, o que requer dados do componente puro. Enquanto que a parte residual se refere primariamente às forças intermoleculares que são responsáveis pela entalpia da mistura e, por essa razão, os dois parâmetros ajustáveis se apresentam nesta parte da equação.

A equação UNIQUAC para energia de Gibbs de excesso é a seguinte:

$$\frac{g^E}{RT} = \left(\frac{g^E}{RT}\right)_{combinatorial} + \left(\frac{g^E}{RT}\right)_{residual} \tag{2.35}$$

Para uma mistura binária:

$$\left(\frac{g^E}{RT}\right)_{combinatorial} = x_1 ln\frac{\Phi_1^*}{x_1} + x_2 ln\frac{\Phi_2^*}{x_2} + \frac{z}{2}\left(x_1 q_1 ln\frac{\theta_1}{\Phi_1^*} + x_2 q_2 ln\frac{\theta_2}{\Phi_2^*}\right) \tag{2.36}$$

$$\left(\frac{g^E}{RT}\right)_{residual} = -x_1 q'_1 ln(\theta'_1 + \theta'_2 \tau_{21}) - x_2 q'_2 ln(\theta'_2 + \theta'_1 \tau_{12}) \tag{2.37}$$

onde o número de coordenação z é igual a 10. A fração de segmento, Φ^*, e as frações de área, θ e θ', são dados por:

$$\Phi_1^* = \frac{x_1 r_1}{x_1 r_1 + x_2 r_2} \text{ e } \Phi_2^* = \frac{x_2 r_2}{x_1 r_1 + x_2 r_2} \tag{2.38}$$

$$\theta_1 = \frac{x_1 q_1}{x_1 q_1 + x_2 q_2} \text{ e } \theta_2 = \frac{x_2 q_2}{x_1 q_1 + x_2 q_2} \tag{2.39}$$

$$\theta'_1 = \frac{x_1 q'_1}{x_1 q'_1 + x_2 q'_2} \text{ e } \theta'_2 = \frac{x_2 q'_2}{x_1 q'_1 + x_2 q'_2} \quad (2.40)$$

Os parâmetros r, q e q' são constantes da estrutura molecular do componente puro que dependem do tamanho molecular e da área da superfície externa.

Para misturas binárias, os parâmetros ajustáveis, τ_{12} e τ_{21} podem ser escritos em termos de energia característica Δu_{12} e Δu_{21} através das equações 2.41 e 2.42.

$$\tau_{12} = exp\left(-\frac{\Delta u_{12}}{RT}\right) \quad (2.41)$$

$$\tau_{21} = exp\left(-\frac{\Delta u_{21}}{RT}\right) \quad (2.42)$$

Os coeficientes de atividade são dados pelas equações 2.43 e 2.44:

$$ln\gamma_1 = ln\frac{\Phi_1^*}{x_1} + \frac{z}{2} q_1 ln\frac{\theta_1}{\Phi_1^*} + \Phi_2^*\left(l_1 - \frac{r_1}{r_2} l_2\right) - q'_1 ln(\theta'_1 + \theta'_2 \tau_{21}) +$$

$$\theta'_2 q'_1 \left(\frac{\tau_{21}}{\theta'_1 + \theta'_2 \tau_{21}} - \frac{\tau_{12}}{\theta'_2 + \theta'_1 \tau_{12}}\right) \quad (2.43)$$

$$ln\gamma_2 = ln\frac{\Phi_2^*}{x_2} + \frac{z}{2} q_2 ln\frac{\theta_2}{\Phi_2^*} + \Phi_1^*\left(l_2 - \frac{r_2}{r_1} l_1\right) - q'_2 ln(\theta'_2 + \theta'_1 \tau_{12}) +$$

$$\theta'_1 q'_2 \left(\frac{\tau_{12}}{\theta'_2 + \theta'_1 \tau_{12}} - \frac{\tau_{21}}{\theta'_1 + \theta'_2 \tau_{21}}\right) \quad (2.44)$$

onde

$$l_1 = \frac{z}{2}(r_1 - q_1) - (r_1 - 1) \quad (2.45)$$

$$l_2 = \frac{z}{2}(r_2 - q_2) - (r_2 - 1) \quad (2.46)$$

A equação UNIQUAC é aplicável a uma grande variedade de misturas líquidas não eletrolíticas contendo fluidos polares e não polares e incluindo misturas parcialmente

miscíveis. Com apenas dois parâmetros binários ajustáveis, a equação UNIQUAC nem sempre representa dados de qualidade com alta precisão, mas para muitas misturas típicas fornece uma descrição bastante satisfatória (PRAUSNITZ, LICHTENTHALER e GOMES DE AZEVEDO, 1999).

2.5.2. Modelos de contribuição de grupos

O primeiro método de contribuição de grupo para a predição dos coeficientes de atividade para o ELV foi o método ASOG (*Analytical SOlution of Groups*) (KOJIMA e TOCHIGI, 1979). O método ASOG utiliza o modelo de Wilson para descrever a dependência da concentração dos grupos de coeficiente de atividade requeridos na ideia de solução de grupos (GMEHLING et al., 2012).

O método de contribuição de grupos UNIFAC (*UNIquac Functional group Activity Coefficients*) foi publicado por Fredenslund, Jones e Prausnitz em 1975 e, como o método ASOG, também é baseado na ideia de contribuição de grupos. O método UNIFAC e seus desenvolvimentos são métodos de contribuição de grupos amplamente utilizados nas indústrias para os cálculos de coeficiente de atividade.

O método baseia-se na abordagem do modelo UNIQUAC, isto é, os coeficientes de atividade são calculados a partir de um termo combinatorial e outro residual. A parte combinatorial é independente da temperatura e leva em consideração o tamanho e forma das moléculas, trata-se da contribuição entrópica. A parte residual considera as interações entálpicas.

$$ln\gamma_i = ln\gamma_i^C + ln\gamma_i^R \tag{2.47}$$

Na versão original do modelo UNIFAC, a parte combinatorial, $ln\gamma_i^C$, pode ser calculada usando a seguinte equação:

$$ln\gamma_i^C = 1 - V_i + lnV_i - 5q_i\left(1 - \frac{V_i}{F_i} + ln\frac{V_i}{F_i}\right) \quad (2.48)$$

onde: $V_i = \frac{r_i}{\sum_j r_j x_j}$ e $F_i = \frac{q_i}{\sum_j q_j x_j}$, r_i e q_i são o volume relativo de van der Waals e a área da superfície relativa de van de Waals, respectivamente.

Para o método de contribuição de grupos UNIFAC, as propriedades relativas de van der Waals, r_i e q_i, podem ser obtidas usando os grupos relativos de volume, R_k, e área de superfície, Q_k, de van der Waals. Valores de R_k e Q_k podem ser obtidos das tabelas publicadas por Hansen et al. (1991) ou pelas tabelas publicadas por Bondi (1968).

$$r_i = \sum_k v_k^{(i)} R_k \quad (2.49)$$

$$q_i = \sum_k v_k^{(i)} Q_k \quad (2.50)$$

onde $v_k^{(i)}$ é o número de grupos funcionais do tipo k no componente i.

O termo residual dependente da temperatura, $ln\gamma_i^R$, leva em consideração as interações entre os diferentes compontentes. No método de contribuição de grupos, essa parte é calculada pelo conceito de soluções de grupos, utilizando-se os coeficientes de atividade de grupo Γ_k e $\Gamma_k^{(i)}$ pela equação 2.51.

$$ln\gamma_i^R = \sum_k v_k^{(i)}\left(ln\Gamma_k - ln\Gamma_k^{(i)}\right) \quad (2.51)$$

onde: Γ_k e $\Gamma_k^{(i)}$ são os coeficientes de atividade de grupo para o grupo k na mistura e no componente puro i, respectivamente.

A descrição da dependência da concentração do coeficiente de atividade de grupo da equação UNIQUAC é apresentada na equação 2.52.

$$ln\Gamma_k = Q_k \left[1 - ln(\sum_m \Theta_m \Psi_{mk}) - \sum_m \frac{\Theta_m \Psi_{km}}{\sum_n \Theta_n \Psi_{nm}}\right] \quad (2.52)$$

sendo:

$$\Theta_m = \frac{Q_m X_m}{\sum_n Q_n X_n} \quad (2.53)$$

$$\mathrm{X}_m = \frac{\sum_j v_m^{(j)} x_j}{\sum_j \sum_n v_n^{(j)} x_j} \quad (2.54)$$

$$\Psi_{mk} = exp\left(-\frac{a_{mn}}{T}\right) \quad (2.55)$$

onde : Θ_m é a fração de área da superfície; X_m é a fração molar de grupo do grupo m e a_{mn} é o parâmetro de interação de grupo entre os grupos funcionais (ou grupos principais) m e n.

No método UNIFAC, para cada combinação de grupo principal dois parâmetros de interação de grupo independentes da temperatura, a_{mn} e a_{nm}, são requeridos.

O modelo UNIFAC modificado (Dortmund) (WEIDLICH e GMEHLING, 1987; GMEHLING, LI e SCHILLER, 1993) e o modelo UNIFAC modificado (Lyngby) (LARSEN, RASMUSSEN e FREDENSLUND, 1987a) são métodos UNIFAC modificados que diferem da abordagem original apenas na representação da dependência da temperatura dos parâmetros de interação de grupo e a utilização de uma parte combinatória ligeiramente modificada. Tais mudanças visam corrigir alguns pontos fracos da abordagem original do método UNIFAC. Para o modelo modificado UNIFAC (Dortmund) tem-se:

$$ln\gamma_i^C = 1 - V'_i + lnV'_i - 5q_i\left(1 - \frac{V_i}{F_i} + ln\frac{V_i}{F_i}\right) \quad (2.56)$$

onde : $V'_i = \frac{r_i^{3/4}}{\sum_j x_j r_j^{3/4}}$ é a fração de volume empiricamente modificada.

E a dependência da temperatura é dada por:

$$\Psi_{mk} = exp\left(-\frac{a_{mn}+b_{mn}.T+c_{mn}.T^2}{T}\right) \quad (2.57)$$

2.6. Coeficiente de Atividade à Diluição Infinita

O coeficiente de atividade à diluição infinita, γ^{∞}, caracteriza o comportamento de um composto dissolvido (soluto) que é completamente envolvido por moléculas do solvente (ALESSI, FERMEGLIA e KIKIC, 1991; DALLINGA, SCHILLER e GMEHLING, 1993; GRUBER, LANGENHEIM e GMEHLING, 1997; KOJIMA, ZHANG e HIAKI, 1997) (ver Figura 2.1); portanto, esta propriedade indica geralmente o máximo de não-idealidade da mistura e fornece informações incisivas sobre as interações soluto-solvente, na ausência de interações soluto-soluto (MCMILLAN e MAYER, 1945). Portanto, trata-se essencialmente de uma propriedade de excesso (KOJIMA, ZHANG e HIAKI, 1997).

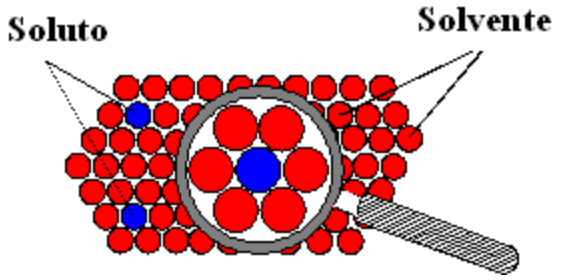

Figura 2.1: Representação esquemática de uma solução altamente diluída (KRUMMEN, 2002).

O coeficiente de atividade à diluição infinita é um parâmetro de extremo interesse não apenas do ponto de vista teórico mas também do ponto de vista prático da química e da engenharia química (DALLINGA, SCHILLER e GMEHLING, 1993; GRUBER, LANGENHEIM e GMEHLING, 1997; KOJIMA, ZHANG e HIAKI, 1997). Do ponto de vista industrial, o γ^{∞} oferece maior aplicabilidade do que qualquer medição em concentração finita, já que pode ser utilizado para prever o comportamento de fase de uma mistura no intervalo inteiro de concentração (KOJIMA, ZHANG e HIAKI, 1997).

Os valores de γ^{∞} têm importância prática pois possuem direta aplicação nos problemas industriais relacionados aos processos de separação, já que podem ser utilizados na seleção de solventes para os processos de destilação e retificação extrativa, absorção ou extração. Além disso, com o auxílio do γ^{∞} como função da temperatura, a ocorrência de pontos de azeotropia pode ser prevista (DALLINGA, SCHILLER e GMEHLING, 1993; GRUBER, LANGENHEIM e GMEHLING, 1997).

Do ponto de vista teórico, o conhecimento do coeficiente de atividade à diluição infinita permite a avaliação dos parâmetros das equações de correlação (WALAS, 1990) assim como o desenvolvimento de novos modelos termodinâmicos (DALLINGA,

SCHILLER e GMEHLING, 1993). A determinação experimental deste parâmetro é particularmente útil, pois permite o cálculo dos parâmetros necessários às expressões de energia de Gibbs de excesso (POLING, PRAUSNITZ e O'CONNELL, 2001) amplamente utilizadas nos cálculos de processos envolvento o equilíbrio de fases.

O coeficiente de atividade à diluição infinita pode ser determinado por vários métodos que, de acordo com Kojima, Zhang e Hiaki (1997), são classificados como diretos e indiretos. Os métodos indiretos incluem as extrapolações a partir de dados de equilíbrio líquido-vapor (ELV) e cálculos a partir de outros dados termodinâmicos, tais como: dados de equilíbrio líquido-líquido (ELL), coeficiente de distribuição líquido-líquido e o coeficiente de partição gás-líquido, entre outros.

A extrapolação dos dados de ELV é realizada utilizando um polinômio flexível de Legendre ou um modelo termodinâmico. No caso de dados de ELL, o γ^{∞} pode ser calculado a partir do critério de isoatividade ($x_i^{\propto}.\gamma_i^{\alpha} = x_i^{\beta}.\gamma_i^{\beta}$), assumindo que $x_i^{\propto}.\gamma_i^{\alpha} = 1$ para fase $\propto$. Os valores de γ^{∞} são obtidos pelo recíproco da solubilidade.

Os métodos diretos incluem o método da cromatografia gás-líquido (GLC), método GLC de *headspace*, método do gás de arraste (*Dilutor Technique*), método da cromatografia líquido-líquido, o método de ebuliometria diferencial e método estático diferencial (KOJIMA, ZHANG e HIAKI, 1997).

Mais informações sobre os diferentes métodos de determinação do coeficiente de atividade à diluição infinita podem ser encontradas nas seguintes referências: Gautreaux Jr. e Coates (1955); Leroi et al. (1977); Letcher (1978); Alessi, Fermeglia e Kikic (1986);

Dohnal e Horáková (1991); Landa, Belfer e Locke (1991); Orbey e Sandler (1991); Dallinga, Schiller e Gmehling (1993); Trampe e Eckert (1993); Eckert e Sherman (1996); Sandler (1996); Kojima, Zhang e Hiaki (1997); Asprion, Hasse e Maurer (1998).

2.7. Entalpia de Excesso

As funções termodinâmicas de excesso são definidas como a diferença (positiva ou negativa) entre um valor atual de uma determinada função e o valor correspondente ao de uma mistura ideal na mesma pressão, temperatura e composição (GUGGENHEIM, 1967; GINER et al., 2006). A descrição do comportamento real dos líquidos quando eles são misturados e a extensão com a qual a solução real desvia da idealidade podem ser obtidas pela análise das propriedades de excesso.

Especificamente, a entalpia de excesso, H^E, fornece informações quantitativas sobre a dependência da energia de Gibbs de excesso, g^E, em relação à temperatura como descrito pela equação de Gibbs-Helmholtz (equação 2.58) (GMEHLING, 1993; HORSTMANN e GMEHLING, 2001; POLING, PRAUSNITZ e O'CONNELL, 2001; THIEDE et al., 2010):

$$\left(\frac{\partial \ln \gamma_i}{\partial 1/T}\right)_{P,x} = \frac{H_i^E}{R} \tag{2.58}$$

Esta informação pode, portanto, ser utilizada em conjunto com outros resultados (dados de equilíbrio de fase líquido-vapor - ELV, e equilíbrio de fase líquido-líquido - ELL, coeficiente de atividade à diluição infinita γ^∞ e dados de azeotropia) para ajustar simultaneamente parâmetros confiáveis para os modelos de g^E em função da temperatura

ou os parâmetros de interação de métodos de contribuição de grupos, tais como o modelo UNIFAC Modificado (Dortmund) (GMEHLING, 1993; ABBOTT et al., 1994; LOHMANN e GMEHLING, 1999).

Propriedades de excesso, assim como a entalpia de excesso, também podem refletir as diferenças entre os efeitos energéticos e estruturais de uma solução em relação aos seus componentes quando não misturados (ABBOTT et al., 1994).

No caso dos compostos de sistemas graxos, no entanto, um número limitado de dados de entalpia de excesso estão disponíveis na literatura. Apenas uma publicação (RESA et al., 2002) reporta dados de entalpia de excesso (H^E) medida para óleos vegetais, mas somente para misturas com álcool e à temperatura ambiente (298,15 K), como a maioria dos dados de H^E publicados (GMEHLING, 1993). Isto significa que dados a temperaturas mais elevadas são ainda necessários.

2.8. Referências Bibliográficas

ABBOTT, M. M. et al. A Field Guide to the Excess Functions. **Chem. Eng. Educ.,** v. 28, p. 18-23,77, 1994.

ABRAMS, D. S.; PRAUSNITZ, J. M. Statistical Thermodynamics of Liquid Mixtures: A New Expression for the Excess Gibbs Energy of Partly or Completely Miscible Systems. **AIChE J.,** v. 21, p. 116-128, 1975.

AKISAWA SILVA, L. Y. et al. Determination of the Vapor Pressure of Ethyl Esters by Differential Scanning Calorimetry. **J. Chem. Thermodyn.,** v. 43, p. 943-947, 2011.

AKISAWA SILVA, L. Y. et al. Vapor Liquid Equilibrium of Fatty Acid Ethyl Esters Determined using DSC. **Thermochimica Acta,** v. 512, p. 178-182, 2011.

ALESSI, P.; FERMEGLIA, M.; KIKIC, I. A Differential Static Apparatus for the Investigation of the Infinitely Diluted Region. **Fluid Phase Equilibr.,** v. 29, n. October, p. 249-256, 1986.

_____. Significance of Dilute Regions. **Fluid Phase Equilibr.,** v. 70, p. 239-250, 1991.

ANDERSON, D. A Primer on Oils Processing Technology. In: HUI, Y. H. (Ed.). **Bailey's Industrial Oil and Fat Products**. 5. New York: John Wiley & Sons, v.4, 1996. p.1-61.

ANSOLIN, M. et al. Experimental Data for Liquid Liquid Equilibrium of Fatty Systems with Emphasis on the Distribution of Tocopherols and Tocotrienols. . **Fluid Phase Equilibr.,** v. 338, p. 78-86, 2013.

ANTONIASSI, R.; ESTEVES, W.; MEIRELLES, A. J. A. Pretreatment of Corn Oil for Physical Refining. **J. Am. Oil Chem. Soc.,** v. 75, n. 10, p. 1411-1415, 1998.

ANVISA. **Resolução RDC nº 270, de 22 de setembro de 2005**. ANVISA, A. N. D. V. S.-. Brasília: D.O.U. - Diário Oficial da União 2005.

ASPRION, N.; HASSE, H.; MAURER, G. Limiting Activity Coefficients in Alcohol-Containing Organic Solutions from Headspace Gas Chromatography. **J. Chem. Eng. Data,** v. 43, n. 1, p. 74–80, 1998.

BAROUTIAN, S. et al. Densities of Ethyl Esters Produced from Different Vegetable Oils. **J. Chem. Eng. Data,** v. 53, n. 9, p. 2222-2225, 2008.

BASSO, R. C.; MEIRELLES, A. J. A.; BATISTA, E. A. C. Liquid Liquid Equilibrium of Pseudoternary Systems Containing Glycerol+Ethanol+Ethylic Biodiesel from Crambe Oil (Crambe abyssinica) at T/K=(298.2, 318.2, 338.2) and Thermodynamic Modeling. **Fluid Phase Equilibr.,** v. 333, p. 55-62, 2012.

_____. Densities and Viscosities of Fatty Acid Ethyl Esters and Biodiesels Produced by Ethanolysis from Palm, Canola, and Soybean Oils: Experimental Data and Calculation Methodologies. **Ind. Eng. Chem. Res.,** v. 52, n. 8, p. 2985–2994, 2013.

BASSO, R. C. et al. LLE Experimental Data, Thermodynamic Modeling and Sensitivity Analysis in the Ethyl Biodiesel from Macauba Pulp Oil Settling Step. **Bioresource Technology,** v. 131, p. 468-475, 2013.

BERA, D. et al. A Novel Azeotropic Mixture Solvent for Solvent Extraction of Edible Oils. **Agricultural Engineering International: the CIGR Ejournal,** v. VIII, n. April, p. Manuscript FP 06 005, 2006.

BOCKISCH, M. **Fats and Oils Handbook**. Champaign, Illinois: AOCS Press, 1998. ISBN 0-935315-82-9.

BONDI, A. **Physical Properties of Molecular Crystals, Liquids, and Glasses**. New York, N.Y.: J. Wiley, 1968. 502.

BRASIL. **Estabelece padrão de identidade e qualidade para óleos e gorduras comestíveis, destinados à alimentação humana.** Decreto-lei no 986 de 21 de outubro de 1969. ALIMENTOS, A. C. D. L. D. São Paulo: ABIA. Resolução CNNPA no22/77 1969.

BROCKMANN, R.; DEMMERING, G.; KREUTZER, U. Fatty Acids. In: KAUDY, L., ROUNSAVILLE, J.F., SCHULZ, A. (Ed.). **Ullmann's Encyclopedia of Industrial Chemistry**. Weinheim: Verlog Chemie, v.A10, 1987. p.245-275.

BURKE, M. R. **Soaps**. Bailey's Industrial Oil and Fat Products. SHAHIDI, F. Hoboken, New Jersey: John Wiley & Sons, Inc. 6**:** 103-136 p. 2005.

CARARETO, N. D. D. et al. Flash Points of Mixtures Containing Ethyl Esters or Ethylic Biodiesel and Ethanol. **Fuel (Guildford),** v. 96, p. 319-326, 2012.

CARARETO, N. D. D. et al. The Solid Liquid Phase Diagrams of Binary Mixtures of even Saturated Fatty Alcohols. **Fluid Phase Equilibr.,** v. 303, p. 191-198, 2011.

CERIANI, R.; COSTA, A. M.; MEIRELLES, A. J. A. Optimization of the Physical Refining of Sunflower Oil Concerning the Final Contents of trans-Fatty Acids. **Ind. Eng. Chem. Res.,** v. 47, p. 681-692, 2008.

CERIANI, R. et al. Group Contribution Model for Predicting Viscosity of Fatty Compounds. **J. Chem. Eng. Data,** v. 52, p. 965-972, 2007.

CERIANI, R.; MEIRELLES, A. J. A. Predicting Vapor–Liquid Equilibria of Fatty Systems. **Fluid Phase Equilibr.,** v. 215, p. 227–236, 2004a.

_____. Simulation of Batch Physical Refining and Deodorization Processes. **J. Am. Oil Chem. Soc.,** v. 81, p. 305–312, 2004b.

_____. Simulation of Continuous Deodorizers: Effects on Product Streams. **J. Am. Oil Chem. Soc.,** v. 81, p. 1059-1069, 2004c.

_____. Modeling Vaporization Efficiency for Steam Refining and Deodorization. **Ind. Eng. Chem. Res.,** v. 44, p. 8377-8386, 2005.

CERIANI, R.; MEIRELLES, A. J. A. Simulation of Continuous Physical Refiners for Edible Oil Deacidification. **J. Food Eng.,** v. 76, p. 261-271, 2006.

CERIANI, R.; MEIRELLES, A. J. A. Formation of Trans PUFA during Deodorization of Canola Oil: A Study through Computational Simulation. **Chem. Eng. Process.,** v. 46, p. 375–385, 2007.

CERIANI, R.; MEIRELLES, A. J. A.; GANI, R. Simulation of Thin-Film Deodorizers in Palm Oil Refining. **J. Food Proc. Eng.,** v. 33, p. 208-225, 2010.

CERIANI, R. et al. Densities and Viscosities of Vegetable Oils of Nutritional Value. **J. Chem. Eng. Data,** v. 53, p. 1846–1853, 2008.

CHIYODA, C. et al. Liquid Liquid Equilibria for Systems composed of Refined Soybean Oil, Free Fatty Acids, Ethanol, and Water at different Temperatures. **Fluid Phase Equilibr.,** v. 299, p. 141-147, 2010.

COSTA, M. C. et al. Phase Diagrams of Mixtures of Ethyl Palmitate with Fatty Acid Ethyl Esters. **Fuel (Guildford),** v. 91, p. 177-181, 2012.

COSTA, M. C. et al. Low-Temperature Behavior of Biodiesel: Solid Liquid Phase Diagrams of Binary Mixtures Composed of Fatty Acid Methyl Esters. **Energy & Fuels,** v. 25, p. 3244-3250, 2011.

COSTA, M. C. et al. Solid-Liquid Equilibrium of Saturated Fatty Acids + Triacylglycerols. **J. Chem. Eng. Data,** v. 55, p. 974-977, 2010.

COSTA, M. C. et al. Solid Liquid Equilibrium of Binary Mixtures Containing Fatty Acids and Triacylglycerols. **J. Chem. Eng. Data,** v. 56, p. 3277-3284, 2011.

COSTA, M. C. et al. Solid-Liquid Equilibrium of Tristearin with Refined Rice Bran and Palm Oils. **J. Chem. Eng. Data,** v. 55, p. 5078-5082, 2010.

CUEVAS, M. S. et al. Vegetable Oils Deacidification by Solvent Extraction: Liquid-Liquid Equilibrium Data for Systems Containing Sunflower Seed Oil at 298.2 K. **J. Chem. Eng. Data,** v. 55, p. 3859-3862, 2010.

DALLINGA, L.; SCHILLER, M.; GMEHLING, J. Measurement of Activity Coefficient at Infinite Dilution using Differential Ebulliometry and Non-Steady-State Gas-Liquid-Chromatography **J. Chem. Eng. Data,** v. 38, n. 1, p. 147-155, 1993.

DDB. **Dortmund Data Bank Dortmund Data Bank Software & Separation Technology** Oldenburg: DDBST GmbH 2011.

DE GREYT, W.; KELLENS, M. **Deodorization**. Bailey's Industrial Oil and Fat Products. SHAHIDI, F. Hoboken, New Jersey: John Wiley & Sons, Inc. 5**:** 341-383 p. 2005.

DE LA FUENTE B., J. C. et al. Phase Equilibria in Mixtures of Triglycerides with Low-Molecular Weight Alkanes. **Fluid Phase Equilibr.,** v. 128 p. 221 - 227, 1997.

DEMARCO, A. Extracción por Solvente. In: J. M. BLOCK, D. B.-A. (Ed.). **Temas Selectos en Aceites y Grasas**. São Paulo: Edgard Blücher, 2009. p.67-95.

DIPPR. **Design Institute for Physical Properties Data Bank** AIChE [2005, 2008, 2009, 2010].

DOHNAL, V.; HORÁKOVÁ, I. A New Variant of the Rayleigh Distillation Method for the Determination of Limiting Activity Coefficients. **Fluid Phase Equilibr.,** v. 68, n. Nov, p. 173–185, 1991.

ECKERT, C. A.; SHERMAN, S. R. Measurement and Prediction of Limiting Activity Coefficients. **Fluid Phase Equilibr.,** v. 116, n. 1-2, p. 333–342, 1996.

ENCINAR, J. M. et al. Biodiesel Fuels from Vegetables Oils: Transesterification of *Cynara cardunculus* L. Oils with Ethanol. **Energ. Fuel,** v. 16, n. 2, p. 443-450, 2002.

ENCINAR, J. M.; GONZÁLEZ, J. F.; RODRIGUEZ-REINARES, A. Ethanolysis of Used Frying Oil. Biodiesel Preparation and Characterization. **Fuel Process. Technol.,** v. 88, p. 513-522, 2007.

ERHAN, S. Z. **Vegetable Oils as Lubricants, Hydraulic Fluids, and Inks**. Bailey's Industrial Oil and Fat Products. SHAHIDI, F. Hoboken, New Jersey: John Wiley & Sons, Inc. 6**:** 259-278 p. 2005.

FALLEIRO, R. M. M. et al. Vapor Pressure Data for Fatty Acids Obtained using an Adaptation of the DSC Technique. **Thermochimica Acta,** v. 547, p. 6-12, 2012.

FALLEIRO, R. M. M.; MEIRELLES, A. J. A.; KRÄHENBÜHL, M. A. Experimental Determination of the (Vapor+Liquid) Equilibrium Data of Binary Mixtures of Fatty Acids by Differential Scanning Calorimetry. **J. Chem. Thermodyn.,** v. 42, p. 70-77, 2010.

FDA. Food Additive Status List. **Investigations Operations Manual (IOM) - Appendix A**, http://www.fda.gov/Food/IngredientsPackagingLabeling/FoodAdditivesIngredients/ucm091048.htm#ftnH, 2011. Acesso em: 05/set/2013.

FOLLEGATTI-ROMERO, L. A. et al. Liquid-Liquid .Equilibrium for Ternary Systems Containing Ethyl Esters, Anhydrous Ethanol and Water at 298.15, 313.15, and 333.15 K. **Ind. Eng. Chem. Res.,** v. 49, p. 12613-12619, 2010.

FOLLEGATTI-ROMERO, L. A. et al. Liquid Liquid Equilibria for Ethyl Esters+Ethanol+Water Systems: Experimental Measurements and CPA EoS Modeling. **Fuel (Guildford),** v. 96, p. 327-334, 2012.

FOLLEGATTI-ROMERO, L. A. et al. Liquid Liquid Equilibria for Ternary Systems Containing Ethyl Esters, Ethanol and Glycerol at 323.15 and 353.15K. **Fuel (Guildford),** v. 94, p. 386-394, 2012.

FORNARI, T.; BOTTINI, S. B.; BRIGNOLE, E. A. Application of UNIFAC to Vegetable Oil-Alkane Mixtures. **J. Am. Oil Chem. Soc.,** v. 71, n. 4, p. 391-395, 1994. ISSN 0003-021X. Disponível em: < http://dx.doi.org/10.1007/BF02540519 >.

FREDENSLUND, A.; GMEHLING, J.; RASMUSSEN, P. **Vapor-Liquid Equilibria Using UNIFAC**. Amsterdam: Elsevier, 1977. 380.

FREDENSLUND, A.; JONES, R. L.; PRAUSNITZ, J. M. Group-Contribution Estimation of Activity Coefficients in Nonideal Liquid Mixtures. **AIChE J.,** v. 21, n. 6, p. 1086-1099, 1975.

FREITAS, S. P.; LAGO, R. C. A. Equilibrium Data for the Extraction of Coffee and Sunflower Oils with Ethanol. **Braz. J. Food Technol.,** v. 10, p. 220-224, 2007.

FREITAS, S. P.; MONTEIRO, P. L.; LAGO, R. C. A. Extração do Óleo da Borra de Café Solúvel com Etanol Comercial. 1o. Simpósio de Pesquisa dos Cafés do Brasil, 2000, Poços de Caldas. p.740-743.

GAUTREAUX JR., M. F.; COATES, J. Activity Coefficients at Infinite Dilution. **AIChE J.,** v. 1, n. 4, p. 496–500, 1955.

GERVAJIO, G. C. **Industrial and Nonedible Products from Oils and Fats**. Bailey's Industrial Oil and Fat Products. SHAHIDI, F. Hoboken, New Jersey: John Wiley & Sons, Inc. 6**:** 1-56 p. 2005.

GINER, B. et al. Study of Weak Molecular Interactions through Thermodynamic Mixing Properties. **J. Phys. Chem. B,** v. 110, n. 35, p. 17683-17690, 2006.

GMEHLING, J. Excess Enthalpies for 1, 1, 1 - Trichloroethane with Alkanes, Ketones, and Esters. **J. Chem. Eng. Data,** v. 38, n. 1, p. 143-146, 1993.

GMEHLING, J. et al. **Chemical Thermodynamics for Process Simulation**. 1st. Weinheim: Wiley-VCH, 2012. 735.

GMEHLING, J.; LI, J.; SCHILLER, M. A modified UNIFAC Model. 2. Present Parameter Matrix and Results for different Thermodynamic Properties. **Ind. Eng. Chem. Res.,** v. 32, n. 1, p. 178-193, 1993. ISSN 0888-5885. Disponível em: < http://dx.doi.org/10.1021/ie00013a024 >.

GMEHLING, J.; ONKEN, J. Calculations of Activity Coefficient from Structural-groups Contribution. **Int. Chem. Eng.,** v. 19, n. 4, p. 566-570, 1979.

GONÇALVES, C. B. et al. Viscosities of Fatty Mixtures: Experimental Data and Prediction. **J. Chem. Eng. Data,** v. 52, p. 2000-2006, 2007.

GONÇALVES, C. B.; PESSÔA FILHO, P. A.; MEIRELLES, A. J. A. Partition of Nutraceutical Compounds in Deacidification of Palm oil by Solvent Extraction. **J. Food Eng.,** v. 81, n. 1, p. 21-27, 2007.

GRUBER, D.; LANGENHEIM, D.; GMEHLING, J. Measurement of Activity Coefficients at Infinite Dilution using Gas-Liquid Chromatography. 6. Results for Systems Exhibiting Gas-Liquid Interface Adsorption with 1-Octanol. **J. Chem. Eng. Data,** v. 42, n. 5, p. 882-885, 1997.

GUGGENHEIM, E. A. **Thermodynamics : an Advanced Treatment for Chemists and Physicists** 5th Amsterdam: North-Holland, 1967. 390.

GUNSTONE, F. D. **Vegetable Oils**. Bailey's Industrial Oil and Fat Products SHAHIDI, F. Hoboken, New Jersey: John Wiley & Sons. 1**:** 606 p. 2005.

GUPTA, M. K. **Edible Oil and Fat Products: Products and Applications**. Bailey's Industrial Oil and Fat Products. SHAHIDI, F. Hoboken, New Jersey: John Wiley & Sons, Inc. 4**:** 1-31 p. 2005.

HAAS, M. J. et al. A Process Model to Estimate Biodiesel Production Costs. **Bioresource Technol.,** v. 97, p. 671–678, 2006

HANSEN, H. K. et al. Vapor-Liquid Equilibria by UNIFAC Group Contribution 5. Revision and Extension. **Ind. Eng. Chem. Res.,** v. 30, n. 10, p. 2352-2355, 1991.

HÉNON, G. et al. Deodorization of Vegetable Oils. Part I: Modelling the Geometrical Isomerization of Polyunsaturated Fatty Acids. **J Am Oil Chem Soc,** v. 76, n. 1, p. 73-81, 1999.

HERNANDEZ, E. **Pharmaceutical and Cosmetic Use of Lipids**. Bailey's Industrial Oil and Fat Products. SHAHIDI, F. Hoboken, New Jersey: John Wiley & Sons, Inc. 6**:** 391-411 p. 2005.

HORSTMANN, S.; GMEHLING, J. Vapor-Liquid Equilibria and Excess Enthalpy Data for the Binary System Propionic Aldehyde + 2-Methyl-2-butanol at 333.15 K. **J. Chem. Eng. Data,** v. 46, n. 6, p. 1487-1489, 2001.

HRON, R. J.; KOLTUN, S. P. An Aqueous Ethanol Extration Process for Cottonseed Oil. **J. Am. Oil Chem. Soc.,** v. 61, n. 9, p. 1457-1460, 1984.

HRON, R. J.; KOLTUN, S. P.; GRACI, A. V. Biorenewable Solvents for Vegetable Oil Extraction. **J. Am. Oil Chem. Soc.,** v. 59, n. 9, p. 674-684, 1982.

JOHNSON, L. A. Recovery of Fats and Oils from Plant and Animal Sources. In: R. D. O'BRIEN, W. E. F., P. J. WAN (Ed.). **Introduction to Fats and Oils Technology**. 2nd. Champaign, Illinois: AOCS Press, 2000. p.20-48.

KEMPER, T. G. **Oil Extraction**. Bailey's Industrial Oil and Fat Products. SHAHIDI, F. Hoboken, New Jersey: John Wiley & Sons, Inc. 5**:** 572 p. 2005.

KOJIMA, K.; TOCHIGI, K. **Prediction of Vapor-Liquid Equilibria by the ASOG Method**. Tokio: Kodansha-Elsevier, 1979.

KOJIMA, K.; ZHANG, S.; HIAKI, T. Measuring Methods of Infinite Dilution Activity Coefficients and a Database for Systems including Water. **Fluid Phase Equilibr.,** v. 131, n. 1-2, p. 145-179, 1997.

KRONICK, P.; KAMATH, Y. K. **Leather and Textile Uses of Fats and Oils**. Bailey's Industrial Oil and Fat Products. SHAHIDI, F. Hoboken, New Jersey: John Wiley & Sons, Inc. 6**:** 353-369 p. 2005.

KRUMMEN, M. **Experimentelle Untersuchung des Aktivitätskoeffizienten bei unendlicher Verdünnung in ausgewählten Lösungsmitteln und Lösungsmittelgemischen als Grundlage für die Synthese thermischer Trennprozesse**. 2002. 198 Thesis (Doktors der Naturwissenschaften). Fachbereich Chemie, Carl von Ossietzky Universität Oldenburg, Oldenburg.

LANDA, I.; BELFER, A. J.; LOCKE, D. C. Measurement of Limiting Activity Coefficients using non-Steady-State Gas Chromatography. **Ind. Eng. Chem. Res.,** v. 30, n. 8, p. 1900–1906, 1991.

LARSEN, B. L.; RASMUSSEN, P.; FREDENSLUND, A. A Modified UNIFAC Group-Contribution Model for Prediction of Phase Equilibria and Heats of Mixing. **Ind. Eng. Chem. Res.,** v. 26, p. 2274-2286, 1987a.

_____. A Modified UNIFAC Group-Contribution Model for Prediction of Phase Equilibria and Heats of Mixing. **Ind. Eng. Chem. Res.,** v. 26, p. 2274-2286, 1987b.

LEROI, J.-C. et al. Accurate Measurement of Activity Coefficients at Infinite Dilution by Inert Gas Stripping and Gas Chromatography. **Ind. Eng. Chem. Proc. DD,** v. 16, n. 1, p. 139-144, 1977.

LETCHER, T. M. Activity Coefficients at Infinite Dilution from Gas-Liquid Chromatography. In: MCGLASHAN, M. L. (Ed.). **Chemical Thermodynamics**. London: The Chemical Society, v.2, 1978. cap. 2, p.46-70.

LIN, K. F. **Paints, Varnishes, and Related Products**. Bailey's Industrial Oil and Fat Products. SHAHIDI, F. Hoboken, New Jersey: John Wiley & Sons, Inc. 6**:** 307-351 p. 2005.

LOHMANN, J.; GMEHLING, J. Bedeutung von Stützstellen bei tiefen und hohen Temperaturen für die Anpassung temperaturabhängiger Modified UNIFAC (Dortmund)-Parameter. **Chem. Tech.,** v. 51, n. 4, p. 184-190, 1999.

LUSAS, E. W.; WATKINS, L. R.; KOSEOGLU, S. S. Isopropyl Alcohol to be Tested as Solvent. **Inform.,** v. 2, p. 970 – 973, 1991.

LYNN JR., J. L. **Detergents and Detergency**. Bailey's Industrial Oil and Fat Products. SHAHIDI, F. Hoboken, New Jersey: John Wiley & Sons, Inc. 6**:** 137-189 p. 2005.

MA, F.; HANNA, M. A. Biodiesel Production: a Review. **Bioresource Technol.,** v. 70, p. 1-15, 1999.

MARCHETTI, J. M.; MIGUEL, V. U.; ERRAZU, A. F. Possible Methods for Biodiesel Production. **Renew Sust. Energ. Rev.,** v. 11, p. 1300-1311, 2007.

MATTIL, K. F. Deodorization. In: K.F. MATTIL, F. A. N., A.J. STIRTON (Ed.). **Bailey's Industrial Oil and Fat Products**. New York: John Wiley & Sons, 1964. p.897-930.

MAZA, A.; ORMSBEE, R. A.; STRECKER, L. R. Effects of Deodorization and Steam.Refining Parameters on Finished Oil Quality **J. Am. Oil Chem. Soc.,** v. 69, n. 10, p. 1003-1008, 1992.

MCMILLAN, W. G.; MAYER, J. E. The Statistical Thermodynamics of Multicomponent Systems. **J. Chem. Phys.,** v. 13, p. 276-305, 1945.

MEHER, L. C.; SAGAR, D. V.; NAIK, S. N. Technical Aspects of Biodiesel Production by Transesterifications: a Review. **Renew. Sust. Energ. Rev.,** v. 10, 2006.

MILLIGAN, E. D.; TANDY, D. C. Distillation and Solvent Recovery. **J. Am. Oil Chem. Soc.,** v. 51, p. 347-350, 1974.

NARINE, S. S.; KONG, X. **Vegetable Oils in Production of Polymers and Plastics**. Bailey's Industrial Oil and Fat Products. SHAHIDI, F. Hoboken, New Jersey: John Wiley & Sons, Inc. 6**:** 279-306 p. 2005.

O'BRIEN, R. D. **Fats and Oils: Formulating and Processing for Applications.** Lancaster: Technomic., 1998. 694.

_____. Fats And Oils Processing. In: R. D. O'BRIEN, W. E. F., AND P. J. WAN (Ed.). **Introduction to Fats and Oils Technology**. 2nd. Illinois: A.O.C.S. Press, Champaign, 2000a. p.90-107.

_____. Introduction to Fats and Oils Technology. In: R. D. O'BRIEN, W. E. F., AND P. J. WAN (Ed.). **Fats And Oils: An Overview**. Illinois: AOCS Press: Champaign, 2000b. p.1-19.

OLIVEIRA, M. B. et al. Phase Equilibria of Ester + Alcohol Systems and their description with the Cubic-Plus-Association Equation of State. **Ind. Eng. Chem. Res. ,** v. 49, n. 7, p. 3452-3458, 2010.

ORBEY, H.; SANDLER, S. I. Relative Measurements of Activity Coefficients at Infinite Dilution by Gas Chromatography. **Ind. Eng. Chem. Res.,** v. 30, n. 8, p. 2006–2011, 1991.

PARAÍSO, P. R. **Modelagem e Análise do Processo de Obtenção de Óleo de Soja.** . 2001. 200 Tese de doutorado (Doutorado). Faculdade de Engenharia Química, UNICAMP, Campinas.

PARAÍSO, P. R.; ANDRADE, C. M. G.; ZEMP, R. J. Destilação da Miscela II: Modelagem e Simulação do Stripping do Hexano. **Ciênc Tecnol Aliment,** v. 25, n. 1, p. 37-44, 2005.

PETRAUSKAITÈ, V.; DE GREYT, W. F.; KELLENS, M. J. Physical Refining of Coconut Oil: Effect of Crude Oil Quality and Deodorization Conditions on Neutral Oil Loss. **J. Am. Oil Chem. Soc.,** v. 77, n. 6, p. 581-586, 2000.

PINA, C. G.; MEIRELLES, A. J. A. Deacidification of Corn Oil by Solvent Extraction in a Perforated Totating Disc Column. **J. Am. Oil Chem. Soc.,** v. 77, p. 553-559, 2000.

PITZER, K. S.; CURL JR., R. F. The Volumetric and Thermodynamic Properties of Fluids. III. Empirical Equation for the Second Virial Coefficient. **J. Am. Chem. Soc.,** v. 79, p. 2369 - 2370, 1957.

POLING, B. E.; PRAUSNITZ, J. M.; O'CONNELL, J. P. **Properties of Gases and Liquids**. 5th. McGraw-Hill, 2001.

PRAUSNITZ, J. M.; LICHTENTHALER, R. N.; GOMES DE AZEVEDO, E. **Molecular Thermodynamics of Fluid-Phase Equilibria**. 3rd New Jersey: Prentice Hall PTR, 1999. 860.

RAO, R. K. et al. Alcoholic Extraction of Vegetable Oils. I. Solubilities of Cottonseed, Peanut, Sesame, and Soybean Oils in Aqueous Ethanol. **J. Am. Oil Chem. Soc.,** v. 32, n. 7, p. 420-423, 1955.

REGITANO-D'ARCE, M. A. B. **Ensaios de Extração de Óleo de Girassol (Helianthus annuus L.) com Álcool Etílico**. 1985. 110 Dissertation (Master Science). ESALQ Universidade de São Paulo, Piracicaba.

_____. **Extração de Óleo de Girassol com Etanol: Cinética, Ácido Clorogênico, Material Insaponificável**. 1991. 145 Thesis (Doctor). ESALQ, Universidade de São Paulo, Piracicaba.

RENON, H.; PRAUSNITZ, J. M. Local Compositions in Thermodynamic Excess Functions for Liquids Mixtures. **AIChE J.,** v. 14, n. 1, p. 135-144, 1968.

RESA, J. M. et al. Enthalpies of Mixing, Heat Capacities, and Viscosities of Alcohol (C1-C4) + Olive Oil Mixtures at 298.15 K. **J. Food Eng.,** v. 52, p. 113-118, 2002.

RITTNER, H. Extraction of Vegetable Oils with Ethyl Alcohol. **Oléagineux,** v. 47, n. jan., p. 29-42, 1992.

ROBUSTILLO, M. D. et al. Solid Liquid Equilibrium in Ternary Mixtures of Ethyl Oleate, Ethyl Laurate and Ethyl Palmitate. **Fluid Phase Equilibr.,** v. 339, p. 58-66, 2013.

RODRIGUES, C. E. C.; ONOYAMA, M. M.; MEIRELLES, A. J. A. Optimization of the Rice Bran Oil Deacidification Process by Liquid-liquid Extraction. **J. Food Eng.,** v. 73, n. 4, p. 370-378, 2006.

SAMPAIO, K. A. et al. Steam Deacidification of Palm Oil. **Food Bioprod. Process.,** v. 89, p. 383-390, 2011.

SANAIOTTI, G. et al. Densities, Viscosities, Interfacial Tensions, and Liquid-Liquid Equilibrium Data for Systems Composed of Soybean Oil + Commercial Linoleic Acid + Ethanol + Water at 298.2 K. . **J. Chem. Eng. Data,** v. 55, n. 11, p. 5237–5245, 2010.

SANDLER, S. I. Infinite Dilution Activity Coefficients in Chemical, Environmental and Biochemical Engineering. **Fluid Phase Equilibr.,** v. 116, p. 343-353, 1996.

_____. **Chemical and Engineering Thermodynamics.** New York: John Wiley & Sons, 1999. 772.

SCHWARZBACH, J. Aspectos de Segurança Relacionados ao Hexano na Extração de Óleos Vegetais. **Óleos e Grãos,** v. mar-abr, p. 27-34, 1997.

SCRIMGEOUR, C. **Chemistry of Fatty Acids**. Bailey's Industrial Oil and Fat Products. SHAHIDI, F. Hoboken, New Jersey: John Wiley & Sons. 1**:** 606 p. 2005.

SILVA, A. E. et al. Liquid-Liquid Equilibrium Data for Systems Containing Palm Oil Fractions + Fatty Acids + Ethanol + Water. **J. Chem. Eng. Data,** v. 56, p. 1892-1898, 2011.

SILVA, C. A. S. et al. Liquid−Liquid Equilibrium Data for Systems Containing Jatropha curcas Oil + Oleic Acid + Anhydrous Ethanol + Water at (288.15 to 318.15) K **J. Chem. Eng. Data,** v. 55, p. 2416-2423, 2010.

SMITH, J. M.; VAN NESS, H. C.; ABBOTT, M. M. **Introdução à Termodinâmica da Engenharia Química.** Rio de Janeiro: LTC, 2000. 697.

SRIVASTAVA, A.; PRASAD, R. Triglycerides-based Diesel Fuels. **Renew. Sust. Energ. Rev.,** v. 4, p. 111-133, 2000.

SWERN, D. Bailey's Industrial Oil and Fat Products. In: SWERN, D. (Ed.). **Bailey's Industrial Oil and Fat Products**. 3rd. New York: Interscience Publisher, v.1, 1964. cap. Physical Properties of Fats and Fatty Acids, p.97-144. (Bailey's Industrial Oil and Fat Products).

TANDY, D. C.; MCPHERSON, W. J. Physical Refining of Edible Oil. **J. Am. Oil Chem. Soc.,** v. 61, n. 7, p. 1253-1258, 1984.

THIEDE, S. et al. Experimental Determination of Vapor-Liquid Equilibria and Excess Enthalpy Data for the Binary System 2-Methyl-1-butanol + 3-Methyl-1-butanol as a Test Mixture for Distillation Columns. **Ind. Eng. Chem. Res.,** v. 49, n. 4, p. 1844–1847, 2010.

TRAMPE, D. B.; ECKERT, C. A. A Dew Point Technique for Limiting Activity Coefficients in Nonionic Solutions. **AIChE J.,** v. 39, n. 6, p. 1045–1050, 1993.

TRUJILLO-QUIJANO, J. A. Óleo de Palma: Um Produto Natural. **Revista Óleos & Grãos**, n. Mar/Abr, p. 19-23, 1997.

TSONOPOULOS, C. An Empirical Correlation of Second ViriaI Coefficients. **AIChE J.,** v. 20, n. 2, p. 263 - 272, 1974.

EUROPEAN UNION. **Extraction Solvents which may be used during the Processing of Raw Materials, of Foodstuffs, of Food Components or of Food Ingredients**. Directive 2009/32/EC. UNION, E. P. A. O. T. C. O. T. E. Strasbourg: Official Journal of the European Union**:** L 141/ 3 - L 141/11 p. 2009.

WALAS, S. M. **Chemical Process Equipament Selection and Design**. Washington: Butterworth-Hunemann, 1990. 754.

WAN, P. J. Properties of Fats and Oils. In: R. D. O'BRIEN, W. E. F., P. J. WAN (Ed.). **Introduction to Fats and Oils Technology**. 2nd. Illinois: A.O.C.S. Press, Champaign, 2000. p.20-48.

WEIDLICH, U.; GMEHLING, J. A Modified UNIFAC Model. 1. Prediction of VLE, h_E and γ^{∞} **Ind. Eng. Chem. Res.,** v. 26, n. 7, p. 1372-1381, 1987.

WILLIAMS, M. A. **Recovery of Oils and Fats from Oilseeds and Fatty Materials**. Bailey's Industrial Oil and Fat Products. SHAHIDI, F. Hoboken, New Jersey: John Wiley & Sons, Inc. 5**:** 572 p. 2005.

WILLIAMS, M. A.; HRON, R. J. Obtaining Oils and Fats from Source Materials. In: HUI, Y. H. (Ed.). **Bailey's Industrial Oil and Fat Products.** 5th. New York: John Wiley & Sons, v.4, 1996. p.61-157.

WILSON, G. M. Vapor-Liquid Equilibrium. XI. A New Expression for the Excess Free Energy of Mixing. **J. Am. Chem. Soc.,** v. 86, p. 127-130, 1964.

XU, X. et al. Pilot Batch Production of Specific-Structured Lipids by Lipase-Catalyzed Interesterification: Preliminary Study on Incorporation and Acyl Migration. **J. Am. Oil Chem. Soc.,** v. 75, n. 2, p. 301-308, 1998.

XU, X. et al. Purification and Deodorization of Structured Lipids by Short Path Distillation. **Eur. J. Lipid Sci. Technol.,** v. 104, p. 745-755, 2002.

XU, X.; SKANDS, A.; ADLER-NISSEN, J. Purification of Specific Structured Lipids by Distillation: Effects on Acyl Migration. **J. Am. Oil Chem. Soc.,** v. 78, n. 7, p. 715-718, 2001.

CAPÍTULO 3: ACTIVITY COEFFICIENT AT INFINITE DILUTION MEASUREMENTS FOR ORGANICS SOLUTES (POLAR AND NON-POLAR) IN FATTY COMPOUNDS: SATURATED FATTY ACIDS

Artigo publicado na revista *The Journal of Chemical Thermodynamics*,

vol. 55, ano: 2012, p. 42-49.

Activity Coefficient at Infinite Dilution Measurements for Organic Solutes (polar and non-polar) in Fatty Compounds: Saturated Fatty Acids.

Patrícia C. Belting[a,b,1], Jürgen Rarey[a*], Jürgen Gmehling[a], Roberta Ceriani[c], Osvaldo Chiavone-Filho[d], Antonio J. A. Meirelles[b]

[a] *Carl von Ossietzky Universität Oldenburg, Technische Chemie (FK V), D-26111 Oldenburg, Federal Republic of Germany*

[b] *Food Engineering Department, Faculty of Food Engineering, State University of Campinas, Av. Monteiro Lobato 50, Cidade Universitária Zeferino Vaz, 13083-970, Campinas-SP, Brazil*

[c] *Faculty of Chemical Engineering, State University of Campinas, Av. Albert Einstein 500, Cidade Universitária Zeferino Vaz, 13083-852, Campinas-SP, Brazil*

[d] *Chemical Engineering Department, Federal University of Rio Grande do Norte, Av. Senador Salgado Filho S/N, 59066-800, Natal-RN, Brazil*

[1 a] *Present address,* [b] *Permanent address*

Abstract

The activity coefficients at infinite dilution , γ_{13}^{∞} (the subscript 1 and 3 correspond to solute and solvent, respectively), for 21 solutes, including alkane, cycloalkane, alkene, aromatic compounds, alcohol, ester, ketone and halogenated hydrocarbons, in four solvents, that are the saturated fatty acids: capric (decanoic) acid, lauric (dodecanoic) acid, myristic (tetradecanoic) acid and palmitic (hexadecanoic) acid, were determined by gas-liquid chromatography at temperatures from 314.10 K to 358.33 K. Comparison with previously published for selected solutes in palmitic (hexadecanoic) acid were also performed. The

values of the partial molar excess Gibbs energy, ΔG_{13}^{∞} , enthalpy, ΔH_{13}^{∞}, and entropy, ΔS_{13}^{∞}, at infinite dilution were calculated from experimental γ_{13}^{∞} values obtained over the temperature range. Results obtained in this work allow a more accurate description of the real behavior of fatty systems.

Keywords: Capric acid; Lauric acid; Myristic acid; Palmitic acid; Limiting activity coefficient; gas-liquid chromatography method.

3.1. Introduction

Fatty acids (FA) are monoacids (general formula for saturated fatty acids: $\mathrm{C_nH_{(2n+1)}COOH}$) which are found in nature in lipids (mainly animal and vegetable fats and oils). They are present, most of the times, combined with glycerol molecules, forming the triacylglycerols (TAGs) and partial- acylglycerols or in free form as free fatty acids (FFAs) [1; 2]. As aliphatic compounds, the fatty acids can be saturated or unsaturated and vary in carbon chain length [1]. Like vegetable oils and others fatty compounds, fatty acids (FA) have very low vapor pressure [3].

Fatty acids are major constituents of fatty systems which are involved in the extraction and refining of edible oils and in the manufacturing of biodiesel and partial glycerides [4-6]. All these processes employ several separation stages, for which thermodynamic equilibrium information is essential during the design and operation of the equipment or for modeling the process via computer simulation, especially because these processes usually

involve multicomponent mixtures [3; 7; 8]. Our research group has provided several studies involving phase equilibria of mixtures containing fatty compounds [3; 7-17].

In case of edible oil processes, the equilibrium relationships are of great importance in the following stages: extraction of vegetable oils from oilseeds using solvents (traditionally hexane-rich petroleum fractions), especially the solvent recovery process [18], and refining steps like deacidification (mainly the physical process) [12] and deodorization [19]. In biodiesel production, the phase equilibrium is required for purification steps of biofuel and for excess alcohol recovery [5; 6; 20].

The activity coefficient at infinite dilution (limiting activity coefficient), γ_{13}^{∞}, represents an important thermodynamic property, both for the development of liquid theories and for the reliable design of thermal separation processes [21-23]. Particularly, it is routinely applied in solvent pre-screening for separation process which involves (vapor + liquid) equilibrium, and (liquid + liquid) equilibrium [24-26].

There are several methods to determine the activity coefficient at infinite dilution. The most important in case of volatile solutes and less or non-volatile solvents are:

- the retention time method (gas-liquid chromatography, GLC) [27],
- the dynamic method (ebulliometry) [28; 29],
- the static method [30],
- the dilutor technique [31].

GLC is the most often reported technique and is being employed in this work.

In this work, we report measurements of activity coefficients at infinite dilution, γ_{13}^{∞}, for 21 solutes (alkane, cycloalkane, alkene, aromatic compounds, alcohol, ester, ketone and halogenated hydrocarbons) in four saturated fatty acids:

- capric (decanoic) acid,
- lauric (dodecanoic) acid,
- myristic (tetradecanoic) acid,
- palmitic (hexadecanoic) acid.

The values of γ_{13}^{∞} were determined at temperatures from (314.10 to 358.33) K. Experimental γ_{13}^{∞} were used to calculate the values of partial molar excess Gibbs energy, ΔG_{13}^{∞}, enthalpy, ΔH_{13}^{∞}, and entropy, ΔS_{13}^{∞}, at infinite dilution.

3.2. Experimental

3.2.1 Materials

The list of fatty acids (solvents), their purity and the suppliers are shown in Table 3.1. The solvents were not subjected to further purification. The solutes had mass fraction purities > 99% and were used without further purification because the GLC technique separates any impurities on the column. Chromosorb P-AW-DMCS 60/80 mesh, supplied by CS-Chromatographie Service GmbH (Germany), was used as solid support material.

TABLE 3.1. Information about the investigated solvents.

Solvent	**Purity (GC) / Mass fraction**	**Supplier**
Capric acid	> 0.99	Lancaster Synthesis
Lauric acid	> 0.99	Fluka
Myristic acid	> 0.995	Fluka
Palmitic acid	> 0.99	Sigma

The structures of the saturated fatty acids used in this work are presented in Figure 3.1.

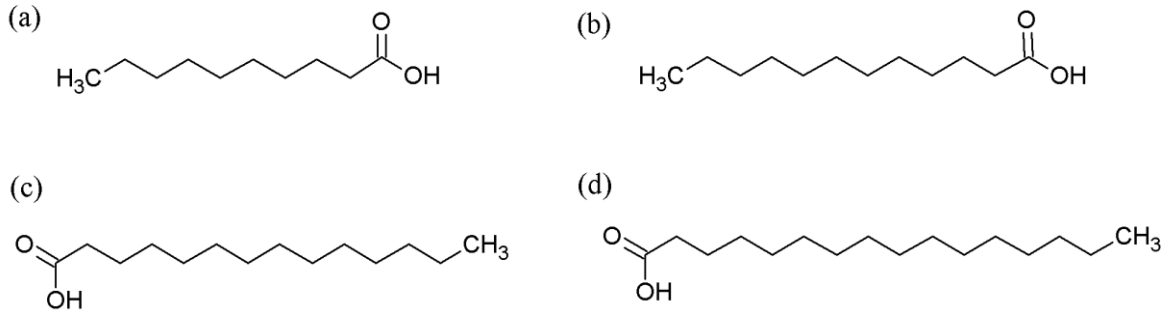

FIGURE 3.1. Structure of the saturated fatty acids: a) Capric acid; b) Lauric acid; c) Myristic acid and d) Palmitic acid.

3.2.2. Apparatus and experimental procedure

The measurements were carried out with a homemade gas-liquid chromatograph whose description is presented in a previous paper [21]. The equipment follows the same principle as presented by Letcher [22]. In our case, there was no need for carrier gas presaturation, due to the negligible vapor pressure of fatty acids, which minimizes the problem of mass loss. Our GLC is equipped with a thermal conductivity detector (Gow-Mac, model 10285) and a catharometer (Pye Unicam) as electrical supply.

Dry Helium (mass fraction purity > 0.9999) was used as carrier gas, its flow rates were within the range (0.65 to 0.85) $cm^3 \cdot s^{-1}$ and were measured using a calibrated Agilent digital gas flow meter (uncertainly of 0.1 $cm^3 \cdot min^{-1}$), which was placed at the inlet of the column. The flow rates were corrected for the calibration parameters of the digital flow meter (101.325 kPa and T = 295.15 K) and were also compared to the value obtained by a soap bubble flow meter installed at the outlet of the column, in all assays we found good agreement. The flow rate was set for a series of runs and was allowed to stabilize for at least 30 min before the beginning of the retention time determination.

For the experiments, a 304 grade stainless steel column (internal bore 4.1 mm and length 25 cm) was used. The column for each stationary phase was prepared by first washing with soapy water, then rinsing with water, distilled water and with acetone, and finally drying in an oven at 70°C. Chloroform (mass fraction purity > 0.999 and dried over molecular sieve) was used as a slurry solvent to aid the uniform coating of the fatty acid onto the inert solid support. Coating the solid support material with fatty acid was performed by adding known quantities of solvent (capric, lauric, myristic or palmitic acid) to a pre-weighed amount of the chromosorb. Chloroform was then added to the mixture, dissolving the fatty acid into support material, and it was removed afterwards by slow evaporation from the mixture (fatty acid + chromosorb) using a rotating evaporator. After the evaporation of the chloroform, the mixture was subjected to a low pressure of approx. 5 kPa at 330 K for at least 15 h. The column was then packed with a known mass of about 2 g of mixture. The masses of stationary phase and solid support were determinate before and after measurements by gravimetric analysis using an analytical balance (Sartorius, model

CP225D, Germany), accurate to ± 0.00001 g, as described in [21]. The solid support material was loaded with around 20% to 30% (w/w) of the solvent. These loadings were deemed to be large enough to avoid residual adsorption effects. For each solvent investigated, two different loadings were used at all temperatures studied.

The injected solute volume was $10^{-4}\ cm^3$, therefore the solute could be considered to be at "infinite dilution" on the column. As the GLC apparatus is equipped with a TCD (Thermal Conductivity detector), air could be used as a non-retainable component. Thus, together with the solute, about $9 \cdot 10^{-4}\ cm^3$of air were injected, using a syringe with a total capacity of $0.001\ cm^3$ (SGE Analytical Science).

The retention times were detected by a Hewlett-Packard HP 3990A integrator. Triple analyses of the solute retention times were performed to ensure reproducibility and stability of the system during the runs. They were generally reproducible to within 0.1% to 2% depending on the temperature and the solute. The temperature of the column was controlled by a thermostatic bath (Lauda) equipped with 2 platinum resistance thermometers (PT-100), with an uncertainly of ± 0.01 K. The column temperature was maintained constant within ± 0.1 K. The column inlet pressure, P_i , was measured by a pressure gauge (accuracy ± 0.3 kPa) and the column outlet pressure, P_o , was measured using a capacitive absolute pressure gauge (accuracy ± 0.2 kPa). The pressure drop $(P_i - P_o)$ varied between 5 kPa and 10 kPa, mainly depending on the flow rate of the carrier gas and the column temperature.

The experiments were carried out at different temperatures in the range from (314.10 to 358.33) K, and at a given temperature, for some solutes, the experiment was repeated two

times (with different loadings) to verify the reproducibility. The results were compared to the available literature values. The estimated overall errors in γ_{13}^{∞} and ΔH_{13}^{∞} were less than 4 % and 20%, respectively, taking into account the possible errors when determining the retention time (< 1%), the solute vapor pressure (< 0.5%), the number of moles of solvent on GLC column (< 2%) and the cross virial coefficient (< 0.2%).

3.3. Theoretical Background

In this work the equation of Everett [32] and Cruickshank *et al.* [33] was used to calculate γ_{13}^{∞} for solutes in saturated fatty acids:

$$\ln \gamma_{13}^{\infty} = \ln\left(\frac{n_3 RT}{V_N P_1^*}\right) - \frac{P_1^*(B_{11} - V_1^*)}{RT} + \frac{P_o J_2^3 (2B_{12} - V_1^{\infty})}{RT} \qquad (3.1)$$

where subscriptions 1, 2 and 3 refer to solute, carrier gas and solvent (in this case the saturated fatty acid), respectively. In this equation: n_3 is the number of moles of solvent on the column packing; R is the gas constant; T is the column temperature; V_N refers to the net retention volume of the solute; P_1^* is the vapor pressure of pure solute; B_{1i}(i = 1, 2) are the second virial coefficient and cross coefficient; V_1^* is the molar volume of pure solute; V_1^{∞} is the partial molar volume of the solute at infinite dilution in the solvent; P_o is the column outlet pressure; and J_2^3 the pressure-correction term (James-Martin [34] coefficient). All temperature and pressure dependent variables are at the column temperature T and column outlet pressure P_o. We assumed that $V_1^{\infty} \approx V_1^*$, as suggested by Everett and Stoddart [27].

The pressure-correction term, J_2^3, is calculated by

$$J_2^3 = \frac{3}{2}\frac{\left({}^{P_i}/_{P_o}\right)^2 - 1}{\left({}^{P_i}/_{P_o}\right)^3 - 1} \tag{3.2}$$

and the net retention volume of solute, V_N, is given by

$$V_N = J_2^3 F_c (t_R - t_G), \tag{3.3}$$

where P_i and P_o are the inlet and outlet pressures of the column, respectively; t_R and t_G are the retention times for the solute and an unretained gas (in this case air), respectively; and F_c is the column outlet flow rate, corrected for the temperature and pressure calibration of the flow meter by

$$F_c = F\left(\frac{P_o}{P_{fm}}\right)\left(\frac{T_{fm}}{T}\right) \tag{3.4}$$

where F is the flow rate measured with a calibrated flow meter; P_o is the outlet pressure and P_{fm} is the calibration pressure of the flow meter (in this case 1013.25 kPa); T is the temperature of the column; and T_{fm} is the calibration temperature of the flow meter (in this case 295.15 K).

The thermophysical properties required for calculating the activity coefficients at infinite dilution were taken from the Dortmund Data Bank (DDB) [35] and the Design Institute for Physical Properties (DIPPR) data bank. The vapor pressures were calculated from Antoine constants stored in the DDB, the liquid molar volumes and second virial coefficients of pure solutes were calculated from the respective DIPPR correlations, whereas the cross second virial coefficients (B_{12}) were estimated from the Tsonopoulos corresponding states correlation [36] coupled with Hudson-McCoubrey mixing rules [37; 38], the ionization energies used in the calculation of $T_{C,12}$ (cross critical temperature) were taken from

reference [39]. The values of P_1^*, V_1^* B_{11} and B_{12} for all solutes in palmitic acid at studied range temperature are given in table 3.S1 and the ionization energy are in table 3.S2 in the Supplementary Data (SD).

The activity coefficients at infinite dilution as function of temperature can be expressed by

$$\ln \gamma_{13}^{\infty} = \frac{\Delta\mu_1^{E,\infty}}{RT} = \frac{\Delta H_1^{E,\infty}}{RT} - \frac{\Delta S_1^{E,\infty}}{R} \tag{3.5}$$

In case of a linear dependence of $\ln \gamma_{13}^{\infty}$ on reciprocal temperature ($\ln \gamma_{13}^{\infty} = {}^{a}/_{T} + b$), the partial molar excess enthalpy at infinite dilution, $\Delta H_{13}^{E,\infty}$, can be calculated from the slope "a", and the partial molar excess entropy at infinite dilution, ΔS_{13}^{∞}, from the intercept "b".

3.4. Results and Discussion

The average values of the experimental γ_{13}^{∞} results for each temperature and the solvents capric (decanoic) acid, lauric (dodecanoic) acid, myristic (tetradecanoic) acid and palmitic (hexadecanoic) acid are presented in tables 3.2 to 3.5, respectively.

TABLE 3.2. Experimental activity coefficients at infinite dilution, γ_{13}^{∞}[a], for solutes in capric (decanoic) acid at different temperatures.

Solute	**314.10 K**	**314.24 K**	**333.26 K**	**333.38 K**	**353.25 K**	**353.30 K**
n-Hexane	1.752	1.774	1.731	1.696		1.653
n-Heptane	1.870	1.901	1.827	1.824		1.754
Isooctane	2.018	1.983	1.914		1.858	
1-Hexene		1.559	1.496	1.494		1.428
Toluene	1.151	1.174	1.122	1.116	1.144	1.156
Cyclohexane	1.436	1.461	1.386	1.391	1.352	1.309
Ethylbenzene			1.278	1.302[b]		1.218
Methanol		2.140		1.845	1.462[c]	1.569
Ethanol	2.115[c]	2.067	1.728	1.783		1.478
1-Propanol	1.887	1.924	1.569	1.600	1.407	1.354
1-Butanol			1.482	1.530[b]	1.342	1.321
2-Propanol	1.560	1.581	1.347	1.357	1.198	1.151
2-Butanol	1.334	1.354	1.167	1.159	1.052	1.037
Chloroform	0.823	0.846	0.850	0.827		0.825
Trichloroethylene	1.048	1.037	1.003	1.009	0.945[d]	0.969
Chlorobenzene			1.163	1.181	1.170	1.151
1,2-Dichloroethane	1.446	1.495	1.354	1.395		1.268
Benzyl Chloride						
Ethylacetate	1.329		1.247	1.299	1.207	
Acetone	1.558		1.458	1.466	1.343	
Anisole					1.432	1.449

[a] uncertainty 4% [b] T= 333.35 K; [c] T= 313.24 K; [d] T= 353.08 K.

TABLE 3.3. Experimental activity coefficients at infinite dilution, γ_{13}^{∞} [a], for solutes in lauric (dodecanoic) acid at different temperatures.

Solute	329.18 K	329.20 K	343.39 K	343.39 K	358.06 K	358.10 K
n-Hexane		1.574	1.532	1.538	1.499	
n-Heptane	1.645	1.666	1.669	1.659	1.591	1.616
Isooctane	1.746	1.771	1.697	1.718	1.674	1.688
1-Hexene		1.389		1.387	1.342	
Toluene	1.064	1.078		1.067	1.040	1.052
Cyclohexane	1.287	1.281		1.253	1.201	1.204
Ethylbenzene		1.222	1.202	1.189	1.178	1.175
Methanol	1.811	1.896[b]	1.672	1.656[c]		1.582
Ethanol	1.924	2.017		1.786	1.561	1.566
1-Propanol	1.758	1.784	1.566	1.605	1.426	1.432
1-Butanol		1.697	1.541	1.509	1.343	1.356
2-Propanol	1.500	1.531	1.334	1.370	1.222	1.238
2-Butanol	1.282	1.298		1.174	1.064	1.077
Chloroform	0.810	0.810	0.832	0.818		0.839
Trichloroethylene	0.952	0.967	0.944	0.951	0.933	
Chlorobenzene	1.108	1.118	1.081	1.075[c]	1.066	
1,2-Dichloroethane	1.380	1.370	1.297	1.318	1.233	
Benzyl Chloride					1.711	1.713
Ethylacetate	1.369	1.360		1.278	1.198	1.214
Acetone	1.592	1.590	1.450	1.466	1.335	1.365
Anisole			1.374	1.347[c]	1.334	1.353

[a] uncertainty 4% [b] T= 328.82 K; [c] T= 343.65 K.

TABLE 3.4. Experimental activity coefficients at infinite dilution, γ_{13}^{∞} [a], for solutes in myristic (tetradecanoic) acid at different temperatures.

Solute	**338.27 K**	**338.29 K**	**348.20 K**	**348.30 K**	**358.33 K**	**358.33 K**
n-Hexane	1.345			1.329	1.335	
n-Heptane	1.451	1.465		1.433	1.402	1.399
Isooctane	1.534			1.505		1.448
1-Hexene		1.240	1.224	1.207		1.182
Toluene	0.926	1.010	0.958			0.930
Cyclohexane	1.091	1.089		1.066	1.047	1.024
Ethylbenzene	1.061			1.059		1.037
Methanol	1.997[b]	1.919	1.732	1.709	1.596[c]	1.564
Ethanol	1.820	1.786	1.666	1.667	1.533	1.519
1-Propanol	1.614	1.651	1.522	1.511	1.373	1.369
1-Butanol	1.488	1.543	1.452	1.420	1.224	1.318
2-Propanol	1.394	1.421	1.305	1.297	1.194	1.187
2-Butanol	1.165	1.206	1.122	1.108	1.053	1.039
Chloroform	0.743	0.743	0.739	0.740	0.746	0.727
Trichloroethylene	0.847	0.843	0.842	0.838	0.842	0.824
Chlorobenzene	0.983	0.998	0.996	0.982	0.979	0.961
1,2-Dichloroethane	1.207	1.237	1.195	1.176	1.132	1.128
Benzyl Chloride			1.615	1.605	1.569	1.548
Ethylacetate	1.240	1.205	1.193	1.188	1.130	1.121
Acetone	1.430	1.458	1.364	1.350	1.296	1.267
Anisole	1.322	1.300	1.286	1.268	1.238	1.208

[a] uncertainty 4% [b] T= 338.29 K; [c] T= 358.31 K.

TABLE 3.5. Average experimental activity coefficients at infinite dilution, γ_{13}^{∞} [a], for solutes in palmitic (hexadecanoic) acid at different temperatures and literature values.

Solute	**This Work**			**Alessi *et al.* [45]**				**Foco *et al.* [46]**		
T/K	340.19	348.01	358.22	346.95	360.65	381.45	395.45	354.75	365.25	374.15
n-Hexane	1.293	1.299	1.301	1.28	1.30	1.43	1.41	1.43	1.47	1.50
n-Heptane	1.399	1.380	1.372	1.39	1.37	1.51	1.51	1.51	1.54	1.59
Isooctane	1.499	1.455	1.416[d]					1.60	1.64	1.68
1-Hexene	1.170[b]	1.178	1.200	1.16	1.24	1.30	1.27	1.32	1.35	1.39
Toluene	0.934	0.935	0.934	0.94	0.93	1.00	1.00	0.99	1.00	1.05
Cyclohexane	1.031	1.022	1.011	1.02	1.03	1.12	1.10	1.12	1.12	1.15
Ethylbenzene	1.039[b]	1.048	1.057	1.04	1.04	1.10	1.10	1.11	1.18	1.15
Methanol	2.088[b]	1.935[c]	1.798[e]	2.13[f]	1.85[g]	1.62[h]	1.34[i]	1.94	1.87	1.83
Ethanol	1.927	1.802	1.624[e]	1.82[f]	1.66[g]	1.43[h]	1.27[i]	1.85	1.76	1.73
Ethanol (rep)	1.918[b]	1.786[c]	1.602[d]							
1-Propanol	1.735	1.627	1.500[d]					1.65	1.56	1.53
1-Butanol	1.647	1.555	1.430[d]					1.58	1.48	1.45
2-Propanol	1.468	1.408	1.291[d]					1.41	1.38	1.35
2-Butanol	1.258	1.199	1.116[d]					1.60	1.18	1.16
Chloroform	0.748	0.739	0.759	0.78[f]	0.77[g]	0.76[h]	0.77[i]	1.01	0.84	0.87
Trichloroethylene	0.831	0.826	0.831					0.89	0.90	0.93
Chlorobenzene	0.974	0.957	0.974					1.27	1.24	1.25

1,2-Dichloroethane	1.220	1.190	1.143					1.60	1.02	1.04
Benzyl Chloride		1.620	1.569					0.83	1.67	1.60
Ethylacetate	1.282	1.201[c]	1.156	1.33[f]	1.25[g]	1.18[h]	1.16[i]	1.36	1.32	1.34
Acetone	1.494	1.417	1.325[e]	1.54[f]	1.43[g]	1.29[h]	1.17[i]	1.60	1.56	1.53
Acetone (rep)	1.494[b]	1.410[c]	1.342[d]							
Anisole	1.303	1.278	1.253					1.31	1.37	1.30

[a] uncertainty 4% [b] T=340.17 K; [c] T=347.93 K; [d] 358.32 K; [e] T=358.23 K; [f] T=344.35 K; [g] T=359.35 K; [h] T=380.75 K; [i] T=395.15 K; rep = repetition.

As shown in tables 3.2 to 3.5, only moderate deviations from ideal mixture behavior were found, the highest values of γ_{13}^{∞} (around 2) were obtained for short-chain alcohols. The combination of a rather long non-polar hydrocarbon chain and the strongly polar carboxylic acid group enables fatty acids to easily dissolve both polar and non-polar compounds.

Higher γ_{13}^{∞} values increase the volatility of the solute and enable more easy separation of the solute from the fatty acid by evaporation. The downside is, that all solutes with a higher activity coefficient in the fatty acids are at the same time associating components with a rather high heat of vaporization, which increases the energy consumption when separating these from the fatty acids.

Analyzing the values of γ_{13}^{∞} for the solutes: n-hexane, n-heptane and isooctane, it was found that the increase of γ_{13}^{∞} with an increase of the solute alkyl chain, as well as the values of γ_{13}^{∞} were lower for cycloalkanes in comparison to linear alkanes (see cyclohexane and n-hexane). That means that aliphatic hydrocarbons with cyclic structure have higher interaction strength than linear alkanes. In this case, the packing effect described by Marciniak [40] can be also considered. Components with lower molar volume reveal higher interactions due to the additional packing effect. That can be observed for cyclohexane (114.374 $cm^3 \cdot mol^{-1}$ at 338.29 K) compared to n-hexane (139.398 $cm^3 \cdot mol^{-1}$ at 338.29 K). By comparing alkene and alkane with the same number of carbons (1-hexene and n-hexane), we found that the interaction of double bond in alkene with the fatty acids leads to lower values of γ_{13}^{∞}.

From the investigated hydrocarbons, the aromatic hydrocarbon toluene has the smallest values of γ_{13}^{∞}. As discussed in previous works [40-42], the reduction of γ_{13}^{∞} in aromatics compounds is a consequence of the availability of localized or delocalized π-electrons clouds in benzene structure, which enhances the interaction of aromatic compounds with the slightly polar part of fatty acid molecules. For the aromatic compounds, γ_{13}^{∞} increases with increasing carbon number of the side chain on the benzene ring. Acetone and ethyl acetate showed intermediate values of γ_{13}^{∞}, between the alcohols and hydrocarbons.

The lowest values of γ_{13}^{∞} are observed for the chlorine-containing compounds: chloroform, trichloroethylene and chlorobenzene, which means that these compounds show the highest interaction with fatty acids. The increased intermolecular interactions is attributed to the effects of both: Van der Waals forces and polarity. Moreover, chlorine-containing compounds are naturally found in many biomolecules, including fatty acids [43; 44].

Table 3.5 lists the experimental values of γ_{13}^{∞} for palmitic acid from this work and from available literature [45; 46]. The data obtained in this work have, in general, good agreement with data from Alessi *et al.* [45], however our values are below those obtained by Focus *et al.* [46].

Comparing the data of γ_{13}^{∞} for palmitic acid of this work to the literature (by interpolation), the data measured show differences of less than 0.01 to 0.25 in absolute values, in some cases the difference is by nearly 15%. Comparing our result only with Alessi *et al.* data, the difference is always less than 9%. For some solutes, like cyclohexane and ethybenzene, the variation of value of γ_{13}^{∞} showed also different trend.

However, it should be remarked that the equations used by other authors to calculate γ_{13}^{∞} were similar but not identical to that used in this work. Although both references also have used the virial equation to correct the non-ideality of the gas phase, in our study, unlike the others cited, the solute-carrier gas interactions were not neglected, being considered in the third term of right side of equation (3.1). For calculation of the critical parameters, the vapor pressure and molar volumes, as well as of the virial coefficient of pure solute (B_{11}), other references were used. Additionally, the carrier gas used by Alessi *et al.* was different; the carrier gas used by Foco *et al.* and in this work was helium and not hydrogen. The method to obtain the net retention time is also different in our work. The method developed by Alessi *et al.* to obtain the net retention time uses the measurements of initial retention time (anti-Langmuir isotherm) or the final retention time (Langmuir isotherm), as described in their paper [47], whereas Foco *et al.* used methane as non-retainable gas to obtain the net retention time. This may be the explanation of the higher values obtained by Foco *et al.* compared to this work and the other reference.

Figures 3.2 to 3.4 show the natural logarithm of the activity coefficients in palmitic (hexadecanoic) acid, as function of the inverse absolute temperature for all investigated solutes. The influence of temperature follows a typical trend for most of the solutes, with the increase temperature was observed a decrease in γ_{13}^{∞} value.

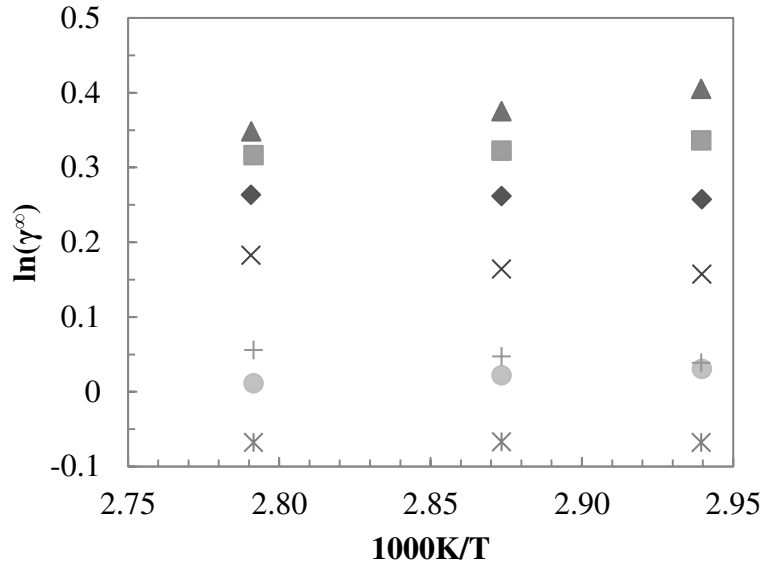

FIGURE 3.2. Plot of $\boldsymbol{ln(\gamma_{13}^{\infty})}$ for palmitic (hexadecanoic) acid *versus* $\mathbf{1/T}$ for the hydrocarbon solutes: ♦ n-Hexane, ■ n-Heptane; ▲Isooctane, × 1-Hexene, ∗ Toluene, ● Cyclohexane, + Ethylbenzene.

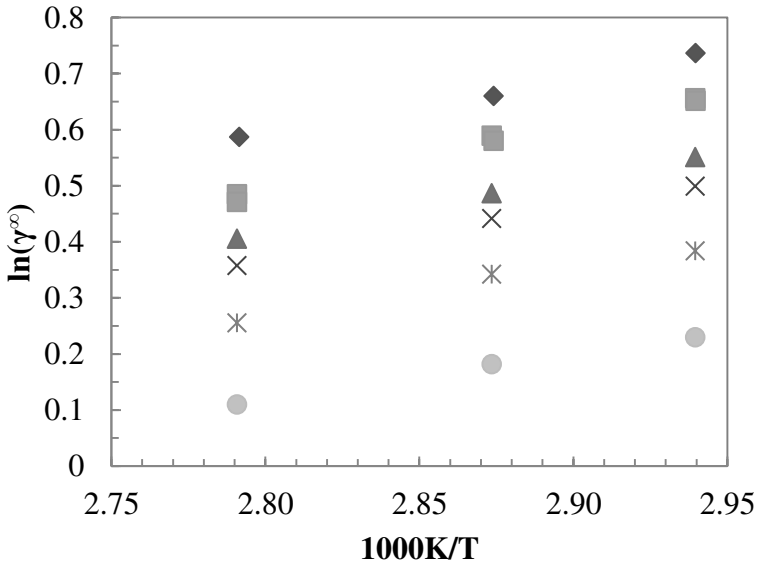

FIGURE 3.3. Plot of $\boldsymbol{ln(\gamma_{13}^{\infty})}$ for palmitic (hexadecanoic) acid *versus* $\mathbf{1/T}$ for the alcohol solutes: ♦ Methanol, ■ Ethanol; ▲1-Propanol, × 1-Butanol, ∗ 2-Propanol, ● 2-Butanol.

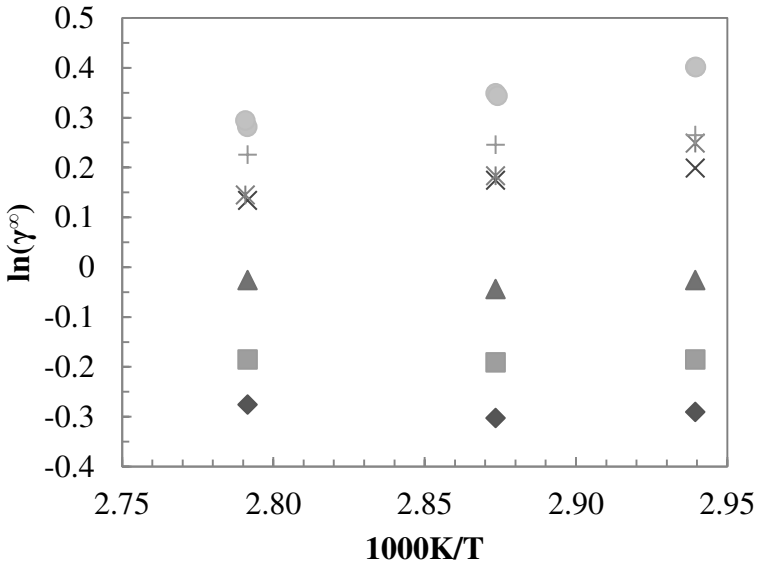

FIGURE 3.4. Plot of $\boldsymbol{ln(\gamma_{13}^{\infty})}$ for palmitic (hexadecanoic) acid *versus* $\boldsymbol{^{1}/_{T}}$ for chloride solute: ♦ Chloroform, ■ Trichloroethylene; ▲Chlorobenzene, × 1,2-Dichloroethane; ketone: ✳ Ethylacetate, ● Acetone, and + Anisole.

Table 3.6 contains values of the partial molar excess enthalpy, $\Delta H_{13}^{E,\infty}$, entropy , ΔS_{13}^{∞}, and Gibbs free energy, ΔG_{13}^{∞} , at infinite dilution calculated from experimental data for capric (decanoic) acid, lauric (dodecanoic) acid, myristic (tetradecanoic) acid and palmitic (hexadecanoic) acid, respectively. The ΔG_{13}^{∞} informs about fundamental interactions between solute and solvent. Most ΔG_{13}^{∞} values are positive. The values of $\Delta H_{13}^{E,\infty}$, determined from the Gibbs-Helmholtz equation, are in general positive. The error in $\Delta H_{13}^{E,\infty}$ is the same as for the linear regression of the natural logarithm of γ_{13}^{∞} as a function of the inverse absolute temperature. The entropy, $T_{ref}\Delta S_{13}^{\infty}$, is relative small for all solute studied, and, in general, the values obtained were positive.

TABLE 3.6. Limiting Values of the partial molar excess enthalpy, ΔH_{13}^{∞}[a], entropy, $T_{ref}\Delta S_{13}^{\infty}$, and Gibbs energy, ΔG_{13}^{∞}, at infinite dilution for solutes in capric, lauric, myristic and palmitic acid at reference temperature 328.15 K.

	Capric Acid			**Lauric Acid**			**Myristic Acid**			**Palmitic Acid**		
Solute	$\Delta H_1^{E,\infty}$/ $kJ.mol^{-1}$	$T_{ref}\Delta S_1^{E,\infty}$/ $kJ.mol^{-1}K^{-1}$	$\Delta G_1^{E,\infty}$/ $kJ.mol^{-1}$	$\Delta H_1^{E,\infty}$/ $kJ.mol^{-1}$	$T_{ref}\Delta S_1^{E,\infty}$/ $kJ.mol^{-1}K^{-1}$	$\Delta G_1^{E,\infty}$/ $kJ.mol^{-1}$	$\Delta H_1^{E,\infty}$/ $kJ.mol^{-1}$	$T_{ref}\Delta S_1^{E,\infty}$/ $kJ.mol^{-1}K^{-1}$	$\Delta G_1^{E,\infty}$/ $kJ.mol^{-1}$	$\Delta H_1^{E,\infty}$/ $kJ.mol^{-1}$	$T_{ref}\Delta S_1^{E,\infty}$/ $kJ.mol^{-1}K^{-1}$	$\Delta G_1^{E,\infty}$/ $kJ.mol^{-1}$
n-Hexane	1.49	0.00	1.49	1.67	0.43	1.24	1.40	0.55	0.85	-0.34	-1.03	0.69
n-Heptane	1.67	0.01	1.66				2.02	0.92	1.09	1.08	0.13	0.95
Isooctane	1.78	-0.04	1.81	1.52	-0.02	1.53	2.88	1.62	1.26	3.17	1.95	1.21
1-Hexene	2.07	0.95	1.12				2.42	1.75	0.66	-1.43	-1.80	0.37
Toluene							4.17	4.03	0.14			
Cyclohexane	2.01	1.09	0.92	2.23	1.53	0.69	2.56	2.25	0.31	1.10	0.98	0.12
Ethylbenzene				1.25	0.71	0.55				0.96	-1.03	1.99
Methanol	7.32	5.56	1.76				10.80	8.66	2.14	8.35	6.05	2.29
Ethanol	8.03	6.38	1.65	7.84	5.95	1.89	8.37	6.51	1.86	9.84	7.70	2.14
1-Propanol	7.61	6.21	1.40	7.27	5.69	1.58	8.75	7.14	1.61	8.14	6.35	1.79
1-Butanol				7.88	6.40	1.48	8.84	7.40	1.43	7.92	6.27	1.65
2-Propanol	6.85	5.93	0.93	7.09	5.94	1.15	8.41	7.22	1.19	7.25	5.93	1.32
2-Butanol	5.96	5.43	0.53	6.33	5.61	0.72	6.28	5.62	0.65	6.72	5.85	0.87
Chloroform												
TCE[b]	2.05	1.99	0.06									

CB[c]				1.58	1.29	0.29						
1,2-DCE[d]	3.42	2.52	0.91	3.63	2.75	0.88	3.95	3.27	0.67	3.68	3.00	0.68
Ethylacetate				0.00								
Acetone	2.26	1.57	0.68	4.19	3.33	0.86	4.14	3.46	0.69	5.70	3.21	2.49
Anisole	3.48	2.41	1.07	5.58	4.30	1.28	5.99	4.00	2.00	6.34	5.03	1.31

[a] uncertainty 20% [b] Trichloroethylene; [c] Chlorobenzene, [d] 1,2-Dichloroethane.

Figures 3.5 and 3.6 present comparisons of γ_{13}^{∞} for alcohols and hydrocarbons, respectively, in the four fatty acids studied. For the series of non-polar solutes, the values of γ_{13}^{∞} decrease with increasing carbon chain of the solvent, when increase the carbon chain of fatty acid. While for polar solutes, γ_{13}^{∞} values increase with increasing solute alkyl chain length. As mentioned above, the increase in carbon chain implies the reduction of solvent polarity, which increases the interaction intermolecular with non-polar solvents and reduces the interaction with polar solvents, reflecting the values of γ_{13}^{∞}. As noted by Alessi *et al.* [45], the effect of the solvent alkyl chain length in γ_{13}^{∞} is as important as the specific nature of functional groups of the solute.

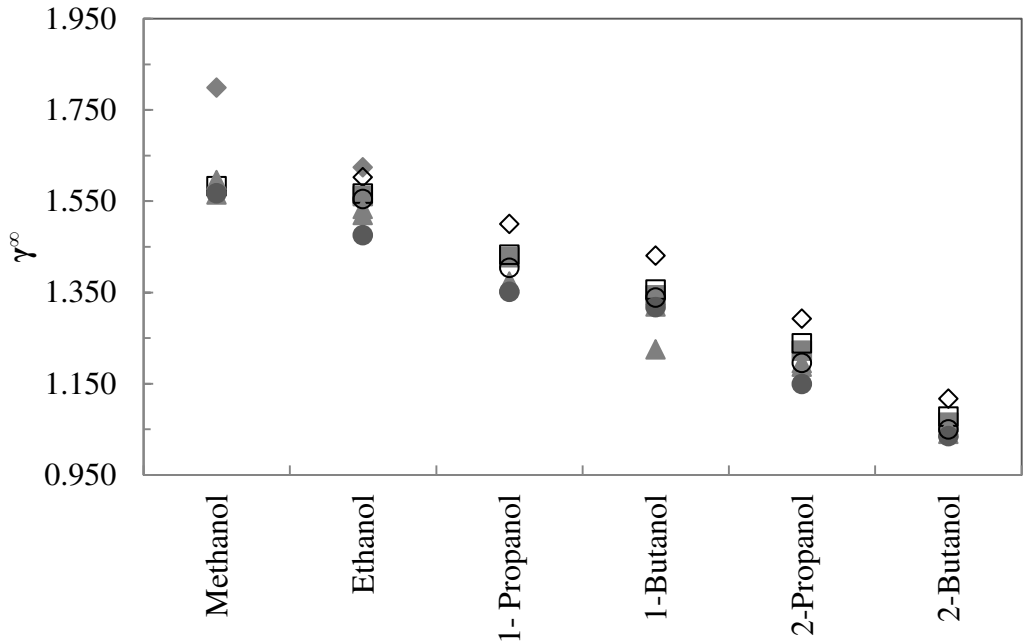

FIGURE 3.5. Plot of $\boldsymbol{\gamma_{13}^{\infty}}$ *versus* $\boldsymbol{T}$ for capric acid ((● T=353.30 K, ○ T= 353.25 K), lauric (■ T=358.06 K, □ T = 358.10 K) acid, myristic acid (▲T = 358.33 K) and palmitic acid (♦ T = 358.23 K, ◊ T = 358.35 K) for alcohols.

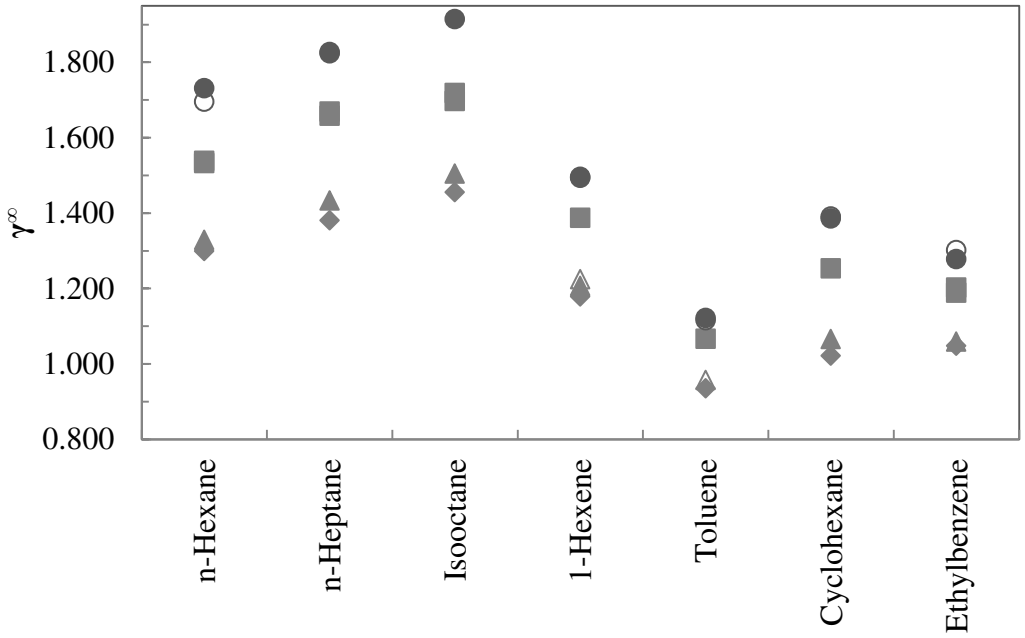

FIGURE 3.6. Plot of $\boldsymbol{\gamma_{13}^{\infty}}$ versus $\boldsymbol{T}$ for capric acid (● T=333.26 K, ○ T= 333.38 K), lauric acid (■ T=343.39 K), myristic acid (▲T = 348.30 K, Δ T = 348.20 K) and palmitic acid (♦ T = 348.01 K) for hydrocarbons.

3.5. Conclusions

Activity coefficients at infinite dilution for 21 solutes in four saturated fatty acids were measured by gas-liquid chromatography at temperatures from (314.10 to 358.33) K and compared to available literature data. The thermodynamic functions at infinite dilution for the same solutes were derived for capric (decanoic) acid, lauric (dodecanoic) acid, myristic (tetradecanoic) acid and palmitic (hexadecanoic) acid. Different trends for polar and non-polar compounds could be identified both in the series of fatty acids and as function of temperature. These results allow a more accurate description of the real behavior of fatty systems.

A further publication under preparation will compare these findings to results of static VLE, dilutor and calorimetric experiments and compare the data to the results of different predictive methods.

Acknowledgment

P. C. Belting wishes to acknowledge CNPq (Conselho Nacional de Desenvolvimento Científico e Tecnológico – 290128/2010-2) and DAAD (Deutscher Akademischer Autausch-Dienst – A/10/71471) for the scholarship. The authors would like to thank the CNPq (304495/2010-7, 480992/2009-6, 307718/2010-7 and 301999/2010-4), FAPESP (Fundação de Amparo à Pesquisa do Estado de São Paulo - 08/56258-8, 09/54137-1 and 2010/16634-0) and INCT-EMA (Institutos Nacionais de Ciência e Tecnologia de Estudos do Meio Ambiente) for the financial support. The authors are grateful to the DDBST GmbH for permitting the use of the Dortmund Data Bank. This work has been supported by the Carl Von-Ossietzky University Oldenburg.

References

[1] P.J. Wan, Properties of Fats and Oils. in: W.E.F. R. D. O'Brien, P. J. Wan, (Ed.), Introduction to Fats and Oils Technology, A.O.C.S. Press, Champaign, Illinois, 2000 pp. 20-48.

[2] R.D. O'Brien, Introduction to Fats and Oils Technology. in: W.E.F. R.D. O'BRIEN, and P.J. WAN, (Ed.), Fats And Oils: An Overview, AOCS Press: Champaign, Illinois, 2000, pp. 1-19.

[3] R. Ceriani, A.J.A. Meirelles, Fluid Phase Equilibr. 215 (2004) 227–236.

[4] J.M. Encinar, J.F. Gonzáles, J.J. Rodriguez, A. Tejedor, Energ. Fuel 16 (2002) 443-450.

[5] J.M. Marchetti, V.U. Miguel, A.F. Errazu, Renew Sust. Energ. Rev. 11 (2007) 1300-1311.

[6] F. Ma, M.A. Hanna, Bioresource Technol. 70 (1999) 1-15.

[7] L.A. Follegatti-Romero, M. Lanza, C.A.S. Silva, E.A.C. Batista, A.J.A. Meirelles, J. Chem. Eng. Data 55 (2010) 2750-2756.

[8] C.A.S. Silva, G. Sanaiotti, M. Lanza, L.A. Follegatti-Romero, A.J.A. Meirelles, E.A.C. Batista, J. Chem. Eng. Data 55 (2010) 440-447.

[9] C.B. Gonçalves, E.C. Batista, A.J.A. Meirelles, J. Chem. Eng. Data 47 (2002) 416-420.

[10] C.B. Gonçalves, A.J.A. Meirelles, Fluid Phase Equilibr 221 (2004) 139-150.

[11] C.B. Gonçalves, P.A. Pessôa Filho, A.J.A. Meirelles, J. Food Eng. 81 (2007) 21-27.

[12] C.G. Pina, A.J.A. Meirelles, J. Am. Oil Chem. Soc. 77 (2000) 553-559.

[13] C.E.C. Rodrigues, R. Antoniassi, A.J.A. Meirelles, J. Chem. Eng. Data 48 (2003) 367-373.

[14] C.E.C. Rodrigues, K.K. Aracava, F.N. Abreu, Int. J. Food Sci. Tech. 45 (2010) 2407–2414.

[15] C.E.C. Rodrigues, A. Fillipini, A.J.A. Meirelles, J. Chem. Eng. Data 51 (2006) 15-21.

[16] C.E.C. Rodrigues, M.M. Onoyama, A.J.A. Meirelles, J. Food Eng. 73 (2006) 370-378.

[17] C.E.C. Rodrigues, P.A. Pessôa Filho, A.J.A. Meirelles, Fluid Phase Equilibr. 216 (2004) 271-283.

[18] E.D. Milligan, D.C. Tandy, J. Am. Oil Chem. Soc. 51 (1974) 347-350.

[19] K.F. Mattil, Deodorization. in: F.A.N. K.F. Mattil, A.J. Stirton, (Ed.), Bailey's Industrial Oil and Fat Products, John Wiley & Sons, New York, 1964, pp. 897-930.

[20] L.C. Meher, D.V. Sagar, S.N. Naik, Renew Sust. Energ. Rev. 10 (2006).

[21] C. Knoop, D. Tiegs, J. Gmehling, J. Chem. Eng. Data 34 (1989) 240-247.

[22] T.M. Letcher, Activity Coefficients at Infinite Dilution from Gas-Liquid Chromatography. in: M.L. McGlashan, (Ed.), Chemical Thermodynamics, The Chemical Society, London, 1978, pp. 46-70.

[23] J. Gmehling, B. Kolbe, M. Kleiber, J. Rarey, Chemical Thermodynamics for Process Simulation, 1st ed., Wiley-VCH, Weinheim, 2012.

[24] J.C. Bastos, M.E. Soares, A.G. Medina, Ind. Eng. Chem. Proc. DD 24 (1985) 420-426.

[25] W. Davida, T.M. Letcher, D. Ramjugernatha, J.D. Raala, J. Chem. Thermodyn. 35 (2003) 1335-1341.

[26] J. Gmehling, C. Möllmann, Ind. Eng. Chem. Res. 37 (1998) 3112-3123.

[27] D.H. Everett, T.H. Stoddart, Trans. Faraday Soc. 57 (1961) 746-754.

[28] E.R. Thomas, B.A. Newman, G.L. Nlcolaldes, C.A. Eckert, J. Chem. Eng. Data 27 (1982) 233-240.

[29] D.L. Bergmann, C.A. Eckert, Fluid Phase Equilibr. 63 (1991) 141-150.

[30] K. Kojima, S. Zhang, T. Hiaki, Fluid Phase Equilibr. 131 (1997) 145-179.

[31] M. Krummen, D. Gruber, J. Gmehling, Ind. Eng. Chem. Res. 39 (2000) 2114-2123.

[32] D.H. Everett, Trans. Faraday Soc. 61 (1965) 1635-1639.

[33] A.J.B. Cruickshank, B.W. Ganey, C.P. Hicks, T.M. Letcher, R.W. Moody, C.L. Young, Trans. Faraday Soc. 65 (1969) 1014-1031.

[34] A.T. James, A.J.P. Martin, Biochem. J. 50 (1952) 679-690.

[35] Dortmund Data Bank Dortmund Data Bank Software & Separation Technology DDBST GmbH, Oldenburg, 2011.

[36] B.E. Poling, J.M. Prausnitz, J.P. O'Connell, Properties of Gases and Liquids, 5th ed., McGraw-Hill, 2001.

[37] H.G. Hudson, J.C. McCoubrey, Trans. Faraday Soc. 56 (1960) 761-766.

[38] J.A. Huff, T.M. Reed, J. Chem. Eng. Data 8 (1963) 306-311.

[39] W.M. Haynes, (Ed.), CRC Handbook of Chemistry and Physics, CRC Press Taylor and Francis Group, LLC, Boulder, Colorado, 2010.

[40] A. Marciniak, J. Chem. Thermodyn. 43 (2011) 1446-1452.

[41] P. Reddy, K.J. Chiyen, N. Deenadayalu, D. Ramjugernath, J. Chem. Thermodyn. 43 (2011) 1178-1184.

[42] P. Reddy, N.V. Gwala, N. Deenadayalu, D. Ramjugernath, J. Chem. Thermodyn. 43 (2011) 754-758.

[43] V.M. Dembitsky, M. Srebnik, Prog. Lipid Res. 41 (2002) 315–367.

[44] G.W. Gribble, J. Nat. Prod. 55 (1992) 1353–1395.

[45] P. Alessi, I. Kikic, A. Alessandri, M. Orlandini Visaberghi, Chem. Eng. Commun. 16 (1982) 377-382.

[46] G. Foco, A. Bermudez, S. Bottini, J. Chem. Eng. Data 41 (1996) 1071-1074.

[47] P. Alessi, I. Kikic, A. Papo, G. Torriano, J. Chem. Eng. Data 23 (1978) 29-33.

Appendix 3.A. Supplementary Data

Supplementary data associated with this article are tables 3.S1 and 3.S2.

TABLE 3.S1. Values of P_1^*, V_1^* B_{11} and B_{12} for all solutes in palmitic acid at studied range temperature.

Solute	T/K	P_1^*/Pa	V_1^*/m^3.mol^{-1}	B_{11}/m^3.mol^{-1}	B_{12}/m^3.mol^{-1}
n-Hexane	340.17	95754	1.3982E-04	-1.342E-03	3.927E-05
n-Hexane	348.01	122151	1.4163E-04	-1.263E-03	3.951E-05
n-Hexane	358.22	164773	1.4413E-04	-1.170E-03	3.980E-05
n-Heptane	340.17	36313	1.5546E-04	-1.983E-03	4.607E-05
n-Heptane	348.01	47884	1.5723E-04	-1.847E-03	4.632E-05
n-Heptane	358.22	67232	1.5965E-04	-1.691E-03	4.663E-05
Isooctane	340.17	36856	1.7458E-04	-2.062E-03	4.653E-05
Isooctane	348.01	48213	1.7649E-04	-1.934E-03	4.678E-05
Isooctane	358.23	67068	1.7909E-04	-1.785E-03	4.710E-05
1-Hexene	340.17	113142	1.3439E-04	-1.202E-03	3.712E-05
1-Hexene	348.01	143422	1.3624E-04	-1.133E-03	3.735E-05
1-Hexene	358.22	191959	1.3879E-04	-1.053E-03	3.762E-05
Toluene	340.19	24332	1.1170E-04	-1.799E-03	3.301E-05
Toluene	348.01	32421	1.1275E-04	-1.677E-03	3.325E-05
Toluene	358.22	46137	1.1417E-04	-1.536E-03	3.356E-05
Cyclohexane	340.17	65831	1.1466E-04	-1.205E-03	3.036E-05
Cyclohexane	348.01	84676	1.1586E-04	-1.127E-03	3.060E-05
Cyclohexane	358.22	115321	1.1751E-04	-1.036E-03	3.090E-05
Ethylbenzene	340.19	9998	1.2828E-04	-2.497E-03	3.909E-05
Ethylbenzene	348.01	13733	1.2940E-04	-2.318E-03	3.936E-05
Ethylbenzene	358.22	20279	1.3091E-04	-2.111E-03	3.968E-05
Methanol	340.17	111500	4.2889E-05	-8.862E-04	2.538E-05
Methanol	347.93	149438	4.3376E-05	-7.819E-04	2.558E-05

Methanol	358.23	215772	4.4060E-05	-6.706E-04	2.582E-05
Ethanol	340.17	63607	6.1731E-05	-1.232E-03	3.196E-05
Ethanol	340.19	63659	6.1732E-05	-1.232E-03	3.196E-05
Ethanol	347.93	87888	6.2387E-05	-1.070E-03	3.217E-05
Ethanol	348.01	88183	6.2394E-05	-1.068E-03	3.217E-05
Ethanol	358.23	131756	6.3307E-05	-8.970E-04	3.243E-05
Ethanol	358.32	132244	6.3316E-05	-8.956E-04	3.243E-05
1-Propanol	340.19	28463	7.8844E-05	-1.402E-03	3.727E-05
1-Propanol	348.01	40651	7.9631E-05	-1.262E-03	3.750E-05
1-Propanol	358.32	63135	8.0721E-05	-1.109E-03	3.778E-05
1-Butanol	340.19	11654	9.6268E-05	-1.896E-03	4.161E-05
1-Butanol	348.01	17163	9.7153E-05	-1.744E-03	4.185E-05
1-Butanol	358.32	27701	9.8371E-05	-1.568E-03	4.216E-05
2-Propanol	340.19	53084	8.1158E-05	-1.387E-03	3.937E-05
2-Propanol	348.01	74540	8.2066E-05	-1.238E-03	3.960E-05
2-Propanol	358.32	113507	8.3335E-05	-1.078E-03	3.987E-05
2-Butanol	340.19	25925	9.7311E-05	-1.502E-03	4.129E-05
2-Butanol	348.01	37207	9.8421E-05	-1.390E-03	4.153E-05
2-Butanol	358.32	58048	9.9958E-05	-1.261E-03	4.182E-05
Chloroform	340.19	122132	8.5158E-05	-8.569E-04	2.435E-05
Chloroform	348.01	155054	8.6134E-05	-8.110E-04	2.458E-05
Chloroform	358.22	208000	8.7472E-05	-7.571E-04	2.485E-05
Trichloroethylene	340.19	52677	9.4842E-05	-1.413E-03	2.688E-05
Trichloroethylene	348.01	68578	9.5810E-05	-1.277E-03	2.711E-05
Trichloroethylene	358.22	94656	9.7128E-05	-1.130E-03	2.741E-05
Chlorobenzene	340.19	11734	1.0654E-04	-1.990E-03	3.161E-05
Chlorobenzene	348.01	15989	1.0739E-04	-1.831E-03	3.188E-05
Chlorobenzene	358.22	23405	1.0855E-04	-1.658E-03	3.220E-05
1,2-	340.19	58364	8.3677E-05	-1.057E-03	2.667E-05

Dichloroethane					
1,2-Dichloroethane	348.01	76071	8.4563E-05	-9.932E-04	2.691E-05
1,2-Dichloroethane	358.22	105382	8.5770E-05	-9.190E-04	2.721E-05
Benzyl Chloride	348.01	2642	1.2073E-04	-3.527E-03	3.901E-05
Benzyl Chloride	358.22	4193	1.2192E-04	-3.097E-03	3.937E-05
Ethylacetate	340.19	72043	1.0466E-04	-1.382E-03	3.564E-05
Ethylacetate	348.01	94241	1.0595E-04	-1.284E-03	3.587E-05
Ethylacetate	358.32	131505	1.0773E-04	-1.172E-03	3.617E-05
Acetone	340.17	144316	7.8859E-05	-1.171E-03	2.837E-05
Acetone	340.19	144403	7.8861E-05	-1.171E-03	2.837E-05
Acetone	347.93	183379	7.9921E-05	-1.074E-03	2.859E-05
Acetone	348.01	183834	7.9933E-05	-1.073E-03	2.859E-05
Acetone	358.23	247530	8.1414E-05	-9.635E-04	2.886E-05
Acetone	358.32	248209	8.1428E-05	-9.625E-04	2.886E-05
Anisole	340.19	4711	1.1366E-04	-2.414E-03	3.740E-05
Anisole	348.01	6722	1.1456E-04	-2.382E-03	3.767E-05
Anisole	358.22	10390	1.1578E-04	-2.289E-03	3.799E-05

TABLE 3.S2. First ionization energy of used solutes [39].

Solute	**eV(particle)$^{-1}$**	**kJ.mol^{-1}**
n-Hexane	10.13	977.39
n-Heptane	9.93	958.10
Isooctane	9.86	951.34
1-Hexene	9.44	910.82
Toluene	8.83	851.73
Cyclohexane	9.86	951.34
Ethylbenzene	8.77	846.17
Methanol	10.85	1046.86
Ethanol	10.43	1006.34
1-Propanol	10.18	982.22
1-Butanol	9.99	963.89
2-Propanol	10.17	981.25
2-Butanol	9.88	953.27
Chloroform	11.37	1097.03
Trichloroethylene	9.46	912.75
Chlorobenzene	9.07	875.12
1,2-Dichloroethane	11.04	1065.19
Benzyl Chloride	9.10	878.01
Ethylacetate	10.01	965.81
Acetone	9.70	936.19
Anisole	8.22	793.11

CAPÍTULO 4: ACTIVITY COEFFICIENT AT INFINITE DILUTION MEASUREMENTS FOR ORGANIC SOLUTES (POLAR AND NONPOLAR) IN FATTY COMPOUNDS – PART II: C18 FATTY ACIDS

Artigo publicado na revista *The Journal of Chemical Thermodynamics*,

vol. 60, ano: 2013, p. 142-149.

Activity Coefficient at Infinite Dilution Measurements for Organic Solutes (polar and non-polar) in Fatty Compounds – Part II: C18 Fatty Acids.

Patrícia C. Belting[a,b,1], Jürgen Rarey[a*], Jürgen Gmehling[a], Roberta Ceriani[c], Osvaldo Chiavone-Filho[d], Antonio J. A. Meirelles[b]

[a] *Carl von Ossietzky Universität Oldenburg, Technische Chemie (FK V), D-26111 Oldenburg, Federal Republic of Germany*

[b] *Food Engineering Department, Faculty of Food Engineering, University of Campinas, Av. Monteiro Lobato 80, Cidade Universitária Zeferino Vaz, 13083-862, Campinas-SP, Brazil*

[c] *Faculty of Chemical Engineering, University of Campinas, Av. Albert Einstein 500, Cidade Universitária Zeferino Vaz, 13083-852, Campinas-SP, Brazil*

[d] *Chemical Engineering Department, Federal University of Rio Grande do Norte, Av. Senador Salgado Filho S/N, 59066-800, Natal-RN, Brazil*

[1 a] *Present address,* [b] *Permanent address*

Abstract

In this work, activity coefficients at infinite dilution (γ_{13}^{∞}) have been measured for 21 solutes (subscript 1) (alkanes, cycloalkanes, alkenes, aromatic compounds, alcohols, esters, ketones and halogenated hydrocarbons), in four solvents (subscript 3), namely one saturated fatty acid and three unsaturated fatty acids: stearic (octadecanoic) acid – C18:0, oleic (*cis*-9-octadecenoic) acid – C18:1 9c, linoleic (*cis*,*cis*-9,12-octadecadienoic) acid – C18:2 9c12c and linolenic (*cis*,*cis*,*cis*-9,12,15-octadecatrienoic) acid – C18:3 9c12c15c, by gas-liquid chromatography. The measurements were carried out at temperatures from

(303.13 to 368.19) K and the partial molar excess Gibbs free energy ($\Delta G_1^{E,\infty}$), enthalpy ($\Delta H_1^{E,\infty}$), and entropy ($\Delta S_1^{E,\infty}$), at infinite dilution were calculated from experimental γ_{13}^{∞} values obtained over the temperature range. The uncertainties in determination of γ_{13}^{∞} and $\Delta H_1^{E,\infty}$ are 4 % and 20 %, respectively. The results for stearic acid obtained in this study have been compared to those available in the Dortmund Data Bank (DDB). The real behavior of fatty systems could be better understood through the results obtained in this work.

Keywords: Stearic acid; Oleic acid; Linoleic acid; Linolenic acid; Limiting activity coefficient; Gas-liquid chromatography method.

4.1. Introduction

Fatty acids, esterified to glycerol, are the main constituents of oils and fats. Most commodity oils contain fatty acids with carbon chain lengths between C16 and C22, with C18 fatty acids dominating in most plant oils [1]. This paper studies C18 fatty acids most commonly found in nature, their nomenclature and additional information are shown in table 4.1 and the chemical structures are illustrated in figure 4.1.

TABLE 4.1. Nomenclature and other data of C18 fatty acids.

Fatty Acid Nomenclature			M[b,d]/ g/mol^{-1}	Melting Point[b]/ K	Significant sources[e]
IUPAC	**Trivial**	**Symbol[a]**			
Octadecanoic acid	Stearic acid	C18:0	284.483	342.50	Cocoa butter, tallow
cis-9-Octadecenoic acid	Oleic acid	C18:1 9c	282.467	289.15	Cottonseed, olive, palm, rapeseed oils
cis,*cis*-9,12-Octadecadienoic acid	Linoleic acid	C18:2 9c12c	280.451	268.15	Corn, soybean, sunflower oils
cis,*cis*,*cis*-9,12,15-Octadecatrienoic acid	Linolenic acid	C18:3 9c12c15c	278.435	262.03	Linseed oil

[a] Cx:y, x = chain length, y = number of double bonds followed by respective position and c = configuration *cis*.
[b] from DDB [2].
[d] M= molar mass.
[e] Ref.: [1].

Table 4.1 also illustrates one of the effects of unsaturation, the melting point of C18 fatty acids decreases with increasing unsaturation.

Storage fats (seed oils and animal adipose tissue) consist chiefly (> 98 %) of triacylglycerols, with the fatty acids distributed among different molecular species. The minor components are partial acylglycerols and free fatty acids, and they may also include phospholipids, sterols, tocopherols, carotenoids, etc. [1; 3-5].

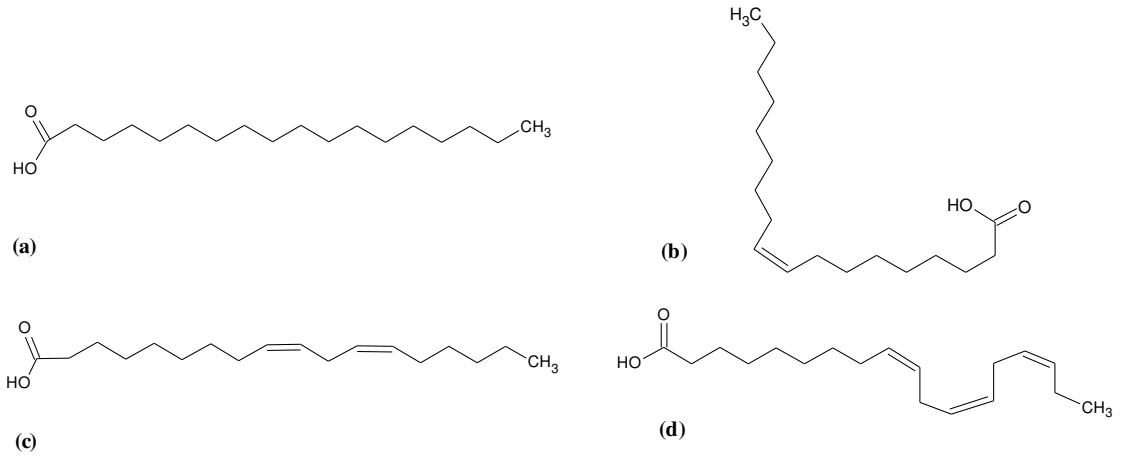

FIGURE 4.1. Structure of the C 18 fatty acids: (a) stearic acid; (b) oleic acid; (c) linoleic acid, and d) linolenic acid.

Figure 4.1 shows that, as in case of other fatty acids, the basic structure of C18 fatty acids consists of a hydrophobic hydrocarbon chain, in this case, with 18 carbons (which can be saturated or unsaturated) with a hydrophilic polar group at one end. It endows fatty acids and their derivatives with distinctive properties, reflected in both their food and industrial use [1; 3]. The most reactive sites in fatty acid molecules are the carboxyl group and double bonds, which are important to the body metabolism and to the reactions used in the food and oleochemical industry [1]. In their pure form as well as in not too dilute solutions, fatty acids are nearly completely dimerized in the liquid phase [6].

Oleic, linoleic and linolenic acids can also be called ω-9, ω-6 and ω-3 fatty acids, respectively. The last two can also be classified as polyunsaturated fatty acids (PUFA), which are produced only by plants and phytoplankton and are essential to all higher organisms, including mammals and fish, because ω-3 and ω-6 fatty acids cannot be interconverted, and both are essential nutrients [7].

In recent years, there is an increasing interest in the thermodynamic property and phase equilibrium data of fatty systems, such as mixtures containing: fatty acids, methyl and ethyl esters of fatty acids, glycerol, partial acylglycerols, triacylglycerols, and multicomponent systems, such as edible oils, fats and biodiesel. All these compounds are directly involved in industrial extraction and refining of edible vegetable oils [8-12], the production and purification of partial acylglycerols [13-17] and in the processing of biodiesel [18-21], all of which are submitted to several separation and purification stages which play an important role in the economics of the processes. This is especially true in case of very high purity requirements, which result in increased investment and operating costs.

From practical and theoretical points of view, the activity coefficient at infinite dilution or the limiting activity coefficient (γ_{13}^{∞}) represents an important property to the practicing chemist and process engineer [22-24]. From the industrial viewpoint, it offers a wider applicability than any measurement at finite concentration, since experimental values at infinite dilution are better suited to predict the phase behavior of a mixture over the entire concentration range than vice versa [25]. They are also especially useful for the selection of selective solvents (e.g. extraction, absorption and extractive distillation) and for reliable design, optimization and modeling of thermal separation processes [24; 26-28]. From a theoretical point of view, the activity coefficients at infinite dilution are important for the development of new thermodynamic models and also for the adjustment of reliable model parameters [24; 28; 29].

In our previous work [30], the γ_{13}^{∞} of several solutes in saturated fatty acids: capric acid (C10:0), lauric acid (C12:0), myristic acid (C14:0) and palmitic acid (C16:0) were

measured and different trends for polar and non-polar solutes could be identified, both in the series of fatty acids and as function of temperature. This paper is a continuation of that work, and it discusses the role of the double bonds in the structure of the fatty acid (solvent) in the solvent-solute interaction with the aim to contribute to the pool of knowledge available to develop a greater understanding of the correlation between structure and function for the various fatty acids.

We report here activity coefficients at infinite dilution, γ_{13}^{∞}, for 21 solutes (alkanes, cycloalkanes, alkenes, aromatic compounds, alcohols, esters, ketones and halogenated hydrocarbons) in four C18 fatty acids:

- stearic (octadecanoic) acid – C18:0;
- oleic (*cis*-9-octadecenoic) acid – C18:1 9c or ω-9;
- linoleic (*cis*,*cis*-9,12-octadecadienoic) acid – C18:2 9c12c or ω-6;
- linolenic (*cis*,*cis*,*cis*-9,12,15-octadecatrienoic) acid – C18:3 9c12c15c or ω-9.

The values of γ_{13}^{∞} were determined at temperatures from (303.13 to 368.19) K. Experimental γ_{13}^{∞} data were used to calculate the values of partial molar excess Gibbs free energy, $\Delta G_1^{E,\infty}$, enthalpy, $\Delta H_1^{E,\infty}$, and entropy, $\Delta S_1^{E,\infty}$, at infinite dilution.

4.2. Experimental

4.2.1. Materials

Table 4.2 presents the list of fatty acids (solvents), their purity and the suppliers; they were not subjected to further purification. The solutes had purities above 0.99 in mass fraction and were used also without further purification since the GLC technique allows the separation of any impurities on the column. As solid support material for all stationary phases, Chromosorb P-AW-DMCS 60/80 mesh, supplied by CS-Chromatographie Service GmbH (Germany) was used. Dry helium (> 0.9999 mass fraction purity) was used as carrier gas.

TABLE 4.2. Information about the investigated solvents.

Solvent	**Purity (GC)**	**Supplier**
	Mass fraction	
Stearic acid	> 0.985	Sigma
Oleic acid	> 0.99	Sigma Aldrich
Linoleic acid	> 0.995	Aldrich
Linolenic acid	> 0.99	Sigma

4.2.2. Apparatus and experimental procedure

A homemade gas-liquid chromatograph was used for the measurements of activity coefficients at infinite dilution. A detailed description is presented by Knoop *et al.* [31]. This apparatus follows the same principle as presented by Letcher [32]. Due to the negligible vapor pressure of fatty acids [33], there was no need for carrier gas pre-saturation, since problems of mass loss are minimized. Our GLC is equipped with a thermal

conductivity detector (Gow-Mac, model 10285) and a catharometer (Pye Unicam) as electrical supply.

The unsaturated solvents were stocked at temperature below – 20 °C. For these compounds, the entire procedure for preparation of the column was carried out under inert atmosphere (nitrogen) and with a minimum exposure to light, since they are sensitive to oxidation [34].

A pre-weighed amount of a pre-dried solid support was coated with a known quantity of solvent (stearic, oleic, linoleic or linolenic acid) with chloroform (0.999 fraction mass purity dried over molecular sieve) as a solubilizer in a rotary evaporator. All chloroform was then removed by slow evaporation (for unsaturated fatty acids under nitrogen atmosphere) and the mixture (fatty acid + chromosorb) was subjected to a low pressure of approximately 5 kPa at 310 K for at least 15 hours.

The column (304 grade stainless steel, length 25 cm and internal diameter 4.1 mm) was carefully filled with a known mass (about 2 g) of coated solid support. As described in [31], before and after the measurements the masses of solvent and solid support were determined gravimetrically using an analytical balance (Sartorius, model CP225D, Germany), accurate to ± 0.00001 g. The solid support material was coated with around 20% to 30% (w/w) of the solvent. These loadings were deemed to be large enough to avoid residual adsorption effects. For each solvent investigated, two different loadings were used.

An adaptation was made in the equipment described by Knoop *et al.* [31]: a calibrated Agilent digital gas flow meter (uncertainly of 0.1 $cm^3 \cdot min^{-1}$) was installed at the inlet of the column for the control and measurement of the carrier gas flow rate. The helium flow

rates were within the range (0.65 to 0.85) $cm^3 \cdot s^{-1}$ and corrected for the calibration parameters of the digital flow meter (101.325 kPa and 295.15 K). In all assays, the flow rate was compared to the value obtained by a soap bubble flow meter installed at the outlet of the column (from original version) and both values were found to be in good agreement. Before the beginning of the retention time determination, the flow rate was set and allowed to stabilize for at least 30 min.

The sample volumes of injected solutes were varied from (0.1 to 0.3) $10^{-3}cm^3$, as recommended by Laub *et al.* [35], therefore the solute could be considered to be at "infinite dilution" on the column. Air was used as a non-retainable component, since the GLC apparatus was equipped with a TCD (Thermal Conductivity detector). Thus, together with the solute, about (0.7 to 0.9) $10^{-3}cm^3$ of air were injected, using a syringe with a total capacity of $10^{-3}cm^3$ (SGE Analytical Science). It was first verified that this quantity of air would not interfere with the obtained retention times.

A Hewlett-Packard HP 3990A integrator was used for the detection of retention times. To ensure reproducibility and stability of the system during the runs, triple analyses of the solute retention times were performed. The reproducibility obtained was generally within 0.1 to 2%, depending on the temperature and the solute. The column temperature was maintained constant within ± 0.1 K and it was controlled by a thermostatic bath (Lauda) equipped with two platinum resistance thermometers (PT-100), with an uncertainly of ± 0.01 K. The column inlet (P_i) and outlet pressure (P_o) were measured by a pressure gauge (accuracy ± 0.3 kPa) and a capacitive absolute pressure gauge (accuracy ± 0.2 kPa),

respectively. Depending on the flow rate of the carrier gas and the column temperature, the column pressure drop $(P_i - P_o)$ varied between (5 and 10) kPa.

The experiments were carried out at different temperatures in the range from (303.13 to 368.19) K, and to verify the reproducibility, at a given temperature, for some solutes, the experiment was repeated twice (with different loadings). The results for the solvent stearic acid were compared to the available literature values. Taking into account the possible errors when determining the retention time (< 1%), the solute vapor pressure (< 0.5%), the number of moles of solvent on GLC column (< 2%) and the cross virial coefficient (< 0.2%), the estimated overall errors in γ_{13}^{∞} and $\Delta H_1^{E,\infty}$ were less than 4 % and 20%, respectively.

4.3. Theoretical Background

The equation proposed by Everett [36] and Cruickshank *et al.* [37] was used in this paper to calculate the activity coefficients at infinite dilution, γ_{13}^{∞}, for solutes in C18 fatty acids, as shown below:

$$\ln \gamma_{13}^{\infty} = \ln\left(\frac{n_3 RT}{V_N P_1^*}\right) - \frac{P_1^*(B_{11} - V_1^*)}{RT} + \frac{P_o J_2^3 (2B_{12} - V_1^{\infty})}{RT} \qquad (4.1)$$

where R is the general gas constant; T is the absolute column temperature and V_N refers to the net retention volume of the solute. In this expression, the subscriptions 1, 2 and 3 refer to solute, carrier gas and solvent (in this case the C18 fatty acid), respectively. Other quantities occurring in equation (4.1) are: n_3, the number of moles of solvent on the column packing; P_1^*, the vapor pressure of pure solute; B_{1i}(i = 1, 2), the second virial coefficient and cross coefficient; V_1^*, the molar volume of pure solute; P_o is the column outlet pressure;

V_1^{∞}, the partial molar volume of the solute at infinite dilution in the solvent (in this work $V_1^{\infty} \approx V_1^*$, as suggested by Everett and Stoddart [38]). The J_2^3 denotes the pressure-correction term (James-Martin [39] coefficient) calculated by equation 2. All temperature and pressure dependent variables were taken at the column temperature T and column outlet pressure P_o.

$$J_2^3 = \frac{3}{2}\frac{\left({}^{P_i}/_{P_o}\right)^2 - 1}{\left({}^{P_i}/_{P_o}\right)^3 - 1} \tag{4.2}$$

where P_i and P_o are the inlet and outlet pressures of the column, respectively.

The net retention volume of solute, V_N, is given by

$$V_N = J_2^3 F_c (t_R - t_G), \tag{4.3}$$

where t_R and t_G are the retention times for the solute and an unretained gas (in this case air), respectively; and F_c is the column outlet flow rate, corrected for the temperature and pressure calibration of the flow meter by

$$F_c = F\left(\frac{P_o}{P_{fm}}\right)\left(\frac{T_{fm}}{T}\right) \tag{4.4}$$

where F is the flow rate measured with a calibrated flow meter; P_o is the outlet pressure and P_{fm} is the calibration pressure of the flow meter, i.e. 1013.25 Pa; T is the absolute temperature of the column; and T_{fm} is the calibration temperature of the flow meter, i.e. 295.15 K.

The thermophysical properties required for developing the activity coefficients at infinite dilution were taken from the Dortmund Data Bank (DDB) [2] and the Design Institute for Physical Properties (DIPPR) data bank [40]. The cross second virial coefficients (B_{12}) were estimated from the Tsonopoulos corresponding states correlation

[29] coupled with Hudson-McCoubrey mixing rules [41; 42], the ionization energies used in the calculation of $T_{C,12}$ (cross critical temperature) were taken from reference [43], whereas the second virial coefficients of pure solutes were calculated from the DIPPR correlations. The vapor pressures were calculated from Antoine constants stored in the DDB and the liquid molar volumes were also calculated from the DIPPR correlations. The values of P_1^*, V_1^* B_{11} and B_{12} for all solutes in stearic acid at studied range temperature are given in Table 4.S1 in the Supplementary Data (SD).

The activity coefficients at infinite dilution were determined as a function of temperature, therefore, $\ln \gamma_{13}^{\infty}$ can be directly related with excess thermodynamics functions at infinite dilution by the following expression:

$$\ln \gamma_{13}^{\infty} = \frac{\Delta \mu_1^{E,\infty}}{RT} = \frac{\Delta H_1^{E,\infty}}{RT} - \frac{\Delta S_1^{E,\infty}}{R} \tag{4.5}$$

Assuming a linear dependence of $\ln \gamma_{13}^{\infty}$ on the reciprocal absolute temperature ($\ln \gamma_{13}^{\infty} = {a}/{T} + b$), the partial molar excess enthalpy at infinite dilution, $\Delta H_1^{E,\infty}$, can be estimated from the slope "a", and the partial molar excess entropy at infinite dilution, $\Delta S_1^{E,\infty}$, from the intercept "b".

4.4. Results and Discussion

Tables 4.3 to 4.6 list the average γ_{13}^{∞} experimental values for different solutes in the investigated fatty acids: stearic (octadecanoic) acid, oleic (*cis*-9-octadecenoic) acid, linoleic (*cis*,*cis*-9,12-octadecadienoic) acid and linolenic (*cis*,*cis*,*cis*-9,12,15-octadecatrienoic) acid over temperature range from (303.13 to 368.19) K, respectively.

TABLE 4.3. Experimental limiting activity coefficients, γ_{13}^{∞}[a], for solutes in stearic (octadecanoic) acid, C18:0, at different temperatures and literature values.

Solute	**This Work**						**Alessi *et al.* (1985)[44]**			**Alessi *et al.* (1995)[45]**			
T / K	349.47	349.48	358.39	358.46	367.93	368.13	354	384	413	347	357	367	377
n-Hexane	1.258		1.239[c]			1.186	1.16	1.12	1.10	1.25	1.27	1.27	1.30
n-Heptane	1.346		1.332[c]			1.279	1.13	1.23	1.22				
Isooctane	1.419		1.407[c]		1.365[d]	1.354							
1-Hexene	1.151		1.134[c]			1.085	1.04	1.03	0.96				
Toluene	0.903	0.892	0.872			0.869	0.85	0.83	0.81				
Cyclohexane	0.985		0.968[c]			0.959[d]	0.91	0.90	0.84				
Ethylbenzene	1.029		1.014[c]		1.020[d]	0.982							
Methanol		1.964	1.924			1.751	1.97	1.55	1.14	2.44	2.24	2.08	1.98
Ethanol		1.811	1.713			1.549	1.70	1.30	1.01				
1-Propanol	1.555[b]	1.582		1.461	1.363	1.387	1.58	1.21	0.98				
1-Butanol	1.501[b]	1.481		1.363	1.307	1.315	1.52	1.17	0.97				
2-Propanol	1.337[b]			1.262	1.175	1.142[d]							
2-Butanol	1.176[b]	1.197		1.088	1.019	1.006[d]							
Chloroform	0.734		0.704			0.694	0.70	0.69	0.64	0.73			
TCE		0.789	0.776		0.741								

Chlorobenzene	0.954		0.936[c]			0.924[d]				
1,2-DCE	1.157	1.142	1.102	1.121[c]	1.096[d]	1.062				
Benzyl Chloride	1.559	1.545	1.486			1.452				
Ethyl acetate		1.245	1.189		1.076	1.090[d]	1.17	1.07	0.97	
Acetone		1.480	1.391			1.304	1.37	1.12	1.06	
Anisole	1.216	1.224	1.189	1.194[c]	1.173[d]	1.157				

[a] Uncertainty 4%.
[b] T=349.38 K.
[c] T=358.40 K.
[d] T = 368.19 K.
TCE = Trichloroethylene.
1,2-DCE = 1,2- Dichloroethane.

Table 4.3 also shows, in addition to the experimental data of this work, the values of γ_{13}^{∞} for stearic acid from available literature [44; 45], as stored in DDB (Dortmund Data Bank) [2]. For most solutes, we observe good agreement between literature values and those obtained in this work. Comparing γ_{13}^{∞} in stearic acid from this work to the results obtained by Alessi *et al.* (1985) [44] (by interpolation), we can find differences of less than 0.02 to 0.21 in absolute values (or mean difference less than 6 %). Comparing our result and those obtained by Alessi *et al.* (1995) [45], for methanol the difference is by nearly 24 %. In fact, if we compare the data from these two available sources, it is possible to check the inconsistence of both values of γ_{13}^{∞} itself and as function of temperature.

The discrepancy between the earlier published γ_{13}^{∞} values for some solutes and one listed in table 4.3 is probably due to different methods used to obtain the retention time, the use of different equations and different references of thermodynamic properties for calculating γ_{13}^{∞}, and the use of different inert carrier gases for the measurements. Since the new values were determined several times and using different loadings for most of the solutes the results show good agreement with references, we believe them to be more accurate.

TABLE 4.4. Experimental limiting activity coefficients, γ_{13}^{∞} [a], for solutes in oleic (*cis*-9-octadecenoic) acid, C18:1 9c, at different temperatures.

Solute	**338.36 K**	**348.29 K**	**348.36 K**	**358.28 K**
n-Hexane	1.401	1.329	1.341	1.302
n-Heptane	1.516	1.428	1.469	1.369
Isooctane	1.627	1.519	1.544	1.477
1-Hexene	1.213	1.205	1.194	1.152
Toluene	0.925	0.893	0.865	0.852
Cyclohexane	1.062	1.001	1.011	1.352
Ethylbenzene	1.052	0.991	0.964	0.962
Methanol	1.573		1.476	1.491
Ethanol	1.451		1.373	1.382
1-Propanol	1.355		1.267	1.244
1-Butanol	1.260		1.226	1.224
2-Propanol	1.199		1.122	1.113
2-Butanol	1.019		0.987	0.975
Chloroform	0.653	0.676		0.628
Trichloroethylene	0.803	0.783		0.742
Chlorobenzene	0.930	0.905		0.877
1,2-Dichloroethane	1.090	1.077		1.011
Benzyl Chloride		1.439		1.385
Ethyl acetate	1.201	1.130		1.091
Acetone	1.311	1.292		1.197
Anisole	1.204	1.170		1.153

[a] Uncertainty 4% .

TABLE 4.5. Experimental limiting activity coefficients, γ_{13}^{∞} [a], for solutes in linoleic (*cis*,*cis*-9,12-octadecadienoic) acid, C18:2 9c12c, at different temperatures.

Solute	**338.28 K**	**338.28 K**	**348.31 K**	**348.28 K**	**358.30 K**
n-Hexane	2.196		2.556	2.524	2.932
n-Heptane	2.322		2.736	2.678	3.232
Isooctane	2.434		2.975	2.962	3.632
1-Hexene	1.726		1.982	2.003	2.360
Toluene	1.097	1.094	1.165	1.192	1.263
Cyclohexane	1.493	1.486	1.709	1.704	2.026
Ethylbenzene	1.271		1.363	1.353	1.487
Methanol	1.454		1.328		
Ethanol	1.362			1.222	1.231
1-Propanol	1.288		1.242		1.220[b]
1-Butanol	1.187			1.181	
2-Propanol	1.134			1.136	1.127[b]
2-Butanol	1.089		1.101		1.100
Chloroform	0.642	0.644	0.674	0.689	0.734
Trichloroethylene					
Chlorobenzene	1.002	0.996	1.072	1.069	1.162
1,2-Dichloroethane	1.048	1.057	1.055	1.082	1.112
Benzyl Chloride			1.531	1.540	1.608
Ethyl acetate	1.228			1.267	1.115[b]
Acetone	1.213			1.161	1.133[b]
Anisole	1.242		1.292	1.317	1.369

[a] Uncertainty 4%.
[b] T= 358.33 K.

TABLE 4.6. Experimental limiting activity coefficients, γ_{13}^{∞} [a], for solutes in linolenic (*cis*,*cis*,*cis*-9,12,15-octadecatrienoic) acid, C18:3 9c12c15c, at different temperatures.

Solute	**303.13 K**	**313.24 K**	**313.25 K**	**323.26 K**
n-Hexane	3.699		2.911	3.306
n-Heptane	3.834		3.066	3.264
Isooctane	4.570		3.535	4.012
1-Hexene	2.520	2.123	2.187	2.454
Toluene			1.171	1.204
Cyclohexane	2.356	1.913	1.880	2.041
Ethylbenzene				
Methanol	1.164		1.291[b]	1.357
Ethanol	1.070		1.216	1.316
1-Propanol				1.271
1-Butanol				
2-Propanol			1.081	1.121
2-Butanol				
Chloroform	0.613		0.621[b]	0.623[c]
Trichloroethylene				
Chlorobenzene				
1,2-Dichloroethane	1.053	1.035	1.020	0.996
Benzyl Chloride				
Ethyl acetate	1.312		1.160[b]	1.178[c]
Acetone	1.099	1.057	1.101	1.111
Anisole				

[a] Uncertainty 4%.
[b] T= 313.24 K.
[c] T= 323.24 K.

In a previous work [30], we have already noted that the combination of a rather long non-polar hydrocarbon chain and the strongly polar carboxylic acid group enables fatty acids to dissolve easily both polar and non-polar compounds. In this study we could observe the influence of the presence and number of *cis* double bonds in fatty acids in the interaction with several solutes. A *cis* double bond introduces a pronounced bend in fatty acid chain and therefore causes a distinct kink in the polyunsaturated fatty acids alkyl chain [1]. The effect of the quantity of fatty acid *cis* double bonds can be seen on magnitude and trend of γ_{13}^{∞} when comparing the results obtained in saturated and mono-saturated fatty acids (stearic and oleic acids, respectively) with data from polyunsaturated fatty acids (linoleic and linolenic acids).

In terms of the overall magnitude of the γ_{13}^{∞} values (maximum around 4.6 for linolenic acid), it can be noted that unlike our previous work with saturated fatty acids [30], the values of γ_{13}^{∞} present more pronounced deviations from ideal mixture behavior. For all solvents investigated the lowest values of γ_{13}^{∞} are observed for chloroform followed by other chlorine-containing compounds (trichloroethylene, chlorobenzene and 1,2-dichloroethane) which means that independently of the presence of *cis* double bonds in the fatty acid chain, chloroform has a strong interaction with fatty acids (unsaturated or not), that can be result from van der Waals forces and polarity effects. It is also worth mentioning that chlorine-containing compounds are naturally found in fatty acids as in many other biomolecules [46].

Figures 4.2 to 4.5 show the limiting activity coefficients in stearic (octadecanoic), oleic (*cis*-9-octadecenoic), linoleic (*cis*,*cis*-9,12-octadecadienoic) and linolenic (*cis, cis, cis*-

9,12,15-octadecatrienoic) acids as function of the absolute temperature for several investigated solutes.

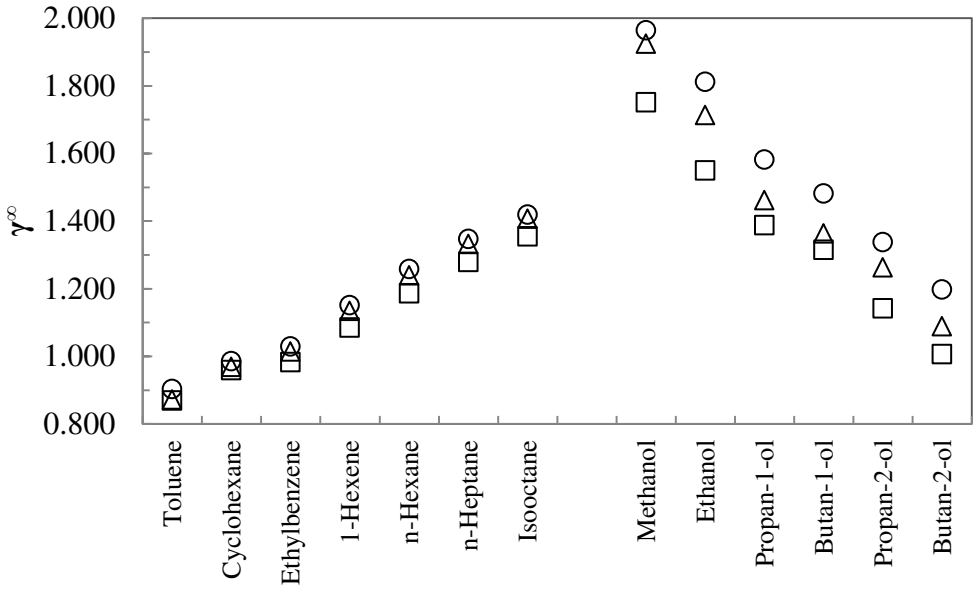

FIGURE 4.2. Plot of $\boldsymbol{\gamma_{13}^{\infty}}$ in stearic (octadecanoic) acid *versus* $\boldsymbol{T}$ for hydrocarbons and alcohols, ○ at T = 349.5 K; Δ at T = 358.4 K; and □ at T = 368.1 K.

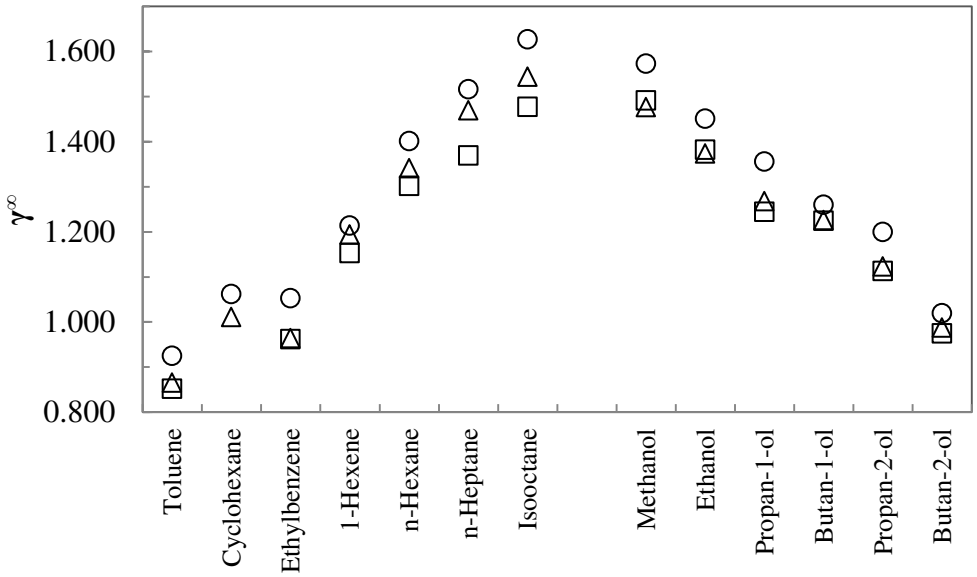

FIGURE 4.3. Plot of $\boldsymbol{\gamma_{13}^{\infty}}$ in oleic (*cis*-9-octadecenoic) acid *versus* $\boldsymbol{T}$ for hydrocarbons and alcohols, ○ at T = 338.4 K; Δ at T = 348.4 K; and □ at T = 358.3 K.

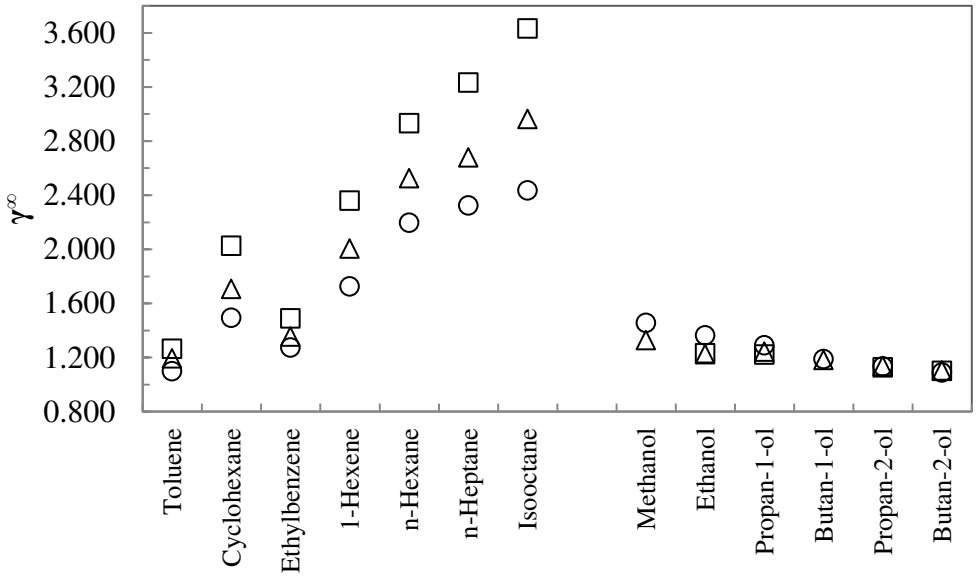

FIGURE 4.4. Plot of $\boldsymbol{\gamma_{13}^{\infty}}$ in linoleic (*cis*,*cis*-9,12-octadecadienoic) acid *versus* $\boldsymbol{T}$ for hydrocarbons and alcohols, ○ at T = 338.3 K; Δ at T = 348.3 K; and □ at T = 358.3 K.

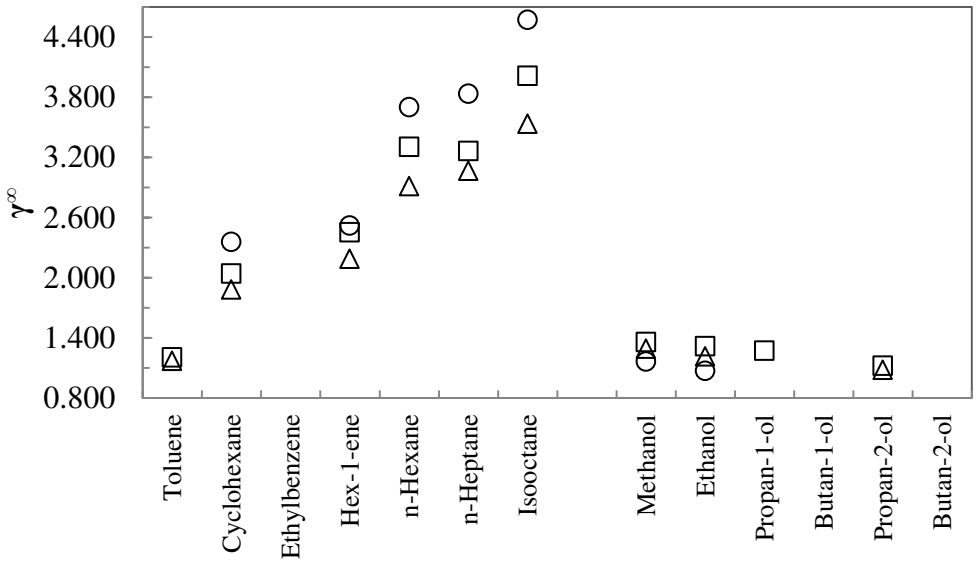

FIGURE 4.5. Plot of $\boldsymbol{\gamma_{13}^{\infty}}$ in linolenic (*cis,cis,cis*-9,12,15-octadecatrienoic) acid *versus* ***T*** for hydrocarbons and alcohols, ○ at T = 303.1 K; Δ at T = 313.3 K; and □ at T = 323.3 K.

For all solvents studied, the values of γ_{13}^{∞} for alkane (n-hexane, n-heptane and isooctane) increase with increasing solute alkyl chain and for alcohols the converse is true, i.e. γ_{13}^{∞} values decrease with increasing solute alkyl chain. For all solvents investigated, toluene shows the smallest γ_{13}^{∞} values from the hydrocarbons series studied. This is the result of the interaction between the slightly polar portion of fatty acid molecules with the localised or delocalised π-electrons clouds in benzene structure. Analysing the values of γ_{13}^{∞} for alkane, alkene and cycloalkane with the same carbon number, it was found the follow hierarchy for the γ_{13}^{∞} values in increasing order: cyclohexane < hex-1-ene < n-hexane. In the case of cycloalkanes, it should be considered that their molar volumes are smaller than those of linear alkane and alkene with the same number of carbons atoms, therefore the packing

effect additionally increases the interaction with fatty acids, the same was observed in previous work [30] and for others solvents as ionic liquids [47-49]. The alkene double bond leads to stronger mutual interactions between the fatty acids and the solute hex-1-ene than between the fatty acids and n-hexane.

As mentioned above the influence of the number of *cis* double bonds follows typical trends for some solutes: for the series of hydrocarbons (non-polar solutes), the values of γ_{13}^{∞} increase with increasing number of *cis* double bonds in the fatty acid alkyl chain. In case of alcohols (polar solutes), γ_{13}^{∞} values decrease with increasing number of *cis* double bonds in the carbon chain of the solvent. We can deduce that the increase in the *cis* double bonds in fatty acid alkyl chain implies the increase of solvent polarity, which reduces the intermolecular interaction with non-polar solvents and increases the interaction with polar solvents, as reflected in the values of γ_{13}^{∞}.

If we compare the magnitude of γ_{13}^{∞} values for non-polar and polar solutes in stearic, oleic, linoleic and linolenic acids, it is possible to observe a significant change in values of γ_{13}^{∞} due the presence of *cis* double bonds in fatty acids (see profiles of γ_{13}^{∞} values for these solutes in figures 4.2 to 4.5). For stearic acid (saturated fatty acid) higher interactions (lower γ_{13}^{∞} values) are observed with non-polar solutes, while for oleic acid (monounsaturated fatty acid) polar and non-polar solutes have the same interaction (about same magnitude of γ_{13}^{∞} values) and for linoleic and linolenic acids (polyunsaturated fatty acids) polar solutes now have higher interaction with the solvent (lower γ_{13}^{∞} values) than non-polar solutes. This is probably consequence of the presence of the hydrogen atom of *cis* double bond in fatty acid, which shows stronger acidic properties and the π-electron of

double bond causes an increase of interactions between unsaturated fatty acids with polar solutes.

For stearic and oleic acids the influence of temperature follows a typical trend for most of the solutes with increasing temperature was observed a decrease in γ_{13}^{∞} value. While for linoleic acid the opposite effect was noted for hydrocarbons solutes, in which the temperature increase was followed by an increase in γ_{13}^{∞} value. For linolenic acid, the effect of the temperature on the magnitude of γ_{13}^{∞} was more difficult to fit into a pattern.

The partial molar excess enthalpy, $\Delta H_1^{E,\infty}$, entropy, $\Delta S_1^{E,\infty}$, and Gibbs free energy, $\Delta G_1^{E,\infty}$, at infinite dilution calculated from stearic (octadecanoic), oleic (*cis*-9-octadecenoic), linoleic (*cis*,*cis*-9,12-octadecadienoic) and linolenic (*cis*,*cis*,*cis*-9,12,15-octadecatrienoic) acids experimental data are shown in table 4.7.

TABLE 4.7. Limiting values of the partial molar excess enthalpy, $\Delta H_1^{E,\infty}$[a], entropy, $\Delta S_1^{E,\infty}$, and Gibbs free energy, $\Delta G_1^{E,\infty}$, for solutes in stearic, oleic, linoleic and linolenic acid at reference temperature 298.15 K.

	Stearic Acid			**Oleic Acid**			**Linoleic Acid**			**Linolenic Acid**		
Solute	$\Delta G_1^{E,\infty}$/ kJ.mol^{-1}	$\Delta H_1^{E,\infty}$/ kJ.mol^{-1}	$T_{ref}\Delta S_1^{E,\infty}$/ kJ.mol^{-1}	$\Delta G_1^{E,\infty}$/ kJ.mol^{-1}	$\Delta H_1^{E,\infty}$/ kJ.mol^{-1}	$T_{ref}\Delta S_1^{E,\infty}$/ kJ.mol^{-1}	$\Delta G_1^{E,\infty}$/ kJ.mol^{-1}	$\Delta H_1^{E,\infty}$/ kJ.mol^{-1}	$T_{ref}\Delta S_1^{E,\infty}$/ kJ.mol^{-1}	$\Delta G_1^{E,\infty}$/ kJ.mol^{-1}	$\Delta H_1^{E,\infty}$/ kJ.mol^{-1}	$T_{ref}\Delta S_1^{E,\infty}$/ kJ.mol^{-1}
n-Hexane	1.07	3.38	2.31	1.27	3.72	2.46	0.24	-14.53	-14.77	3.27	16.84	13.57
n-Heptane	1.18	2.97	1.78	1.65	5.15	3.50	0.12	-16.62	-16.74			
Isooctane	1.26	2.59	1.33	1.77	4.89	3.12	-0.17	-20.14	-19.97			
1-Hexene	0.86	3.39	2.54	0.81	2.60	1.79	-0.52	-15.73	-15.21	2.73	15.65	12.92
Toluene							-0.62	-7.16	-6.54			
Cyclohexane	0.18	1.54	1.36				-0.80	-15.13	-14.32	2.29	13.87	11.58
Ethylbenzene	0.47	2.67	2.21	0.63	4.36	3.73	-0.34	-7.85	-7.51			
Methanol										0.30	-6.23	-6.53
Ethanol	2.80	8.98	6.18				1.37	5.08	3.72	0.06	-8.40	-8.46
1-Propanol	2.21	7.55	5.34				0.95	2.76	1.81			
1-Butanol	2.06	7.40	5.34									
2-Propanol	1.95	8.38	6.43	0.88	3.80	2.92						
2-Butanol	1.76	9.08	7.32				0.58	3.25	2.66			
Chloroform	-0.32	3.17	3.49				-1.86	-6.48	-4.61	-1.22	-0.67	0.55
TCE[b]	-0.05	3.63	3.68	-0.06	3.97	4.03						

CB[c]	0.31	2.87	2.56	0.18	2.98	2.80	-0.89	-7.50	-6.61			
1,2-DCE[d]				0.68	3.76	3.07				0.17	2.28	2.11
Ethyl acetate	1.66	3.93	2.27									
Acetone	1.77	8.27	6.50	1.03	4.88	3.86				0.26	2.15	1.89
Anisole	2.03	7.24	5.21	1.24	4.58	3.34	0.88	3.45	2.57			

[a] Uncertainty 20%.
[b] TCE = Trichloroethylene.
[c] CB = Chlorobenzene.
[d] 1,2-DCE = 1,2-Dichloroethane.

In case of the solvents stearic and oleic acids, positive values of $\Delta G_1^{E,\infty}$, and $\Delta H_1^{E,\infty}$ were found for all solutes and the entropy values are relative small and positive. The positive values for $\Delta H_1^{E,\infty}$ mean a weak association between the solutes studied and these two fatty acids. However for stearic acid, we could see the same trend as observed for others saturated fatty acids in our previous study [30]. Both for alkanes and for alcohol solutes, the calculated values of $\Delta H_1^{E,\infty}$ decrease with an increase in carbon number of the solute. Furthermore, for alcohols the decreasing $\Delta H_1^{E,\infty}$ values occur with decrease of γ_{13}^{∞} values and the opposite is observed for alkanes. In the case of polyunsaturated fatty acids we obtained negative $\Delta H_1^{E,\infty}$ values for some solutes. The negative values of partial molar excess enthalpies at infinite dilution indicate that interactions of solute-solvent pairs are higher than for solute-solute pairs. For linolenic acid, the strong association occurred with alcohols (polar solute), whereas for linoleic acid, as observed also in figure 4.4, the strong negative $\Delta H_1^{E,\infty}$ values is a result of the stark increase of γ_{13}^{∞} values with increasing temperature. It should be noted that the $\Delta H_1^{\mathrm{E},\infty}$ values for the polyunsaturated fatty acids were calculated from different ranges of temperature.

4.5. Conclusions

Limiting activity coefficients at infinite dilution for 21 solutes in four saturated and unsaturated fatty acids were measured by gas-liquid chromatography at temperatures from (303.13 to 368.19) K and compared to available literature data. The thermodynamic functions at infinite dilution for the same solutes were derived for stearic (octadecanoic), oleic (*cis*-9-octadecenoic), linoleic (*cis*,*cis*-9,12-octadecadienoic) and linolenic (*cis*,*cis*,*cis*-

9,12,15-octadecatrienoic) acids. For all solvents different trends could be identified for polar and non-polar compounds as function of temperature. It appears that both the presence and the number of *cis* double bonds in the fatty acid alkyl chain have influence on the solvent-solute and solute-solute interactions and hence on the values of γ_{13}^{∞}. These results allow a more accurate description of the real behaviour of fatty systems.

Acknowledgment

P. C. Belting wishes to acknowledge CNPq (Conselho Nacional de Desenvolvimento Científico e Tecnológico – 290128/2010-2) and DAAD (Deutscher Akademischer Autausch-Dienst – A/10/71471) for the scholarship. The authors would like to thank the CNPq (304495/2010-7, 480992/2009-6, 307718/2010-7 and 301999/2010-4), FAPESP (Fundação de Amparo à Pesquisa do Estado de São Paulo - 08/56258-8, 09/54137-1 and 2010/16634-0) and INCT-EMA (Instituto Nacional de Ciência e Tecnologia de Estudos do Meio Ambiente) for the financial support. The authors are grateful to the DDBST GmbH for permitting the use of the Dortmund Data Bank. This work has been supported by the Carl von-Ossietzky University Oldenburg.

References

[1] C. Scrimgeour, Chemistry of Fatty Acids. in: F. Shahidi, (Ed.), Bailey's Industrial Oil and Fat Products, John Wiley & Sons, Hoboken, New Jersey, 2005, pp. 606.

[2] DDB, Dortmund Data Bank Dortmund Data Bank Software & Separation Technology DDBST GmbH, Oldenburg, 2011.

[3] P.J. Wan, Properties of Fats and Oils. in: W.E.F. R. D. O'Brien, P. J. Wan, (Ed.), Introduction to Fats and Oils Technology, A.O.C.S. Press, Champaign, Illinois, 2000, pp. 20-48.

[4] R.D. O'Brien, Introduction to Fats and Oils Technology. in: W.E.F. R. D. O'Brien, and P. J. Wan, (Ed.), Fats And Oils: An Overview, AOCS Press: Champaign, Illinois, 2000, pp. 1-19.

[5] F.D. Gunstone, Vegetable Oils. in: F. Shahidi, (Ed.), Bailey's Industrial Oil and Fat ProductsJohn Wiley & Sons, Hoboken, New Jersey, 2005, pp. 606.

[6] L.W. Reeves, Trans. Faraday Soc. 55 (1959) 1684-1688.

[7] A.C. Rustan, C.A. Drevon, Fatty Acids: Structures and Properties, eLS, John Wiley & Sons, Ltd, 2001.

[8] R.D. O'Brien, Fats And Oils Processing. in: W.E.F. R. D. O'Brien, and P. J. Wan, (Ed.), Introduction to Fats and Oils Technology, A.O.C.S. Press, Champaign, Illinois, 2000, pp. 90-107.

[9] C.B. Gonçalves, E.C. Batista, A.J.A. Meirelles, J. Chem. Eng. Data 47 (2002) 416-420.

[10] E.D. Milligan, D.C. Tandy, J. Am. Oil Chem. Soc. 51 (1974) 347-350.

[11] K.F. Mattil, Deodorization. in: F.A.N. K.F. Mattil, A.J. Stirton, (Ed.), Bailey's Industrial Oil and Fat Products, John Wiley & Sons, New York, 1964, pp. 897-930.

[12] C.G. Pina, A.J.A. Meirelles, J. Am. Oil Chem. Soc. 77 (2000) 553-559.

[13] Z. Guo, X. Xu, Green Chem. 8 (2006) 54–62.

[14] L.-Z. Cheong, H. Zhang, Y. Xu, X. Xu, J. Agric. Food Chem. 57 (2009) 5020–5027.

[15] X. Xu, S. Balchena, C.-E. Høyb, J. Adler-Nissena, J. Am. Oil Chem. Soc. 75 (1998) 301-308.

[16] X. Xu, C. Jacobsenb, N.S. Nielsenb, M.T. Heinrichb, D. Zhoua, Eur. J. Lipid Sci. Technol. 104 (2002) 745-755.

[17] X. Xu, A. Skands, J. Adler-Nissen, J. Am. Oil Chem. Soc. 78 (2001) 715-718.

[18] J.M. Encinar, J.F. Gonzáles, J.J. Rodriguez, A. Tejedor, Energ. Fuel 16 (2002) 443-450.

[19] F. Ma, M.A. Hanna, Bioresource Technol. 70 (1999) 1-15.

[20] J.M. Marchetti, V.U. Miguel, A.F. Errazu, Renew. Sust. Energ. Rev. 11 (2007) 1300-1311.

[21] I.M. Atadashi, M.K. Aroua, A. Abdul Aziz, Renew. Sust. Energ. Rev. 14 (2010) 1999-2008.

[22] P. Alessi, M. Fermeglia, I. Kikic, Fluid Phase Equilibr. 70 (1991) 239-250.

[23] D. Gruber, D. Langenheim, J. Gmehling, J. Chem. Eng. Data 42 (1997) 882-885.

[24] L. Dallinga, M. Schiller, J. Gmehling, J. Chem. Eng. Data 38 (1993) 147-155.

[25] K. Kojima, S. Zhang, T. Hiaki, Fluid Phase Equilibr. 131 (1997) 145-179.

[26] M. Krummen, P. Wassrscheid, J. Gmehling, J. Chem. Eng. Data 47 (2002) 1411-1417.

[27] J. Gmehling, A. Brehm, Grundoperationen, Thieme-Verlag, Stuttgart, 1996.

[28] J. Gmehling, B. Kolbe, M. Kleiber, J. Rarey, Chemical Thermodynamics for Process Simulation, 1st ed., Wiley-VCH, Weinheim, 2012.

[29] B.E. Poling, J.M. Prausnitz, J.P. O'Connell, Properties of Gases and Liquids, 5th ed., McGraw-Hill, 2001.

[30] P.C. Belting, J. Rarey, J. Gmehling, R. Ceriani, O. Chiavone-Filho, A.J.A. Meirelles, J. Chem. Thermodyn. 55 (2012) 42-49.

[31] C. Knoop, D. Tiegs, J. Gmehling, J. Chem. Eng. Data 34 (1989) 240-247.

[32] T.M. Letcher, Activity Coefficients at Infinite Dilution from Gas-Liquid Chromatography. in: M.L. McGlashan, (Ed.), Chemical Thermodynamics, The Chemical Society, London, 1978, pp. 46-70.

[33] R. Ceriani, A.J.A. Meirelles, Fluid Phase Equilibr. 215 (2004) 227–236.

[34] B.H.J. Bielski, R.L. Arudi, M.W. Sutherland, J. Biol. Chem. 258 (1983) 4759-4761.

[35] R.J. Laub, J.H. Purnell, P.S. Williams, M.W.P. Harbison, D.E. Martire, J. Chromatogr. A 155 (1978) 233–240.

[36] D.H. Everett, Trans. Faraday Soc. 61 (1965) 1635-1639.

[37] A.J.B. Cruickshank, B.W. Ganey, C.P. Hicks, T.M. Letcher, R.W. Moody, C.L. Young, Trans. Faraday Soc. 65 (1969) 1014-1031.

[38] D.H. Everett, T.H. Stoddart, Trans. Faraday Soc. 57 (1961) 746-754.

[39] A.T. James, A.J.P. Martin, Biochem. J. 50 (1952) 679-690.

[40] DIPPR, Design Institute for Physical Properties Data Bank AIChE, [2005, 2008, 2009, 2010].

[41] H.G. Hudson, J.C. McCoubrey, Trans. Faraday Soc. 56 (1960) 761-766.

[42] J.A. Huff, T.M. Reed, J. Chem. Eng. Data 8 (1963) 306-311.

[43] W.M. Haynes, (Ed.), CRC Handbook of Chemistry and Physics, CRC Press Taylor and Francis Group, LLC, Boulder, Colorado, 2010.

[44] P. Alessi, I. Kikic, M. Orlandini, Evaluation of the Influence of Polar Groups on the Activity Coefficients at Infinite Dilution, Private Communication, 1985, pp. 1-11.

[45] P. Alessi, A. Cortesi, P. Sacomani, S. Bottini, Latin Am. Appl. Res. 25 (1995) 37-45.

[46] V.M. Dembitsky, M. Srebnik, Prog. Lipid Res. 41 (2002) 315–367.

[47] A. Marciniak, J. Chem. Thermodyn. 43 (2011) 1446-1452.

[48] P. Reddy, N.V. Gwala, N. Deenadayalu, D. Ramjugernath, J. Chem. Thermodyn. 43 (2011) 754-758.

[49] K. Paduszyński, U. Domańska, J. Phys. Chem. B 115 (2011) 8207-8215.

Appendix 4.A. Supplementary Data

Supplementary data associated with this article is table 4.S1.

TABLE 4.S1. Values of P_1^*, V_1^* B_{11} and B_{12} for all solutes in stearic acid at studied range temperature.

Solute	**T/K**	P_1^***/Pa**	V_1^***/m^3.mol^{-1}**	B_{11}**/m^3.mol^{-1}**	B_{12}**/m^3.mol^{-1}**
n-Hexane	368.13	216386	1.4671E-04	-1.090E-03	4.006E-05
n-Hexane	349.47	127638	1.4198E-04	-1.249E-03	3.955E-05
n-Hexane	358.40	165592	1.4417E-04	-1.169E-03	3.980E-05
n-Heptane	368.13	91512	1.6213E-04	-1.559E-03	4.692E-05
n-Heptane	349.47	50333	1.5757E-04	-1.824E-03	4.637E-05
n-Heptane	358.40	67611	1.5969E-04	-1.689E-03	4.664E-05
Isooctane	368.13	90538	1.8176E-04	-1.657E-03	4.738E-05
Isooctane	349.47	50607	1.7685E-04	-1.911E-03	4.683E-05
Isooctane	358.40	67428	1.7914E-04	-1.782E-03	4.710E-05
Isooctane	368.19	90692	1.8177E-04	-1.656E-03	4.738E-05
1-Hexene	368.13	250288	1.4144E-04	-9.829E-04	3.787E-05
1-Hexene	349.47	149694	1.3659E-04	-1.121E-03	3.739E-05
1-Hexene	358.40	192888	1.3884E-04	-1.051E-03	3.763E-05
Toluene	349.48	34160	1.1295E-04	-1.655E-03	3.330E-05
Toluene	368.13	63554	1.1561E-04	-1.417E-03	3.383E-05
Toluene	358.39	46398	1.1419E-04	-1.534E-03	3.356E-05
Toluene	349.47	34147	1.1295E-04	-1.656E-03	3.330E-05
Cyclohexane	349.47	88608	1.1609E-04	-1.113E-03	3.065E-05
Cyclohexane	358.40	115912	1.1754E-04	-1.035E-03	3.090E-05
Cyclohexane	368.19	152925	1.1919E-04	-9.584E-04	3.116E-05
Ethylbenzene	368.13	28874	1.3244E-04	-1.936E-03	3.997E-05
Ethylbenzene	349.47	14544	1.2961E-04	-2.287E-03	3.940E-05
Ethylbenzene	358.40	20410	1.3094E-04	-2.108E-03	3.969E-05
Ethylbenzene	368.19	28931	1.3244E-04	-1.935E-03	3.998E-05

Methanol	349.48	158180	4.3476E-05	-7.634E-04	2.561E-05
Methanol	368.13	300698	4.4761E-05	-5.858E-04	2.604E-05
Methanol	358.39	217011	4.4071E-05	-6.691E-04	2.582E-05
Ethanol	349.48	93577	6.2522E-05	-1.041E-03	3.221E-05
Ethanol	368.13	189820	6.4251E-05	-7.661E-04	3.266E-05
Ethanol	358.39	132590	6.3323E-05	-8.946E-04	3.243E-05
1-Propanol	358.46	63492	8.0736E-05	-1.107E-03	3.778E-05
1-Propanol	349.38	43178	7.9772E-05	-1.240E-03	3.754E-05
1-Propanol	367.93	92524	8.1794E-05	-9.917E-04	3.803E-05
1-Propanol	349.48	43369	7.9783E-05	-1.238E-03	3.754E-05
1-Propanol	368.13	93237	8.1817E-05	-9.895E-04	3.803E-05
1-Butanol	358.46	27871	9.8388E-05	-1.566E-03	4.216E-05
1-Butanol	349.38	18326	9.7311E-05	-1.719E-03	4.189E-05
1-Butanol	367.93	41993	9.9564E-05	-1.427E-03	4.242E-05
1-Butanol	368.13	42345	9.9589E-05	-1.425E-03	4.242E-05
2-Propanol	358.46	114121	8.3353E-05	-1.076E-03	3.987E-05
2-Propanol	349.38	78954	8.2230E-05	-1.214E-03	3.963E-05
2-Propanol	367.93	163703	8.4598E-05	-9.579E-04	4.010E-05
2-Propanol	349.48	79286	8.2242E-05	-1.212E-03	3.964E-05
2-Propanol	368.13	164913	8.4625E-05	-9.557E-04	4.011E-05
2-Butanol	358.46	58378	9.9979E-05	-1.259E-03	4.183E-05
2-Butanol	349.38	39548	9.8620E-05	-1.372E-03	4.157E-05
2-Butanol	367.93	85290	1.0147E-04	-1.157E-03	4.208E-05
2-Butanol	349.48	39725	9.8635E-05	-1.370E-03	4.157E-05
2-Butanol	368.19	86143	1.0151E-04	-1.154E-03	4.208E-05
Chloroform	349.47	161892	8.6321E-05	-8.029E-04	2.462E-05
Chloroform	358.40	209014	8.7495E-05	-7.562E-04	2.486E-05
Chloroform	368.19	272088	8.8853E-05	-7.102E-04	2.510E-05
Trichloroethylene	358.46	95342	9.7160E-05	-1.127E-03	2.741E-05

Trichloroethylene	349.38	71705	9.5983E-05	-1.255E-03	2.716E-05
Trichloroethylene	367.93	125877	9.8440E-05	-1.017E-03	2.766E-05
Trichloroethylene	368.13	126592	9.8468E-05	-1.015E-03	2.767E-05
Trichloroethylene	358.39	95144	9.7151E-05	-1.128E-03	2.741E-05
Trichloroethylene	349.47	71915	9.5995E-05	-1.254E-03	2.716E-05
Chlorobenzene	358.46	23607	1.0858E-04	-1.654E-03	3.221E-05
Chlorobenzene	349.38	16851	1.0755E-04	-1.806E-03	3.192E-05
Chlorobenzene	367.93	32879	1.0969E-04	-1.522E-03	3.249E-05
Chlorobenzene	349.48	16916	1.0756E-04	-1.804E-03	3.193E-05
Chlorobenzene	368.13	33103	1.0972E-04	-1.519E-03	3.249E-05
Chlorobenzene	358.39	23548	1.0857E-04	-1.655E-03	3.221E-05
1,2-Dichloroethane	349.38	79569	8.4721E-05	-9.827E-04	2.695E-05
1,2-Dichloroethane	349.48	79831	8.4733E-05	-9.819E-04	2.696E-05
1,2-Dichloroethane	368.13	141698	8.7000E-05	-8.552E-04	2.748E-05
1,2-Dichloroethane	358.39	105933	8.5791E-05	-9.179E-04	2.722E-05
1,2-Dichloroethane	358.40	105952	8.5792E-05	-9.178E-04	2.722E-05
1,2-Dichloroethane	368.19	141935	8.7007E-05	-8.549E-04	2.748E-05
Benzyl Chloride	349.48	2829	1.2090E-04	-3.459E-03	3.906E-05
Benzyl Chloride	368.13	6384	1.2311E-04	-2.764E-03	3.970E-05
Benzyl Chloride	358.39	4224	1.2194E-04	-3.091E-03	3.938E-05
Benzyl Chloride	349.47	2827	1.2090E-04	-3.459E-03	3.906E-05
Ethylacetate	367.93	175842	1.0949E-04	-1.081E-03	3.642E-05
Ethylacetate	349.48	98962	1.0619E-04	-1.267E-03	3.592E-05
Ethylacetate	358.39	131787	1.0774E-04	-1.171E-03	3.617E-05
Ethylacetate	368.19	177173	1.0954E-04	-1.079E-03	3.643E-05
Acetone	349.48	192101	8.0140E-05	-1.056E-03	2.863E-05
Acetone	368.13	324429	8.2947E-05	-8.741E-04	2.910E-05
Acetone	358.39	248689	8.1438E-05	-9.619E-04	2.886E-05
Anisole	349.48	7171	1.1474E-04	-2.371E-03	3.771E-05

Anisole	368.13	15403	1.1701E-04	-2.170E-03	3.828E-05
Anisole	358.39	10462	1.1580E-04	-2.287E-03	3.799E-05
Anisole	349.47	7167	1.1473E-04	-2.372E-03	3.771E-05
Anisole	358.40	10465	1.1580E-04	-2.287E-03	3.799E-05
Anisole	368.19	15437	1.1701E-04	-2.169E-03	3.828E-05

CAPÍTULO 5: MEASUREMENTS OF ACTIVITY COEFFICIENTS AT INFINITE DILUTION IN VEGETABLE OILS AND CAPRIC ACID USING THE DILUTOR TECHNIQUE

Artigo submetido à revista Fluid Phase Equilibria.

Measurements of Activity Coefficients at Infinite Dilution in Vegetable Oils and Capric Acid Using the Dilutor Technique

Patrícia C. Belting[a,b,1], Jürgen Rarey[a], Jürgen Gmehling[a], Roberta Ceriani[c], Osvaldo Chiavone-Filho[d], Antonio J. A. Meirelles[b,*]

[a] *Carl von Ossietzky Universität Oldenburg, Technische Chemie (FK V), D-26111 Oldenburg, Federal Republic of Germany*

[b] *Food Engineering Department, Faculty of Food Engineering, University of Campinas, Av. Monteiro Lobato 80, Cidade Universitária Zeferino Vaz, 13083-862, Campinas-SP, Brazil*

[c] *Faculty of Chemical Engineering, University of Campinas, Av. Albert Einstein 500, Cidade Universitária Zeferino Vaz, 13083-852, Campinas-SP, Brazil*

[d] *Chemical Engineering Department, Federal University of Rio Grande do Norte, Av. Senador Salgado Filho S/N, 59066-800, Natal-RN, Brazil*

[1] [a] *Present address,* [b] *Permanent address*

Abstract

This paper reports experimental activity coefficients at infinite dilution, γ_i^{∞}, for methanol, ethanol and n-hexane in three refined vegetable oils: soybean oil, sunflower oil, and rapeseed oil measured using the dilutor technique (inert gas stripping method). The measurements were carried out in the temperature range between 313.15 K to 353.15 K. Furthermore, activity coefficients at infinite dilution for various solutes (acetone, methanol, ethanol, n-hexane, cyclohexane and toluene) were measured in capric (decanoic) acid using the same technique at temperatures from 313.13 K to 353.30 K. The new data obtained for capric acid and soybean oil were compared with already published experimental data.

Additionally, densities of the investigated vegetable oils were measured in the temperature range from 293.15 K to 353.15 K. Using the experimental γ_i^{∞} values obtained over the temperature range, the partial molar excess Gibbs energy ($\Delta G_i^{E,\infty}$), enthalpy ($\Delta H_i^{E,\infty}$), and entropy ($\Delta S_i^{E,\infty}$), at infinite dilution were determined. The relative error for the γ_i^{∞} measurements carried out using the dilutor technique is approximately ± 2.5 %. The measured γ_i^{∞} data in the investigated refined vegetable oils were also compared with the results of the group contribution methods original UNIFAC and modified UNIFAC (Dortmund) and an extension of the latter method to triacylglycerols was proposed.

Keywords: Limiting activity coefficient, Fatty compounds, Inert gas stripping method, original UNIFAC model, Modified UNIFAC (Dortmund) model.

5.1. Introduction

Natural vegetable oils are composed primarily of triacylglycerols (TAGs), a ester of one molecule of glycerol and three molecules of fatty acids, and some minor components such as free fatty acids (FFA), partial acylglycerols (mono- and diacylglycerols) and also small amounts of other compounds such as phospholipids, sterols, tocopherols and tocotrienols, vitamins, carotenes, chlorophylls, and other coloring matters [1-4]. When refined, they are subjected to several purification steps, therefore they are composed mainly of TAGs (above 98 %) [3, 5].

Some vegetable oils dominate production and export and have become more dominant with the passage of time. These are soybean oil (produced mainly in the United States,

Brazil, Argentina, and China), palm oil (Malaysia and Indonesia), rapeseed oil (China, European Union, India, and Canada), and sunflower oil (Russia, European Union, and Argentina) [1]. Thereby, soybean, rapeseed, and sunflower oils, along with four materials of animal origin and more nine other vegetable oils are treated as commodity [1, 6], and for this reason were chosen for this study.

The application of vegetable oils in the processing of food products as feedstock or ingredient is well-known. However there are several non-edible industrial products manufactured from vegetable oils, such as biodiesel [7-10], soap, detergents and surfactants [6, 11, 12], lubricants [13], polymers [14], pharmaceutical and cosmetics products [15], paint and varnishes [16], and textile products [17]. In many of these industries, as well as in industrial extraction and refining of edible vegetable oils [18-23] and in the production and purification of partial acylglycerols [24-28], there are several separation and purification stages which are important for the final product quality and in the economics of these processes. Thereby equilibrium relationships and thermodynamical properties, such as activity coefficient at infinite dilution (γ_i^{∞}), are required for the reliable design, optimization and modeling of thermal separation processes [29, 30] and for development of new thermodynamic models as well as for the adjustment of reliable model parameters [30-32].

This paper is a part of our ongoing systematic measurements of thermophysical properties of fatty compounds for the development of predictive thermodynamic models. In previous papers, activity coefficients at infinite dilution (γ_i^{∞}) of twenty one solutes in

saturated and unsaturated fatty acids (capric, lauric, myristic, palmitic, stearic, oleic, linoleic, and, linolenic acids) have already been reported [33, 34].

In this work, activity coefficients at infinite dilution (γ_i^{∞}) of methanol, ethanol and n-hexane in three refined vegetable oils (soybean, sunflower, and rapeseed oils), at temperatures from 313.15 K to 353.15 K, have been measured using the dilutor technique (inert gas stripping method). Additionally, densities of the investigated vegetable oils were measured in temperature range from 293.15 K to 353.15 K. The experimental γ_i^{∞} data were compared to the results predicted by original UNIFAC [35, 36] (UNIFAC) and modified UNIFAC (Dortmund) [37, 38] (mod. UNIFAC) methods and were used to calculate the values of partial molar excess Gibbs free energy, ($\Delta G_i^{E,\infty}$), enthalpy ($\Delta H_i^{E,\infty}$), and entropy ($\Delta S_i^{E,\infty}$) at infinite dilution over the temperature range. Based on these results a modification of mod. UNIFAC for an improved description of γ_i^{∞} in triacylglycerols was proposed. Furthermore, activity coefficients at infinite dilution for various solutes (acetone, methanol, ethanol, n-hexane, cyclohexane and toluene) were measured in capric (decanoic) acid using the dilutor technique at temperatures from 313.13 K to 353.30 K. The new experimental data obtained for capric acid and soybean oil were compared with those available in literature [33, 39].

5.2. Experimental

5.2.1. Materials

The chemicals used in this work including their purity and the suppliers are summarized in Table 5.1. Refined soybean oil was purchased from Vandermoortele Deutschland GmbH, refined sunflower oil and refined rapeseed oil were purchased from Brökelmann + Co and Oelmühle GmbH + Co. Before the measurements the refined vegetable oils were dried over molecular sieve and subjected to vacuum (absolute pressure about 5 kPa) for at least 24 hours to remove volatile impurities. The water content of all chemicals and vegetable oil was determined by Karl Fischer titration and was less than 100 $\mathrm{mg.kg^{-1}}$.

Table 5.1. Information about the chemicals used.

Component	**Purity (GC) Mass fraction**	**W[a]/ (mg.kg^{-1})**	**Supplier**
Methanol	> 0.998	80	VWR International GmbH
Ethanol	> 0.998	48	VWR International GmbH
Acetone	> 0.999	50	Fisher Scientific
n-Hexane	> 0.99	30	Carl Roth GmbH
Cyclohexane	> 0.998	28	Fisher Scientific
Toluene	> 0.999	33	AnalaR Normapur
Capric Acid	> 0.99		Lancaster Synthesis

[a] W = Water content.

The fatty acid (FA) compositions of the refined vegetable oils studied in this work are presented in Table 5.2. These compositions were determined by gas chromatography of fatty acid methyl esters using the official method (1-62) of the American Oil Chemists' Society (AOCS) [40]. Prior to the chromatographic analysis, the fatty acids of the refined vegetable oils were converted to their corresponding methyl esters according to the method of Hartman and Lago [41], as used by Lanza et al. [42], Silva et al. [43] and Follegatti-Romero et al. [44]. The samples were submitted to a CGC Agilent 6850 Series CG capillary gas chromatography system under the following experimental conditions: DB-23 Agillent capillary column (50 % cyanopropyl-methylpolysilloxane), 0.25 μm, 60 m x 0.25 mm i.d.; helium as carrier gas at a rate of 1.0 $\mathrm{mL.\,min^{-1}}$; linear velocity of 24 $\mathrm{cm.\,s^{-1}}$; split ratio 1:50; injection temperature of 523.15 K; injection volume $10^{-3}\mathrm{cm^3}$; column temperature of 383.15 K for 5 min, 383.15 K to 523.15 K at rate of 5 $\mathrm{K.\,min^{-1}}$, followed by 488.15 K for 24 min; and detection temperature of 553.15 K. The fatty acid methyl esters were identified by comparison with the retention times of the Nu Check Prep (Elysian/MN, U. S. A.) standards, and the quantification was performed by internal normalization.

The free fatty acid content of refined vegetable oils expressed as mass fractions of oleic acid was determined by titration according to the official AOCS method Ca 5a-40 [40]. The Iodine value (IV) was calculated from the fatty acid composition according to the official AOCS method Cd 1c-85 [40].

Table 5.2. Fatty acid composition of refined vegetable oils.

Fatty Acid Nomenclature				M^a/	**Soybean oil**		**Sunflower oil**		**Rapeseed oil**	
IUPAC	**Trivial**	**Symbol**	**Cz:y**[b]	$(\mathbf{g.mol^{-1}})$	**100** x^c	**100** w^d	**100** x	**100** w	**100** x	**100** w
dodecanoic	Lauric	L	C12:0	200.32	0.05	0.03	0.07	0.05	0.06	0.05
tetradecanoic	Myristic	M	C14:0	228.38	0.10	0.09	0.11	0.09	0.09	0.07
pentadecanoic			C15:0	242.40	0.04	0.04	0.05	0.04	0.04	0.04
hexadecanoic	Palmitic	P	C16:0	256.43	11.46	10.55	6.94	6.36	4.89	4.46
cis-hexadec-9-enoic	Palmitoleic	Po	C16:1	254.42	0.11	0.10	0.13	0.12	0.22	0.20
heptadecanoic	Margaric	Ma	C17:0	270.45	0.09	0.09	0.04	0.04	0.06	0.06
cis-heptadeca-10-enoic			C17:1	268.43	0.06	0.06	0.04	0.04	0.07	0.07
octadecanoic	Stearic	S	C18:0	284.49	3.40	3.47	3.02	3.07	1.78	1.79
cis-octadeca-9-enoic	Oleic	O	C18:1	282.47	28.90	29.30	25.52	25.76	62.98	63.18
cis,cis-octadeca-9,12-dienoic	Linoleic	Li	C18:2	280.45	48.73	49.04	62.47	62.61	18.64	18.56
trans-trans-octadeca-9,12-dienoic	Linoelaidic		C18:2T[e]	278.44	0.19	0.19	0.40	0.40	0.10	0.10
all-*cis*-octadeca-9,12,15-trienoic	Linolenic	Le	C18:3	278.44	5.20	5.20	0.09	0.09	7.47	7.39
all-*trans*-octadeca-9,12,15-trienoic			C18:3T[e]	278.44	0.57	0.57			1.14	1.13
icosanoic	Arachidic	A	C20:0	312.54	0.32	0.36	0.21	0.23	0.51	0.57

cis-icos-9-enoic	Gadoleic	Ga	$C_{20:1}$	310.52	0.27	0.30	0.20	0.22	1.27	1.40
docosanoic	Behenic	Be	$C_{22:0}$	340.59	0.38	0.47	0.52	0.64	0.25	0.30
docos-13-enoic	Erucic		$C_{22:1}$	338.57					0.34	0.40
tetracosanoic	Lignoceric	Lg	$C_{24:0}$	368.65	0.12	0.16	0.18	0.24	0.10	0.13
cis-tetracos-15-enoic	Nervonic	Ne	$C_{24:1}$	366.63					0.10	0.13
FFA[f]						0.0002		0.0002		0.0002
W[g]/ $mg.kg^{-1}$						< 72		< 73		< 70
IV[h]						123.18		130.67		107.43

[a] *M* = Molar mass; [b] C z:y, where z = number of carbons and y = number of double bonds; [c] molar fraction; [d] mass fraction; [e]Trans isomers; [f] Free fatty acid in mass fraction of oleic acid; [g] W = Water content; [h] IV = calculated Iodine value.

The probable triacylglycerol (TAG) compositions (Table 5.3) were obtained by gas chromatography and by an algorithm suggested by Antoniossi Filho at al. [45]. The sample diluted in tetrahydrofuran (10 $\mathrm{mg.\,mL^{-1}}$) were submitted to a CGC Agilent 6850 Series CG capillary gas chromatograph system under the following experimental conditions: DB-17 HT Agilent Catalog: 122-1811 capillary column (50% phenyl-methylpolysiloxane), 0.15 μm, 10 m x 0.25 mm i.d.; helium as carrier gas at rate of 1.0 $\mathrm{ml.\,min^{-1}}$; linear velocity of 40 $\mathrm{cm.\,s^{-1}}$; injection temperature of 633.15 K; column temperature 523.15 K to 623.15 K at a rate of 5 $\mathrm{K.\,min^{-1}}$, followed by 623.15 K for 20 min; detection temperature of 648.2 K; and injection volume of $10^{-3}\mathrm{cm^3}$, split 1:100. Most TAG groups were identified by comparison with the retention times of the Nu Check Prep (Elysian/MN, U. S. A.) standards. Since it is not possible to identify all peaks due to the lack of standards, for determination of the complete TAG composition the results of the algorithm developed by Antoniossi Filho et al. [45] were also used. The TAG group quantification was performed by internal normalization. As input data to the algorithm, the quantities of trans isomers (see table 5.2) were computed with their respective cis isomers, as suggested by Follegatti-Romero et al. [44].

The average molar mass of the vegetable oils was calculated using their respective fatty acid compositions (Table 5.2), assuming that all fatty acids are esterified to glycerol molecules to form triacylglycerols. The values obtained for the refined soybean, sunflower and rapeseed oils are 874.04 $\mathrm{g.\,mol^{-1}}$, 875.55 $\mathrm{g.\,mol^{-1}}$, and 882.83 $\mathrm{g.\,mol^{-1}}$, respectively.

Table 5.3. Probable triacylglycerol composition of refined vegetable oils.

		M^a/	Soybean oil		Sunflower oil		Rapeseed oil	
main TAG[b]	**Cz:y[c]**	**(g. mol^{-1})**	**100 x^d**	**100 w^e**	**100 x**	**100 w**	**100 x**	**100 w**
POP	C50:1[c]	833.36	1.46	1.40			0.55	0.52
PLiP	C50:2	831.34	3.29	3.14	1.34	1.27		
POS	C52:1	861.42	0.89	0.89			0.59	0.58
POO	C52:2	859.40	5.42	5.35	2.06	2.02	8.26	8.07
POLi	C52:3	857.38	11.92	11.74	7.79	7.63	5.94	5.79
PLeO	C52:4	855.36					2.83	2.75
PLiLi	C52:4	855.36	14.85	14.59	11.80	11.52		
PLeLi	C52:5	853.35	1.95	1.91				
SOO	C54:2	887.46	1.74	1.77	0.66	0.67	2.66	2.68
SOLi	C54:3	885.43	6.87	6.99	3.60	3.64		
OOO	C54:3	885.43	2.79	2.83	2.69	2.72	34.98	35.21
OOLi	C54:4	883.42	13.39	13.58	16.74	16.89	23.44	23.54
OLiLi	C54:5	881.40	16.61	16.82	29.60	29.80		
OOLe	C54:5	881.40					14.39	14.42
LiLiLi	C54:6	879.38	16.95	17.12	23.71	23.82		
OLiLe	C54:6	879.38					4.15	4.15
LiLiLe	C54:7	877.37	1.87	1.88				
OOA	C56:2	915.51					0.60	0.63
OOGa	C56:3	913.50					1.00	1.04
OLiGa	C56:4	911.48					0.60	0.62

[a] M = Molar mass; [b] Groups with a total triacylglycerol (TAG) composition lower than 0.5 % were ignored; [c] C z:y, where z = number of carbons (except carbons of glycerol) and y = number of double bonds; [d] molar fraction; [e] mass fraction.

5.2.2. Apparatus and Experimental Procedure

The dilutor (inert gas stripping) technique was used for the measurements of the activity coefficients at infinite dilution, γ_i^{∞}, for methanol, ethanol and n-hexane in refined soybean, sunflower and rapeseed oils and for various solutes (acetone, methanol, ethanol, n-hexane, cyclohexane and toluene) in capric (decanoic) acid. The apparatus and principle of the method have been described in previous papers [46, 47]. The equipment follows the same principle as proposed by Leroi et al. [48], improved by Richon et al. [49, 50] and optimized by Krummen [51].

In the dilutor apparatus, a highly diluted component, the solute ($x_i < 10^{-3}$), is injected into the measurement cell via a septum and it is stripped under isothermal conditions from a solvent or solvent mixture (in our case refined vegetable oil) by a constant inert gas flow (helium with mass fraction purity > 0.99996). As shown in previous work [47], the dilutor technique is particularly suited for the measurements of limiting activity coefficients in solvent mixtures because the use of the saturator cell guarantees a constant solvent composition in the measurement cell (the double cell technique was discussed in detail by Bao and Han [52, 53]). The flow of the carrier gas helium was controlled and measured by using a digital mass flow controller (Bronkhorst Hi-TEC; F-201-RA 33V). In the measurements, the typical carrier gas flow rate used (helium) was 10 $\mathrm{cm}^3.\mathrm{min}^{-1}$ to 15 $\mathrm{cm}^3.\mathrm{min}^{-1}$.

The limiting activity coefficient can be determined by measuring the composition of the carrier gas leaving the measurement cell by a gas chromatograph (Hewlett-Packard; HP

6890) as a function of time. To guarantee reliable γ_i^∞ values, at least 15 % of the solute was removed from the system during the measurement, as recommended by Krummen et al. [54]. Phase equilibrium can be assumed as very small gas bubbles are generated via a capillary and the residence time in the solvent is further improved by stirring.

The γ_i^∞ was calculated by equation (5.1):

$$\gamma_i^\infty = -\frac{n_{solv}RT}{\varphi_i^S P_i^S \left[\frac{F_{He}\left(1+P_{solv}^S/P\right)}{a}+V_g\right]} \tag{5.1}$$

where n_{solv} is the number of moles of solvent in the measurement cell; R is the general gas constant; T is the absolute measurement cell temperature; φ_i^S and P_i^S are the saturation fugacity coefficient and saturation vapor pressure of the solute i, respectively; F_{He} is the carrier gas flow rate; P_{solv}^S is the saturation vapor pressure of the solvent; P is the measurement cell pressure; V_g is the vapor volume in measurement cell; a is the slope of the natural logarithm of the peak area of the solute i versus time.

The activity coefficients at infinite dilution were determined as a function of temperature, therefore $\Delta H_i^{E,\infty}$ can be calculated from the Gibbs-Helmholtz equation[32]:

$$\left(\frac{\partial ln\gamma_i^\infty}{\partial 1/T}\right)_{P,x} = \frac{\Delta H_i^{E,\infty}}{R} \tag{5.2}$$

and $\ln \gamma_i^\infty$ can be directly related to excess thermodynamics functions at infinite dilution by the following expression:

$$ln\,\gamma_i^\infty = \frac{\mu_i^{E,\infty}}{RT} = \frac{\Delta H_i^{E,\infty}}{RT} - \frac{\Delta S_i^{E,\infty}}{R} \tag{5.3}$$

Assuming a linear dependence of $\ln \gamma_i^\infty$ on the reciprocal absolute temperature ($ln\,\gamma_i^\infty = {}^{c}/_{T} + b$), the partial molar excess enthalpy at infinite dilution, $\Delta H_i^{E,\infty}$, can be estimated

from the slope "c", and the partial molar excess entropy at infinite dilution, $\Delta S_i^{E,\infty}$, from the intercept "b".

The thermophysical properties required for calculating the activity coefficients at infinite dilution were taken from the Dortmund Data Bank (DDB) [55] and the Design Institute for Physical Properties (DIPPR) data bank [56]. The P_i^s and the P_{solv}^s for capric acid were calculated from Wagner constants stored in the DDB, the P_{solv}^s values for refined vegetable oil were estimated according to the group contribution method proposed by Ceriani and Meirelles [57] using their compositions (Table 5.3), and the second virial coefficients of pure solutes, used to calculate φ_i^s, were obtained from the respective DIPPR correlations. The V_g was obtained from the amount and density of solvent and the well-known cell volume. The vapor pressures of the refined vegetable oils and capric acid are very low; therefore we could assume a constant amount of solvent in the measurement cell. This was also confirmed by weighing the cell before and after each measurement. The densities of the refined vegetable oils were measured with a vibrating tube densimeter (Anton Paar Model 4500) with a precision of (5.10^{-5}g.cm^{-3}) and the values are given in Table 5.4, the density of capric acid was taken from the DDB.

Table 5.4. Density of refined vegetable oils in the temperature range from (293.15 to 353.15) K.

Soybean Oil		**Sunflower Oil**		**Rapeseed Oil**	
T/K	$\boldsymbol{\rho}^{a}$**/** $(\mathbf{g.cm^{-3}})$	**T/K**	$\boldsymbol{\rho}$**/** $(\mathbf{g.cm^{-3}})$	**T/K**	$\boldsymbol{\rho}$**/** $(\mathbf{g.cm^{-3}})$
293.16	0.92014	293.16	0.92062	293.16	0.91728
303.14	0.91332	303.14	0.91382	303.14	0.91046
313.14	0.90651	313.14	0.90702	313.13	0.90368
323.13	0.89977	323.13	0.90028	323.13	0.89691
333.14	0.89306	333.15	0.89357	333.13	0.89019
343.13	0.88640	343.14	0.88690	343.14	0.88360
353.12	0.87976	353.13	0.88027	353.14	0.87695

[a] uncertainty ± 0.00005 $\mathrm{g.cm^{-3}}$.

The experiments were carried out at different temperatures in the range from 313.13 K to 353.30 K. The estimated relative error in γ_i^{∞} and $\Delta H_i^{E,\infty}$ are approximately 2.5% and 20 %, respectively, taking into account the accuracy of the temperature (± 0.05 K), the cross virial coefficient (< 0.2%), the saturation fugacity coefficient (± 0.5 %), the helium flow rate (< 0.85 %) and the solute vapor pressure (< 0.5%).

5.3. Results and Discussion

Table 5.5 and Figs. 5.1 and 5.2 present the experimental activity coefficient at infinite dilution, γ_i^{∞}, for the solvent capric acid from this work, measured with the help of dilutor technique, and from available literature [33], measured with the help of gas-liquid chromatography method (GLC). Although the reproducibility and reliability of the method and equipment used in this work have already been proved on several previous studies for

pure solvents [46, 52, 54, 58-61] and solvents mixtures [47, 52, 53, 62, 63], the data obtained for capric acid by these two methods were compared in order to evaluate the performance of dilutor technique for fatty compounds.

Table 5.5. Experimental data of γ_i^{∞} for several solutes in capric acid from this work [a] and from literature [b].

T/K	**Acetone**	**T/K**	**Methanol**	**T/K**	**Ethanol**
313.20	1.583	313.13	2.224	313.13	2.196
314.10	1.558*	314.24	2.140*	313.24	2.115*
333.22	1.538	333.38	1.845*	314.24	2.067*
333.26	1.458*	353.08	1.462*	318.11	2.025
333.38	1.466*	353.30	1.569*	328.15	1.704
353.23	1.496			333.14	1.757
353.25	1.343*			333.26	1.728*
				333.38	1.783*
				338.13	1.611
				353.30	1.478*
T/K	n-Hexane	T/K	Cyclohexane	T/K	Toluene
313.17	1.918	313.13	1.470	314.10	1.151*
314.10	1.752*	314.10	1.436*	314.24	1.174*
314.24	1.774*	314.24	1.461*	333.11	1.162
318.19	1.915	333.26	1.386*	333.26	1.122*
328.21	1.759	333.38	1.391*	333.38	1.116*
333.26	1.731*	353.19	1.344	353.25	1.144*
333.38	1.696*	353.25	1.352*	353.30	1.156*
338.11	1.692	353.30	1.309*		
353.30	1.653*				

[a] uncertainty 2.5%; [b] uncertainty 4%; * data from ref.: [33].

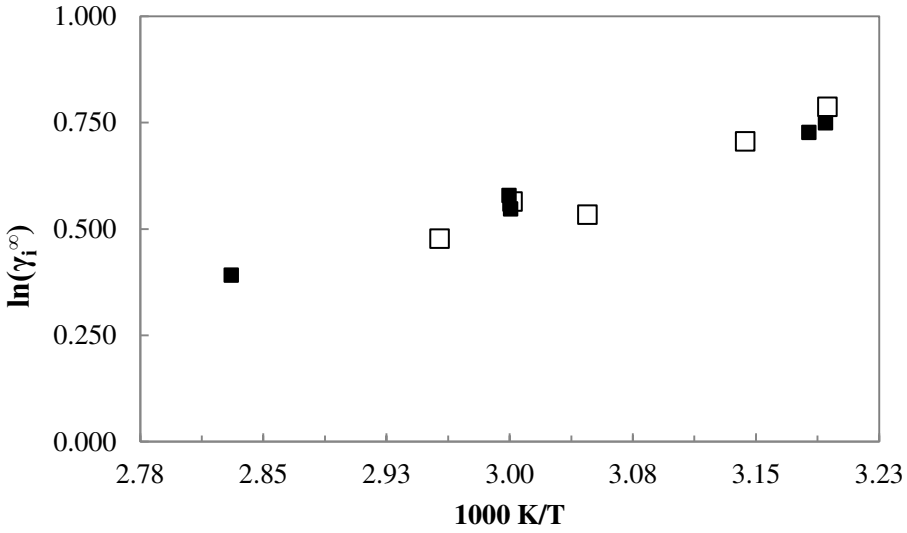

Fig. 5.1. Comparison of the experimental γ_i^{∞} data from (■) this work with (□) published data [33] for ethanol in capric acid.

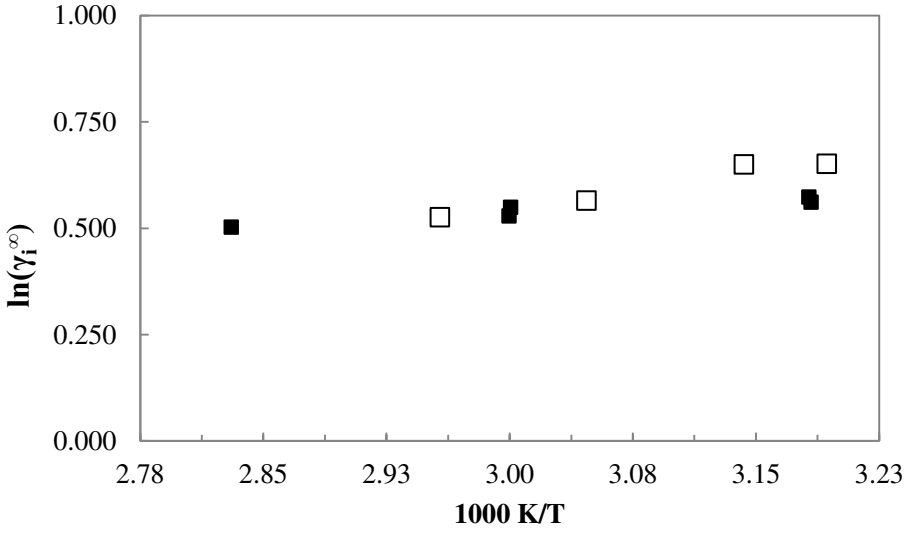

Fig. 5.2. Comparison of the experimental γ_i^{∞} data from (■) this work with (□) published data [33] for n-hexane in capric acid.

The data obtained in this work measured by dilutor technique are in good agreement with data from Belting et al. measured by gas-liquid chromatography (GLC) [33]. Comparing the data of γ_i^∞ for capric acid of this work to the literature (by interpolation), the data measured show differences of less than 0.001 to 0.168 in absolute values and the average deviation is below 2 %. The differences between values measured by the dilutor technique and GLC method can be justified by their uncertainties, 2.5 % and 4 %, respectively.

The experimental γ_i^∞ data of the solutes: methanol, ethanol and n-hexane in refined vegetable oils and the data predicted by UNIFAC (original) and mod. UNIFAC (Dortmund) are listed in Tables 5.6 to 5.8. Table 5.6 present also the experimental values of γ_i^∞ for soybean oil from the available literature [39]. The predictions of activity coefficient at infinite dilution by the group contribution methods were performed considering the probable triacylglycerol compositions of refined vegetable oils shown in Table 5.3.

Figs. 5.3 to 5.5 depict the natural logarithm of limiting activity coefficients in the refined soybean, sunflower and rapeseed oils as function of the inverse absolute temperature for all investigated solutes, respectively. Fig. 5.3 shows also the published data.

Table 5.6. Experimental data from this work[a] and from literature [39] and predicted data of γ_i^{∞} in refined soybean oil.

T/K	Solute								
	Methanol			Ethanol			n-Hexane		
		UNIFAC			UNIFAC			UNIFAC	
	expt[b]	orig[c]	Dort[d]	expt[b]	orig[c]	Dort[d]	expt[b]	orig[c]	Dort[d]
313.15	3.524	1.414	2.331	2.025	1.491	1.728	0.515	0.336	0.649
323.15	3.166	1.321	2.155	1.731	1.408	1.562	0.505	0.335	0.642
331.85	1.80*			1.79*			0.588*		
333.15	2.838	1.239	1.988	1.508	1.333	1.415	0.497	0.333	0.636
343.15	2.584	1.165	1.830	1.365	1.265	1.284	0.490	0.332	0.630
352.15	1.51*			1.34*			0.585*		
353.15	2.356	1.099	1.681	1.211	1.204	1.166	0.480	0.331	0.625
374.05	1.23*			1.07*			0.562*		
396.55	1.02*			0.881*			0.572*		

[a] uncertainty 2.5%; [b] experimental data; [c] data predicted by UNIFAC model, [d]data predicted by mod. UNIFAC model, * data from ref. [39].

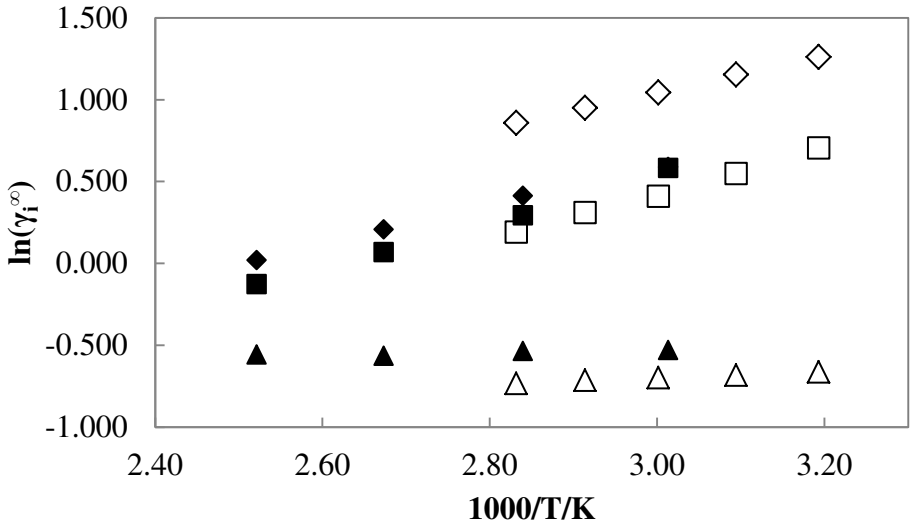

Fig. 5.3. Plot of $ln(\gamma_i^{\infty})$ for refined soybean oil versus $1/T$. Data from this work for: (◊) methanol, (□) ethanol, and (Δ) n-hexane, and data from ref. [39] for: (♦) methanol, (■) ethanol, and (▲) n-hexane.

As is apparent from the entries in Table 5.6 and observed in Fig. 5.3, the γ_i^{∞} data obtained in this work for ethanol in soybean oil are in good agreement with the data from King and List [39]. However our values for n-hexane and for methanol are far from those given in this reference. Comparing the data of γ_i^{∞} in soybean oil from this work with published data (by interpolation), the data measured show differences of less than 0.016 to 0.822 in absolute values, for methanol the difference is nearly 63 %. But in both studies, the variation of γ_i^{∞} follows similar trends for all solutes, i.e., γ_i^{∞} decreases with increasing temperature.

It should be mentioned that the methodology used by King and List [39] (inverse gas chromatography) is different to that used in this work (dilutor technique with double cells). Although the authors have taken care to use only data which the interfacial adsorption at

the support surface was not observed and also verified that there was no solvent loss during the experimental runs, since soybean oil is a mixture, it is not possible to guarantee that there was no separation of its components in the three-foot-long column during the runs, in this case the results could be heavily influenced.

Table 5.7. Experimental and predicted data of γ_i^{∞} in refined sunflower oil.

***T*/K**	**Solute**								
	Methanol			**Ethanol**			**n-Hexane**		
		UNIFAC			**UNIFAC**			**UNIFAC**	
	expt[a]	**orig[b]**	**Dort[c]**	**expt[a]**	**orig[b]**	**Dort[c]**	**expt[a]**	**orig[b]**	**Dort[c]**
313.15	3.577	1.410	2.335	2.186	1.489	1.729	0.514	0.333	0.645
323.15	3.199	1.317	2.158	1.976	1.406	1.563	0.504	0.332	0.638
333.15	2.906	1.235	1.990	1.426	1.330	1.416	0.499	0.330	0.632
343.15	2.601	1.161	1.831	1.216	1.263	1.284	0.489	0.329	0.626
353.15	2.094	1.096	1.682	0.837	1.201	1.166	0.475	0.328	0.622

[a] experimental data (uncertainty 2.5%); [b] data predicted by UNIFAC model; [c] data predicted by mod. UNIFAC model.

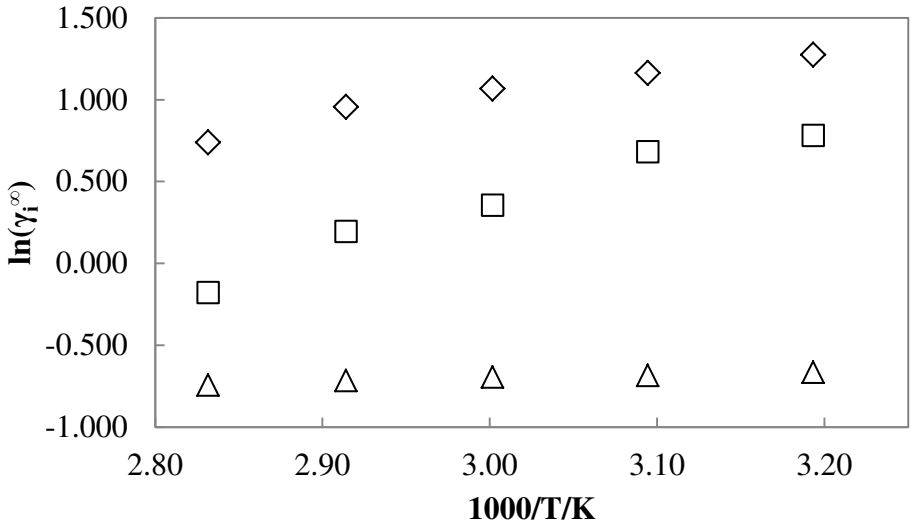

Fig. 5.4. Plot of $ln(\gamma_i^{\infty})$ for refined sunflower oil versus $1/T$ for (◊) methanol, (□) ethanol and (Δ) n-hexane.

Table 5.8. Experimental and predicted data of γ_i^{∞} in refined rapeseed oil.

T/K	Solute								
	Methanol			Ethanol			n-Hexane		
		UNIFAC			UNIFAC			UNIFAC	
	expt[a]	orig[b]	Dort[c]	expt[a]	orig[b]	Dort[c]	expt[a]	orig[b]	Dort[c]
313.15	3.622	1.409	2.386	2.080	1.529	1.743	0.471	0.333	0.634
323.15	3.093	1.317	2.203	1.627	1.444	1.576	0.466	0.331	0.628
333.15	2.559	1.235	2.030	1.414	1.367	1.428	0.460	0.330	0.623
343.15	2.076	1.162	1.866	1.229	1.297	1.294	0.453	0.329	0.618
353.15	1.816	1.096	1.712	0.920	1.234	1.175	0.445	0.328	0.614

[a] experimental data (uncertainty 2.5%); [b] data predicted by UNIFAC model; [c] data predicted by mod. UNIFAC model.

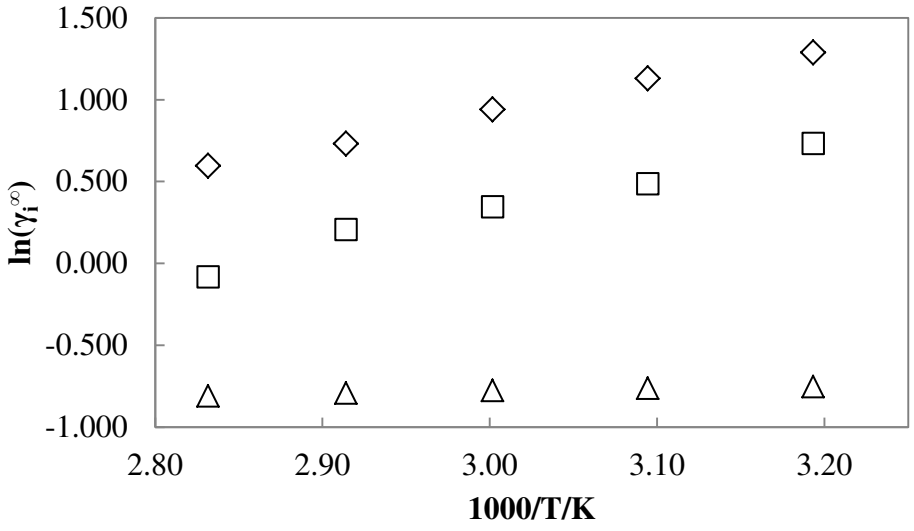

Fig. 5.5. Plot of $ln(\gamma_i^{\infty})$ for refined rapeseed oil versus $1/T$ for (◊) methanol, (□) ethanol and (Δ) n-hexane.

As presented in Tables 5.6 to 5.8, the experimental and predicted results for all solutes show significant deviations, however the temperature dependence of γ_i^{∞} is well represented. Comparing the experimental γ_i^{∞} data in refined vegetable oil with data predicted by UNIFAC and mod. UNIFAC, the average deviations are about 34 % and 22 %, respectively. UNIFAC parameters are nearly solely based on vapor-liquid equilibrium data for mixtures of components of similar size and the Staverman-Guggenheim combinatorial expression in the model leads to systematic deviations for asymmetric mixtures [64]. This was corrected in mod. UNIFAC and, among others, γ^{∞}- data were used to regress the model parameters. As also reported in the work of Weidlich and Gmehling [38], data predicted with UNIFAC in this work show larger deviation from experiment. For mod. UNIFAC, the authors [38] report a mean deviation ranging from 3.3 % to 8.6 % in

γ^{∞}. Unfortunately larger deviations were observed in our work. However it should be appreciated that there is probably a strong proximity effect in case of the three ester groups connected to each other in the triacylglycerol backbone and this structure is probably not well represented by the common ester group in mod. UNIFAC.

Results for methanol are strongly and those for ethanol mildly underpredicted while γ^{∞} for n-hexane were overpredicted. This leads to the conclusion that both UNIFAC models assume the vegetable oils to be more polar than determined experimentally. The polar triacylglycerol core in natural vegetable oils is shielded by long hydrocarbon chains and this may lead to a decrease in polarity, which is not apparent from type and frequency of the structural groups. In addition the close proximity of three ester groups may lead to a lower effective number of ester groups.

In order to improve the predictive capability of mod. UNIFAC for mixtures containing triacylglycerols, the frequency of the ester groups can be artificially reduced. Figs. 5.6 to 5.8 show the comparison of the predicted values by mod. UNIFAC model considering two and three ester groups together with the experimental data. UNIFAC is not further considered here as it is not applicable to asymmetric mixtures due to its combinatorial contribution.

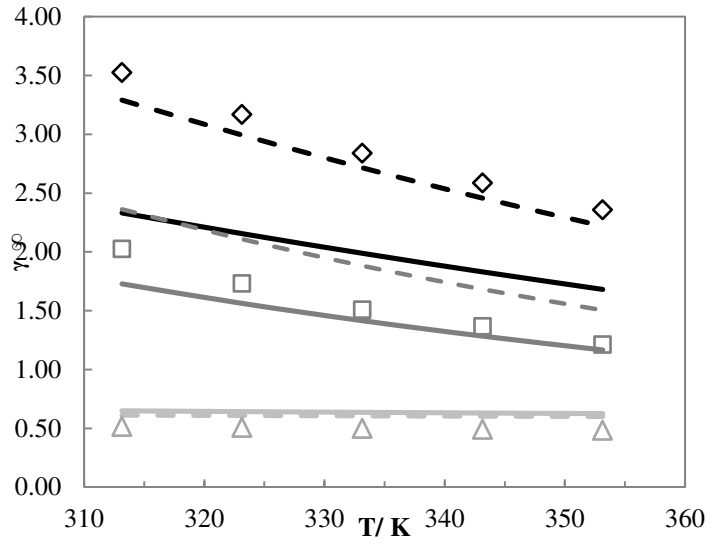

Fig. 5.6. Experimental and predicted activity coefficients at infinite dilution, γ_i^∞ in soybean oil. Experimental data: (◊) methanol, (□) ethanol and (Δ) n-hexane. (──) mod. UNIFAC (- - -) mod. UNIFAC using only 2 ester groups.

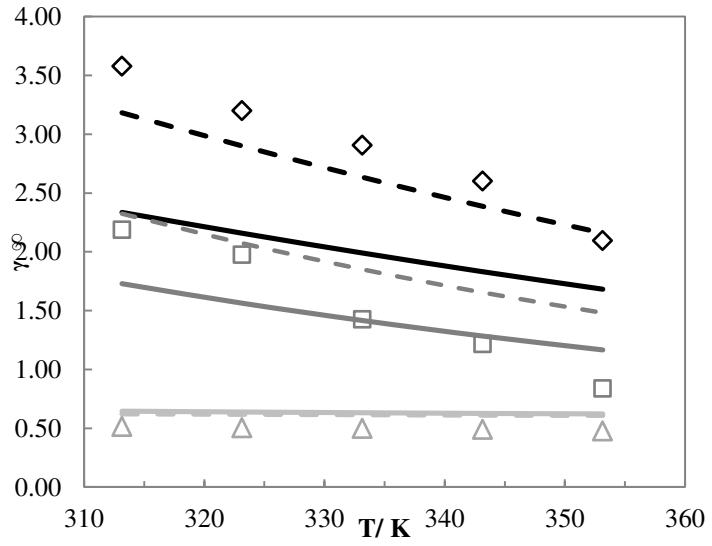

Fig. 5.7. Experimental and predicted activity coefficients at infinite dilution, γ_i^∞, in sunflower oil. Experimental data: (◊) methanol, (□) ethanol and (Δ) n-hexane. (──) mod. UNIFAC (- - -) mod. UNIFAC using only 2 ester groups.

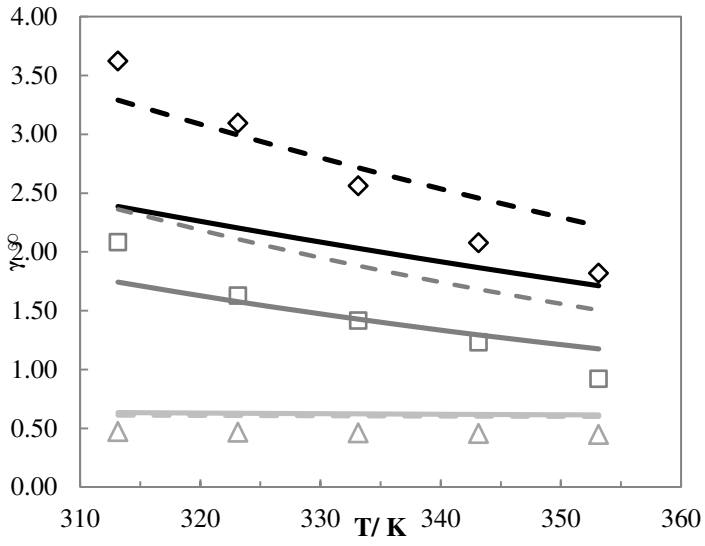

Fig. 5.8. Experimental and predicted activity coefficients at infinite dilution, γ_i^∞, in rapeseed oil. Experimental data: (◊) methanol, (□) ethanol and (Δ) n-hexane. (──) mod. UNIFAC (- - -) mod. UNIFAC using only 2 ester groups.

As can be seen, the proposed "tweak" reduces the deviations significantly for mixtures with methanol and slightly for mixtures with n-hexane. For ethanol the deviations have increased, however the description of the temperature dependence was improved. Due to the importance of triacylglycerols we propose the introduction of a new ester subgroup for the triacylglycerol backbone with approx. two times the Q-value and three times the R-value of the basic ester group. The exact values would need to be regressed to all available data for mixtures containing glycerol triesters. With this modification, mod. UNIFAC could become a viable option for the synthesis and separation processes of fatty systems.

Figs. 5.3 to 5.5 show that in all investigated refined vegetable oils γ_i^∞decreases with an increase of the temperature, this trend was verified for both a non-polar solute (n-hexane) and the polar solutes (methanol and ethanol). As mentioned above, this tendency was also observed for soybean oil by King and List [39]. For purified olive oil, Lebert and Richon

[65] observed an opposite behavior for n-hexane, i.e. γ_i^∞ values increase with increasing temperature. However, if we considered the reported error in each limiting activity coefficient value for any solute n-alkane in olive oil, it appears that the effect of the temperature upon the magnitude of γ_i^∞ is difficult to fit into a pattern.

Experimental data indicate moderate deviation from ideal mixture behavior: the short-chain alcohols presented positive deviation while n-hexane exhibited a considerable negative deviation from ideal behavior, as was also observed by King and List [39]. Then, as the infinite dilution activity coefficient is greater than 1, we can say that the concentration of alcohols in the vapor phase at equilibrium is higher than it would be in the case of an ideal solution, as also reported by Lebert and Richon [65]. The experimental data also confirm the tendency already discussed by Williams [23], which influences the vegetable oil extraction process, since the boiling point of mixtures of dissolved oils and n-hexane or other hydrocarbons , at solvent concentrations lower than 10% by weight, becomes so high that the steam stripping process is essential in the final stages of solvent recovery.

γ_i^∞ values increase in the same order for the solutes investigated in this study, namely: n-hexane < ethanol < methanol, as also observed by King and List [39] and Lebert and Richon [65] for soybean oil and purified olive oil, respectively. The lowest values of γ_i^∞ results from the combinatorial contribution. The extrapolated value for hexane in an n-alkane of a molecular size similar to the vegetable oil would be around 0.5 to 0.6 [38]. In case of methanol and ethanol, a positive deviation from Raoult's law is observed that is similar to that of the alcohols in other less polar solvents. Vrbka et al. [66] reported a γ^∞

of 58.8 for ethanol in hexane at 25°C. In larger alkane solvents this is decreased by the combinatorial contribution while the residual (enthalpic) part would not be affected. For ethanol in an alkane of similar size than the vegetable oil, a γ^{∞} of 25 to 30 could be expected, which is significantly higher than the experimental result of approx. 2. This indicates that while hexane molecules in the oil do not behave different than in a vegetable oil sized alkane, alcohol molecules are able to "find" and interact with the polar ester groups. In case of methanol, this effect is not sufficient to avoid a broad miscibility gap with the oil. The results indicate that the solubility of alcohols in vegetable oils increases with increasing size of the hydrocarbon chain and with increasing temperature, this tendency was also observed in soybean oil [39] and purified olive oil [65]. Higher γ_i^{∞} values increase the volatility of the solute and enable a more easy separation of the solute from the vegetable oil. This is why higher alcohols beyond ethanol are not suitable for oil extraction as they would be difficult to remove via evaporation due to both the lower pure component vapor pressure and the lower activity coefficient. They could still be removed by liquid-liquid extraction using e.g. water but recovering the solvent from the diluted solution in water would not be feasible.

Both properties, solubility and volatility, play an important role in vegetable oil industrial processes. Since in the solvent extraction process the vegetable oil fraction of the oleaginous material is separated from the meal fraction by dissolving the oil fraction in a solvent, n-hexane seems to have the best performance in this process. It is no coincidence that the solvent used in the majority of oilseed solvent extraction plants around the world is commercial hexane, a mixture of hydrocarbons (most n-hexane, approximately 65 %)

generally boiling in the temperature range of 338.15 K to 342.15 K [18, 22]. The results of this study indicate that the alcohols methanol and ethanol, would also be suitable extraction solvents, if the extraction process is carried out at higher temperatures. This would improve the solubility of alcohols in vegetable oil (indicated by the lower γ_i^{∞} values at higher temperatures).

On the other hand, considering the industrial processes to separate these components from vegetable oil, such as: desolventization process, solvent recovery in vegetable oil extraction process [19, 22, 23], and solvent recovery in biodiesel production [67], it can be inferred that alcohols have an advantage over n-hexane, due to their easier separation from vegetable oil by evaporation, since the higher γ_i^{∞} values of methanol and ethanol indicate higher volatility.

Table 5.9 lists the partial molar excess enthalpy, $\Delta H_i^{E,\infty}$, entropy, $\Delta S_i^{E,\infty}$, and Gibbs energy, $\Delta G_i^{E,\infty}$, at infinite dilution determined by linear regression of the γ_i^{∞} experimental data according equation (5.3).

Table 5.9. Limiting values of the partial molar excess enthalpy, $\Delta H_i^{E,\infty}$, entropy, $\Delta S_i^{E,\infty}$, and Gibbs energy, $\Delta G_i^{E,\infty}$, for solutes in refined soybean, sunflower and rapeseed oils at reference temperature 298.15 K.

Solvent	Solute	$\Delta H_i^{E,\infty,a}$ /kJ. mol^{-1}	$T_{ref}\Delta S_i^{E,\infty,b}$ /kJ. mol^{-1}	$\Delta G_i^{E,\infty}$ /kJ. mol^{-1}
Soybean oil	Methanol	9.28	5.71	3.57
	Ethanol	11.66	9.38	2.28
	n-Hexane	1.57	3.14	-1.57
Sunflower oil	Methanol	11.68	7.89	3.79
	Ethanol	22.00	18.81	3.18
	n-Hexane	1.72	3.28	-1.56
Rapeseed oil	Methanol	16.36	12.34	4.01
	Ethanol	17.55	14.89	2.65
	n-Hexane	1.30	3.10	-1.80

[a] uncertainty 20%; [b] $T_{ref} = 298.15$ K.

The $\Delta H_i^{E,\infty}$ and $\Delta S_i^{E,\infty}$ values are all slightly positive and the $\Delta G_i^{E,\infty}$ values are negative for the solute n-hexane. The positive values of $\Delta H_i^{E,\infty}$ indicate that the interaction in solute-solute pairs is slightly higher than in case of solute-solvent pairs. The higher values of $\Delta H_i^{E,\infty}$ for alcohols again reflect the weak association with refined vegetable oil. In addition, it was found that the $\Delta H_i^{E,\infty}$ values are a little bit higher for ethanol than in case of methanol. This behavior should not be employed for the extrapolation to larger alcohol as methanol as the first member of the homologous series may show an untypical behavior.

5.4. Conclusions

In this work, activity coefficient at infinite dilution data for n-hexane, methanol and ethanol in 3 refined vegetable oils have been measured using the gas stripping method (dilutor technique) in the temperature range of 313.15 K to 353.15 K. In addition, the thermodynamic functions at infinite dilution for the same solutes were derived for refined soybean, sunflower and rapeseed oils. It has been shown that the results of limiting activity coefficients obtained for fatty compounds using the dilutor technique have high reliability, since the data for capric acid measured in this work had good agreement with data measured by GLC, with average deviation of about 2 %.

The results demonstrate that in all cases studied there is a decrease in the γ_i^{∞} values with increasing temperature, which results in positive values of partial molar excess enthalpy at infinite dilution. Deviations from ideal behavior, positive for alcohols and negative for n-hexane, have also been experimentally determined. The data obtained do not show good agreement with predicted data using UNIFAC and mod. UNIFAC but a physically realistic modification of mod. UNIFAC improved the results considerably. Based on this observation, introduction of a special ester subgroup for triacylglycerol in mod. UNIFAC is proposed. The experimental information reported here might be useful for practical applications and as a basis for model testing purposes.

Acknowledgements

P. C. Belting wishes to acknowledge CNPq (Conselho Nacional de Desenvolvimento Científico e Tecnológico – 142122/2009-2 and 290128/2010-2) and DAAD (Deutscher Akademischer Austauschdienst – A/10/71471) for the scholarship. The authors would like to thank the CNPq (304495/2010-7, 483340/2012-0, 307718/2010-7 and 301999/2010-4), FAPESP (Fundação de Amparo à Pesquisa do Estado de São Paulo - 08/56258-8, 09/54137-1 and 2010/16634-0) and INCT-EMA (Instituto Nacional de Ciência e Tecnologia de Estudos do Meio Ambiente) for the financial support. The authors are grateful to the DDBST GmbH for permitting the use of the Dortmund Data Bank and Mr. G. J. Maximo for the help with the computer program. This work has been supported by the Carl von-Ossietzky University Oldenburg.

List of Symbols

GLC	gas-liquid chromatography
GC	gas chromatography
TAG	triacylglycerol
FA	fatty acid
FFA	free fat acid
M	molar mass
C z:y	z = number of carbons and y = number of double bonds
x	molar fraction
w	mass fraction
T	trans isomers
W	water content
IV	iodine value

L	lauric acid
M	myristic acid
P	palmitic acid
Po	palmitoleic acid
Ma	margaric acid
S	stearic acid
O	oleic acid
Li	linoleic acid
Le	linolenic acid
A	arachidic acid
Ga	gadoleic acid
Be	behenic acid
Lg	lignoceric acid
Ne	nervonic acid
x_i	solute molar fraction in liquid phase
n_{solv}	number of moles of solvent
R	general gas constant
T	absolute temperature
P_i^s	saturation vapor pressure of the solute i
F_{He}	carrier gas flow rate
P_{solv}^s	saturation vapor pressure of the solvent
P	pressure
V_g	vapor volume in measurement cell
a	parameter in equation 5.1
b	intersection
c	slope
$\Delta H_i^{E,\infty}$	partial molar excess enthalpy at infinite dilution
$\Delta G_i^{E,\infty}$	partial molar excess Gibbs energy at infinite dilution
$\Delta S_i^{E,\infty}$	partial molar excess entropy at infinite dilution

Greek letters

φ_i^s	saturation fugacity coefficient
γ_i^∞	activity coefficient at infinite dilution or limiting activity coefficient
ρ	density

Subscripts

i	solute identification
$solv$	solvent identification
He	helium
ref	reference

Superscripts

E	excess property
s	at saturation
∞	at infinite dilution

References

[1] F.D. Gunstone, Vegetable Oils, in: F. Shahidi (Ed.) Bailey's Industrial Oil and Fat Products John Wiley & Sons, Hoboken, New Jersey, 2005, pp. 606.

[2] R. Przybylski, T. Mag, N.A.M. Eskin, B.E. McDonald, Canola Oil, in: F. Shahidi (Ed.) Bailey's Industrial Oil and Fat Products, John Wiley & Sons, Inc., Hoboken, New Jersey, 2005, pp. 61-121.

[3] P.J. Wan, Properties of Fats and Oils, in: W.E.F. R. D. O'Brien, P. J. Wan (Ed.) Introduction to Fats and Oils Technology, A.O.C.S. Press, Champaign, Illinois, 2000 pp. 20-48.

[4] R.D. O'Brien, Introduction to Fats and Oils Technology, in: W.E.F. R.D. O'Brien, and P.J. Wan (Ed.) Fats And Oils: An Overview, AOCS Press: Champaign, Illinois, 2000, pp. 1-19.

[5] W. De Greyt, M. Kellens, Deodorization, in: F. Shahidi (Ed.) Bailey's Industrial Oil and Fat Products, John Wiley & Sons, Inc., Hoboken, New Jersey, 2005, pp. 341-383.

[6] M.R. Burke, Soaps, in: F. Shahidi (Ed.) Bailey's Industrial Oil and Fat Products, John Wiley & Sons, Inc., Hoboken, New Jersey, 2005, pp. 103-136.

[7] I.M. Atadashi, M.K. Aroua, A. Abdul Aziz, High quality biodiesel and its diesel engine application: A review, Renew. Sust. Energ. Rev., 14 (2010) 1999-2008.

[8] J.M. Marchetti, V.U. Miguel, A.F. Errazu, Possible methods for biodiesel production, Renew Sust. Energ. Rev., 11 (2007) 1300-1311.

[9] J.M. Encinar, J.F. Gonzáles, J.J. Rodriguez, A. Tejedor, Biodiesel Fuels from Vegetables Oils: Transesterification of Cynara cardunculus L. Oils with Ethanol, Energ. Fuel, 16 (2002) 443-450.

[10] F. Ma, M.A. Hanna, Biodiesel production: a review, Bioresource Technol., 70 (1999) 1-15.

[11] C. Scrimgeour, Chemistry of Fatty Acids, in: F. Shahidi (Ed.) Bailey's Industrial Oil and Fat Products, John Wiley & Sons, Hoboken, New Jersey, 2005, pp. 606.

[12] J.L. Lynn Jr., Detergents and Detergency, in: F. Shahidi (Ed.) Bailey's Industrial Oil and Fat Products, John Wiley & Sons, Inc., Hoboken, New Jersey, 2005, pp. 137-189.

[13] S.Z. Erhan, Vegetable Oils as Lubricants, Hydraulic Fluids, and Inks, in: F. Shahidi (Ed.) Bailey's Industrial Oil and Fat Products, John Wiley & Sons, Inc., Hoboken, New Jersey, 2005, pp. 259-278.

[14] S.S. Narine, X. Kong, Vegetable Oils in Production of Polymers and Plastics, in: F. Shahidi (Ed.) Bailey's Industrial Oil and Fat Products, John Wiley & Sons, Inc., Hoboken, New Jersey, 2005, pp. 279-306.

[15] E. Hernandez, Pharmaceutical and Cosmetic Use of Lipids, in: F. Shahidi (Ed.) Bailey's Industrial Oil and Fat Products, John Wiley & Sons, Inc., Hoboken, New Jersey, 2005, pp. 391-411.

[16] K.F. Lin, Paints, Varnishes, and Related Products, in: F. Shahidi (Ed.) Bailey's Industrial Oil and Fat Products, John Wiley & Sons, Inc., Hoboken, New Jersey, 2005, pp. 307-351.

[17] P. Kronick, Y.K. Kamath, Leather and Textile Uses of Fats and Oils, in: F. Shahidi (Ed.) Bailey's Industrial Oil and Fat Products, John Wiley & Sons, Inc., Hoboken, New Jersey, 2005, pp. 353-369.

[18] R.D. O'Brien, Fats And Oils Processing, in: W.E.F. R.D. O'Brien, and P.J. Wan (Ed.) Introduction to Fats and Oils Technology, A.O.C.S. Press, Champaign, Illinois, 2000, pp. 90-107.

[19] E.D. Milligan, D.C. Tandy, Distillation and Solvent Recovery, J. Am. Oil Chem. Soc., 51 (1974) 347-350.

[20] K.F. Mattil, Deodorization, in: F.A.N. K.F. Mattil, A.J. Stirton (Ed.) Bailey's Industrial Oil and Fat Products, John Wiley & Sons, New York, 1964, pp. 897-930.

[21] C.G. Pina, A.J.A. Meirelles, Deacidification of Corn Oil by Solvent Extraction in a Perforated Totating Disc Column., J. Am. Oil Chem. Soc., 77 (2000) 553-559.

[22] T.G. Kemper, Oil Extraction, in: F. Shahidi (Ed.) Bailey's Industrial Oil and Fat Products, John Wiley & Sons, Inc., Hoboken, New Jersey, 2005, pp. 572.

[23] M.A. Williams, Recovery of Oils and Fats from Oilseeds and Fatty Materials, in: F. Shahidi (Ed.) Bailey's Industrial Oil and Fat Products, John Wiley & Sons, Inc., Hoboken, New Jersey, 2005, pp. 572.

[24] Z. Guo, X. Xu, Lipase-catalyzed glycerolysis of fats and oils in ionic liquids: a further study on the reaction system, Green Chem., 8 (2006) 54–62.

[25] L.-Z. Cheong, H. Zhang, Y. Xu, X. Xu, Physical Characterization of Lard Partial Acylglycerols and Their Effects on Melting and Crystallization Properties of Blends with Rapeseed Oil, J. Agric. Food Chem. , 57 (2009) 5020–5027.

[26] X. Xu, S. Balchena, C.-E. Høyb, J. Adler-Nissena, Pilot Batch Production of Specific-Structured Lipids by Lipase-Catalyzed Interesterification: Preliminary Study on Incorporation and Acyl Migration, J. Am. Oil Chem. Soc., 75 (1998) 301-308.

[27] X. Xu, C. Jacobsenb, N.S. Nielsenb, M.T. Heinrichb, D. Zhoua, Purification and deodorization of structured lipids by short path distillation, Eur. J. Lipid Sci. Technol., 104 (2002) 745-755.

[28] X. Xu, A. Skands, J. Adler-Nissen, Purification of Specific Structured Lipids by Distillation: Effects on Acyl Migration, J. Am. Oil Chem. Soc., 78 (2001) 715-718.

[29] J. Gmehling, A. Brehm, Grundoperationen, Thieme-Verlag, Stuttgart, 1996.

[30] J. Gmehling, B. Kolbe, M. Kleiber, J. Rarey, Chemical Thermodynamics for Process Simulation, 1st ed., Wiley-VCH, Weinheim, 2012.

[31] L. Dallinga, M. Schiller, J. Gmehling, Measurement of activity coefficient at infinite dilution using differential ebulliometry and non-steady-state gas-liquid-chromatography, J. Chem. Eng. Data, 38 (1993) 147-155.

[32] B.E. Poling, J.M. Prausnitz, J.P. O'Connell, Properties of Gases and Liquids, 5th ed., McGraw-Hill, 2001.

[33] P.C. Belting, J. Rarey, J. Gmehling, R. Ceriani, O. Chiavone-Filho, A.J.A. Meirelles, Activity Coefficient at Infinite Dilution Measurements for Organic Solutes (polar and nonpolar) in Fatty Compounds: Saturated Fatty Acids, J. Chem. Thermodyn., 55 (2012) 42-49.

[34] P.C. Belting, J. Rarey, J. Gmehling, R. Ceriani, O. Chiavone-Filho, A.J.A. Meirelles, Activity coefficient at infinite dilution measurements for organic solutes (polar and non-polar) in fatty compounds – Part II: C18 fatty acids, J. Chem. Thermodyn., 60 (2013) 142–149.

[35] A. Fredenslund, J. Gmehling, P. Rasmussen, Vapor-liquid equilibria using UNIFAC: a group contribution method, Elsevier Scientific Publishing Company, Amsterdam, 1977.

[36] H.K. Hansen, P. Rasmussen, A. Fredenslund, M. Schiller, J. Gmehling, Vapor-Liquid Equilibria by UNIFAC Group Contribution 5. Revision and Extension, Ind. Eng. Chem. Res., 30 (1991) 2352-2355.

[37] J. Gmehling, J. Li, M. Schiller, A Modified UNIFAC Model.2. Present Parameter Matrix and Results for Different Thermodynamic Properties, Ind. Eng. Chem. Res., 32 (1993) 178-193.

[38] U. Weidlich, J. Gmehling, A Modified UNIFAC Model. 1. Prediction of VLE, hE and $\gamma\infty$ Ind. Eng. Chem. Res., 26 (1987) 1372-1381.

[39] J.W. King, G.R. List, A Solution Thermodynamic Study of Soybean Oil/Solvent Systems by Inverse Gas Chromatography, J. Am. Oil Chem. Soc., 67 (1990) 424-430.

[40] AOCS, Official Methods and recommended Practices of the American Oil Chemists' Society, 5 th ed., AOCS Press, Champaign, IL, 2004.

[41] L. Hartman, R.C.A. Lago, Rapid Preparation of Fatty Acid Methyl Esters from Lipids, Lab. Pract., 22 (1973) 475–476.

[42] M. Lanza, G. Sanaiotti, E. Batista, R.J. Poppi, A.J.A. Meirelles, Liquid-Liquid Equilibrium Data for Systems Containing Vegetable Oils, Anhydrous Ethanol, and Hexane at (313.15, 318.15, and 328.15) K, J. Chem. Eng. Data, 54 (2009) 1850-1859.

[43] C.A.S. Silva, G. Sanaiotti, M. Lanza, L.A. Follegatti-Romero, A.J.A. Meirelles, E.A.C. Batista, Mutual Solubility for Systems Composed of Vegetable Oil + ethanol + Water at Different Temperatures, J. Chem. Eng. Data, 55 (2010) 440-447.

[44] L.A. Follegatti-Romero, M. Lanza, C.A.S. Silva, E.A.C. Batista, A.J.A. Meirelles, Mutual Solubility of Pseudobinary Systems Containing Vegetable Oils and Anhydrous Ethanol from (298.15 to 333.15) K, J. Chem. Eng. Data, 55 (2010) 2750-2756.

[45] N.R. Antoniossi Filho, O.L. Mendes, F.M. Lanças, Computer prediction of triacylglycerol composition of vegetable oils by HRGC, Chromatographia, 40 (1995) 557-562.

[46] D. Gruber, M. Krummen, J. Gmehling, The determination of activity coefficients at infinite dilution with the help of the dilutor technique (inert gas stripping), Chem. Eng. Technol., 22 (1999) 827-831.

[47] M. Krummen, D. Gruber, J. Gmehling, Measurement of activity coefficients at infinite dilution in solvent mixtures using the dilutor technique, Ind. Eng. Chem. Res., 39 (2000) 2114-2123.

[48] J.-C. Leroi, J.-C. Masson, H. Renon, J.-F. Fabries, H. Sannier, Accurate measurement of activity coefficients at infinite dilution by inert gas stripping and gas chromatography, Ind. Eng. Chem. Proc. DD, 16 (1977) 139-144.

[49] D. Richon, P. Antoine, H. Renon, Infinite dilution activity coefficients of linear and branched alkanes from C1 to C9 in n-hexadecane by inert gas stripping, Ind. Eng. Chem. Proc. DD, 19 (1980) 144-147.

[50] D. Richon, H. Renon, Infinite dilution Henry's constants of light hydrocarbons in n-hexadecane, n-octadecane, and 2,2,4,4,6,8,8-heptamethylnonane by inert gas stripping, J. Chem. Eng. Data, 25 (1980) 59-60.

[51] M. Krummen, Experimentelle Untersuchung des Aktivitätskoeffizienten bei unendlicher Verdünnung in ausgewählten Lösungsmitteln und Lösungsmittelgemischen als Grundlage für die Synthese thermischer Trennprozesse, in: Fachbereich Chemie, Carl von Ossietzky Universität Oldenburg, Oldenburg, 2002, pp. 198.

[52] J.-B. Bao, S.-J. Han, Infinite dilution activity coefficients for various types of systems, Fluid Phase Equilibr., 112 (1995) 307-316.

[53] J.-B. Bao, S.-J. Han, Measurements of Infinite-Dilution Ternary Activity Coefficients by Gas Stripping. Acetonitrile-Benzene-n-Heptane at 318.15 K, Ind. Eng. Chem. Res., 35 (1996) 2773-2776.

[54] M. Krummen, P. Wasserscheid, J. Gmehling, Measurement of activity coefficients at infinite dilution in ionic liquids using the dilutor technique, J. Chem. Eng. Data, 47 (2002) 1411-1417.

[55] Dortmund Data Bank Dortmund Data Bank Software & Separation Technology in, DDBST GmbH, Oldenburg, 2011.

[56] Design Institute for Physical Properties Data Bank in, AIChE, [2005, 2008, 2009, 2010].

[57] R. Ceriani, A.J.A. Meirelles, Predicting vapor–liquid equilibria of fatty systems, Fluid Phase Equilibr., 215 (2004) 227–236.

[58] D. Gruber, M. Krummen, J. Gmehling, Die Bestimmung von Aktivitätskoeffizienten bei unendlicher Verdünnung mit Hilfe der Dilutor-Technik Chem.-Ing.-Tech., 71 (1999) 503-508

[59] Z. Atik, D. Gruber, M. Krummen, J. Gmehling, Measurement of Activity Coefficients at Infinite Dilution of Benzene, Toluene, Ethanol, Esters, Ketones, and Ethers at Various Temperatures in Water Using the Dilutor Technique, J. Chem. Eng. Data, 49 (2004) 1429-1432.

[60] R. Kato, J. Gmehling, Activity coefficients at infinite dilution of various solutes in the ionic liquids [MMIM]+[CH3SO4]−, [MMIM]+[CH3OC2H4SO4]−, [MMIM]+[(CH3)2PO4]−, [C5H5NC2H5]+[(CF3SO2)2N]− and [C5H5NH]+[C2H5OC2H4OSO3]−, Fluid Phase Equilibr., 226 (2004) 37-44.

[61] M. Bahlmann, S. Nebig, J. Gmehling, Activity coefficients at infinite dilution of alkanes and alkenes in 1-alkyl-3-methylimidazolium tetrafluoroborate, Fluid Phase Equilibr., 282 (2009) 113-116.

[62] M. Krummen, J. Gmehling, Measurement of activity coefficients at infinite dilution in N-methyl-2-pyrrolidone and N-formylmorpholine and their mixtures with water using the dilutor technique, Fluid Phase Equilibr., 215 (2004) 283-294.

[63] S. Çehreli, J. Gmehling, Phase equilibria for benzene–cyclohexene and activity coefficients at infinite dilution for the ternary systems with ionic liquids, Fluid Phase Equilibr., 295 (2010) 125–129.

[64] I. Kikic, P. Alessi, P. Rasmussen, A. Fredenslund, On the Combinatorial Part of the UNIFAC and UNIQUAC Models., Can. J. Chem. Eng., 58 (1980) 253-258.

[65] A. Lebert, D. Richon, Infinite Dilution Activity Coefficients of n -Alcohols as a Function of Dextrin Concentration in Water-Dextrin Systems, J. Agric. Food Chem., 32 (1984) 1156-1161.

[66] P. Vrbka, B. Hauge, L. Frydendal, V. Dohnal, Limiting Activity Coefficients of Lower 1-Alkanols in n-Alkanes: Variation with Chain Length of Solvent Alkane and Temperature, J. Chem. Eng. Data, 47 (2002) 1521–1525.

[67] L.C. Meher, D.V. Sagar, S.N. Naik, Technical aspects of biodiesel production by transesterifications: a review, Renew Sust. Energ. Rev., 10 (2006).

CAPÍTULO 6: EXCESS ENTHALPIES FOR VARIOUS BINARY MIXTURES WITH VEGETABLE OIL AT TEMPERATURES BETWEEN 298.15 K AND 383.15 K

Artigo submetido à revista Fluid Phase Equilibria.

Excess Enthalpies for Various Binary Mixtures with Vegetable Oil at Temperatures between 298.15 K and 383.15 K

Patrícia C. Belting[a,b,1], Jürgen Gmehling[a], Rainer Bölts[a], Jürgen Rarey[a], Roberta Ceriani[c], Osvaldo Chiavone-Filho[d], Antonio J. A. Meirelles[b,*]

[a] *Carl von Ossietzky Universität Oldenburg, Technische Chemie (FK V), D-26111 Oldenburg, Federal Republic of Germany*

[b] *Food Engineering Department, Faculty of Food Engineering, University of Campinas, Av. Monteiro Lobato 80, Cidade Universitária Zeferino Vaz, 13083-862, Campinas-SP, Brazil*

[c] *Faculty of Chemical Engineering, University of Campinas, Av. Albert Einstein 500, Cidade Universitária Zeferino Vaz, 13083-852, Campinas-SP, Brazil*

[d] *Chemical Engineering Department, Federal University of Rio Grande do Norte, Av. Senador Salgado Filho S/N, 59066-800, Natal-RN, Brazil*

[1 a] *Present address,* [b] *Permanent address*

Abstract

This paper presents excess enthalpies (H^E) for the following systems containing refined vegetable oils: soybean oil + methanol (at 353.15 K/ 722 kPa), soybean oil + ethanol (at 353.15 K/ 687 kPa and 383.15 K/ 653 kPa), soybean oil + n-hexane (at 353.15 K/ 722 kPa and 383.15 K/ 756 kPa), soybean oil + propan-2-ol (at 298.15 K/ 998 kPa), sunflower oil + methanol (at 353.15 K/ 791 kPa), sunflower oil + ethanol (at 353.15 K/ 894 kPa and 383.15 K/ 860 kPa), sunflower oil + n-hexane (at 353.15 K/ 894 kPa and 383.15 K/ 756 kPa), sunflower oil + propan-2-ol at (298.15 K/ 929 kPa), rapeseed oil + methanol (at 353.15 K/ 963 kPa), rapeseed oil + ethanol (at 353.15 K/ 998 kPa and 383.15 K/ 1136 kPa), and

rapeseed oil + n-hexane (at 353.15 K/ 894 kPa and 383.15 K/ 1136 kPa). The measurements were carried out with a commercially available isothermal flow calorimeter. The experimental H^E values have been fitted to the Redlich-Kister polynomial equation. The results for systems with propan-2-ol and some values of partial molar excess enthalpies at infinite dilution, $H_i^{E,\infty}$, obtained in this study have been compared to those available in literature. The systems were also compared in terms of molecular interactions.

Keywords: Molar excess enthalpy, Heat of mixing, Refined vegetable oil, Isothermal flow calorimetry.

6.1. Introduction

In recent years, vegetable oils and related compounds are playing an important role not only for the food processing industry. The interest in these components is growing since they are considered as potential renewable source of biofuels. Additionally vegetable oils can also be used as feedstock in the production of several non-edible industrial goods.

Commercially important vegetable oils, as others edible fat and oils, have as main constituents the triacilglycerols (TAGs), which can be formed from the condensation reaction of glycerol and fatty acids. Partial acylglycerols (mono- and diacylglycerols) and free fatty acids (FFA) are normally present as minor compounds, and also traces of phospholipids, sterols, tocopherols and tocotrienols, vitamins, and coloring matters as carotenes and chlorophylls. Most natural vegetable oils are complex mixtures of many different triacylglycerols, and their exact composition further varies with the sources [1-3].

In vegetable oil industrial processes there are several separation steps, such as solvent extraction (mainly solvent recovery steps) [4-6], fatty acids distillation [7], fatty alcohols fractionation, production and purification of partial acylglycerols [7-9], physical refining (mainly deacidification process) [10, 11], and deodorization of vegetable oils [12, 13], as well as in biodiesel production (biofuel purification and recovery of excess alcohol) [14-16], in which the thermophysical properties and phase equilibrium data are of great importance [17-19].

In spite of the great variety and practical importance of fatty compounds, experimental data for mixtures as vegetable oils are scarce in the literature and even less data are available for pure fatty components. Therefore, our reseach group has conducted a series of studies involving data measurement and model development for the estimation and prediction of fatty compound properties [20-30].

Excess enthalpy or heat of mixing (H^E) is an interesting thermodynamic property, because, when measured at different temperatures, together with phase equilibrium (as vapor-liquid equilibrium –VLE and liquid-liquid equilibrium - LLE) data it can be used for the revision and extension of group contribution methods, such as Modified UNIFAC (Dortmund) or for fitting reliable temperature-dependent G^E model parameters [31-33], since H^E data sets measured at various temperatures deliver the correct temperature dependence of the activity coefficients, which is described quantitatively by the Gibbs-Helmholtz equation [18]. This equation provides a direct relationship between the temperature dependence of the activity coefficient and the partial molar excess enthalpy [18, 31]. Excess properties, like excess enthalpies, can also reflect differences between

energetic and structural effects in a solution relative to those in the unmixed components [33].

In the case of fatty compounds systems however, a very limited number of excess enthalpy data are available in the literature. We are aware of only one report (Resa et al. [34]) dealing with excess enthalpy (H^E) measurements for vegetable oils but just for mixtures with alcohols and at ambient temperature (298.15 K), as most of the published H^E data [31]. This means that data at higher temperatures are still required. Other three papers have reported data of partial molar excess enthalpies at infinite dilution deduced from activity coefficient data at infinite dilution: namely a recent publication from our group for three refined vegetable oils (soybean, sunflower and rapeseed oils) [25], and other reports for olive oil [35] and soybean oil [36].

In this work, systematic H^E measurements for binary mixtures with refined vegetable oils (soybean, sunflower and rapeseed oils) were carried out at temperature from 298.15 K to 383.15 K using a commercially available isothermal flow calorimeter. The systems presented in this paper were chosen to extend the H^E database at higher temperatures, which is required for the systematic further development of Modified UNIFAC (Dortmund).

6.2. Experimental

6.2.1. Materials

Methanol and ethanol were supplied by VWR International GmbH (mass fraction purity of 0.998 and water content 80 $mg.kg^{-1}$and 48 $mg.kg^{-1}$, respectively). Propan-2-ol was supplied by Riedel-de Haen (mass fraction purity 0.998 and water content 50 $mg.kg^{-1}$) and n-hexane was supplied by Carl Roth GmbH (mass fraction purity 0.99 and water content 30 $mg.kg^{-1}$). The purities were checked by gas chromatography. Refined soybean oil was purchased from Vandermoortele Deutschland GmbH, refined sunflower and refined rapeseed oils were purchased from Brökelmann + Co and Oelmühle GmbH + Co. The refined vegetable oils were further dried over molecular sieve and subjected to vacuum for at least 24 hours. These procedures removed any water and volatile impurities from the vegetable oils. The water content of all chemicals and vegetable oils was analyzed by the Karl Fischer titration technique. The results obtained have shown the water content was less than 100 $mg.\,kg^{-1}$.

Fatty acid (FA) compositions of the investigated refined vegetable oils were determined by gas chromatography of fatty acid methyl esters using the official method (1-62) of the American Oil Chemists' Society (AOCS) [37] and are presented in Table 6.1. Prior to the chromatographic analysis, the fatty acids of the samples were converted to their respective methyl esters using the method of Hartman and Lago [38] as used by Lanza et al. [39], Silva et al. [40] and Follegatti-Romero et al. [28]. The chromatographic analyses were

carried out using a CGC Agilent 6850 Series CG capillary gas chromatography system under the same experimental conditions described by Belting et al. [25].

The free fatty acid content of refined vegetable oils was determined by titration according to the official AOCS method Ca 5a-40 [37]. The Iodine value (IV) was calculated from the fatty acid composition according to the official AOCS method Cd 1c-85 [37].

Table 6.1. Fatty acid composition of refined vegetable oils investigated.

Fatty Acid Nomenclature				M^a/	Soybean oil		Sunflower oil		Rapeseed oil	
IUPAC	**Trivial**	**Symbol**	**Cz:y[b]**	**($\mathbf{g.mol^{-1}}$)**	**100 x^c**	**100 w^d**	**100 x**	**100 w**	**100 x**	**100 w**
dodecanoic	Lauric	L	C12:0	200.32	0.05	0.03	0.07	0.05	0.06	0.05
tetradecanoic	Myristic	M	C14:0	228.38	0.10	0.09	0.11	0.09	0.09	0.07
pentadecanoic			C15:0	242.40	0.04	0.04	0.05	0.04	0.04	0.04
hexadecanoic	Palmitic	P	C16:0	256.43	11.46	10.55	6.94	6.36	4.89	4.46
cis-hexadec-9-enoic	Palmitoleic	Po	C16:1	254.42	0.11	0.10	0.13	0.12	0.22	0.20
heptadecanoic	Margaric	Ma	C17:0	270.45	0.09	0.09	0.04	0.04	0.06	0.06
cis-heptadeca-10-enoic			C17:1	268.43	0.06	0.06	0.04	0.04	0.07	0.07
octadecanoic	Stearic	S	C18:0	284.49	3.40	3.47	3.02	3.07	1.78	1.79
cis-octadeca-9-enoic	Oleic	O	C18:1	282.47	28.90	29.30	25.52	25.76	62.98	63.18
cis,cis-octadeca-9,12-dienoic	Linoleic	Li	C18:2	280.45	48.73	49.04	62.47	62.61	18.64	18.56
trans-trans-octadeca-9,12-dienoic	Linoelaidic		C18:2T[e]	278.44	0.19	0.19	0.40	0.40	0.10	0.10
all-*cis*-octadeca-9,12,15-trienoic	Linolenic	Le	C18:3	278.44	5.20	5.20	0.09	0.09	7.47	7.39
all-*trans*-octadeca-9,12,15-trienoic			C18:3T[e]	278.44	0.57	0.57			1.14	1.13
icosanoic	Arachidic	A	C20:0	312.54	0.32	0.36	0.21	0.23	0.51	0.57

cis-icos-9-enoic	Gadoleic	Ga	C20:1	310.52	0.27	0.30	0.20	0.22	1.27	1.40
docosanoic	Behenic	Be	C22:0	340.59	0.38	0.47	0.52	0.64	0.25	0.30
docos-13-enoic	Erucic		C22:1	338.57					0.34	0.40
tetracosanoic	Lignoceric	Lg	C24:0	368.65	0.12	0.16	0.18	0.24	0.10	0.13
cis-tetracos-15-enoic	Nervonic	Ne	C24:1	366.63					0.10	0.13
FFA[f]						0.0002		0.0002		0.0002
W[g]/ mg.kg^{-1}						< 72		< 73		< 70
IV[h]						123.18		130.67		107.43

[a] *M* = Molar mass; [b] C z:y, where z = number of carbons and y = number of double bonds; [c] molar fraction; [d] mass fraction; [e]Trans isomers; [f] Free fatty acid expressed as mass fractions of oleic acid; [g] W = Water content; [h] IV = calculated Iodine value.

The probable triacylglycerol (TAG) compositions (Table 6.2) were obtained by gas chromatography and by the algorithm suggested by Antoniossi Filho et al. [41] as described in previous work [25].

The average molar mass of the vegetable oils was calculated using the respective fatty acid compositions present in Table 6.1, assuming that all fatty acids are esterified to the glycerol molecules to form triacylglycerols. The values obtained for the refined soybean, sunflower and rapeseed oils are 874.04 $\mathrm{g.mol^{-1}}$, 875.55 $\mathrm{g.mol^{-1}}$, and 882.83 $\mathrm{g.mol^{-1}}$, respectively.

Table 6.2. Probable triacylglycerol composition of refined vegetable oils investigated.

		M^a/	Soybean oil		Sunflower oil		Rapseed oil	
main TAG[b]	**Cz:y[c]**	**($g.mol^{-1}$)**	**100 x^d**	**100 w^e**	**100 x**	**100 w**	**100 x**	**100 w**
POP	C50:1[c]	833.36	1.46	1.40			0.55	0.52
PLiP	C50:2	831.34	3.29	3.14	1.34	1.27		
POS	C52:1	861.42	0.89	0.89			0.59	0.58
POO	C52:2	859.40	5.42	5.35	2.06	2.02	8.26	8.07
POLi	C52:3	857.38	11.92	11.74	7.79	7.63	5.94	5.79
PLeO	C52:4	855.36					2.83	2.75
PLiLi	C52:4	855.36	14.85	14.59	11.80	11.52		
PLeLi	C52:5	853.35	1.95	1.91				
SOO	C54:2	887.46	1.74	1.77	0.66	0.67	2.66	2.68
SOLi	C54:3	885.43	6.87	6.99	3.60	3.64		
OOO	C54:3	885.43	2.79	2.83	2.69	2.72	34.98	35.21
OOLi	C54:4	883.42	13.39	13.58	16.74	16.89	23.44	23.54
OLiLi	C54:5	881.40	16.61	16.82	29.60	29.80		
OOLe	C54:5	881.40					14.39	14.42
LiLiLi	C54:6	879.38	16.95	17.12	23.71	23.82		
OLiLe	C54:6	879.38					4.15	4.15
LiLiLe	C54:7	877.37	1.87	1.88				
OOA	C56:2	915.51					0.60	0.63
OOGa	C56:3	913.50					1.00	1.04
OLiGa	C56:4	911.48					0.60	0.62

[a] M = Molar mass; [b] Groups with a total triacylglycerol (TAG) composition lower than 0.5 % were ignored; [c] C z:y, where z = number of carbons (except carbons of glycerol) and y = number of double bonds; [d] molar fraction; [e] mass fraction.

6.2.2. Apparatus and Experimental Procedure

The molar excess enthalpies (H^E) data were measured using a commercially available isothermal flow calorimeter from Hart Scientific (model 7501). The apparatus and procedure have been previously described by Gmehling [31]. In the calorimeter, two syringe pumps (model LC 2600, ISCO) provide a flow of constant composition and temperature through a thermostated flow cell equipped with a pulsed heater, a calibration heater, and a Peltier cooler mounted in a stainless steel cylinder. A back pressure regulator keeps the pressure constant (up to 2.10^4 kPa) and prevents evaporation and degassing effects. Flow rates were selected to cover the whole mole fraction range. This device enables the detection of endothermic and exothermic mixing effects since the Peltier cooler works at constant power, producing a constant heat loss from the calorimeter cell, which is compensated by the pulsed heater. The energy per pulse was determined by electrical calibration with precision of ca. 0.5 %. From the recorded frequency change of the pulsed heater (between base line and actual measurements) and the flow rates, the molar excess enthalpies could be obtained from the energy evolved per pulse, the densities of both components at pump temperature, the given pressure and the molar mass of the compounds. The densities of the refined vegetable oils were obtained (by interpolation) from experimental data measured with the help of a vibrating tube densimeter (Anton Paar Model 4500) with a precision of ($5.10^{-5}\mathrm{g.cm^{-3}}$), the vegetable oil molar masses were estimated as described above. The densities and molar mass of the other components were taken from the Dortmund Data Bank (DDB) [42]. The experimental uncertainties are ± 0.01

K in temperature and less than 0.0005 in mole fraction. The uncertainty in H^E measurements was estimated to be less than 1%.

The results have been fitted using a Redlich-Kister polynomial equation (Equation 6.1) and the objective function presented in Equation 6.2 as function of composition.

$$H^E/(x_1x_2) = \sum_{i=1}^{m} \mathrm{A_i}(2x_1 - 1)^{i-1} \quad (6.1)$$

$$F = \sum[(H^E/x_1x_2)_{exptl} - (H^E/x_1x_2)_{calcd}]^2 \quad (6.2)$$

where H^E is the molar excess enthalpy, $\mathrm{A_i}$ are the adjustable parameters obtained by the least-square equation method, m is the number of parameters, x_1 and x_2 are the mole fractions of the compounds 1 and 2, respectively, and the subscripts $exptl$ and $calcd$ indicate the experimental and calculated data, respectively.

6.3. Results and discussion

The 17 experimental excess enthalpy (H^E) data sets are given in Tables 6.3 to 6.13 with information about the temperature and the pressure used in the measurements. During the H^E measurements at temperatures 353.15 K and 383.15 K, no reaction was observed because of the short residence time in the calorimeter cel caused by the flow principle.

Table 6.3. Experimental H^E data for the system n-Hexane (1) + Soybean oil (2).

x_1[a]	$H^{Eb}/\ (J.mol^{-1})$	x_1	$H^E/\ (J.mol^{-1})$	x_1	$H^E/\ (J.mol^{-1})$
		353.15 K and 722 kPa			
0.0551	29.9	0.3871	192.2	0.7207	263.3
0.1104	60.0	0.4425	214.5	0.7764	255.6
0.1650	89.9	0.4980	234.6	0.8323	228.0
0.2210	114.9	0.5536	248.1	0.8881	191.6
0.2758	140.4	0.6095	261.0	0.9440	122.7
0.3321	167.7	0.6648	269.1		
		383.15 K and 756 kPa			
0.0502	10.7	0.5978	106.4	0.9395	1.3
0.0993	26.1	0.6981	95.6	0.9496	-4.4
0.1982	48.7	0.7986	68.5	0.9596	-6.5
0.2986	77.7	0.8488	45.8	0.9698	-8.9
0.3976	92.7	0.8992	19.9	0.9798	-7.8
0.4981	103.0	0.9244	6.5	0.9899	-5.1

[a] Uncertainty < 0.0005 in mole fraction; [b] Uncertainty < 1%.

Table 6.4. Experimental H^E data for the system Methanol (1) + Soybean oil (2).

x_1[a]	$H^{Eb}/\ (J.mol^{-1})$	x_1	$H^E/\ (J.mol^{-1})$	x_1	$H^E/\ (J.mol^{-1})$
		353.15 K and 722 kPa			
0.0569	595.0	0.4073	3478.3	0.7033	3680.2
0.1184	1231.8	0.4680	3728.1	0.7623	3313.2
0.1727	1721.5	0.5265	3818.8	0.8217	2683.4
0.2333	2280.6	0.5848	3886.9	0.8811	1826.1
0.2912	2748.1	0.6435	3811.5	0.9405	925.2
0.3505	3134.5				

[a] Uncertainty < 0.0005 in mole fraction; [b] Uncertainty < 1%.

Table 6.5. Experimental H^E data for the system Ethanol (1) + Soybean oil (2).

x_1[a]	H^E[b]/ $(J.\mathrm{mol}^{-1})$	x_1	H^E/ $(J.\mathrm{mol}^{-1})$	x_1	H^E/ $(J.\mathrm{mol}^{-1})$
		353.15 K and 687 kPa			
0.0570	583.6	0.4087	3670.9	0.7027	3927.3
0.1157	1216.0	0.4666	3988.9	0.7621	3610.0
0.1745	1767.9	0.5260	4108.2	0.8212	3118.2
0.2321	2274.0	0.5843	4193.6	0.8808	2417.9
0.2902	2857.8	0.6432	4126.6	0.9403	1452.8
0.3492	3318.2				
		383.15 K and 653 kPa			
0.0571	625.4	0.4090	3894.7	0.7029	4559.6
0.1158	1335.3	0.4668	4215.3	0.7623	4261.5
0.1746	1949.5	0.5262	4554.9	0.8216	3747.3
0.2323	2490.6	0.5846	4671.8	0.8809	2964.5
0.2904	3057.3	0.6442	4679.8	0.9404	1798.0
0.3494	3498.8				

[a] Uncertainty < 0.0005 in mole fraction; [b] Uncertainty < 1%.

Table 6.6. Experimental H^E data for the system Propan-2-ol (1) + Soybean oil (2).

x_1[a]	H^E[b]/ $(J.\mathrm{mol}^{-1})$	x_1	H^E/ $(J.\mathrm{mol}^{-1})$	x_1	H^E/ $(J.\mathrm{mol}^{-1})$
		298.15 K and 998 kPa			
0.0535	465.4	0.3864	2857.8	0.6829	2985.9
0.1082	953.6	0.4429	3012.5	0.7444	2746.8
0.1601	1450.3	0.5023	3133.7	0.8070	2366.4
0.2167	1911.6	0.5619	3149.8	0.8705	1832.0
0.2711	2341.0	0.6214	3119.4	0.9348	1075.3
0.3285	2632.1				

[a] Uncertainty < 0.0005 in mole fraction; [b] Uncertainty < 1%.

Table 6.7. Experimental H^E data for the system n-Hexane (1) + Sunflower oil (2).

x_1[a]	H^E[b]/ $(J.mol^{-1})$	x_1	H^E/ $(J.mol^{-1})$	x_1	H^E/ $(J.mol^{-1})$
		353.15 K and 756 kPa			
0.0553	29.5	0.3878	187.2	0.7213	264.1
0.1107	61.0	0.4433	210.3	0.7769	254.9
0.1654	83.0	0.4988	226.0	0.8327	233.0
0.2215	113.5	0.5543	243.9	0.8884	190.2
0.2764	134.5	0.6102	255.8	0.9442	123.3
0.3327	166.6	0.6655	264.8		
		383.15 K and 894 kPa			
0.0505	8.5	0.6994	99.8	0.9399	1.9
0.0999	21.9	0.7595	86.0	0.9499	-0.3
0.1992	48.7	0.8296	61.2	0.9599	-5.1
0.2999	74.2	0.8798	36.2	0.9700	-5.8
0.3991	98.3	0.8998	22.7	0.9800	-4.9
0.4997	109.3	0.9198	13.7	0.9399	1.9
0.5993	111.2				

[a] Uncertainty < 0.0005 in mole fraction; [b] Uncertainty < 1%.

Table 6.8. Experimental H^E data for the system Methanol (1) + Sunflower oil (2).

x_1[a]	H^E[b]/ $(J.mol^{-1})$	x_1	H^E/ $(J.mol^{-1})$	x_1	H^E/ $(J.mol^{-1})$
		353.15 K and 791 kPa			
0.0570	596.5	0.4082	3508.2	0.7038	3670.3
0.1135	1242.1	0.4690	3729.1	0.7628	3290.9
0.1686	1731.2	0.5274	3876.5	0.8221	2663.6
0.2340	2257.9	0.5857	3926.2	0.8814	1821.6
0.2920	2704.7	0.6444	3850.6	0.9406	925.6
0.3513	3215.4				

[a] Uncertainty < 0.0005 in mole fraction; [b] Uncertainty < 1%.

Table 6.9. Experimental H^E data for the system Ethanol (1) + Sunflower oil (2).

x_1[a]	H^E[b]/ $(J.mol^{-1})$	x_1	H^E/ $(J.mol^{-1})$	x_1	H^E/ $(J.mol^{-1})$
		353.15 K and 894 kPa			
0.0573	543.2	0.4101	3606.3	0.7049	3885.6
0.1163	1094.7	0.4694	3949.2	0.7638	3563.5
0.1753	1761.7	0.5285	4064.2	0.8203	3077.4
0.2359	2243.0	0.5875	4114.3	0.8819	2388.9
0.2938	2794.5	0.6460	4095.2	0.9409	1423.9
0.3525	3323.2				
		383.15 K and 860 kPa			
0.0574	522.4	0.4084	4018.0	0.7039	4640.6
0.1163	1205.9	0.4680	4409.7	0.7628	4355.2
0.1753	1822.8	0.5262	4679.9	0.8220	3830.9
0.2331	2424.8	0.5857	4847.4	0.8813	3042.6
0.2914	2951.3	0.6446	4836.1	0.9406	1855.5
0.3505	3560.4				

[a] Uncertainty < 0.0005 in mole fraction; [b] Uncertainty < 1%.

Table 6.10. Experimental H^E data for the system Propan-2-ol (1) + Sunflower oil (2).

x_1[a]	H^E[b]/ $(J.mol^{-1})$	x_1	H^E/ $(J.mol^{-1})$	x_1	H^E/ $(J.mol^{-1})$
		298.15 K and 929 kPa			
0.0524	591.1	0.3873	3055.4	0.6846	3057.8
0.1079	1168.2	0.4457	3203.3	0.7464	2796.9
0.1626	1728.7	0.5048	3284.1	0.8086	2398.4
0.2178	2164.4	0.5642	3283.1	0.8717	1872.6
0.2742	2519.7	0.6238	3206.2	0.9354	1108.3
0.3302	2830.8				

[a] Uncertainty < 0.0005 in mole fraction; [b] Uncertainty < 1%.

Table 6.11. Experimental H^E data for the system n-Hexane (1) + Rapeseed oil (2).

x_1[a]	H^E[b]/ $(J.mol^{-1})$	x_1	H^E/ $(J.mol^{-1})$	x_1	H^E/ $(J.mol^{-1})$
		353.15 K and 894 kPa			
0.0998	45.3	0.5012	229.0	0.9003	173.5
0.2012	96.5	0.6008	250.5	0.9502	113.9904
0.3013	147.0	0.7008	259.9	0.9801	48.5102
0.4008	190.8	0.8007	239.9		
		383.15 K and 1136 kPa			
0.1002	23.3	0.4994	100.4	0.8999	23.7
0.1998	47.3	0.5998	105.5	0.9400	-6.7
0.2996	72.5	0.6996	89.7	0.9602	-9.5
0.4000	92.3	0.7998	58.1	0.9901	-3.3

[a] Uncertainty < 0.0005 in mole fraction; [b] Uncertainty < 1%.

Table 6.12. Experimental H^E data for the system Methanol (1) + Rapeseed oil (2).

x_1[a]	H^E[b]/ $(J.mol^{-1})$	x_1	H^E/ $(J.mol^{-1})$	x_1	H^E/ $(J.mol^{-1})$
		353.15 K and 963 kPa			
0.0577	526.3	0.4508	3736.0	0.7654	3461.2
0.1200	1168.9	0.5509	4010.9	0.8241	2800.5
0.1750	1650.4	0.5999	4019.4	0.8828	1835.1
0.2361	2270.9	0.6480	4019.7	0.9413	925.2
0.2944	2829.1	0.7063	3854.2	0.9801	330.9
0.3540	3281.7				

[a] Uncertainty < 0.0005 in mole fraction; [b] Uncertainty < 1%.

Table 6.13. Experimental H^E data for the system Ethanol (1) + Rapeseed oil (2).

x_1[a]	H^E[b]/ $(J.mol^{-1})$	x_1	H^E/ $(J.mol^{-1})$	x_1	H^E/ $(J.mol^{-1})$
		353.15 K and 998 kPa			
0.0573	581.1	0.4100	3783.1	0.7049	3999.5
0.1163	1243.0	0.4694	4062.7	0.7638	3656.0
0.1753	1845.6	0.5285	4214.9	0.8229	3150.8
0.2331	2443.2	0.5875	4251.0	0.8819	2437.1
0.2937	2978.6	0.6459	4195.5	0.9409	1457.1
0.3525	3427.7				
		383.15 K and 1136 kPa			
0.0578	641.5	0.4120	3921.4	0.7061	4531.0
0.1171	1287.7	0.4700	4244.3	0.7645	4208.4
0.1764	1863.7	0.5294	4492.8	0.8234	3689.2
0.2345	2401.7	0.5876	4659.6	0.8823	2910.6
0.2930	2974.8	0.6471	4657.0	0.9412	1777.0
0.3522	3454.1				

[a] Uncertainty < 0.0005 in mole fraction; [b] Uncertainty < 1%.

A description of the enthalpic real mixture behavior of these liquids will be made from the analysis of the experimental excess enthalpies data presented in this paper.

The results obtained for systems of alcohol + vegetable oil (see tables 6.4-6.6, 6.8-6.10, 6.12, and 6.13) present high excess enthalpies. These systems are strongly endothermic, as also observed by Resa et al. [34] at 298.15 K, and the H^E values increase with increasing temperature.

The mixture alcohols + vegetable oil show a limited miscibility and thus a positive deviation from Raoult's law depending on temperature and composition. Silva et al. [28] and Chiyoda et al. [43] showed that the miscibility of vegetable oil and absolute ethanol increases with increasing temperature. At temperatures and concentrations studied in this work, no miscibility gap was observed. Our data are in agreement with the results obtained by Follegatti-Romero et al. [29] and Silva et al. [28], which presented the extrapolated critical solution temperatures (predicted by NRTL model) for the systems: soybean oil + ethanol (342.25 K), sunflower oil + ethanol (343.55 K) and rapeseed oil + ethanol (347.00 K), respectively, lower than the experimental temperatures used in this work.

The H^E data of n-hexane + vegetable oil are mostly positive but relatively small and decrease with increasing temperature. This is a typical behavior for mixtures between a slightly polar compound (vegetable oil) and a non-polar compound (n-hexane), as also observed by Gmehling [44]. However these binary mixtures at 383.15 K and at high concentration of n-hexane (above 0.94 molar fraction) presented negative values of H^E.

In Figs. 6.1 to 6.4 the experimental results for the vegetable oil systems are compared with the Redlich-Kister fits. The symbols represent the experimental data and the lines

correspond to the fitting carried out with the Redlich-Kister polynomial equation. It is worth noting that at present vapor-liquid equilibrium (VLE) data are not available in literature for the systems studied and liquid-liquid equilibrium (LLE) data are available for only a few of them [26, 39, 45]. Therefore, instead of simultaneous data regression using e.g. NRTL we have used the Redlich-Kister equation to fit the H^E results only.

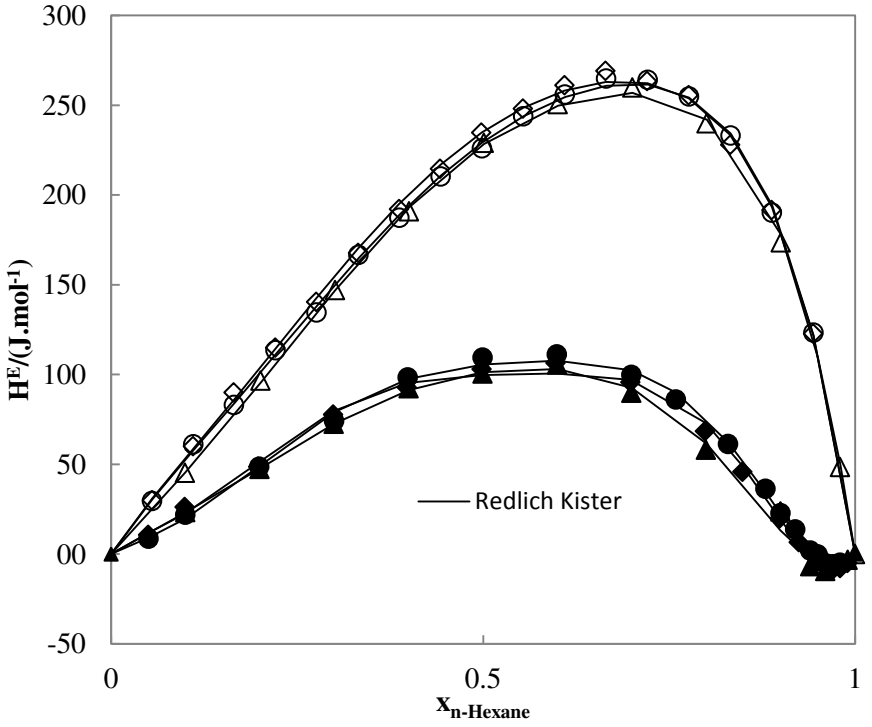

Fig. 6.1. Excess enthalpies (H^E) for the systems: n-hexane (1) + soybean oil (2) at 353.15 K (◊) and at 383.15 K (♦), n-hexane (1) + sunflower oil (2) at 353.15 K (○) and at 383.15 K (●), and n-hexane + rapeseed oil (2) at 353.15 K (Δ) and at 383.15 K (▲).

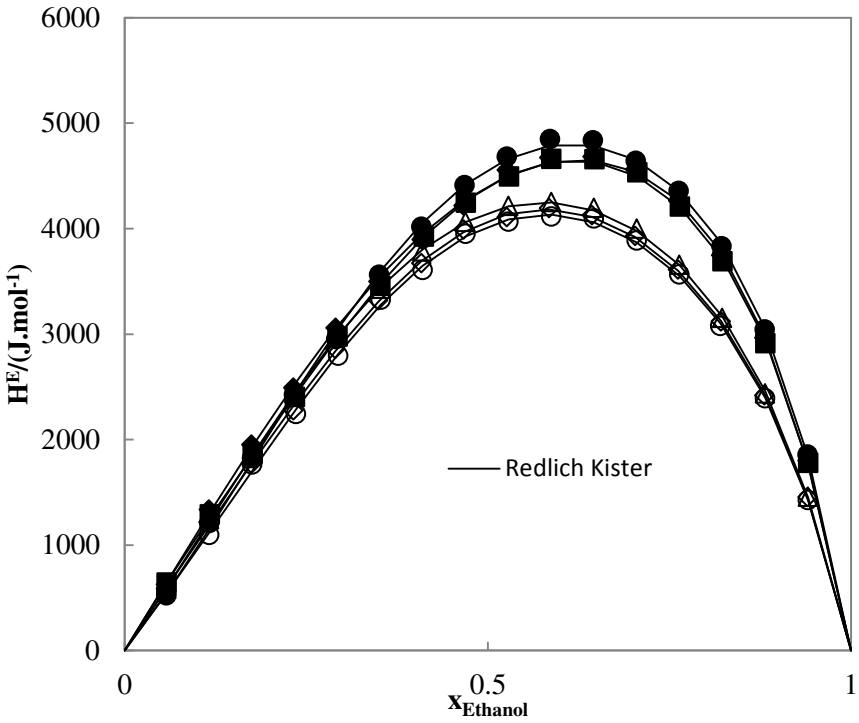

Fig. 6.2. Excess enthalpies (H^E) for the systems: ethanol (1) + soybean oil (2) at 353.15 K (◊) and at 383.15 K (♦), ethanol (1) + sunflower oil (2) at 353.15 K (○) and at 383.15 K (●) and ethanol + rapeseed oil (2) at 353.15 K (∆) and at 383.15 K (▲).

Comparing the results from mixtures of different vegetable oils with the same compound at the same temperature, very similar trends were found, as can be seen in Figs. 6.1 and 6.2. Therefore, the diagram for the further investigated mixtures was only presented for the case of soybean oil (Fig. 6.3).

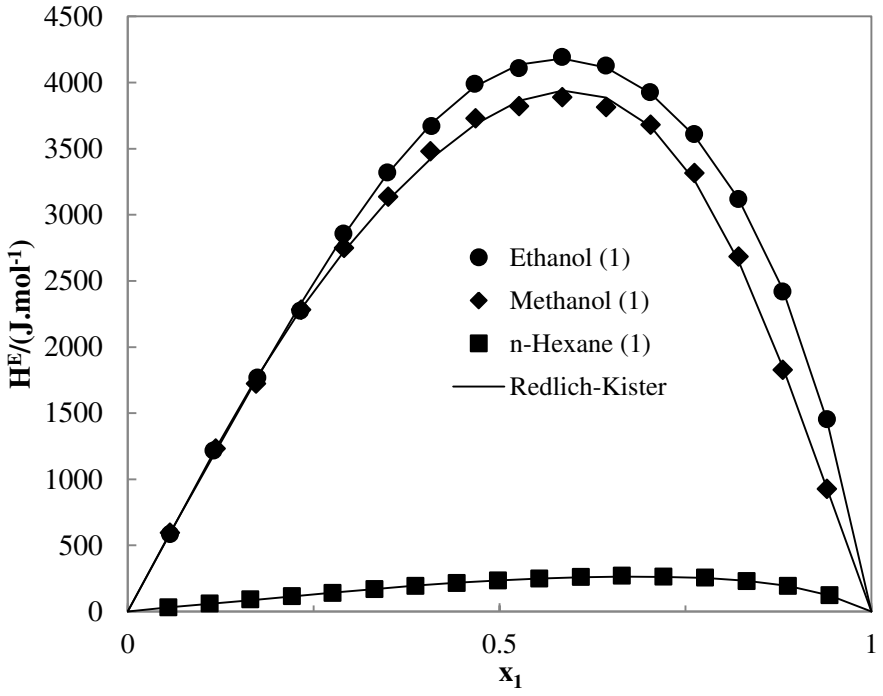

Fig. 6.3. Comparison of the experimental H^E data of mixtures of different solvents (1) with soybean oil (2) at 353.15 K.

The comparison of excess enthalpy data obtained for different mixtures with soybean oil at 353.15 K are presented in Fig. 6.3. Analysing the diagrams, it can be seen that all investigated mixtures show endothermic behavior. Furthermore the following hierarchy was found for the H^E values in increasing order: n-hexane < methanol < ethanol. The non-ideality of these mixtures can be attributed on one hand to structural effects: interstitial accommodation, changes in free volume, and differences in shape and size of the mixed components and, on the other hand, to the energetic effects, this means molecular interactions that can be weakened or destroyed or established during the mixing process [46].

From Figs. 6.2 and 6.3 it can be concluded that the molar excess enthalpies for mixtures with alcohols present large positive values. This behavior is usually observed when polar and associating compounds, such as alcohols, are mixed with polar but non associating molecules, such as esters, which constitute the vegetable oils. Our results are therefore consistent with the rule established by Abbott et al. [33], in their "field guide to the excess functions". This type of mixtures belongs to "region I" (enthalpy dominates) and have usually positive and large H^E values. This suggests that the overall amount of interactions of these two unmixed compounds diminishes upon mixing due to complex molecular effects in operation. In this type of mixture association or eletrostatic interactions (as the strong hydrogen-bonds) between like molecules (alcohol) may be partially compensated by solvation between unlike species (esters), i.e., probably strong dipolar interactions and hydrogen-bonds between the oxygen in the alcohols and the π-electrons of the ester (vegetable oil) are formed in place of the association effects or eletrostatic interactions between alcohol molecules. Comparing the results for mixtures with methanol and vegetable oils with ethanol and vegetable oils at same temperature (353.15 K) we can observe that the mixtures with ethanol presented always higher H^E values (see Tables 6.4 and 6.5 for soybean oil, 6.8 and 6.9 for sunflower oil, and 6.12 and 6.13 for rapeseed oil). Our results agree with those presented by Resa et al. [34]. They also verified that the disruption of the hydrogen-bonding effect which involves the absorption of energy increases with the size of the alcohol, i.e., alcohols with longer chain show more significant depression of hydrogen-bonding effect and consequently higher H^E values.

Comparing the H^E values for mixtures of n-hexane with vegetable oils with mixtures of vegetable oils and alcohol, higher interaction between the n-hexane (nonpolar compound) and the vegetable oil (polar but non associating compound) are observed. The low value of H^E *i*ndicates that the mixture of n-hexane and vegetable oil shows a quasi ideal enthalpic behavior.

Binary systems of vegetable oil + alcohols and vegetable oil + water have a strongly temperature dependent miscibility gap. This special behavior can be applied, for example, for the recovery of the solvents used in vegetable oil extraction by alcohols or for the recovery of excess alcohol normaly used in the transesterification reaction in biodiesel production.

The H^E-data of the systems propan-2-ol + soybean oil and propan-2-ol + sunflower oil at 298.15 K are compared to previously published data [34] in Fig. 6.4. For propan-2-ol + sunflower oil our results agree within ± 2 % with those obtained by other authors. In case of the system propan-2-ol + soybean oil our data are on average 15 % lower than those reported in literature. However, it should be mentioned that the equipment and methodology used in reference [34] differ considerably from the one used in this work and the vegetable oils used in both studies have slightly different compositions.

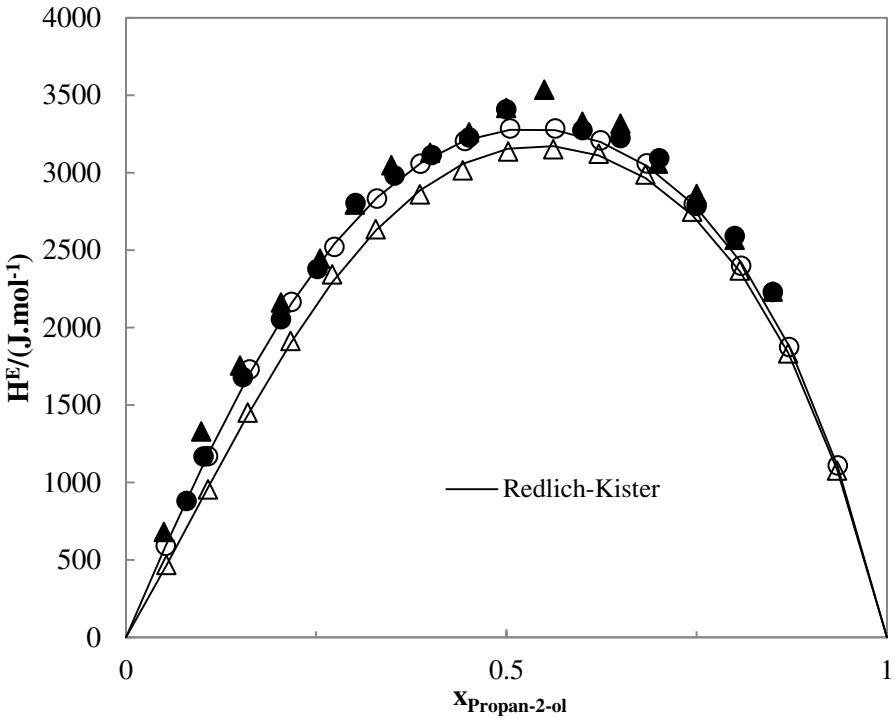

Fig. 6.4. Comparison of the experimental H^E data of mixtures with propan-2-ol (1) and vegetable oils at 298.15 K from this work (Δ - soybean oil, ○ - sunflower oil) and from Resa et al.[34] (▲ - soybean oil, ● – sunflower oil).

It was found (by both Resa et al. [34] and this study) that the variation of vegetable oil composition has no strong influence on the excess enthalpies, since these compounds are basically mixtures of triacylglycerols (esters) with a very similar average molar mass and similar chemical characteristics. It was observed that the variation of temperature and vegetable oil concentration had a much larger influence (see Figs. 6.1 and 6.2).

The equipment used by Resa et al. [34] works at ambient temperature and pressure. This means that the temperatures of the two compounds and the mixture are dependent on room temperature control. Unlike temperature and mixture composition, it is reasonable to consider that the pressure has little effect on H^Emeasurements, as long as it does not

promote changes in mixture physical state. In the equipment used in this work, the temperature control of the 2 components and of the mixture in flow cell is performed by thermostated syringe liquid pumps and silicon oil bath, respectively. The temperatures are monitored with a Hart Scientific platinum resistance thermometer (model 1006 Micro-Therm) with an accuracy of ± 0.005 K and the pressure is maintained constant (to avoid any evaporation) with help of a back pressure regulator.The methodology for calculating H^E is also different: in our work H^E is obtained from the energy envolved per pulse of the pulsed heater, while Resa et al. [34] use the variation of the temperature after mixing the components, i.e. the results are significantly influenced by the initial temperature of the components and by ambient temperature. Since the new values were determined several times with precise control, we believe them to be more accurate.

The fitted Redlich-Kister parameters A_i and the root mean square deviation (*RMSD*) for all investigated mixtures are given in Table 6.14.

Table 6.14. Redlich-Kister parameters (A_i) and the root mean square deviation (*RMSD*) for systems with refined vegetable oil.

Component 1	**Component 2**	**T/ K**	$\mathbf{A_1}$	$\mathbf{A_2}$	$\mathbf{A_3}$	$\mathbf{A_4}$	$\mathbf{A_5}$	$\mathbf{A_6}$	***RMSD*[a]/ ($\mathbf{J.mol^{-1}}$)**
n-hexane	soybean oil	353.15	941.533	566.75	255.21	499.31	486.59		2.75
n-hexane	soybean oil	383.15	399.105	29.601	266.36	617.32	-827.56	-1103.1	2.54
methanol	soybean oil	353.15	15170.4	5920.5	2392.8	-3595.4	-5403.3		37.53
ethanol	soybean oil	353.15	16305.1	5389.9	-538.38	3834.1	4189.3		19.63
ethanol	soybean oil	383.15	17621.8	7650.6	3895.1	4710.6	2085.6		33.69
propan-2-ol	soybean oil	298.15	12606.8	2021.2	1253.5	3635.5			21.91
water	soybean oil	353.15	3649.58	-664.85	282.67	-3351.4	-1297.5	4504.4	22.57
n-hexane	sunflower oil	353.15	918.391	592.20	311.16	481.55	457.52		2.34
n-hexane	sunflower oil	383.15	422.334	87.553	174.64	458.22	-732.63	-881.91	2.23
methanol	sunflower oil	353.15	15278.9	5832.7	2041.2	-3679.3	-4903.6		37.04
ethanol	sunflower oil	353.15	16103.1	5420.3	-745.32	4310.3	3756.8		29.80
ethanol	sunflower oil	383.15	18250.8	8236.3	1137.3	6158.4	3991.7		35.32
propan-2-ol	sunflower oil	298.15	13096.2	1303.1	2676.7	3038.2			12.41
water	sunflower oil	353.15	3491.78	-220.88	1967.2	-5696.8	-3285.7	6692.5	21.50
n-hexane	rapeseed oil	353.15	911.989	569.00	230.18	549.92	449.76		2.43
n-hexane	rapeseed oil	383.15	405.422	120.85	5.0906	73.920	-507.56	-583.44	3.74

methanol	rapeseed oil	353.15	15827.8	6518.1	798.51	-2723.6	-4771.5		57.01
ethanol	rapeseed oil	353.15	16616.9	4946.0	544.98	4665.0	2398.7		14.49
ethanol	rapeseed oil	383.15	17614.9	8196.9	1395.8	3988.4	5326.1		20.37
water	rapeseed oil	353.15	3679.06	-1220.1	246.31	-1442.4	-433.91	1632.3	2.75

[a]Root mean square deviation - $RMSD(H^E) = \left[\sum \frac{\left(H^E_{calcd} - H^E_{exptl}\right)^2}{N}\right]^{1/2}$, where N is the number of experimental values.

Table 6.15 summarizes the calculated values of the partial molar excess enthalpy at infinite dilution, $H_i^{E,\infty}$, for systems with various solvents (component 1) and refined vegetable oil (component 2) from this work (obtained by fitting a Redlich-Kister polynomial to the experimental calorimetric data) and available literature (derived from the slopes of the linear plot of $ln(\gamma_i^{\infty})$ the measured versus $1/T$ according to the Gibbs-Helmholtz equation). It can be seen that the $H_i^{E,\infty}$values obtained from the calorimetric data are in the range of the $H_i^{E,\infty}$ values obtained from the linear plots.

Table 6.15. Excess enthalpies at infinite dilution ($H_i^{E,\infty}$) for systems with various solvents (1) and refined vegetable oil (2).

		This work				Ref. [36][b]	Ref. [25][b]
Component 1	**Component 2**	$\boldsymbol{H_1^{E,\infty}/}$ $\boldsymbol{(kJ.mol^{-1})}$ **at 353.15 K**	$\boldsymbol{H_2^{E,\infty}/}$ $\boldsymbol{(kJ.mol^{-1})}$ **at 353.15 K**	$\boldsymbol{H_1^{E,\infty}/}$ $\boldsymbol{(kJ.mol^{-1})}$ **at 383.15 K**	$\boldsymbol{H_2^{E,\infty}/}$ $\boldsymbol{(kJ.mol^{-1})}$ **at 383.15 K**	$\boldsymbol{H_1^{E,\infty}/}$ $\boldsymbol{(kJ.mol^{-1})}$	$\boldsymbol{H_1^{E,\infty}/}$ $\boldsymbol{(kJ.mol^{-1})}$
n-hexane	soybean oil	0.62	2.75	0.29	-0.62	0.59	1.57
methanol	soybean oil	9.83	14.48			9.72	9.28
ethanol	soybean oil	10.73	29.18	11.24	35.96	12.15	11.66
propan-2-ol	soybean oil	8.20[a]	19.52 [a]				
water	soybean oil	2.15	3.12				
n-hexane	sunflower oil	0.61	2.76	0.20	-0.47		1.72
methanol	sunflower oil	10.26	14.57				11.68
ethanol	sunflower oil	9.38	28.85	8.99	37.77		22.00
propan-2-ol	sunflower oil	11.43 [a]	20.11 [a]				
water	sunflower oil	1.40	2.95				
n-hexane	rapeseed oil	0.47	2.71	0.29	-0.49		1.30
methanol	rapeseed oil	8.06	15.65				16.36
ethanol	rapeseed oil	9.95	29.17	12.15	36.52		17.55
water	rapeseed oil	4.52	2.46				

[a] Data obtained at 298.15 K, [b] estimated from linear dependence of $ln(\gamma_i^{\infty})$on the reciprocal absolute temperature, uncetainty ± 20%.

Table 6.15 shows similar values of $H_i^{E,\infty}$ for mixtures with the same solvent in the different vegetable oils and for almost all mixtures investigated the obtained values at infinite dilution correspond to endothermal partial molar excess enthalpies ($H_i^{E,\infty} > 0$), except for mixtures of vegetable oil at infinite dilution in n-hexane at 383.15 K, as observed in experimental H^E values (see Tables 6.3, 6.7, and 6.11). The positive and large $H_i^{E,\infty}$ values for alcohols at infinite dilution again reflect the weak association with the vegetable oils.

Comparing the partial molar excess enthalpies values at infinite dilution of n-hexane in the vegetable oils of this work to the literature, the data measured show differences of less than 0.03 $\mathrm{kJ.mol^{-1}}$ to 1.52 $\mathrm{kJ.mol^{-1}}$ in absolute values. Comparing our results for methanol and ethanol at infinite dilution in soybean oil with available literature data, the difference is always less than 12%. It should be considered that the values of $H_i^{E,\infty}$ from both available references have about 20% error by the fact that $H_i^{E,\infty}$ is determined from the difference of log terms.

6.4. Conclusions

Excess enthalpies were measured for 20 mixtures containing refined vegetable oils in the temperature range from 298.15 K to 383.15 K with the objective of extending the excess enthalpy database at higher temperatures, which is required for the further development of the modified UNIFAC (Dortmund). Because at this moment vapor-liquid and liquid-liquid equilibrium data are only available for part of the studied systems, the results have been

fitted to the Redlich-Kister polynomial equation instead of using a thermodynamic model based on the local composition concept.

All systems investigated showed deviation from the ideal behavior and their experimental H^E data are mostly positive. The strong endothermic effect observed in mixtures with alcohols is mainly due to the disruption of hydrogen-bonds upon mixing.

A further publication under preparation will compare these findings with the results of static vapor-liquid equilibrium (VLE) measurements obtained for the same vegetable oils and compared with the results of different predictive methods. Thus, it will be possible to evaluate the need to define new groups and/or to fit new group interaction parameters for the modified UNIFAC method.

Acknowledgements

P. C. Belting wishes to acknowledge CNPq (Conselho Nacional de Desenvolvimento Científico e Tecnológico – 142122/2009-2 and 290128/2010-2) and DAAD (Deutscher Akademischer Austauschdienst – A/10/71471) for the scholarship. The authors would like to thank the CNPq (304495/2010-7, 483340/2012-0, 307718/2010-7 and 301999/2010-4), FAPESP (Fundação de Amparo à Pesquisa do Estado de São Paulo - 08/56258-8, 09/54137-1 and 2010/16634-0) and INCT-EMA (Instituto Nacional de Ciência e Tecnologia de Estudos do Meio Ambiente) for the financial support. The authors are grateful to the DDBST GmbH for permitting the use of the Dortmund Data Bank. This work has been supported by the Carl von-Ossietzky University Oldenburg.

List of Symbols

H^E	excess enthalpy or heat of mixing
TAG	triacylglycerol
FA	fatty acid
FFA	free fatty acid
VLE	vapor-liquid equilibrium
LLE	liquid-liquid equilibrium
G^E	excess Gibbs energy
AOCS	American Oil Chemists' Society
GC	gas chromatography
M	molar mass
C z:y	z = number of carbons and y = number of double bonds
x	molar fraction
w	mass fraction
T	trans isomers
W	water content
IV	iodine value
L	lauric acid
M	myristic acid
P	palmitic acid
Po	palmitoleic acid
Ma	margaric acid
S	stearic acid
O	oleic acid
Li	linoleic acid
Le	linolenic acid
A	arachidic acid
Ga	gadoleic acid
Be	behenic acid

Lg	lignoceric acid
Ne	nervonic acid
x_1	mole fraction of component 1
x_2	mole fraction of component 2
A_i	adjustable parameter of the Redlich-Kister equation
m	number of parameters of the Redlich-Kister equation
$RMSD$	root mean square deviation
N	number of experimental values
T	absolute temperature
$H_i^{E,\infty}$	partial molar excess enthalpy at infinite dilution of compound i

Subscripts

i	identification of component
i	identification of Redlich-Kister parameter
$exptl$	experimental data
$calcd$	calculated data

Superscripts

E	excess property
∞	at infinite dilution

References

[1] R.D. O'Brien, Fats And Oils Processing, in: W.E.F. R. D. O'Brien, and P. J. Wan (Ed.) Introduction to Fats and Oils Technology, A.O.C.S. Press, Champaign, Illinois, 2000, pp. 90-107.

[2] P.J. Wan, Properties of Fats and Oils, in: W.E.F. R. D. O'Brien, P. J. Wan (Ed.) Introduction to Fats and Oils Technology, A.O.C.S. Press, Champaign, Illinois, 2000, pp. 20-48.

[3] F.D. Gunstone, Vegetable Oils, in: F. Shahidi (Ed.) Bailey's Industrial Oil and Fat Products John Wiley & Sons, Hoboken, New Jersey, 2005, pp. 606.

[4] E.D. Milligan, D.C. Tandy, Distillation and Solvent Recovery, J. Am. Oil Chem. Soc., 51 (1974) 347-350.

[5] A. Demarco, Extracción por Solvente, in: D.B.-A. J. M. Block (Ed.) Temas Selectos en Aceites y Grasas, Edgard Blücher, São Paulo, 2009, pp. 67-95.

[6] M.A. Williams, Recovery of Oils and Fats from Oilseeds and Fatty Materials, in: F. Shahidi (Ed.) Bailey's Industrial Oil and Fat Products, John Wiley & Sons, Inc., Hoboken, New Jersey, 2005, pp. 572.

[7] X. Xu, C. Jacobsenb, N.S. Nielsenb, M.T. Heinrichb, D. Zhoua, Purification and deodorization of structured lipids by short path distillation, Eur. J. Lipid Sci. Technol., 104 (2002) 745-755.

[8] X. Xu, S. Balchena, C.-E. Høyb, J. Adler-Nissena, Pilot Batch Production of Specific-Structured Lipids by Lipase-Catalyzed Interesterification: Preliminary Study on Incorporation and Acyl Migration, J. Am. Oil Chem. Soc., 75 (1998) 301-308.

[9] X. Xu, A. Skands, J. Adler-Nissen, Purification of Specific Structured Lipids by Distillation: Effects on Acyl Migration, J. Am. Oil Chem. Soc., 78 (2001) 715-718.

[10] C.B. Gonçalves, P.A. Pessôa Filho, A.J.A. Meirelles, Partition of Nutraceutical Compounds in Deacidification of Palm oil by Solvent Extraction., J. Food Eng., 81 (2007) 21-27.

[11] C.G. Pina, A.J.A. Meirelles, Deacidification of Corn Oil by Solvent Extraction in a Perforated Totating Disc Column., J. Am. Oil Chem. Soc., 77 (2000) 553-559.

[12] K.F. Mattil, Deodorization, in: F.A.N. K.F. Mattil, A.J. Stirton (Ed.) Bailey's Industrial Oil and Fat Products, John Wiley & Sons, New York, 1964, pp. 897-930.

[13] W. De Greyt, M. Kellens, Deodorization, in: F. Shahidi (Ed.) Bailey's Industrial Oil and Fat Products, John Wiley & Sons, Inc., Hoboken, New Jersey, 2005, pp. 341-383.

[14] F. Ma, M.A. Hanna, Biodiesel Production: a Review, Bioresource Technol., 70 (1999) 1-15.

[15] L.C. Meher, D.V. Sagar, S.N. Naik, Technical aspects of biodiesel production by transesterifications: a review, Renew Sust. Energ. Rev., 10 (2006).

[16] J.M. Marchetti, V.U. Miguel, A.F. Errazu, Possible methods for biodiesel production, Renew Sust. Energ. Rev., 11 (2007) 1300-1311.

[17] J. Gmehling, B. Kolbe, M. Kleiber, J. Rarey, Chemical Thermodynamics for Process Simulation, 1st ed., Wiley-VCH, Weinheim, 2012.

[18] B.E. Poling, J.M. Prausnitz, J.P. O'Connell, Properties of Gases and Liquids, 5th ed., McGraw-Hill, 2001.

[19] J. Gmehling, A. Brehm, Grundoperationen, Thieme-Verlag, Stuttgart, 1996.

[20] R. Ceriani, A.J.A. Meirelles, Predicting Vapor–Liquid Equilibria of Fatty Systems, Fluid Phase Equilibr., 215 (2004) 227–236.

[21] R. Ceriani, C.B. Gonçalves, J. Rabelo, M. Caruso, A.C.C. Cunha, F.W. Cavaleri, E.A.C. Batista, A.J.A. Meirelles, Group Contribution Model for Predicting Viscosity of Fatty Compounds, J. Chem. Eng. Data, 52 (2007) 965-972.

[22] C.B. Gonçalves, R. Ceriani, J. Rabelo, M.C. Maffia, A.J.A. Meirelles, Viscosities of Fatty Mixtures: Experimental Data and Prediction, J. Chem. Eng. Data, 52 (2007) 2000-2006.

[23] J. Rabelo, E. Batista, F.W. Cavaleri, A.J.A. Meirelles, Viscosity Prediction for Fatty Systems, J. Am. Oil Chem. Soc., 77 (2000) 1255-1262.

[24] P.C. Belting, J. Rarey, J. Gmehling, R. Ceriani, O. Chiavone-Filho, A.J.A. Meirelles, Activity Coefficient at Infinite Dilution Measurements for Organic Solutes (polar and nonpolar) in Fatty Compounds: Saturated Fatty Acids, J. Chem. Thermodyn., 55 (2012) 42-49.

[25] P.C. Belting, J. Rarey, J. Gmehling, R. Ceriani, O. Chiavone-Filho, A.J.A. Meirelles, Measurements of Activity Coefficients at Infinite Dilution in Vegetable Oils and Capric Acid Using the Dilutor Technique, (2013).

[26] E. Batista, S. Monnerat, K. Kato, L. Stragevitch, A.J.A. Meirelles, Liquid-Liquid Equilibrium for Systems of Canola Oil, Oleic Acid, and Short-Chain Alcohols, J. Chem. Eng. Data, 44 (1999) 1360-1364.

[27] M.C. Costa, L.A.D. Boros, M.P. Rolemberg, M.A. Krähenbühl, A.J.A. Meirelles, Solid-Liquid Equilibrium of Saturated Fatty Acids + Triacylglycerols, J. Chem. Eng. Data, 55 (2010) 974-977.

[28] C.A.S. Silva, G. Sanaiotti, M. Lanza, L.A. Follegatti-Romero, A.J.A. Meirelles, E. Batista, Mutual Solubility for Systems Composed of Vegetable Oil + ethanol + Water at Different Temperatures, J. Chem. Eng. Data, 55 (2010) 440-447.

[29] L.A. Follegatti-Romero, M. Lanza, C.A.S. Silva, E.A.C. Batista, A.J.A. Meirelles, Mutual Solubility of Pseudobinary Systems Containing Vegetable Oils and Anhydrous Ethanol from (298.15 to 333.15) K, J. Chem. Eng. Data, 55 (2010) 2750-2756.

[30] P.C. Belting, J. Rarey, J. Gmehling, R. Ceriani, O. Chiavone-Filho, A.J.A. Meirelles, Activity coefficient at infinite dilution measurements for organic solutes (polar 3 and non-polar) in fatty compounds – Part II: C18 fatty acids, J. Chem. Thermodyn., (2013).

[31] J. Gmehling, Excess Enthalpies for 1, 1, 1 - Trichloroethane with Alkanes, Ketones, and Esters, J. Chem. Eng. Data, 38 (1993) 143-146.

[32] J. Lohmann, J. Gmehling, Bedeutung von Stützstellen bei tiefen und hohen Temperaturen für die Anpassung temperaturabhängiger Modified UNIFAC (Dortmund)-Parameter, Chem. Tech., 51 (1999) 184-190.

[33] M.M. Abbott, M.V. Ariyapadi, N. Balsara, S. Dasgupta, J.S. Furno, P. Futerko, D.P. Gapinski, T.A. Grocella, R.D. Kaminsky, S.G. Karlsruher, E.W. Kiewra, A.S. Narayan, K.K. Nass, J.P. O'Connell, C.J. Parks, D.F. Rogowski, G.S. Roth, M.B. Sarsfield, K.M. Smith, M. Sujanani, J.J. Tee, N. Tzouvaras, A Field Guide to the Excess Functions, Chem. Eng. Educ., 28 (1994) 18-23,77.

[34] J.M. Resa, C. González, M.A. Fanega, S. Ortiz de Landaluce, J. Lanz, Enthalpies of Mixing, Heat Capacities, and Viscosities of Alcohol (C1-C4) + Olive Oil Mixtures at 298.15 K, J. Food Eng., 52 (2002) 113-118.

[35] A. Lebert, D. Richon, Infinite Dilution Activity Coefficients of n -Alcohols as a Function of Dextrin Concentration in Water-Dextrin Systems, J. Agric. Food Chem., 32 (1984) 1156-1161.

[36] J.W. King, G.R. List, A Solution Thermodynamic Study of Soybean Oil/Solvent Systems by Inverse Gas Chromatography, J. Am. Oil Chem. Soc., 67 (1990) 424-430.

[37] AOCS, Official Methods and Recommended Practices of the American Oil Chemists' Society, 5 th ed., AOCS Press, Champaign, IL, 2004.

[38] L. Hartman, R.C.A. Lago, Rapid Preparation of Fatty Acid Methyl Esters from Lipids, Lab. Pract., 22 (1973) 475–476.

[39] M. Lanza, G. Sanaiotti, E. Batista, R.J. Poppi, A.J.A. Meirelles, Liquid-Liquid Equilibrium Data for Systems Containing Vegetable Oils, Anhydrous Ethanol, and Hexane at (313.15, 318.15, and 328.15) K, J. Chem. Eng. Data, 54 (2009) 1850-1859.

[40] C.A.S. Silva, G. Sanaiotti, M. Lanza, L.A. Follegatti-Romero, A.J.A. Meirelles, E.A.C. Batista, Mutual Solubility for Systems Composed of Vegetable Oil + ethanol + Water at Different Temperatures, J. Chem. Eng. Data, 55 (2010) 440-447.

[41] N.R. Antoniossi Filho, O.L. Mendes, F.M. Lanças, Computer prediction of triacylglicerol composition of vegetable oils by HRGC, J. Chromatog., 40 (1995) 557-562.

[42] Dortmund Data Bank Dortmund Data Bank Software & Separation Technology in, DDBST GmbH, Oldenburg, 2011.

[43] C. Chiyoda, E.C.D. Peixoto, A.J.A. Meirelles, C.E.C. Rodrigues, Liquid–liquid equilibria for systems composed of refined soybean oil, free fatty acids, ethanol, and water at different temperatures, Fluid Phase Equilib., 299 (2010) 141–147.

[44] J. Gmehling, Excess enthalpies of tert-butyl methyl ether (MTBE) + butane at 323.15 Kand 1.8 MPa and of tert-amyl methyl ether (TAME) + methanol at 363.13 K and 2.4 MPa, J. Phys.-Chem. Data, 2 (1996) 131-134.

[45] M. Mohsen-Nia, H. Modarress, H.R. Nabavi, Measuring and Modeling Liquid–Liquid Equilibria for a Soybean Oil, Oleic Acid, Ethanol, and Water System, J. Am. Oil Chem. Soc., 85 (2008) 973–978.

[46] B. Giner, S. Martín, H. Artigas, M.C. López, C. Lafuente, Study of Weak Molecular Interactions through Thermodynamic Mixing Properties, J. Phys. Chem. B, 110 (2006) 17683-17690.

CAPÍTULO 7: MEASUREMENT, CORRELATION AND PREDICTION OF ISOTHERMAL VAPOR-LIQUID EQUILIBRIA OF DIFFERENT SYSTEMS CONTAINING VEGETABLE OIL

Artigo submetido à revista Fluid Phase Equilibria.

Measurement, correlation and prediction of isothermal vapor-liquid equilibria of different systems containing vegetable oil

Patrícia C. Belting[a,b,1], Rainer Bölts[a], Jürgen Rarey[a], Jürgen Gmehling[a], Roberta Ceriani[c], Osvaldo Chiavone-Filho[d], Antonio J. A. Meirelles[b*]

[a] Carl von Ossietzky Universität Oldenburg, Technische Chemie (FK V), D-26111 Oldenburg, Federal Republic of Germany

[b] Food Engineering Department, Faculty of Food Engineering, University of Campinas, Av. Monteiro Lobato 80, Cidade Universitária Zeferino Vaz, 13083-862, Campinas-SP, Brazil

[c] Faculty of Chemical Engineering, University of Campinas, Av. Albert Einstein 500, Cidade Universitária Zeferino Vaz, 13083-852, Campinas-SP, Brazil

[d] Chemical Engineering Department, Federal University of Rio Grande do Norte, Av. Senador Salgado Filho S/N, 59066-800, Natal-RN, Brazil

[1 a] Present address, [b] Permanent address

Abstract

Thermodynamic properties, in particular vapor–liquid equilibria (VLE) data, are required for the development of reliable predictive models for systems with fatty compounds. Isothermal VLE data have been measured for methanol, ethanol, and n-hexane with the refined vegetable oils: soybean, sunflower and rapeseed oils at 348.15 K and 373.15 K with the help of a computer-driven static apparatus. For mixtures containing vegetable oils and n-hexane a negative deviation from Raoult's law was observed and a

homogeneous behavior (no miscibility gap) was found, while mixtures with vegetable oils and alcohols exhibited positive deviation from ideal behavior and, in some cases, limited miscibility. On the basis of the composition of the studied vegetable oils, their relative van der Waals volume and surface area parameters were estimated by the Bondi method and their vapor pressure by a group contribution method developed by Ceriani and Meirelles [1]. The experimental VLE data were correlated together with available excess enthalpies (H^E) and activity coefficients at infinite dilution (γ_i^∞) data using the UNIQUAC model. For the fitting process the refined vegetable oil was treated as a single triacylglycerol (pseudo-component) which has the corresponding degree of unsaturation, number of carbon and molar mass of the original oil composition. The overall-average error (AAE) using UNIQUAC model are 4.46 % for VLE, 7.07 % for γ_i^∞ and 5.80 % for H^E. The experimental data were also compared with the predicted results using mod. UNIFAC (Dortmund) and an extension of these method proposed to triacylglycerols in previous work was also tested.

Keywords: Refined vegetable oil, Vapor-liquid equilibria, UNIQUAC, Modified UNIFAC (Dortmund).

7.1. Introduction

The use of lipids in the food, chemical, petrochemical, pharmaceutical, and cosmetic industries is a long used practice [2-8]. Therefore some vegetable oils and animal fats are treated as commodities [2]. In recent years the interest in fatty compounds has been motivated by the optimization and development of new technologies in edible oil processing [9-14], by the search for alternative solvents for oil extraction from oilseeds [15-20], and mainly by the growing concern in finding alternative non-fossil fuels as biodiesel [21-23].

Natural vegetable oils are composed mainly of triacylglycerols (TAGs) that are esters composed of one molecule of glycerol and three fatty acid molecules, which may either be saturated or unsaturated [9, 10, 24, 25], i.e. vegetable oils are normally complex mixtures of many different TAGs [24].

In industrial processes that involve vegetable oils there are several separation steps in which information about phase equilibria and thermophysical properties is essential for the design and operation of equipment, especially because these processes involve multicomponent mixtures. Particularly the vapor-liquid equilibrium (VLE) is of great importance in the following edible oil and related compounds industry processes: recovery of the solvent from the oil-solvent mixture, fatty acids distillation, fatty alcohols fractionation, and physical refining and deodorization of vegetable oils [1, 14, 19, 20, 26-31].

Unfortunately the number of published vapor-liquid equilibrium (VLE) data sets for fatty compounds, especially for vegetable oils, is very limited. Reliable vapor-liquid

equilibrium (VLE) data would allow checking whether the standard g^E-models like NRTL or UNIQUAC can be used for the description of the real liquid mixture behavior of binary systems with fatty compounds and if group contribution model and g^E-model parameters can successfully be applied to the prediction of the VLE behavior of systems containing fatty compounds as vegetable oils. Predictive models are of great importance, especially for vegetable oils, due to the broad variety of molecular species and composition varying widely with the sources [24].

This paper presents results of a part of our research work in field of fatty compounds and complements the study of thermophysical properties of these components for the development of predictive thermodynamic models. In previous papers, activity coefficients at infinite dilution (γ_i^∞) in saturated and unsaturated fatty acids (capric, lauric, myristic, palmitic, stearic, oleic, linoleic, and, linolenic acids) and in refined vegetable oils have already been reported [32-34], besides excess enthalpies (H^E) of systems containing refined vegetable oils that were also published [35]. In this work, vapor-liquid equilibria (VLE) for systems containing refined soybean, sunflower and rapeseed oils have been measured at 348.15 K and 373.15 K. Additionally, the experimental VLE, γ_i^∞ [34] and H^E [35] data were correlated simultaneously using temperature-dependent interaction for the g^E-model UNIQUAC [36] and predicted by modified UNIFAC Dortmund (mod. UNIFAC) [37, 38] model. The modification of mod. UNIFAC proposed in previous work [34] was also used and its performance was evaluated.

7.2. Experimental

7.2.1. Materials

The supplier, the purity, and the water content of the chemicals and refined vegetable oils used in this work are listed in Table 7.1. The chemicals were used without further treatment. At the beginning of the measurement all vegetable oils were dried over molecular sieves and were purified by vacuum evaporation to remove the last traces of volatile compounds. The vegetable oil composition was analyzed in terms of fatty acid (FA) and triacylglycerol (TAG) content (Tables 7.2 and 7.3, respectively) using the procedure described below. The water content was controlled by Karl Fischer titration for every compound including vegetable oils. The water concentration determined with this method was in all cases less than 100 $\mathrm{mg.kg^{-1}}$. Prior to the VLE measurements, all components were degassed according to the method of Van Ness and Abbott [39].

Table 7.1. Supplier, purity, and water content of the chemicals and the refined vegetable oils.

Component	**Supplier**	**Purity (GC)**	**Water content/**
		Mass fraction	$(\mathbf{mg.kg^{-1}})$
Methanol	VWR International GmbH	> 0.998	80
Ethanol	VWR International GmbH	> 0.998	48
n-Hexane	Carl Roth GmbH	> 0.99	30
Soybean oil	Vandermoortele Deutschland GmbH		72
Sunflower Oil	Brökelmann + Co and Oelmühle GmbH + Co		73
Rapeseed Oil	Brökelmann + Co and Oelmühle GmbH + Co		70

Table 7.2 presents the fatty acid (FA) compositions of the investigated refined vegetable oils. The analysis was performed by gas chromatography of fatty acid methyl esters using the official method (1-62) of the American Oil Chemists' Society (AOCS) [40]. Before performing the chromatographic analysis, the fatty acids of the vegetable oils were converted to their respective methyl esters using the method of Hartman and Lago [41], as used in previous works [34, 35]. The chromatographic analyses were carried out using a CGC Agilent 6850 Series CG capillary gas chromatography system, the experimental conditions are described in detail by Belting et al. [34].

The free fatty acid content and the Iodine value (IV) of refined vegetable oils were determined according to the official AOCS methods [40] Ca 5a-40 and Cd 1c-85, respectively.

The vegetable oil average molar mass was calculated from the respective fatty acid compositions presented in Table 7.2. It was considered that all fatty acids are esterified to the glycerol molecules to form triacylglycerols. The values obtained for the refined soybean, sunflower and rapeseed oils are 874.04 $\mathrm{g.mol^{-1}}$, 875.55 $\mathrm{g.mol^{-1}}$, and 882.83 $\mathrm{g.mol^{-1}}$, respectively.

To determine the probable triacylglycerol (TAG) compositions (Table 7.3), samples of vegetable oil diluted in tetrahydrofuran (10 $\mathrm{mg.mL^{-1}}$) were submitted to a CGC Agilent 6850 Series CG capillary gas chromatograph system under the same experimental conditions as described in previous work [34]. Most TAG groups were identified by comparison with the retention times of the Nu Check Prep (Elysian/MN, U. S. A.) standards. Since it is not possible to identify all chromatogram peaks due to the lack of standards, for determination of the complete TAG composition the algorithm developed by Antoniossi Filho et al. [42] was employed. The TAG group quantification was performed by internal normalization. As input data to the algorithm, the quantities of *trans* isomers (see table 7.2) were computed with their respective *cis* isomers, as suggested by Follegatti-Romero et al. [43].

Table 7.2. Fatty acid composition of refined vegetable oils investigated in this work.

Fatty Acid Nomenclature				M^a/	**Soybean oil**		**Sunflower oil**		**Rapeseed oil**	
IUPAC	**Trivial**	**Symbol**	**Cz:y[b]**	$(\mathbf{g.mol^{-1}})$	**100 x^c**	**100 w^d**	**100 x**	**100 w**	**100 x**	**100 w**
dodecanoic	Lauric	L	C12:0	200.32	0.05	0.03	0.07	0.05	0.06	0.05
tetradecanoic	Myristic	M	C14:0	228.38	0.10	0.09	0.11	0.09	0.09	0.07
pentadecanoic			C15:0	242.40	0.04	0.04	0.05	0.04	0.04	0.04
hexadecanoic	Palmitic	P	C16:0	256.43	11.46	10.55	6.94	6.36	4.89	4.46
cis-hexadec-9-enoic	Palmitoleic	Po	C16:1	254.42	0.11	0.10	0.13	0.12	0.22	0.20
heptadecanoic	Margaric	Ma	C17:0	270.45	0.09	0.09	0.04	0.04	0.06	0.06
cis-heptadeca-10-enoic			C17:1	268.43	0.06	0.06	0.04	0.04	0.07	0.07
octadecanoic	Stearic	S	C18:0	284.49	3.40	3.47	3.02	3.07	1.78	1.79
cis-octadeca-9-enoic	Oleic	O	C18:1	282.47	28.90	29.30	25.52	25.76	62.98	63.18
cis,cis-octadeca-9,12-dienoic	Linoleic	Li	C18:2	280.45	48.73	49.04	62.47	62.61	18.64	18.56
trans-trans-octadeca-9,12-dienoic	Linoelaidic		C18:2T[e]	278.44	0.19	0.19	0.40	0.40	0.10	0.10
all-*cis*-octadeca-9,12,15-trienoic	Linolenic	Le	C18:3	278.44	5.20	5.20	0.09	0.09	7.47	7.39
all-*trans*-octadeca-9,12,15-trienoic			C18:3T[e]	278.44	0.57	0.57			1.14	1.13

icosanoic	Arachidic	A	C20:0	312.54	0.32	0.36	0.21	0.23	0.51	0.57
cis-icos-9-enoic	Gadoleic	Ga	C20:1	310.52	0.27	0.30	0.20	0.22	1.27	1.40
docosanoic	Behenic	Be	C22:0	340.59	0.38	0.47	0.52	0.64	0.25	0.30
docos-13-enoic	Erucic		C22:1	338.57					0.34	0.40
tetracosanoic	Lignoceric	Lg	C24:0	368.65	0.12	0.16	0.18	0.24	0.10	0.13
cis-tetracos-15-enoic	Nervonic	Ne	C24:1	366.63					0.10	0.13
FFA[f]						0.0002		0.0002		0.0002
IV[g]						123.18		130.67		107.43

[a] *M* = Molar mass; [b] C z:y, where z = number of carbons and y = number of double bonds; [c] molar fraction; [d] mass fraction; [e]Trans isomers; [f] Free fatty acid expressed as mass fractions of oleic acid; [g] IV = calculated Iodine value.

Table 7.3. Probable triacylglycerol composition of refined vegetable oils investigated.

		M^a/	Soybean oil		Sunflower oil		Rapseed oil	
main TAG[b]	**Cz:y[c]**	**($g.mol^{-1}$)**	**100 x^d**	**100 w^e**	**100 x**	**100 w**	**100 x**	**100 w**
POP	C50:1[c]	833.36	1.46	1.40			0.55	0.52
PLiP	C50:2	831.34	3.29	3.14	1.34	1.27		
POS	C52:1	861.42	0.89	0.89			0.59	0.58
POO	C52:2	859.40	5.42	5.35	2.06	2.02	8.26	8.07
POLi	C52:3	857.38	11.92	11.74	7.79	7.63	5.94	5.79
PLeO	C52:4	855.36					2.83	2.75
PLiLi	C52:4	855.36	14.85	14.59	11.80	11.52		
PLeLi	C52:5	853.35	1.95	1.91				
SOO	C54:2	887.46	1.74	1.77	0.66	0.67	2.66	2.68
SOLi	C54:3	885.43	6.87	6.99	3.60	3.64		
OOO	C54:3	885.43	2.79	2.83	2.69	2.72	34.98	35.21
OOLi	C54:4	883.42	13.39	13.58	16.74	16.89	23.44	23.54
OLiLi	C54:5	881.40	16.61	16.82	29.60	29.80		
OOLe	C54:5	881.40					14.39	14.42
LiLiLi	C54:6	879.38	16.95	17.12	23.71	23.82		
OLiLe	C54:6	879.38					4.15	4.15
LiLiLe	C54:7	877.37	1.87	1.88				
OOA	C56:2	915.51					0.60	0.63
OOGa	C56:3	913.50					1.00	1.04
OLiGa	C56:4	911.48					0.60	0.62

[a] M = Molar mass; [b] Groups with a total triacylglycerol (TAG) composition lower than 0.5 % were ignored; [c] C z:y, where z = number of carbons (except carbons of glycerol) and y = number of double bonds; [d] molar fraction; [e] mass fraction.

For regression of UNIQUAC model parameters and the prediction by mod.UNIFAC, the refined vegetable oil was represented by a pseudo-component, a single triacylglycerol which has the same degree of unsaturation, number of carbon atoms and average molar mass as the original vegetable oil according to the composition presented in Table 7.3. This approach assumes that the different triacylglycerols present in the vegetable oil behave in a very similar way in the vapor-liquid system under analysis. In this case such compounds can be adequately replaced by a unique representative component having the corresponding average physical-chemical properties. This approach was already evaluated by Lanza et al. [44] who proved its veracity for the liquid-liquid equilibrium.

The structures of the representative components of the refined vegetable oils investigated in this work are shown in Fig. 7.1.

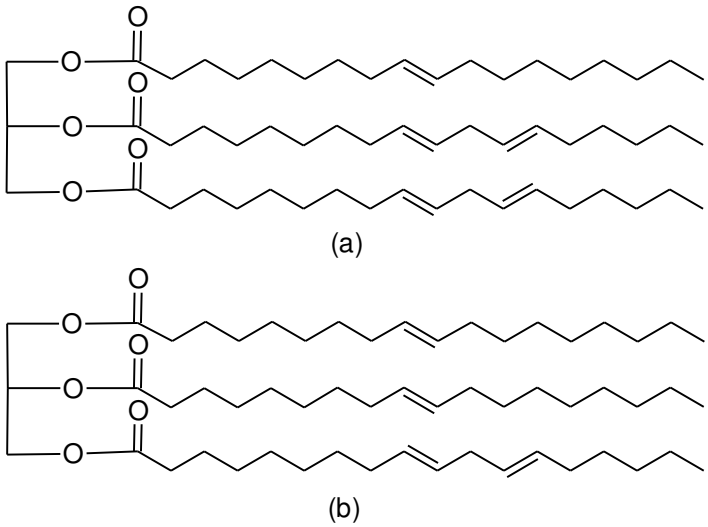

Fig 7.1. Representative components of the investigated refined vegetable oils. (a) 2,3-di(octadeca-9,12-dienoyloxy)propyl octadec-9-enoate (OLiLi) for soybean and sunflower oils; (b) (3-octadeca-9,12-dienoyloxy-2-octadec-9-enoyloxypropyl) octadec-9-enoate (OOLi) for rapeseed oil.

7.2.2. Apparatus and Experimental Procedure

The isothermal VLE data ($P - x$) were measured on a computer-driven static apparatus at 348.15 K and 373.15 K. Principle of the method [45], description of the device [46], and measurement procedure are presented in previous papers [46-48]. The stainless steel equilibrium cell of known volume is immersed in a large oil bath, thoroughly stirred and equipped with a high precision thermostatization. The cell temperature is measured using a Pt100 resistance thermometer (Model 1506, Hart Scientific) pre-calibrated by NIST and with resolution of ± 1 mK. A Digiquartz pressure sensor (Model 245 A, Paroscientific) is connected to the equilibrium cell. The pressure inside the cell is monitored with an accuracy of approximately 0.0005% of maximum pressure. Exactly known amounts of purified, degassed and thermostated components are introduced into the evacuated

equilibrium cell via automatic valves using stepping motor driven piston injectors. The liquid phase composition is obtained by solving mass and volume balance equations, taking into account the vapor-liquid equilibrium (evidenced by the constant temperature and pressure). In this study (low system pressure), the calculated liquid compositions were considered identical to the feed compositions within ± 0.002. The apparatus can be applied for highly precise $P-x$ -measurement up to 388K and 0.35 MPa. The experimental uncertainties of this apparatus are as follows: σ(T)= 0.03 K, σ(P)= 20 Pa + 0.0001 (P/Pa), $\sigma(x_i)$=0.0001.

7.3. Results and discussion

The experimental vapor-liquid equilibrium (VLE) data measured at 348.15 K and 373.15 K for the systems with refined vegetable oils are listed in Tables 7.4-7.9. No pressure increase inside the equilibrium cell was observed during the VLE determination, which leads us to conclude that no reaction with either formation or loss of volatile components takes place in the temperature range covered. In addition, after each VLE-measurement, it was determined the water content of the resulting mixture (vegetable oil + solvent) in equilibrium cell by Karl Fischer titration and no change was observed.

Table 7.4. Vapor-liquid equilibria for methanol (1), ethanol (1), and n-hexane (1) with soybean oil (2) at 348.15 K.

Methanol (1)		**Ethanol (1)**		**n-Hexane (1)**	
x_1	P/kPa	x_1	P/kPa	x_1	P/kPa
0.0000	0.061	0.0000	0.053	0.0000	0.050
0.0962	21.421	0.0344	4.109	0.0303	2.031
0.1415	31.995	0.0675	8.077	0.0786	5.194
0.1919	43.439	0.1006	11.991	0.1132	7.592
0.2323	52.745	0.1367	16.327	0.1329	8.996
0.2665	60.555	0.1680	20.180	0.1713	11.810
0.2985	67.685	0.1968	23.657	0.2059	14.439
0.3298	74.613	0.2211	26.595	0.2256	16.013
0.3570	80.525	0.2682	32.257	0.2533	18.349
0.4121	92.084	0.3034	36.394	0.2745	20.200
0.4993	109.202	0.3899	46.443	0.3370	25.974
0.5901	125.186	0.4817	56.598	0.4006	32.413
0.6795	138.335	0.5757	65.952	0.4721	40.530
0.7573	147.335	0.6704	74.259	0.5530	50.917
0.8118	150.534	0.7401	79.435	0.6215	60.816
0.8532	150.588	0.7947	82.820	0.6813	70.365
0.8973	150.641	0.8397	85.057	0.7315	79.348
0.9184	150.654	0.8763	86.422	0.7359	79.789
0.9380	150.654	0.9060	87.174	0.7775	87.565
0.9560	150.654	0.9304	87.611	0.7849	88.715
0.9693	150.654	0.9475	87.745	0.8239	96.051
0.9788	150.641	0.9613	87.825	0.8283	96.815
0.9858	150.654	0.9723	87.877	0.8648	103.647
0.9909	150.641	0.9807	87.939	0.8697	104.334
0.9943	150.641	0.9870	88.002	0.8956	109.270

0.9966	150.628	0.9913	88.097	0.9061	110.508
0.9981	150.641	0.9942	88.190	0.9336	114.755
0.9991	150.668	0.9961	88.282	0.9545	117.625
0.9997	150.694	0.9975	88.350	0.9702	119.581
1.0000	150.708	0.9984	88.405	0.9811	120.854
		0.9990	88.447	0.9885	121.723
		0.9995	88.478	0.9937	122.306
		0.9998	88.518	0.9971	122.718
		1.0000	88.587	0.9990	122.935
				1.0000	123.125

Table 7.5. Vapor-liquid equilibria for methanol (1), ethanol (1), and n-hexane (1) with soybean oil (2) at 373.15 K.

Methanol (1)		**Ethanol (1)**		**n-Hexane (1)**	
x_1	P/kPa	x_1	P/kPa	x_1	P/kPa
0.0000	0.087	0.0000	0.088	0.0000	0.080
0.1145	44.366	0.0401	9.020	0.0543	5.829
0.1828	73.847	0.1103	25.178	0.0884	10.292
0.2449	101.477	0.1395	32.005	0.1093	13.094
0.2998	126.927	0.1705	40.039	0.1333	16.395
0.3512	150.908	0.1975	46.812	0.1643	20.794
0.3930	170.319	0.2487	59.866	0.1974	25.721
0.4327	189.024	0.2710	65.753	0.2206	29.298
0.4659	204.583	0.3026	74.114	0.2333	31.297
0.4927	217.302	0.3661	91.238	0.2700	37.413
0.5547	246.113	0.4385	110.912	0.3595	53.856
0.6192	274.471	0.5178	132.560	0.4563	74.622
0.6914	303.735	0.6053	155.974	0.5406	95.608
0.7615	328.253	0.6931	178.025	0.6161	117.136
0.8135	342.838	0.7576	192.677	0.6754	136.069
0.8537	351.078	0.8061	202.477	0.7181	151.441
0.8867	352.118	0.8502	210.196	0.7199	151.374
0.8956	352.118	0.8811	214.556	0.7622	166.813
0.9168	352.104	0.9112	217.875	0.7674	169.239
0.9367	352.131	0.9362	219.862	0.8023	181.958
0.9549	352.131	0.9551	220.942	0.8189	188.611
0.9684	352.131	0.9688	221.608	0.8392	196.184
0.9781	352.131	0.9789	222.075	0.8648	205.916
0.9853	352.158	0.9864	222.488	0.8716	208.543
0.9905	352.158	0.9914	222.848	0.9017	219.115

0.9940	352.171	0.9949	223.315	0.9300	228.381
0.9964	352.184	0.9972	223.648	0.9516	234.767
0.9980	352.211	0.9986	223.928	0.9681	239.154
0.9990	352.411	0.9995	224.035	0.9795	242.033
0.9996	352.544	1.0000	224.368	0.9873	243.967
1.0000	352.638			0.9929	245.353
				0.9966	246.286
				0.9988	246.820
				1.0000	247.220

Table 7.6. Vapor-liquid equilibria for methanol (1), ethanol (1), and n-hexane (1) with sunflower oil (2) at 348.15 K.

Methanol (1)		**Ethanol (1)**		**n-Hexane (1)**	
x_1	P/kPa	x_1	P/kPa	x_1	P/kPa
0.0000	0.030	0.0000	0.020	0.0000	0.041
0.0592	13.100	0.0523	5.990	0.0462	3.022
0.1153	25.601	0.0950	11.187	0.0881	5.796
0.1681	37.625	0.1373	16.457	0.1275	8.601
0.2152	48.389	0.1726	20.825	0.1567	10.768
0.2582	58.342	0.2060	24.913	0.1908	13.411
0.2999	68.002	0.2346	28.487	0.2180	15.569
0.3309	75.076	0.2649	32.233	0.2342	16.931
0.3638	82.469	0.2907	35.402	0.2533	18.546
0.4362	97.769	0.3373	41.007	0.2939	22.152
0.5194	113.764	0.4211	50.596	0.3461	27.146
0.6035	128.044	0.5102	60.195	0.4040	33.105
0.6798	139.069	0.6011	68.872	0.4746	41.213
0.7577	147.881	0.6882	76.100	0.5550	51.637
0.8126	150.508	0.7530	80.647	0.6231	61.564
0.8540	150.601	0.8035	83.588	0.6827	71.181
0.8871	150.628	0.8456	85.530	0.7294	79.015
0.8977	150.601	0.8588	86.162	0.7371	80.729
0.9135	150.668	0.8802	86.698	0.7756	87.303
0.9187	150.601	0.8868	87.004	0.7859	89.787
0.9345	150.654	0.9083	87.335	0.8222	95.851
0.9383	150.628	0.9133	87.522	0.8684	104.205
0.9506	150.681	0.9379	87.787	0.9050	110.439
0.9561	150.628	0.9479	87.778	0.9328	114.661
0.9693	150.628	0.9563	87.887	0.9539	117.496

0.9788	150.614	0.9697	87.945	0.9698	119.458
0.9857	150.628	0.9795	87.987	0.9807	120.723
0.9908	150.628	0.9867	88.047	0.9882	121.599
0.9942	150.641	0.9916	88.142	0.9935	122.197
0.9965	150.628	0.9949	88.234	0.9969	122.589
0.9981	150.641	0.9972	88.335	0.9990	122.849
0.9991	150.668	0.9987	88.430	1.0000	123.034
0.9997	150.694	0.9995	88.491		
1.0000	150.694	1.0000	88.585		

Table 7.7. Vapor-liquid equilibria for methanol (1), ethanol (1), and n-hexane (1) with sunflower oil (2) at 373.15 K.

Methanol (1)		**Ethanol (1)**		**n-Hexane (1)**	
x_1	P/kPa	x_1	P/kPa	x_1	P/kPa
0.0000	0.053	0.0000	0.088	0.0000	0.061
0.0860	34.510	0.0401	9.020	0.0516	6.240
0.1614	66.511	0.1103	25.178	0.0991	12.359
0.2315	97.712	0.1395	32.005	0.1294	16.909
0.2950	126.963	0.1705	40.039	0.1599	21.484
0.3488	151.961	0.1975	46.812	0.1881	25.595
0.3980	174.772	0.2487	59.866	0.2167	29.987
0.4358	192.438	0.2710	65.753	0.2408	33.831
0.4713	209.329	0.3026	74.114	0.2717	38.925
0.5051	225.208	0.3661	91.238	0.3861	63.936
0.5653	252.739	0.4385	110.912	0.4678	81.283
0.6293	280.217	0.5178	132.560	0.5433	99.566
0.6967	307.121	0.6053	155.974	0.6149	119.264
0.7649	330.333	0.6931	178.025	0.6695	135.962
0.8158	344.198	0.7576	192.677	0.7153	151.081
0.8555	351.918	0.8061	202.477	0.7247	153.694
0.8878	352.171	0.8502	210.196	0.7591	166.440
0.8956	352.211	0.8811	214.556	0.7706	170.199
0.9141	352.251	0.9112	217.875	0.8002	181.572
0.9168	352.211	0.9362	219.862	0.8172	187.545
0.9349	352.291	0.9551	220.942	0.8380	195.704
0.9366	352.251	0.9688	221.608	0.8637	204.823
0.9548	352.251	0.9789	222.075	0.8709	207.876
0.9683	352.238	0.9864	222.488	0.8994	218.075
0.9780	352.238	0.9914	222.848	0.9011	218.102

0.9852	352.238	0.9949	223.315	0.9297	227.368
0.9904	352.238	0.9972	223.648	0.9517	233.701
0.9939	352.238	0.9986	223.928	0.9683	238.087
0.9963	352.238	0.9995	224.035	0.9798	240.940
0.9980	352.251	1.0000	224.368	0.9876	242.860
0.9991	352.411			0.9932	244.220
0.9996	352.544			0.9967	245.140
1.0000	352.624			0.9988	245.660
				1.0000	245.993

Table 7.8. Vapor-liquid equilibria for methanol (1), ethanol (1), and n-hexane (1) with rapeseed oil (2) at 348.15 K.

Methanol (1)		Ethanol (1)		n-Hexane (1)	
x_1	P/kPa	x_1	P/kPa	x_1	P/kPa
0.0000	0.046	0.0000	0.062	0.0000	0.039
0.0585	13.331	0.0410	5.440	0.0350	2.313
0.1135	26.209	0.0858	10.875	0.0602	3.972
0.1658	38.581	0.1256	15.887	0.0873	5.755
0.2066	48.195	0.1645	20.681	0.1097	7.266
0.2506	58.429	0.1980	24.853	0.1358	9.146
0.2885	67.108	0.2320	29.075	0.1575	10.740
0.3213	74.554	0.2576	32.148	0.1782	12.287
0.3499	80.925	0.2858	35.593	0.1973	13.756
0.4043	92.644	0.3359	41.514	0.2160	15.217
0.4953	110.442	0.4208	51.181	0.2817	20.678
0.5813	125.547	0.5116	60.782	0.3528	27.299
0.6654	137.989	0.6032	69.401	0.4351	35.810
0.7497	147.815	0.6899	76.484	0.5266	46.824
0.8084	150.508	0.7540	80.907	0.6027	57.321
0.8518	150.548	0.8045	83.805	0.6682	67.460
0.8861	150.574	0.8465	85.706	0.7271	77.455
0.9131	150.601	0.8600	86.276	0.7316	78.455
0.9344	150.601	0.8810	86.838	0.7775	86.682
0.9438	150.614	0.8878	87.042	0.7792	86.918
0.9507	150.614	0.9141	87.542	0.8238	95.235
0.9612	150.614	0.9309	87.747	0.8246	95.475
0.9634	150.628	0.9385	87.774	0.8626	102.670
0.9721	150.641	0.9567	87.857	0.8696	103.602
0.9739	150.614	0.9700	87.894	0.8943	108.566

0.9777	150.641	0.9797	87.927	0.9059	109.895
0.9832	150.614	0.9868	87.981	0.9335	114.239
0.9898	150.601	0.9917	88.074	0.9543	117.174
0.9943	150.628	0.9949	88.174	0.9701	119.194
0.9971	150.628	0.9972	88.278	0.9809	120.495
0.9988	150.628	0.9987	88.370	0.9883	121.367
0.9997	150.654	0.9996	88.435	0.9936	121.990
1.0000	150.668	1.0000	88.535	0.9970	122.415
		1.0000	88.587	0.9990	122.635
				1.0000	122.845

Table 7.9. Vapor-liquid equilibria for methanol (1), ethanol (1), and n-hexane (1) with rapeseed oil (2) at 373.15 K.

Methanol (1)		Ethanol (1)		n-Hexane (1)	
x_1	P/kPa	x_1	P/kPa	x_1	P/kPa
0.0000	0.119	0.0000	0.104	0.0000	0.129
0.1041	40.186	0.0607	16.077	0.0481	6.058
0.1771	71.610	0.1042	27.916	0.0866	10.770
0.2446	101.872	0.1347	36.318	0.1093	13.659
0.3038	129.987	0.1607	43.446	0.1512	19.333
0.3508	152.481	0.2039	55.253	0.1694	21.874
0.3977	174.946	0.2425	66.056	0.1870	24.433
0.4380	194.451	0.2631	71.847	0.2234	29.974
0.4744	211.743	0.2988	82.272	0.2572	35.282
0.5066	226.595	0.3318	91.840	0.2740	38.042
0.5664	254.126	0.4033	112.301	0.3689	55.214
0.6213	278.337	0.4841	134.536	0.4603	74.441
0.6870	304.748	0.5738	158.200	0.5376	93.251
0.7592	330.066	0.6654	180.052	0.6133	114.420
0.8126	344.785	0.7324	194.224	0.6683	131.487
0.8537	352.211	0.7858	203.943	0.7190	148.708
0.8870	352.278	0.8309	210.863	0.7261	151.801
0.8922	352.384	0.8400	212.329	0.7621	164.306
0.9136	352.331	0.8675	215.382	0.7718	168.399
0.9201	352.398	0.8710	215.902	0.8027	179.625
0.9347	352.331	0.8979	218.262	0.8182	185.958
0.9425	352.411	0.9007	218.582	0.8400	193.997
0.9509	352.331	0.9286	220.342	0.8645	203.610
0.9603	352.424	0.9496	221.262	0.8724	206.423
0.9636	352.291	0.9650	221.835	0.9016	217.169

0.9722	352.371	0.9763	222.208	0.9301	226.688
0.9733	352.398	0.9846	222.542	0.9519	233.234
0.9778	352.371	0.9902	222.915	0.9684	237.754
0.9827	352.424	0.9941	223.262	0.9798	240.674
0.9896	352.438	0.9967	223.568	0.9877	242.620
0.9942	352.438	0.9984	223.795	0.9932	244.007
0.9971	352.464	0.9994	224.088	0.9967	244.887
0.9988	352.531	1.0000	224.315	0.9988	245.420
0.9997	352.704			1.0000	245.793
1.0000	352.704				

The experimental VLE data for the systems with refined vegetable oils were correlated with the g^E- model UNIQUAC considering the vegetable oil as a pseudo-component, as already mentioned above (see Fig. 7.1). To obtain reliable results for the whole composition and large temperature range besides the VLE data also activity coefficients at infinite dilution, γ_i^∞ [34], and excess enthalpies, H^E [35], were used. In order to consider temperature dependency, quadratic temperature-dependent binary interaction parameters were employed. The six parameters were fitted by the following expression:

$$\Delta u_{ij}/cal.mol^{-1} = a_{ij} + b_{ij}\,T/K + c_{ij}\,T^2/K^2 \qquad (7.1)$$

These adjustable parameters were fitted simultaneously to the experimental VLE, γ_i^∞ and H^E data using the Simplex-Nelder-Mead method [49], whereby the data points inside the miscibility gap were not taken into account during the fitting procedure. The objective function F was defined as follows:

$$F = \Delta VLE + \Delta\gamma_i^\infty + \Delta H^E \qquad (7.2)$$

with

$$\Delta VLE = g_{VLE} \sum_{i=1}^{nw} \left(\frac{P_{i,cal} - P_{i,exp}}{P_{i,exp}} \right)^2 \tag{7.3}$$

$$\Delta \gamma_i^{\infty} = g_{\gamma^{\infty}} \sum_{i=1}^{nw} \left(\frac{\gamma_{i,cal}^{\infty} - \gamma_{i,exp}^{\infty}}{\gamma_{i,exp}^{\infty}} \right)^2 \tag{7.4}$$

$$\Delta H^E = g_{H^E} \sum_{i=1}^{nw} \left(H_{i,cal}^E - H_{i,exp}^E \right)^2 \tag{7.5}$$

where nw is the number of data points and g is the weighting factor for each property.

The required data for the UNIQUAC model are listed in Table 7.10. For methanol, ethanol and n-hexane, the critical data, van der Waals properties r_i and q_i, and coefficients A_i, B_i and C_i of the Antoine equation:

$$P_v/\text{mmHg} = 10^{A_i - \frac{B_i}{T/^{\circ}\text{C} - C_i}} \tag{7.6}$$

which were used for fitting the parameters, were taken from the Dortmund Data Bank (DDB) [50]. For the refined vegetable oils, the relative van der Waals properties r_i and q_i of the UNIQUAC model were estimated from Bondi [51] and the critical constants were estimated according to the group contribution method proposed by Nannoolal et al. [52]. Since, at the moment, no vapor pressure data for vegetable oils are available, for the temperature range covered, this thermodynamic property was predicted according to the group contribution method proposed by Ceriani and Meirelles [1] and the Antoine equation parameters were fitted by the Pure Component Equations tool from DDBSP - Dortmund Data Bank Software Package [50].

Figs. 7.2-7.4 show the VLE experimental data ($P - x$ diagrams) of the nine systems investigated, together with the correlation results of the UNIQUAC model. Figs. 7.5-7.7 show a comparison of the experimental γ_i^{∞} data with correlated results from UNIQUAC

model for the same systems. The activity coefficients at infinite dilution, γ_i^{∞}, as calculated from the regressen parameters are also given in Figs. 7.5-7.7. In Figs. 7.8-7.10 the experimental and calculated H^E data for methanol, ethanol and n-hexane with the three refine vegetable oils investigated in this work are shown.

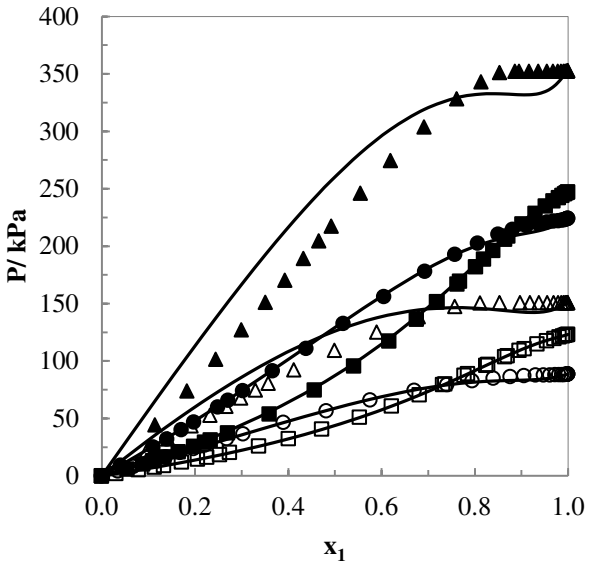

Fig. 7.2. Experimental and correlated VLE data for the investigated systems with soybean oil (2) and: (Δ at 348.15 K and ▲ at 373.15 K) methanol (1); (○ at 348.15 K and ● at 373.15 K) ethanol (1); (□ at 348.15 K and ■ at 373.15 K) n-hexane (1). (—) UNIQUAC.

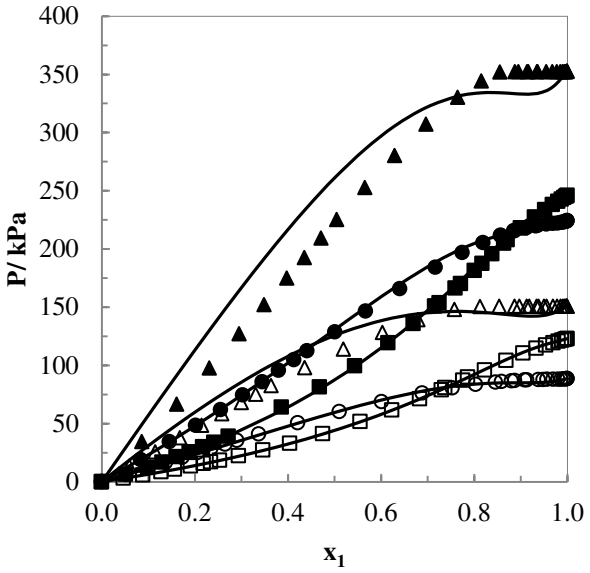

Fig. 7.3. Experimental and correlated VLE data for the investigated systems with sunflower oil (2) and: (Δ at 348.15 K and ▲ at 373.15 K) methanol (1); (○ at 348.15 K and ● at 373.15 K) ethanol (1); (□ at 348.15 K and ■ at 373.15 K) n-hexane (1). (—) UNIQUAC.

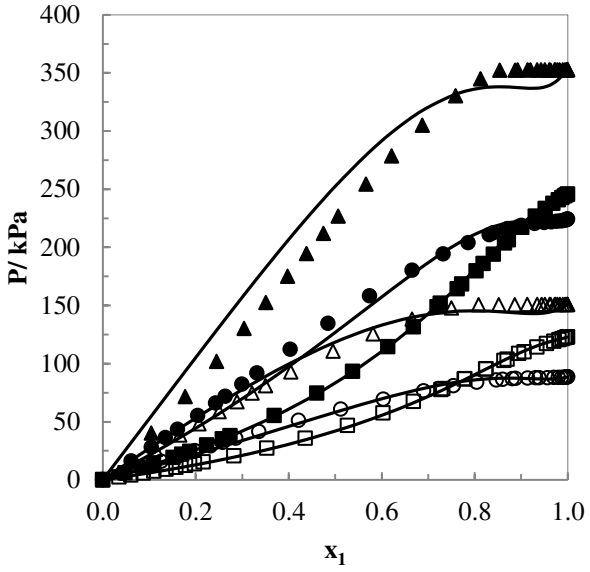

Fig. 7.4. Experimental and correlated VLE data for the investigated systems with rapeseed oil (2) and: (Δ at 348.15 K and ▲ at 373.15 K) methanol (1); (○ at 348.15 K and ● at 373.15 K) ethanol (1); (□ at 348.15 K and ■ at 373.15 K) n-hexane (1). (—) UNIQUAC.

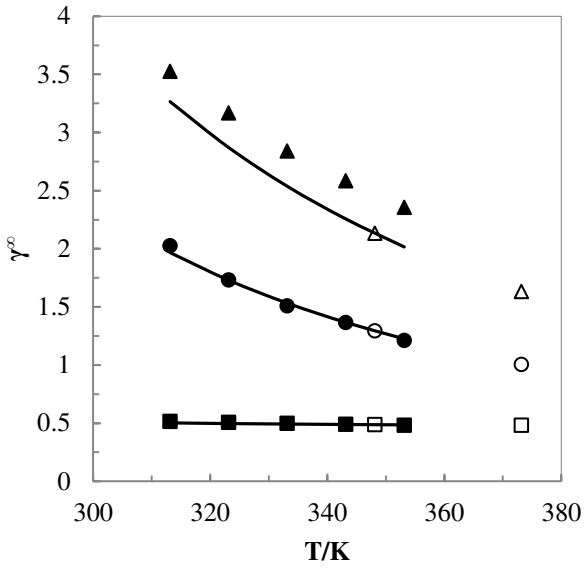

Fig. 7.5. Experimental and correlated γ_i^{∞} data of various solutes (1): (▲) methanol; (●) ethanol; (■) n-hexane in soybean oil (2), (—) UNIQUAC, and γ_i^{∞}-values derived from VLE data: (Δ) methanol, (○) ethanol and (□) n-hexane.

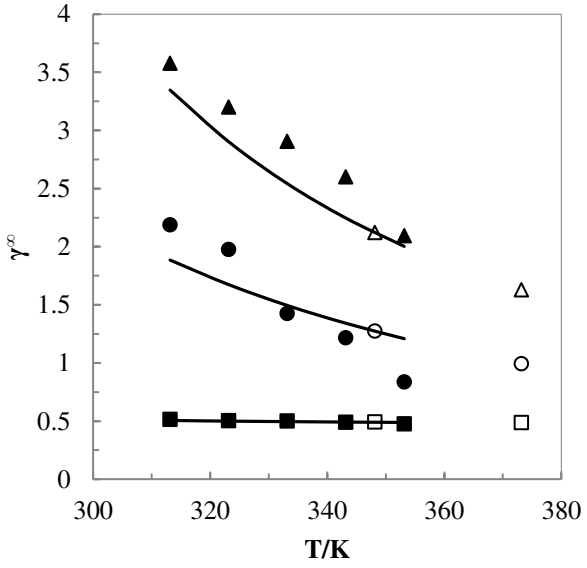

Fig. 7.6. Experimental and correlated γ_i^{∞} data of various solutes (1): (▲) methanol; (●) ethanol; (■) n-hexane in sunflower oil (2), (—) UNIQUAC, and γ_i^{∞}-values derived from VLE data: (Δ) methanol, (○) ethanol and (□) n-hexane.

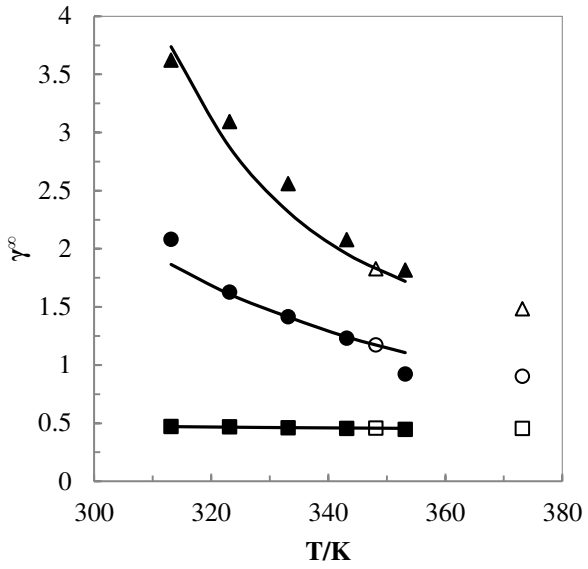

Fig. 7.7. Experimental and correlated γ_i^{∞} data of various solutes (1): (▲) methanol; (●) ethanol; (■) n-hexane in rapeseed oil (2), (─) UNIQUAC, and $\boldsymbol{\gamma_i^{\infty}}$-values derived from VLE data: (Δ) methanol, (○) ethanol and (□) n-hexane.

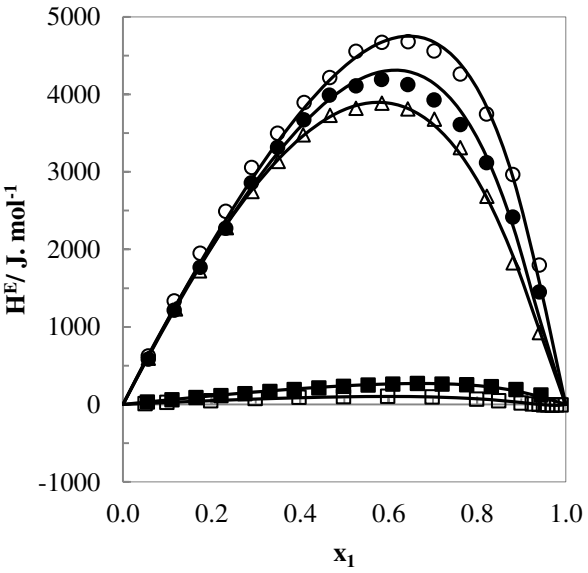

Fig. 7.8. Experimental and correlated H^E data of various solutes (1): (Δ at 353.15 K) methanol; (○ at 353.15 K and ● at 383.15 K) ethanol; (□ at 353.15 K and ■ at 383.15 K) n-hexane in soybean oil (2), (─) UNIQUAC.

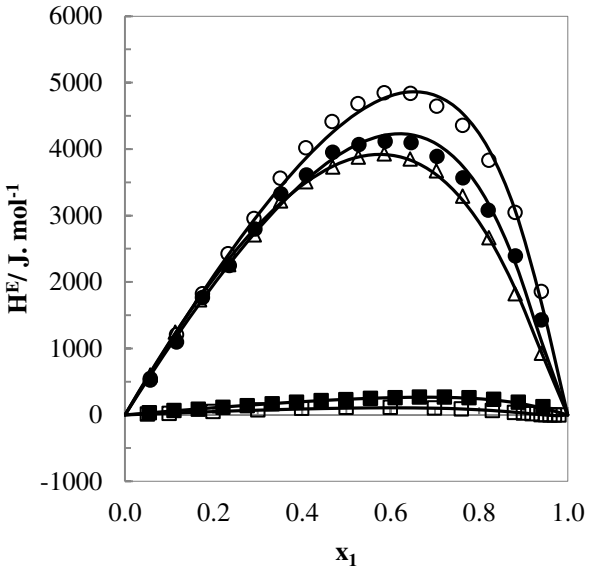

Fig. 7.9. Experimental and correlated H^E data of various solutes (1): (Δ at 353.15 K) methanol; (○ at 353.15 K and ● at 383.15 K) ethanol; (□ at 353.15 K and ■ at 383.15 K) n-hexane in sunflower oil (2), (─) UNIQUAC.

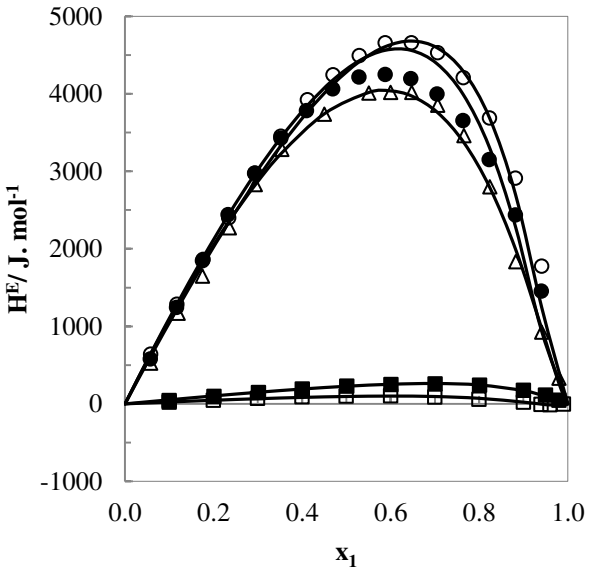

Fig. 7.10. Experimental and correlated H^E data of various solutes (1): (Δ at 353.15 K) methanol; (○ at 353.15 K and ● at 383.15 K) ethanol; (□ at 353.15 K and ■ at 383.15 K) n-hexane in rapeseed oil (2), (─) UNIQUAC.

Comparing the results from mixtures of different vegetable oils with the same compound at the same temperature, very similar VLE behavior was found, as can be seen in Figs. 7.2-7.4. The systems with the alcohols (methanol and ethanol) and n-hexane differ in their non-ideality. The systems containing n-hexane show a negative deviation from Raoult's law, this agrees with the results obtained by Pollard et al. [28] and Belting et al. [34], whereas the systems with methanol and ethanol show a positive deviation from ideal behavior as observed in our previous work [34].

n-hexane is miscible with the three vegetable oils over the entire composition range at both investigated temperatures. In spite of the relatively small positive deviation from Raoult's law a miscibility gap is found for the systems containing alcohols. For systems with methanol + vegetable oil the miscibility gap begins at methanol mole fraction of approximately 0.66 for soybean and sunflower oils and 0.73 for rapeseed oil at 348.15 K and 0.80 at 373.15 K. For systems with ethanol + vegetable oil the miscibility gap begins at ethanol mole fraction of approximately 0.89 and 0.83 for sunflower and rapeseed oil at 348.15 K, respectively. At 373.15 K, only mixtures with ethanol and rapeseed oil shown miscibility gap ($x_{ethanol}$ > 0.88). No miscibility gap was observed in the systems with ethanol and soybean oil. As can be seen from Figs. 7.2-7.4, the miscibility gap becomes larger with decreasing carbon number of the alcohol chain. The complete miscibility of the mixtures with n-hexane can be understood as a result of its large similarity with the fatty compounds. In case of the alcohols, intermolecular hydrogen bonds are broken when the molecule is removed from the pure liquid and these can be formed to a much lesser degree in the mixtures with vegetable oil. This leads to the increase of activity coefficients typically also observed in alkane-alkanol mixtures. In contrast to methanol, ethanol

molecules are less polar due to the longer hydrocarbon part attached to the alcohol group and at the same time are able to form cyclic tetramers and thus retain a higher percentage of their hydrogen bonding even in unpolar solvents. The observed miscibility gaps for alcohols can be used for the separation of fatty compounds (for example deacidification of vegetable oils, biodiesel purification and solvent recover processes) by liquid-liquid extraction, as discussed already in previous works of our research group [31, 44, 53-56].

The fitted interaction UNIQUAC parameters and the data set weighting factors used in the fitting procedure are presented in Table 7.11 together with the overall-average errors (AAE).

As shown in Figs. 7.2-7.4 the correlated results for VLE are in good agreement with the experimental findings. Only systems with methanol were not described satisfactorily. Figs. 7.5-7.7 shows that also the calculated results for γ_i^∞ using UNIQUAC model are in good agreement with the experimental data obtained with help of dilutor technique. Also the γ_i^∞-values derived from VLE data measured at 373.15 K are in good agreement with the γ_i^∞ measured at lower temperatures. In Figs. 7.8-7.10 it can be seen that the experimental and correlated data show a satisfactory agreement. The overall average deviation with UNIQUAC model 4.46 % for VLE, 7.07 % for γ_i^∞ and 5.80 % for H^E taking into account all the systems modeled.

Table 7.10. Antoine coefficients A_i, B_i and C_i, relative van der Waals volumes r_i and surfaces q_i, and critical data of the investigated compounds.

Compounds	A_i	B_i	C_i	T_{min} /K	T_{max} /K	r_i	q_i	T_c /K	P_c /atm	V_c /cm^3.mo	ω
Methanol	8.08097	1582.27	239.700	288.15	373.15	1.4311	1.4320	512.60	79.90	118.00	0.5590
Ethanol	8.20417	1642.89	230.300	216.15	353.15	2.1055	1.9720	516.20	63.00	167.00	0.6350
n-Hexane	7.01051	1246.33	232.988	178.15	508.15	4.4998	3.8560	507.40	29.75	370.00	0.2975
Soybean oil	13.31790	8560.17	261.766	313.15	423.15	38.7157	31.3470	856.58	2.67	3997.90	3.5423
Sunflower Oil	13.31780	8560.12	261.765	313.15	423.15	38.7157	31.3470	856.59	2.67	3997.90	3.5422
Rapeseed Oil	12.45280	7866.99	245.322	313.15	423.15	38.9478	31.5600	872.80	2.62	4161.80	3.3379

Table 7.11. Quadratic temperature-dependent UNIQUAC interaction parameters, weigthing factors (g) and the overall-average error (AAE).

Component 1	Component 2	i	j	a_{ij}	b_{ij}	c_{ij}	g^1 / AAE^2 (%)		
				$/cal.mol^{-1}$	$/cal.mol^{-1}.K^{-}$	$/cal.mol^{-1}.K^{-2}$	VLE	γ_i^{∞}	H^E
Methanol	Soybean oil	1	2	-1143.7071	5.6331	$-8.2046.10^{-3}$	1 / 11.10	1 / 10.86	120 / 2.03
		2	1	2919.0971	-6.1118	$6.8621.10^{-3}$			
Ethanol	Soybean oil	1	2	-241.0424	-0.3125	$1.0370.10^{-3}$	1 / 1.33	1 / 1.19	1 / 3.64
		2	1	1704.2474	1.6257	$-1.0596.10^{-4}$			
n-Hexane	Soybean oil	1	2	-108.3200	-0.8449	$5.3345.10^{-4}$	1 / 1.69	1 / 1.23	1 / 3.96
		2	1	268.2199	0.7088	$-1.3947.10^{-1}$			
Methanol	Sunflower oil	1	2	-47.7623	-0.6059	$6.7685.10^{-4}$	1 / 10.23	1 / 9.23	110 / 1.78
		2	1	2415.4631	-3.1860	$2.5874.10^{-3}$			
Ethanol	Sunflower oil	1	2	-317.7332	0.1311	$6.0005.10^{-4}$	100 / 1.28	1 / 17.74	30 / 4.42
		2	1	1469.5418	-0.5078	$-2.6586.10^{-3}$			
n-Hexane	Sunflower oil	1	2	13.3053	-0.3057	$1.3898.10^{-3}$	3 / 0.89	2 / 1.30	1 / 16.01
		2	1	145.1232	-0.2589	$-2.6365.10^{-4}$			
Methanol	Rapeseed oil	1	2	1099.2901	-7.1851	$-1.0197.10^{-2}$	1 / 6.77	1 / 6.14	37 / 5.50
		2	1	10026.7741	-46.4593	$-6.3408.10^{-1}$			
Ethanol	Rapeseed oil	1	2	267.7288	-3.8881	$7.6477.10^{-3}$	1 / 5.32	1 / 6.57	20 / 5.66
		2	1	2005.0950	-2.5595	$-1.8370.10^{-3}$			

n-Hexane	Rapeseed oil	1	2	156.6363	-0.9254	$2.5746.10^{-3}$	2 / 2.11	3 / 0.85	1 / 3.88
		2	1	27.9881	0.1631	$-1.1057.10^{-3}$			

[1] Weighting factor used in the simultaneous fitting procedure, [2] Overall-average error – AAE $(\%) = 100 \times \frac{\sum_{i=1}^{nw}|M_{exp}-M_{cal}|/M_{exp}}{nw}$, where nw is the number of experimental values and M_{exp} and M_{calc} are the experimental and calculated values for the thermodynamic properties VLE, $\gamma_i^{\infty}$and H^E, respectively.

The VLE, $\gamma_i^{\infty}$and H^E data for the systems containing vegetable oils were predicted using mod. UNIFAC. The vegetable oil was regarded as a single pseudo-component (see Fig. 7.1) as employed in UNIQUAC correlation. In previous work [**34**] a modification of the mod. UNIFAC model was proposed in order to improve its predictive capability for mixtures containing triacylglycerols. In this new model, the frequency of the ester groups was artificially reduced. The mod. UNIFAC using only 2 ester groups was also used in this work. The group assignment adopted in this study for both UNIFAC models is showed in Table 7.12.

In Figs. 7.11-7.13 the predicted results using the group contribution methods mod. UNIFAC and mod. UNIFAC using only 2 ester groups are shown in graphical form together with the VLE, , $\gamma_i^{\infty}$and H^E experimental data, respectively.

Table 7.12. UNIFAC group assignment in this study.

Compounds	Groupname	Maingroup	Subgroup	Frequency	
				mod. UNIFAC[1]	proposed mod. UNIFAC
Methanol	CH_3OH	6	15	1	1
Ethanol	CH_3	1	1	1	1
	CH_2	1	2	1	1
	OH	5	14	1	1
n-Hexane	CH_3	1	1	2	2
	CH_2	1	2	4	4
OLiLi (Soybean and	CH_3	1	1	3	3
Sunflower oils)	CH_2	1	2	37	37
	CH	1	3	1	1
	$CH=CH$	2	6	5	5
	CH_2COO	11	22	3	2
OOLi (Rapeseed Oil)	CH_3	1	1	3	3
	CH_2	1	2	39	39
	CH	1	3	1	1
	$CH=CH$	2	6	4	4
	CH_2COO	11	22	3	2

[1]according to DDB[50].

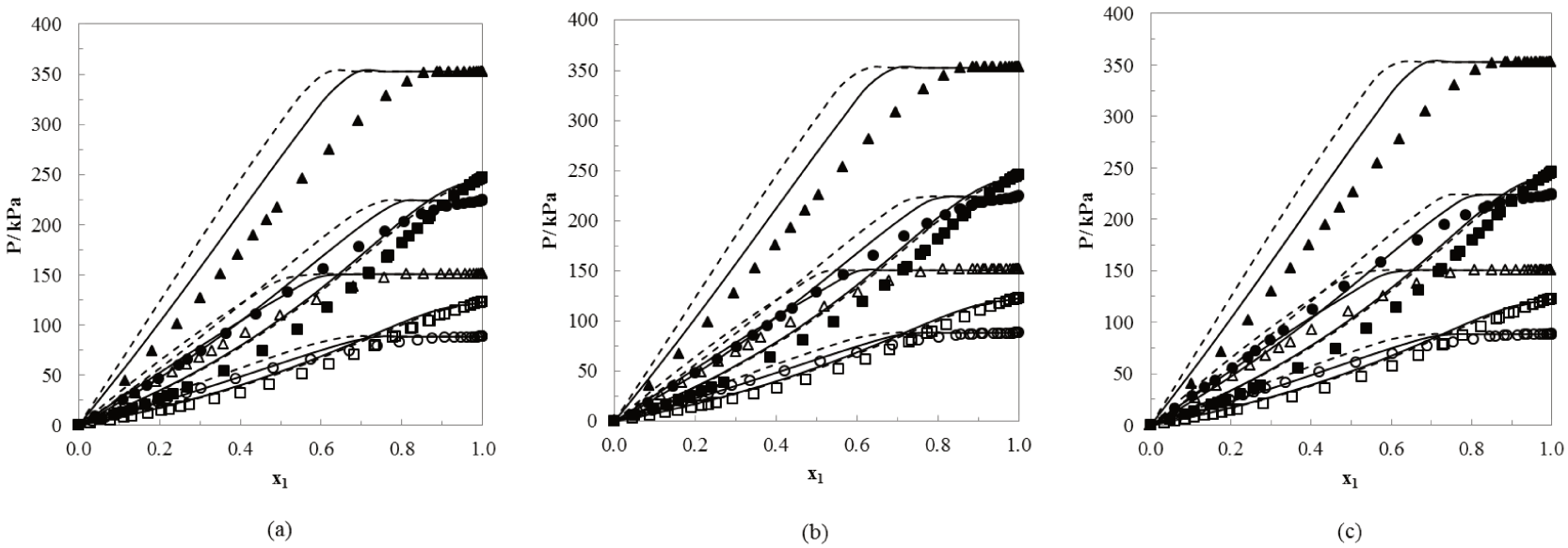

Fig. 7.11. Experimental and predicted VLE data for the investigated systems with (a) soybean, (b) sunflower and (c) rapeseed oils (2): at 348.15 K (○) and 373.15 K (◊) and: (Δ at 348.15 K and ▲ at 373.15 K) methanol (1); (○ at 348.15 K and ● at 373.15 K) ethanol (1); (□ at 348.15 K and ■ at 373.15 K) n-hexane (1). (—) mod. UNIFAC, (- - -) mod. UNIFAC with 2 ester groups.

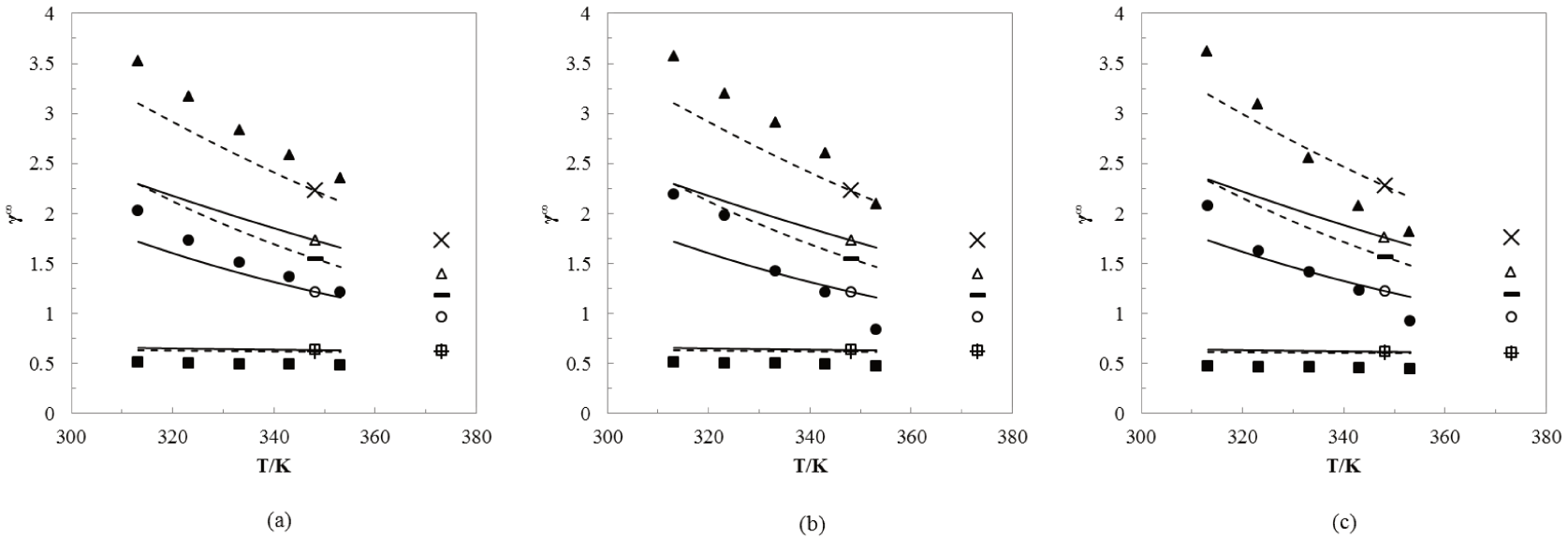

Fig. 7.12. Experimental and predicted γ_i^{∞} data of various solutes (1): (▲) methanol; (●) ethanol; (■) n-hexane in (a) soybean, (b) sunflower and (c) rapeseed oils (2), γ_i^{∞}-values derived from VLE data: (Δ) methanol, (○) ethanol and (□) n-hexane by (—) mod. UNIFAC, and (×) methanol, (▬) ethanol and (+) n-hexane by (- - -) mod. UNIFAC with 2 ester groups.

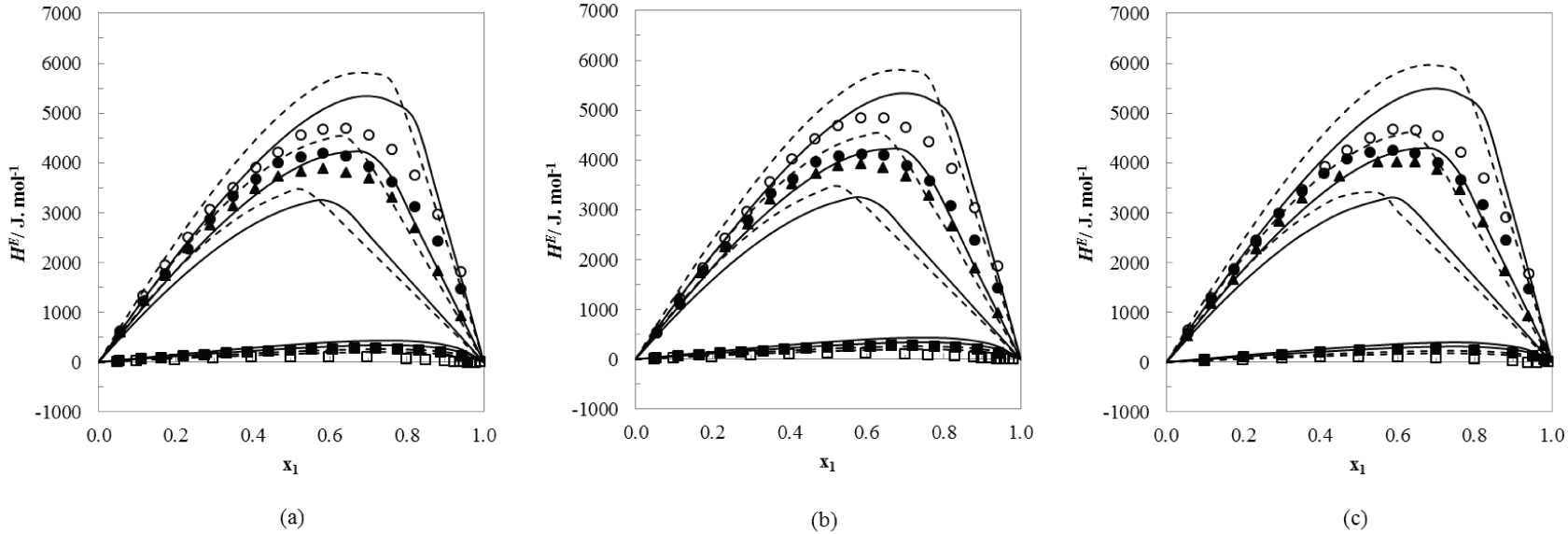

Fig. 7.13. Experimental and predicted H^E data data of various solutes (1): (Δ at 353.15 K and ▲ at 383.15 K) methanol; (○ at 353.15 K and ● at 383.15 K) ethanol; (□ at 353.15 K and ■ at 383.15 K) n-hexane in (a) soybean, (b) sunflower and (c) rapeseed oils (2). (─) mod. UNIFAC, (- - -) mod. UNIFAC with 2 ester groups.

The degree of agreement between the experimental data and predicted results by mod. UNIFAC and mod. UNIFAC using 2 ester groups changes for the different systems. For systems with n-hexane and methanol, mod. UNIFAC predicts a higher pressure over the entire range of composition, whereas systems with ethanol the pressure in the higher vegetable oil concentration is slighty lower than experimental results. The mod. UNIFAC with 2 ester groups overpredicts the pressure for all investigated systems.

The predicted results of both mod. UNIFAC models for the systems with alcohols shown miscibility gap at high solvent concentrations. The composition range of heterogeneous region was larger than observed by experimental data.

The proposed modification in mod. UNIFAC model unfortunally did not improve the prediction of VLE for vegetable oil as observed for γ_i^{∞} and H^E.

Systems with vegetable oils and ethanol show a relatively good agreement between predicted by mod. UNIFAC and experimental results (AAE were less than 5.3 %). For systems with methanol and n-hexane a quantitative prediction of the VLE was not possible with mod. UNIFAC model, nonetheless the calculated results can be used as rough estimates, because they describe the correct phenomenology. The development of reliable predictive models would be in particular desirable for synthesis, design, simulation and optimization of various separation processes in edible oil, biodiesel, and related compounds industries. However, for this development to be feasible, still many more experimental data for different vegetable oils and others fatty compounds are required. It should be remarked that the investigated systems are strongly size-assymmetric, thus we can assume that the temperature-independent combinatorial (entropic) contribution to the activity coefficients for mod. UNIFAC model is more important than the residual term, therefore the

combinatorial part should be focused, since it relates to size and shape differences between molecules.

4. Conclusions

In this work VLE data for 9 systems consisting of three organic solvents (methanol, ethanol and n-hexane) with three vegetable oils (soybean, sunflower and rapeseed oils) were measured at 348.15 K and 373.15 K. For mixtures with methanol and ethanol miscibility gaps were found. The experimental VLE data were correlated simultaneously with γ_i^{∞} and H^E data by using quadratic temperature-dependent UNIQUAC parameters. The results of the correlation show very good agreement with measured data for systems with ethanol and n-hexane. The systems with methanol were not described satisfactorily (deviations about 10 %). The overall average errors were 4.46 % for VLE, 7.07 % for γ_i^{∞} and 5.80 % for H^E. Mod. UNIFAC and mod. UNIFAC using 2 ester groups models gave just a qualitative description for all the investigated systems. For VLE data, the proposed modification of mod. UNIFAC did not improved the results as observed for γ_i^{∞} data in previous work [34]. That means that the development of predictive models is still required for design and simulation of separation processes in oil and oleochemical industries. But for this development of predictive models many more experimental data for different vegetable oils and others fatty compounds have to be measured.

Acknowledgements

P. C. Belting wishes to acknowledge CNPq (Conselho Nacional de Desenvolvimento Científico e Tecnológico – 142122/2009-2 and 290128/2010-2) and DAAD (Deutscher Akademischer Austauschdienst – A/10/71471) for the scholarship. The authors would like to thank the CNPq (304495/2010-7, 483340/2012-0, 307718/2010-7 and 301999/2010-4), FAPESP (Fundação de Amparo à Pesquisa do Estado de São Paulo - 08/56258-8, 09/54137-1 and 2010/16634-0) and INCT-EMA (Instituto Nacional de Ciência e Tecnologia de Estudos do Meio Ambiente) for the financial support. The authors are grateful to the DDBST GmbH for permitting the use of the Dortmund Data Bank. This work has been supported by the Carl von-Ossietzky University Oldenburg.

List of Symbols

VLE	vapor-liquid equilibrium
UNIQUAC	UNIversal QUAsi-Chemical
UNIFAC	UNIversal Functional Activity Coefficient
TAG	triacylglycerol
FA	fatty acid
FFA	free fat acid
γ^{∞}	activity coefficient at infinite dilution
g^E- model	excess Gibbs energy model
AOCS	American Oil Chemists' Society
GC	gas chromatography
M	molar mass
C z:y	z = number of carbons and y = number of double bonds
x	molar fraction

w	mass fraction
T	trans isomers
W	water content
IV	iodine value
L	lauric acid
M	myristic acid
P	palmitic acid
Po	palmitoleic acid
Ma	margaric acid
S	stearic acid
O	oleic acid
Li	linoleic acid
Le	linolenic acid
A	arachidic acid
Ga	gadoleic acid
Be	behenic acid
Lg	lignoceric acid
Ne	nervonic acid
x_1	molar fraction of component 1
P	pressure
T	absolute temperature
Δu_{ij}	binary interaction parameters of UNIQUAC model
r	van der Waals volume parameter
q	van der Waals surface area parameter
$a_{ij},\ b_{ij}, c_{ij}$	quadratic interaction parameters of UNIQUAC model
A_i, B_i, C_i	Antoine equation coefficients
P_v	vapor pressure
DDB	Dortmund Data Bank
DDBSP	Dortmund Data Bank Software Package
AAE	Overall-average error

n	number of experimental values

Subscripts

i	identification of compounds
exp	experimental value
$calc$	calculated value

Superscripts

E	excess property
∞	at infinite dilution

References

[1] R. Ceriani, A.J.A. Meirelles, Predicting vapor–liquid equilibria of fatty systems, Fluid Phase Equilibr., 215 (2004) 227–236.

[2] M.R. Burke, Soaps, in: F. Shahidi (Ed.) Bailey's Industrial Oil and Fat Products, John Wiley & Sons, Inc., Hoboken, New Jersey, 2005, pp. 103-136.

[3] C. Scrimgeour, Chemistry of Fatty Acids, in: F. Shahidi (Ed.) Bailey's Industrial Oil and Fat Products, John Wiley & Sons, Hoboken, New Jersey, 2005, pp. 606.

[4] K.F. Lin, Paints, Varnishes, and Related Products, in: F. Shahidi (Ed.) Bailey's Industrial Oil and Fat Products, John Wiley & Sons, Inc., Hoboken, New Jersey, 2005, pp. 307-351.

[5] J.L. Lynn Jr., Detergents and Detergency, in: F. Shahidi (Ed.) Bailey's Industrial Oil and Fat Products, John Wiley & Sons, Inc., Hoboken, New Jersey, 2005, pp. 137-189.

[6] S.Z. Erhan, Vegetable Oils as Lubricants, Hydraulic Fluids, and Inks, in: F. Shahidi (Ed.) Bailey's Industrial Oil and Fat Products, John Wiley & Sons, Inc., Hoboken, New Jersey, 2005, pp. 259-278.

[7] E. Hernandez, Pharmaceutical and Cosmetic Use of Lipids, in: F. Shahidi (Ed.) Bailey's Industrial Oil and Fat Products, John Wiley & Sons, Inc., Hoboken, New Jersey, 2005, pp. 391-411.

[8] S.S. Narine, X. Kong, Vegetable Oils in Production of Polymers and Plastics, in: F. Shahidi (Ed.) Bailey's Industrial Oil and Fat Products, John Wiley & Sons, Inc., Hoboken, New Jersey, 2005, pp. 279-306.

[9] R.D. O'Brien, Fats And Oils Processing, in: W.E.F. R.D. O'Brien, and P.J. Wan (Ed.) Introduction to Fats and Oils Technology, A.O.C.S. Press, Champaign, Illinois, 2000, pp. 90-107.

[10] R.D. O'Brien, Introduction to Fats and Oils Technology, in: W.E.F. R.D. O'Brien, and P.J. Wan (Ed.) Fats And Oils: An Overview, AOCS Press: Champaign, Illinois, 2000, pp. 1-19.

[11] D. Bera, D. Lahiri, A. Nag, Kinetic studies on bleaching of edible oil using charred sawdust as a new adsorbent, J. Food Eng., 65 (2004) 33 - 36.

[12] R. Ceriani, A.J.A. Meirelles, Simulation of Batch Physical Refining and Deodorization Processes, J. Amer. Oil Chem. Soc., 81 (2004) 305-312.

[13] R. Ceriani, A.J.A. Meirelles, Simulation of Continuous Deodorizers: Effects on Product Streams, J. Am.Oil.Chem.Soc., 81 (2004) 1059-1069.

[14] R. Ceriani, A.J.A. Meirelles, Simulation of Physical Refiners for Edible Oil Deacidification, J. Food Eng., 76 (2006) 261-271.

[15] D. Bera, D. Lahiri, A. De Leonardis, K. De, A. Nag, A Novel Azeotropic Mixture Solvent for Solvent Extraction of Edible Oils, Agricultural Engineering International: the CIGR Ejournal, VIII (2006) Manuscript FP 06 005.

[16] H. Rittner, Extraction of vegetable oils with ethyl alcohol, Oléagineux, 47 (1992) 29-42.

[17] R.J. Hron, S.P. Koltun, An Aqueous Ethanol Extration Process for Cottonseed Oil, J. Am. Oil Chem. Soc., 61 (1984) 1457-1460.

[18] R.J. Hron, S.P. Koltun, A.V. Graci, Biorenewable Solvents for Vegetable Oil Extraction, J. Am. Oil Chem. Soc., 59 (1982) 674-684.

[19] L.A. Johnson, E.W. Lusas, Comparison of Alternative Solvents for Oils Extraction, J. Am. Oil Chem. Soc., 60 (1983) 181-194.

[20] C.E.C. Rodrigues, K.K. Aracava, F.N. Abreu, Thermodynamic and statistical analysis of soybean oil extraction process using renewable solvent, Int. J. Food Sci. Tech., 45 (2010) 2407–2414.

[21] J.M. Encinar, J.F. Gonzáles, J.J. Rodriguez, A. Tejedor, Biodiesel Fuels from Vegetables Oils: Transesterification of *Cynara cardunculus* L. Oils with Ethanol, Energ. Fuels, 16 (2002) 443-450.

[22] F. Ma, M.A. Hanna, Biodiesel production: a review, Bioresour. Technol., 70 (1999) 1-15.

[23] L.C. Meher, D.V. Sagar, S.N. Naik, Technical aspects of biodiesel production by transesterifications: a review, Renew. Sust. Energ. Rev., 10 (2006).

[24] F.D. Gunstone, Vegetable Oils, in: F. Shahidi (Ed.) Bailey's Industrial Oil and Fat Products John Wiley & Sons, Hoboken, New Jersey, 2005, pp. 606.

[25] P.J. Wan, Properties of Fats and Oils, in: W.E.F. R. D. O'Brien, P. J. Wan (Ed.) Introduction to Fats and Oils Technology, A.O.C.S. Press, Champaign, Illinois, 2000 pp. 20-48.

[26] E.D. Milligan, D.C. Tandy, Distillation and Solvent Recovery, J. Am. Oil Chem. Soc., 51 (1974) 347-350.

[27] A. Demarco, Extracción por Solvente, in: D.B.-A. J. M. Block (Ed.) Temas Selectos en Aceites y Grasas, Edgard Blücher, São Paulo, 2009, pp. 67-95.

[28] E.F. Pollard, H.L.E. Vix, E.A. Gastrock, Solvent Extraction of Cottonseed and Peanut Oils., Ind. Eng. Chem., 37 (1945) 1022-1026

[29] C.B. Gonçalves, P.A. Pessôa Filho, A.J.A. Meirelles, Partition os nutraceutical compounds in deacidification of palm oil by solvent extraction., J. Food Eng., 81 (2007) 21-27.

[30] C.G. Pina, A.J.A. Meirelles, Deacidification of Corn Oil by Solvent Extraction in a Perforated Totating Disc Column., J. Am. Oil Chem. Soc., 77 (2000) 553-559.

[31] C.E.C. Rodrigues, M.M. Onoyama, A.J.A. Meirelles, Optimization of the Rice Bran Oil Deacidification Process by Liquid-liquid Extraction, J. Food Eng., 73 (2006) 370-378.

[32] P.C. Belting, J. Rarey, J. Gmehling, R. Ceriani, O. Chiavone-Filho, A.J.A. Meirelles, Activity Coefficient at Infinite Dilution Measurements for Organic Solutes (polar and nonpolar) in Fatty Compounds: Saturated Fatty Acids, J. Chem. Thermodyn., 55 (2012) 42-49.

[33] P.C. Belting, J. Rarey, J. Gmehling, R. Ceriani, O. Chiavone-Filho, A.J.A. Meirelles, Activity coefficient at infinite dilution measurements for organic solutes (polar and non-

polar) in fatty compounds – Part II: C18 fatty acids, J. Chem. Thermodyn., 60 (2013) 142–149.

[34] P.C. Belting, J. Rarey, J. Gmehling, R. Ceriani, O. Chiavone-Filho, A.J.A. Meirelles, Measurements of Activity Coefficients at Infinite Dilution in Vegetable Oils and Capric Acid Using the Dilutor Technique, (2013).

[35] P.C. Belting, R. Bölts, J. Rarey, J. Gmehling, R. Ceriani, O. Chiavone-Filho, A.J.A. Meirelles, Excess Enthalpies for Various Binary Mixtures with Vegetable Oil at Temperatures between 298.15 K and 383.15 K, (2013).

[36] D.S. Abrams, J.M. Prausnitz, Statistical Thermodynamics of Liquid Mixtures: A New Expression for the Excess Gibbs Energy of Partly or Completely Miscible Systems, AIChE Journal, 21 (1975) 116-128.

[37] U. Weidlich, J. Gmehling, A Modified UNIFAC Model. 1. Prediction of VLE, h_E and γ^{∞} Ind. Eng. Chem. Res., 26 (1987) 1372-1381.

[38] J. Gmehling, J. Li, M. Schiller, A modified UNIFAC model. 2. Present parameter matrix and results for different thermodynamic properties, Ind. Eng. Chem. Res., 32 (1993) 178-193.

[39] H.C. Van Ness, M.M. Abbott, A Procedure for Rapid Degassing of Liquids, Ind. Eng. Chem. Fundam., 17 (1978) 66-67.

[40] AOCS, Official Methods and recommended Practices of the American Oil Chemists' Society, 5 th ed., AOCS Press, Champaign, IL, 2004.

[41] L. Hartman, R.C.A. Lago, Rapid Preparation of Fatty Acid Methyl Esters from Lipids, Lab. Pract., 22 (1973) 475–476.

[42] N.R. Antoniossi Filho, O.L. Mendes, F.M. Lanças, Computer prediction of triacylglycerol composition of vegetable oils by HRGC, Chromatographia, 40 (1995) 557-562.

[43] C.A.S. Silva, G. Sanaiotti, M. Lanza, L.A. Follegatti-Romero, A.J.A. Meirelles, E.A.C. Batista, Mutual Solubility for Systems Composed of Vegetable Oil + ethanol + Water at Different Temperatures, J. Chem. Eng. Data, 55 (2010) 440-447.

[44] M. Lanza, W. Borges Neto, E. Batista, R.J. Poppi, A.J.A. Meirelles, Liquid-Liquid Equilibria Data for Reactional Systems of Ethanolysis at 298.3 K, J. Chem. Eng. Data, 53 (2008) 5-15.

[45] R.E. Gibbs, H.C. Van Ness, Vapor-Liquid equilibria from total-pressure measurements. A new apparatus., Ind. Eng. Chem. Fundam., 11 (1972) 410-413.

[46] J. Rarey, J. Gmehling, Computer-operated differential static apparatus for the measurement of vapor-liquid equilibrium data, Fluid Phase Equilibr., 83 (1993) 279-287.

[47] S. Nebig, R. Bölts, J. Gmehling, Measurement of vapor-liquid equilibria (VLE) and excess enthalpies (H^E) of binary systems with 1-alkyl-3-methylimidazolium bis(trifluoromethylsufonyl)imide and prediction of these properties and γ^∞ using modified UNIFAC (Dortmund), Fluid Phase Equilib., 258 (2007) 168-178.

[48] J. Rarey, S. Horstmann, J. Gmehling, Vapor-liquid equilibria and vapor pressure data for systems ethyl *tert*-butyl ether + ethanol and ethyl *tert*-butyl ether + water., J. Chem. Eng. Data, 44 (1999) 532-538.

[49] J.A. Nelder, R. Mead, A simplex method for function minimization, Comput. J., 7 (1965) 308-313.

[50] Dortmund Data Bank Dortmund Data Bank Software & Separation Technology in, DDBST GmbH, Oldenburg, 2011.

[51] A. Bondi, Physical properties of molecular crystals, liquids, and glasses, J. Wiley, New York, N.Y., 1968.

[52] Y. Nannoolal, J. Rarey, J. Ramjugernath, Estimation of pure component properties Part 2. Estimation of critical property data by group contribution, Fluid Phase Equilib., 252 (2007) 1-27.

[53] C.B. Gonçalves, E.C. Batista, A.J.A. Meirelles, Liquid-Liquid Equilibrium Data for the System Corn Oil + Oleic Acid + Ethanol + Water at 298.15 K, J. Chem. Eng. Data, 47 (2002) 416-420.

[54] C.B. Gonçalves, A.J.A. Meirelles, Liquid-Liquid Equilibrium Data for the System Palm Oil + Fatty Acids + Ethanol + Water at 318.2 K, Fluid Phase Equilibr., 221 (2004) 139-150.

[55] C.B. Gonçalves, A.J.A. Meirelles, Liquid-Liquid Equilibrium Data for the System Palm Oil + Fatty Acids + Ethanol + Water at 318.2 K, Fluid Phase Equilib., 221 (2004) 139-150.

[56] M. Lanza, G. Sanaiotti, E. Batista, R.J. Poppi, A.J.A. Meirelles, Liquid-Liquid Equilibrium Data for Systems Containing Vegetable Oils, Anhydrous Ethanol, and Hexane at (313.15, 318.15, and 328.15) K, J. Chem. Eng. Data, 54 (2009) 1850-1859.

CAPÍTULO 8: VAPOR-LIQUID EQUILIBRIUM FOR SYSTEMS CONTAINING REFINED VEGETABLE OIL (COTTONSEED AND SOYBEAN OILS) AND SOLVENT (N-HEXANE AND ETHANOL) AT 41.3 KPA AND 101.3 KPA

Artigo submetido à revista *Journal of Chemical Engineering Data*.

Vapor-liquid equilibrium for systems containing refined vegetable oil (cottonseed and soybean oils) and solvent (n-hexane and ethanol) at 41.3 kPa and 101.3 kPa

Patrícia C. Belting[†], Osvaldo Chiavone-Filho[‡*], Roberta Ceriani[§], Antonio J. A. Meirelles[†]

[†] *Food Engineering Department, Faculty of Food Engineering, University of Campinas, Av. Monteiro Lobato 80, Cidade Universitária Zeferino Vaz, 13083-862, Campinas-SP, Brazil*

[‡] *Chemical Engineering Department, Federal University of Rio Grande do Norte, Av. Senador Salgado Filho S/N, 59066-800, Natal-RN, Brazil*

[§] *Faculty of Chemical Engineering, University of Campinas, Av. Albert Einstein 500, Cidade Universitária Zeferino Vaz, 13083-852, Campinas-SP, Brazil*

Abstract

The objective of this work was to determine vapor-liquid equilibrium data for systems of interest in vegetable oil industry and biodiesel production. The following systems were investigated: refined cottonseed oil + n-hexane at 41.3 kPa and refined soybean oil + ethanol at 101.3 kPa. The measurements were performed using a modified Othmer-type ebulliometer. An oscillating tube densimeter was applied to determine the concentrations of the liquid and vapor phases. The excess volume behavior has also been found on the basis of density-composition calibration curve. The results obtained for the system cottonseed oil + n-hexane showed good agreement with available data. The vapor-liquid equilibrium data

($PTxy$) were well correlated using the UNIQUAC model (average global deviation to respect to temperature and pressure less than 1%) and thermodynamic consistency test of these data have been checked using a maximum likelihood data reduction. The experimental data were compared with the predicted results using original UNIFAC and mod. UNIFAC (Dortmund), with the pseudo-binary mixture assumption.

Keywords: Vapor-liquid equilibria, Vegetable oil, Othmer-type ebulliometer, UNIQUAC model, UNIFAC models.

8.1. Introduction

n-hexane is the most widely used solvent for vegetable oil extraction. The solvent recovery is accomplished by evaporation and steam stripping[1-3]. The residual solvent content in vegetable oil must be only a few $mg \cdot kg^{-1}$ (ppm) and for this reason, this step plays an important role in the economics process, since it requires large amounts of energy. In this context, an accurate knowledge of thermodynamic properties, in particular vapor-liquid equilibrium data, of systems as vegetable oil + solvent are necessary for the reliable design, optimization and modeling of thermal separation processes[3, 4].

It must also be considered that due to recent petroleum price increases and safety, environmental and health concerns, alternatives solvents for extraction of oilseeds become interesting[1, 5-7]. Therefore, various studies have been conducted in search of alternative solvents and, inter alia, ethanol appears as a reliable n-hexane substitute[6, 8-11]. Nowadays,

the study of phase equilibrium of mixtures with vegetable oil and ethanol becomes even more interesting because it is also a system of interest in biodiesel process.

This paper continues our study of thermodynamic properties and vapor-liquid equlibrium (VLE) data for fatty compounds systems[12-16]. New experimental isobaric VLE data for systems with refined vegetable oils (cottonseed oil + n-hexane at 41.3 kPa and soybean oil + ethanol at 101.3 kPa) are reported and analysed. The measured ($PTxy$) data were correlated with the UNIQUAC model and predicted using original UNIFAC and modified UNIFAC (Dortmund) models.

8.2. Experimental Section

8.2.1 Materials

The solvents used in this work were anhydrous ethanol from Merck (Germany), with a purity of 99.9 %, and n-hexane, also from Merck, with purity greater than 99 %. The chemicals were used without further treatment. Refined soybean oil was purchased from Bunge Alimentos S. A. (Luis Eduardo Magalhães/BA, Brazil). The refined cottonseed oil was kindly supplied by Cargill (Itumbiara/GO, Brazil). The water content (<100 $\mathrm{mg.kg^{-1}}$) of chemicals and vegetable oil was checked by Karl Fischer titration.

The vegetable oils compositions in terms of fatty acid (FA) and triacylglycerol (TAG) are present in Tables 8.1 and 8.2, respectively. Both analyzes were performed by gas chromatography. Procedure and experimental conditions is described in detail im previous work[14].

For the mixture approach and UNIQUAC correlation, the vegetable oils were treated as a single triacylglycerol with the same unsaturation degree, number of carbon and average molar mass of the original vegetable oil composition (Table 8.2). For this reason, the average molar masses of the vegetable oils were calculated using the respective fatty acid compositions (Table 8.1), considering that all fatty acids present in the vegetable oil are esterified to glycerol molecules to form triacylglycerols. The values obtained are also listed in Table 8.2. For prediction with UNIFAC models, the entire TAG composition of the vegetable oil (Table 8.2) was deemed.

Table 8.1. Fatty acid composition of refined cottonseed and soybean oils.

Fatty Acid Nomenclature				M^a/	Cottonseed oil		Soybean oil	
IUPAC	**Trivial**	**Symbol**	**Cz:y[b]**	$(\mathbf{g.mol^{-1}})$	**100 x^c**	**100 w^d**	**100 x**	**100 w**
dodecanoic	Lauric	L	C12:0	200.32	0.04	0.03	0.00	0.00
tetradecanoic	Myristic	M	C14:0	228.38	0.85	0.71	0.10	0.08
pentadecanoic			C15:0	242.40	0.03	0.03	0.04	0.04
hexadecanoic	Palmitic	P	C16:0	256.43	24.19	22.59	12.14	11.18
cis-hexadec-9-enoic	Palmitoleic	Po	C16:1	254.42	0.50	0.46	0.09	0.08
heptadecanoic	Margaric	Ma	C17:0	270.45	0.11	0.11	0.10	0.10
cis-heptadeca-10-enoic			C17:1	268.43	0.04	0.04	0.05	0.05
octadecanoic	Stearic	S	C18:0	284.49	2.28	2.36	3.72	3.80
cis-octadeca-9-enoic	Oleic	O	C18:1	282.47	14.91	15.34	22.25	22.57
trans-octadeca-9-enoic			C18:1T[e]	282.47	0.13	0.13		
cis,cis-octadeca-9,12-dienoic	Linoleic	Li	C18:2	280.45	55.82	57.01	53.95	54.35
trans-trans-octadeca-9,12-dienoic	Linoelaidic		C18:2T[e]	278.44	0.13	0.13	0.00	0.00
all-*cis*-octadeca-9,12,15-trienoic	Linolenic	Le	C18:3	278.44	0.16	0.16	6.27	6.27
all-*trans*-octadeca-9,12,15-trienoic			C18:3T[e]	278.44	0.32	0.32	0.28	0.28
icosanoic	Arachidic	A	C20:0	312.54	0.26	0.30	0.34	0.38
cis-icos-9-enoic	Gadoleic	Ga	C20:1	310.52	0.05	0.06	0.18	0.20
docosanoic	Behenic	Be	C22:0	340.59	0.10	0.12	0.38	0.47
docos-13-enoic	Erucic		C22:1	338.57	0.07	0.10	0.11	0.15

tetracosanoic	Lignoceric	Lg	C24:0	368.65	0.04	0.03	0.00	0.00
cis-tetracos-15-enoic	Nervonic	Ne	C24:1	366.63	0.85	0.71	0.10	0.08
FFA [f]						0.003		0.002
IV[g]						130.2		112.90

[a] *M* = Molar mass; [b] C z:y, where z = number of carbons and y = number of double bonds; [c] molar fraction; [d] mass fraction; [e]Trans isomers; [f] Free fatty acid expressed as mass fractions of oleic acid according to the official AOCS method Ca 5a-40[17]; [g] IV = Iodine value calculated from the fatty acid composition according to the official AOCS method Cd 1c-85[17].

Table 8.2. Probable triacylglycerol composition of refined cottonseed and soybean oils.

			M[a]/	Cottonseed oil		Soybean oil
main TAG[b]	**Cz:y**[c]	$(\mathrm{g.mol^{-1}})$	**100** x[d]	**100** w[e]	**100** x	**100** w
PPP	C48:0	807.32	1.35	1.26		
PLiM	C48:2	803.29	0.63	0.59		
POP	C50:1	833.36	2.65	2.56	0.94	0.89
PLiP	C50:2	831.34	9.88	9.52	2.26	2.16
MLiLi	C50:4	827.31	0.78	0.75		
POS	C52:1	861.41			0.62	0.61
PLiS	C52:2	859.39	3.72	3.71		
POO	C52:2	859.39			3.32	3.27
POLi	C52:3	857.38	12.96	12.87	9.04	8.88
PLiLi	C52:4	855.36	23.99	23.78	11.76	11.52
PLeLi	C52:5	853.35			2.58	2.53
SOO	C54:2	887.45			0.85	0.86
SOLi	C54:3	885.43	1.70	1.74	4.14	4.20
OOLi	C54:4	883.41	6.73	6.89	12.55	12.70
OLiLi	C54:5	881.40	15.94	16.28	22.84	23.07
LiLiLi	C54:6	879.38	19.67	20.05	21.96	22.13
LiLiLe	C54:7	877.37			6.40	6.44
LiLeLe	C54:8	875.35			0.74	0.74
M[a]/ $(\mathrm{g.mol^{-1}})$				873.20		861.87

[a] M = Molar mass; [b] Groups with a total triacylglycerol (TAG) composition lower than 0.5 % were ignored; [c] *C z:y*, where z = number of carbons (except carbons of glycerol) and y = number of double bonds; [d] molar fraction; [e] mass fraction.

8.2.2 Apparatus and Procedures.

8.2.2.1. Determination of Vapor-Liquid Equilibrium Data.

A modified Othmer-type ebulliometer18 was used for the VLE measurements. The apparatus have been described previously18-20. The experimental procedure for determination of the VLE (PTxy) data is based on that proposed by Othmer in which the temperature is measured for different compositions at constant total pressure21. The apparatus promotes only the recirculation of the condensed vapor phase, allowing its use in systems with higher viscosity. The equipment consists of an all-glass ebulliometer with external heater (FISATOM, mod. 5, 1600 W) and connected to a pressure control system. The pressure accuracy is aproximately 0.07 kPa. The temperatures are measured using a calibrated platinum resistance thermometer with precision of ±0.1 K. The appatatus can be applied at temperatures between 288 and 488 K and pressures between 40 and 210 kPa. The compositions of both phases (liquid and condensed vapor) were determined by measuring the density at 298.15 K and comparing the results with densities of mixtures of known composition, via inverse interpolation. The densities were measured with an Anton Paar digital densimeter (Model 4500) with a precision of $5.10^{-5}\,\mathrm{g.cm^{-3}}$. The experimental procedure for determining VLE data may be summarized in the following steps: (i) charge a pure componente or a mixture of adequate composition in the ebulliometer; (ii) set up the pressure and turn on the heating; (iii) wait for the recirculation of condensed vapor phase and steadystate condition (recirculation of 40 to 60 drops per minute and stabilization of the temperatures); (iv) after 30 minutes of steady state at the constant pressure, observed also

by the constancy of the condensed vapor drops inside the cell to the boiler, record the temperature of the cell; (v) open the system and take samples of the liquid and vapor phases for analysis in the densimeter. After sampling, the composition is changed in order to describe the phase behavior.

8.2.2.2. Density-Composition Calibration Curves.

For each mixture of vegetable oil and solvent about nine mixtures of known composition were prepared gravimetrically, with a precision of ± 0.00001 g. The density of mixtures with cottonseed oil and n-hexane was deteminated direct in densimeter, while the mixtures with soybean oil and ethanol, as wel as the phase samples, were previously diluted with n-heptane (purity > 99 %, Tedia, USA) to avoid their separation into two liquid phases at ambient temperature. The compositions covered the whole studied concentration range. The measured densities of the calibration curves were fitted with a third-order polynomial. The fitted composition-density function was used to determine the unknown compositions of liquid samples from the ebulliometer. The accuracy in the compositions with this procedure is estimated to be better than 0.0005 mole fraction and the global uncertainty of 0.002. The molar excess volume, V^E, of a binary mixture can be calculated by[22]:

$$V^E = x_1 M_1 \left(\frac{1}{\rho} - \frac{1}{\rho_1}\right) + x_2 M_2 \left(\frac{1}{\rho} - \frac{1}{\rho_2}\right) \quad (8.1)$$

where x_i is the mole fraction of component i, ρ_i is the density of the pure component i, ρ is the density of the mixture, or solution, and M_i is the molar mass of component i. For the excess volume correlation at constant temperature and atmospheric pressutre, a Redlich-Kister polynomial equation is appropriate[22]:

$$V^E/(x_1x_2) = \sum_{i=1}^{m} A_i(2x_1 - 1)^{i-1} \quad (8.2)$$

where V^E is the molar excess enthalpy, A_i are the adjustable parameters obtained by the least-square equation method, m is the number of parameters, x_1 and x_2 are the mole fractions of the components 1 and 2, respectively.

8.2.2.3. Thermodynamic Modelling.

The experimental VLE data were fitted by UNIQUAC equation. As already mentioned, the vegetable oil was regarded as a single pseudo-component, as present in Figure 8.1. The UNIQUAC structural parameters r_i and q_i for the refined vegetable oils were estimated from Bondi[23] and the critical constants were estimated according to the group contribution method proposed by Marrero and Gani[24]. This was necessary for the determination of the fugacity coefficients that were applied the Hayden and O´Connell correlation. Values of the radii of giration, moment dipole and association parameter were collected from AIChE DIPPR (Design Institute for Physical Properties) data bank[25]. The Antoine equation parameters for the vegetable oils were fitted from data predicted according to the group contribution method proposed by Ceriani and Meirelles[26]. For the other compounds the critical data, van der Waals radii for r_i and q_i, and coefficients A_i, B_i and C_i of the Antoine equation were also taken from DIPPR. The following objective function was used for fitting the required UNIQUAC parameters:

$$\mathrm{F} = \min = \frac{\sum\left(T_{\exp} - T_{\mathrm{calc}}\right)^2}{\sigma_T} + \frac{\sum\left(P_{\exp} - P_{\mathrm{calc}}\right)^2}{\sigma_P} + \frac{\sum\left(x_{\exp} - x_{\mathrm{calc}}\right)^2}{\sigma_x} + \frac{\sum\left(y_{\exp} - y_{\mathrm{calc}}\right)^2}{\sigma_y} \quad (8.3)$$

Thermodynamic consistency deviation tests of VLE data have been checked using a maximum likelihood data reduction[27].

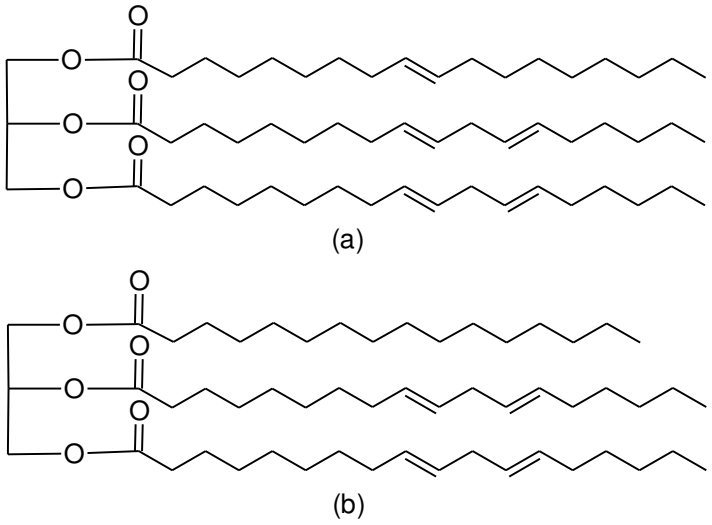

Figure 8.1. Representative components of the investigated refined vegetable oils. (a) 2,3-di(octadeca-9,12-dienoyloxy)propyl octadec-9-enoate (OLiLi) for soybean oil; (b) [3-hexadecanoyloxy-2-[(9E,12E)-octadeca-9,12-dienoyl]oxypropyl] (9E,12E)-octadeca-9,12-dienoate (PLiLi) for cottonseed oil.

The VLE data for the systems (cottonseed oil + n-hexane and soybean oil + ethanol) were predicted using the original UNIFAC[28, 29] and the modified UNIFAC (Dortmund)[30, 31]. correlation. For the prediction, the vegetable oils were considered multicomponent systems according their TAG composition present in Table 8.2.

8.3. Results and Discussion

Table 8.3 and Table 8.4 and Figure 8.2 present the density-composition calibration curves and the excess volume behavior for the system cottonseed oil (1) + n-hexane fitted to the Redlich-Kister polynomial equation.

Table 8.3. Density for cottonseed oil (1) + n-hexane (2) at 298.15 K.

x_1	ρ / g cm^{-3}	V^E / cm^3 mol^{-1}	x_1	ρ / g cm^{-3}	V^E / cm^3 mol^{-1}
0.00000	0.65522	0	0.13050	0.79633	-1.88207
0.01100	0.67596	-0.32155	0.18880	0.82378	-2.04525
0.02440	0.69760	-0.62070	0.27800	0.85105	-2.03671
0.04120	0.72054	-0.93811	0.47400	0.88321	-1.55386
0.06230	0.74425	-1.25909	1.00000	0.91548	0
0.09060	0.76916	-1.49223			

Table 8.4. Redlich-Kister parameters (A_i) and the root mean square deviation (RMSD*).

Component 1	Component 2	T/ K	A_1	A_2	A_3	A_4	A_5	A_6	RMSD*/ ($cm^3.mol^{-1}$)
cottonseed oil	n-hexane	298.15	0.624	182.878	951.392	2105.040	2065.282	760.972	0.024

*Root mean square deviation - RMSD$(V^E) = \left[\sum \frac{\left(V^E_{calcd} - V^E_{exptl}\right)^2}{N}\right]^{1/2}$, where N is the number of experimental values.

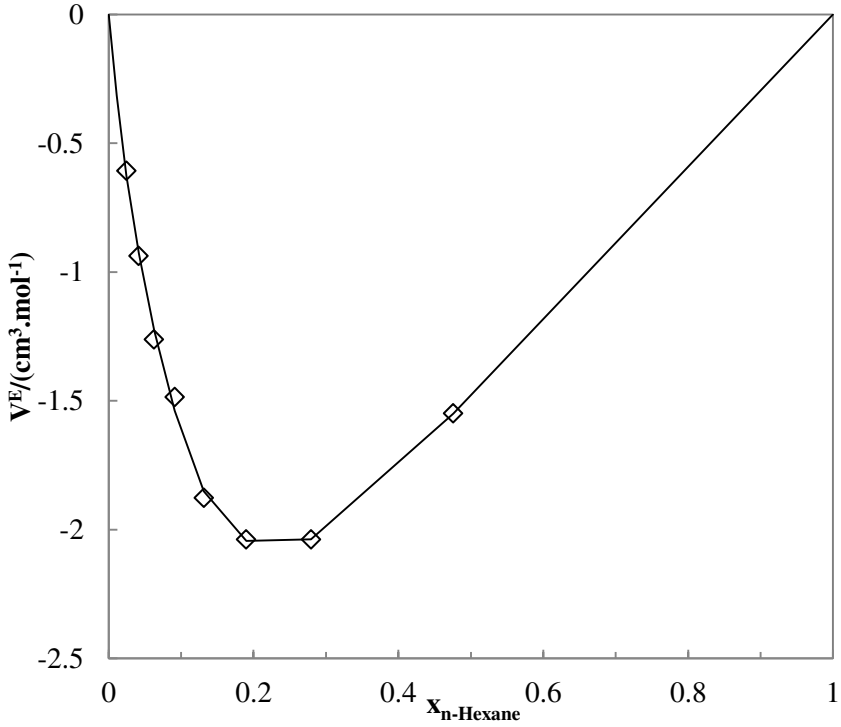

Figure 8.2. Measured and correlated excess volumes of the system cottonseed oil (1) + n-hexane (2) at 298.15 K.

From the mixture densities measurements negative excess volumes have been obtained as can be seen in Figure 8.2. This exothermic effect indicates the accomodation and attraction of the molecules. The negative deviation from Raoult's law can also indicate a affinity between the components of the mixture.

In Tables 8.5 and 8.6 the experimental VLE data measured for refined cottonseed oil + n-hexane at 41.3 kPa and refined soybean oil + ethanol at 101.3 kPa are reported. Figures 8.3 and 8.4 show the experimental ($PTxy$) data and calculated values from UNIQUAC equation for the studied pseudobinary systems.

The required data for the UNIQUAC model are listed in Table 8.7. The fitted binary UNIQUAC parameters are listed in Table 8.8.

Table 8.5. Vapor-liquid equilibria data for refined cottonseed oil (1) + n-hexane (2) at 41.3 kPa.

x_1	T / K	y_1	P / kPa	x_1	T / K	y_1	P / kPa
0.07048	316.25	0.00000	41.44	0.42439	347.00	0.00001	41.48
0.07340	316.17	0.00000	41.42	0.44544	349.27	0.00001	41.20
0.09200	317.70	0.00000	41.15	0.47408	357.56	0.00005	40.96
0.09460	317.90	0.00002	41.25	0.49272	355.82	0.00001	41.23
0.15874	322.36	0.00003	40.94	0.52162	361.79	0.00004	41.60
0.16506	323.80	0.00003	40.99	0.53876	368.92	0.00003	41.39
0.18963	324.14	0.00001	41.53	0.61123	377.19	0.00005	41.15
0.19823	325.58	0.00002	41.51	0.68687	381.67	0.00005	41.51
0.23113	327.56	0.00001	41.14	0.69577	378.45	0.00006	41.05
0.23866	327.81	0.00001	41.63	0.75825	396.23	0.00011	41.33
0.28226	333.45	0.00002	41.25	0.79211	390.96	0.00009	41.37
0.30040	334.21	0.00002	40.87	0.87259	403.20	0.00050	41.34
0.34695	339.53	0.00002	41.69	0.96944	435.97	0.00220	41.68
0.37189	343.73	0.00003	41.65				

Table 8.6. Vapor-liquid equilibria data for refined soybean oil (1) + ethanol (2) at 101.3 kPa.

x_1	T / K	y_1	P / kPa	x_1	T / K	y_1	P / kPa
0.00998	351.62	0.00000	100.99	0.24916	351.72	0.00061	100.91
0.01572	351.62	0.00000	101.12	0.27325	351.72	0.00110	100.92
0.03490	351.72	0.00000	100.75	0.28349	351.72	0.00028	100.65
0.06934	351.72	0.00060	101.02	0.31214	351.82	0.00061	100.88
0.07626	351.72	0.00060	101.01	0.32009	352.38	0.00398	100.82
0.09210	351.72	0.00048	100.95	0.33456	351.72	0.00094	100.83
0.13660	351.72	0.00038	100.74	0.40783	354.24	0.00029	100.85
0.14219	351.72	0.00037	100.62	0.42160	354.64	0.00096	100.99
0.17481	351.72	0.00026	100.61	0.46250	358.66	0.00084	100.82
0.17828	351.72	0.00051	100.88	0.47197	360.07	0.00076	100.72
0.19157	351.72	0.00020	100.75	0.54710	365.8	0.00000	101.01
0.22210	351.72	0.00070	100.89	0.55210	365.9	0.00368	100.73
0.22415	351.72	0.00041	100.62	0.71431	375.16	0.00023	101.00
0.22429	351.72	0.00043	100.91	0.72275	376.46	0.00100	101.10
0.23777	351.72	0.00043	100.78	0.77471	391.15	0.00040	101.03
0.24310	351.72	0.00089	100.90				

Table 8.7. Antoine coefficients A_i, B_i and C_i, relative van der Waals volumes r_i and surfaces q_i, and critical data of the investigated compounds.

Compounds	A_i	B_i	C_i	T_{min} /K	T_{max} /K	r_i	q_i	T_c /K	P_c /atm	V_c /cm^3.mo	ω
Ethanol	8.20417	1642.89	230.300	216.15	353.15	2.1055	1.9720	516.20	63.00	167.00	0.6350
n-Hexane	7.01051	1246.33	232.988	178.15	508.15	4.4998	3.8560	507.40	29.75	370.00	0.2975
Soybean oil	12.3354	7738.96	243.931	313.15	423.15	38.7157	31.3470	1035.19	7.21	3235.10	1.4203
Cottonseed oil	13.6509	8732.92	270.201	313.15	423.15	37.5972	30.4680	1058.25	7.11	3530.38	0.9124

Table 8.8. Estimated[a] UNIQUAC interaction parameters and the mean deviations.

T range/K	P /kPa	a_{12}[b]/K	a_{21}/K	AAD (x_1)[c]	ΔT [d] (%)	AAD (y_1)	ΔP (%)
Cottonseed oil (1) + n-hexane (2)							
315-436	41.3	-336.3	1129.0	0.01154	0.83	0.00043	0.40
Soybean oil (1) + ethanol (2)							
351-391	101.3	504.6	-91.70	0.00181	0.31	0.00111	0.03

[a]Uncertainties assigned: σ_x = 0.002, σ_y = 0.002, σ_T = 0.5 K e σ_P = 0.133 kPa; [b]Binary UNIQUAC parameters: $a_{ij} \equiv (u_{ij} - u_{jj})/R$; [c] $AAD = (1/N)\sum_1^N |\text{exp - calc}|_i$; [d] $\Delta = (100/N)\sum_1^N |(\text{exp - calc})/\text{exp}|_i$,

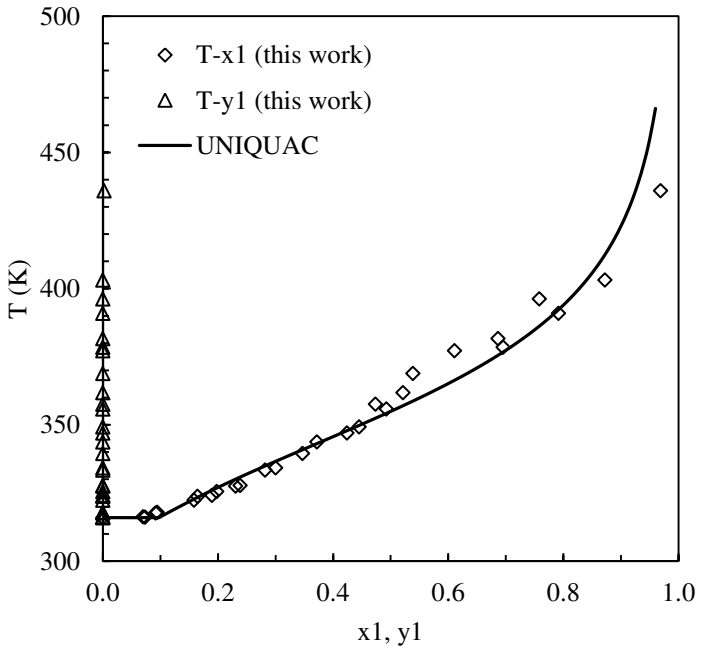

Figure 8.3. Experimental and correlated VLE data for the system cottonseed oil (1) + n-hexane (2) at 41.3 kPa.

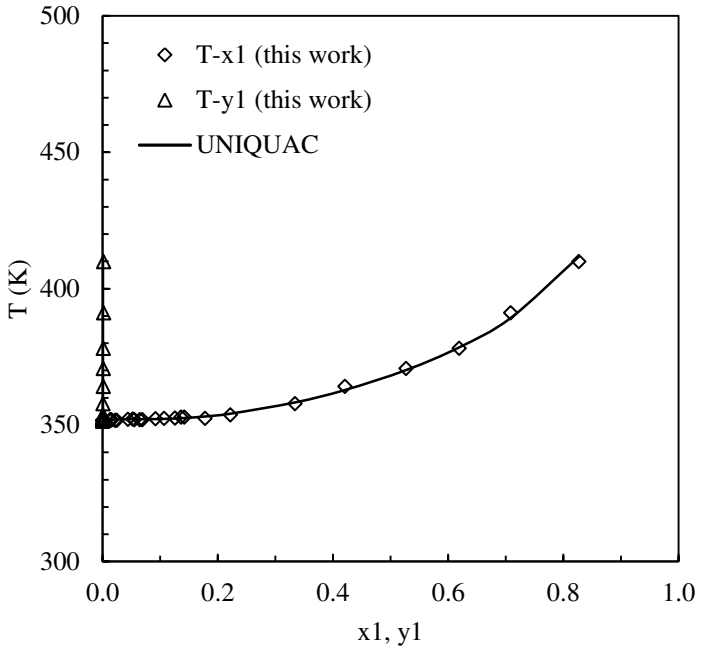

Figure 8.4 Experimental and correlated VLE data for the system soybean oil (1) + ethanol (2) at 101.3 kPa.

The correction of the vapor phase in terms of the fugacity coefficients in the mixture for the components was found to be relevant, and the order of magnitude ranged from 0.84 to 1.045 and 0.481 to 1.747, therefore the deviations of the vapor phase was described with help of the system virial equation of state, truncated after the second term, as presented by Hayden and O'Connell[32].

The maximum likelihood principle[27] was applied to correlate the VLE data and provided a deviation test of the consistency of each isobaric data set. On the basis of these calculations, the data measured are considered to be consistent.

Figure 8.5 show the VLE experimental data of system cottonseed oil (1) + n-hexane (2) obtained in this work and by Pollard et al.[2], together with the predicted results using original UNIFAC and modified UNIFAC (Dortmund).

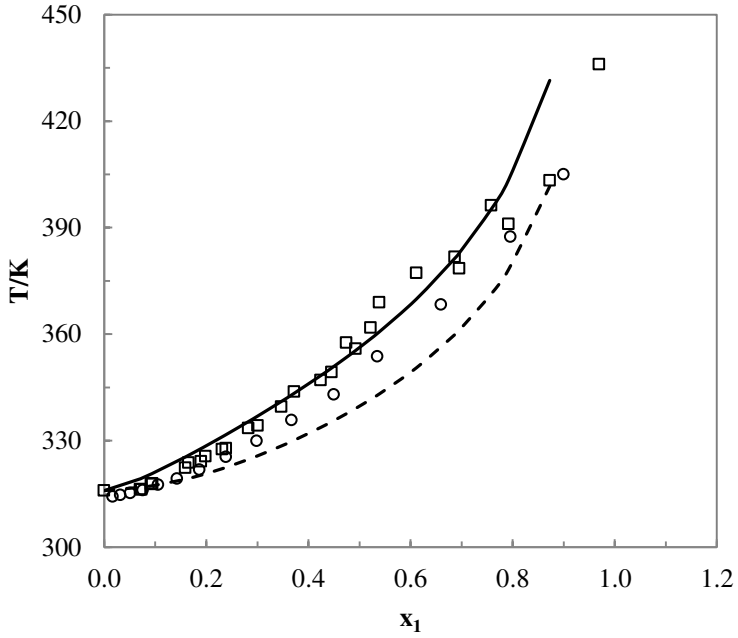

Figure 8.5. Diagram T-x_1 for the system cottonseed oil (1) + n-hexane (2) at 41.3 kPa. (□) Experimental Data from this work; (○) Experimental data from Pollard et al. [2]; (——) Original UNIFAC; (-----) Modified UNIFAC (Dortmund).

Comparing the experimental data from this work to the results obtained by Pollard et al.[2], it was observed mean difference less than 5.5% in temperature. However it should be mentioned that the equipment and methodology used in reference [2] differ considerably from those used in this work. Furthermore, both cottonseed oil and hexane used in both studies have significatively different composition. Pollard et al. have used crude cottonseed oil with an acidity of 3.5% and iodine value (IV) of 105.5 cg I2/100g, and as solvent, they used

a commercial mixture of hexane while for this work we used a refined cottonseed oil with 0.05% acidity (oleic acid) and IV equal to 112.9 cg I_2/100g, and, n-hexane with high purity (mass fraction> 0,99) as solvent.

As can be seen in Figure 8.5, the predicted results are in relative good agreement with the experimental findings. Suprisingly, the system was better predicted by original UNIFAC.

8.4. Conclusions

The results demostrated the consistency of the experimental and computational approches used in this work. The consistency of the VLE data sets has been checked and found to be satisfactory with the maximum likelihood method.

The UNIQUAC model could be applied successfully to the correlation of the VLE experimental data. The average deviation between the experimental and calculates results is less than 1 %. Moreover, with the help of UNIQUAC parameters it is possible to model and simulate, with acceptable acurancy, separation process in vegetable oils industry and biodiesel process. The performance of original UNIFAC and modified UNIFAC (Dortmund) was checked. The original UNIFAC described better the behavior of the system cottonseed-oil + n-hexane.

Acknowledgements

P. C. Belting wishes to acknowledge CNPq (Conselho Nacional de Desenvolvimento Científico e Tecnológico – 142122/2009-2). The authors would like to thank the CNPq

(304495/2010-7, 483340/2012-0, 307718/2010-7 and 301999/2010-4), FAPESP (Fundação de Amparo à Pesquisa do Estado de São Paulo - 08/56258-8, 09/54137-1 and 2010/16634-0) and INCT-EMA (Instituto Nacional de Ciência e Tecnologia de Estudos do Meio Ambiente) for the financial support. This work has been supported by the Federal University of Rio Grande do Norte.

References

1. Johnson, L. A., Recovery of Fats and Oils from Plant and Animal Sources. In *Introduction to Fats and Oils Technology*, 2nd. ed.; R. D. O'Brien, W. E. F., P. J. Wan, Ed. AOCS Press: Champaign, Illinois, 2000; pp 20-48.

2. Pollard, E. F.; Vix, H. L. E.; Gastrock, E. A., Solvent Extraction of Cottonseed and Peanut Oils. *Ind. Eng. Chem.* **1945,** 37, (10), 1022-1026

3. Fornari, T.; Bottini, S.; Brignole, E., Application of UNIFAC to vegetable oil-alkane mixtures. *J. Am. Oil Chem. Soc.* **1994,** 71, (4), 391-395.

4. Gmehling, J.; Kolbe, B.; Kleiber, M.; Rarey, J., *Chemical Thermodynamics for Process Simulation*. 1st ed.; Wiley-VCH: Weinheim, 2012; p 735.

5. Lusas, E. W.; Watkins, L. R.; Koseoglu, S. S., Isopropyl alcohol to be tested as solvent. *Inform.* **1991,** 2, 970 – 973.

6. Rittner, H., Extraction of vegetable oils with ethyl alcohol. *Oléagineux* **1992,** 47, (jan.), 29-42.

7. Bera, D.; Lahiri, D.; De Leonardis, A.; De, K.; Nag, A., A Novel Azeotropic Mixture Solvent for Solvent Extraction of Edible Oils. *Agricultural Engineering International: the CIGR Ejournal* **2006,** VIII, (April), Manuscript FP 06 005.

8. Freitas, S. P.; Lago, R. C. A., Equilibrium data for the extraction of coffee and sunflower oils with ethanol. *Braz. J. Food Technol.* **2007,** 10, 220-224.

9. Hron, R. J.; Koltun, S. P., An Aqueous Ethanol Extration Process for Cottonseed Oil. *J. Am. Oil Chem. Soc.* **1984,** 61, (9), 1457-1460.

10. Rao, R. K.; Krishna, M. G.; Zaheer, S. H.; Arnold, L. K., Alcoholic Extraction of Vegetable Oils. I. Solubilities of Cottonseed, Peanut, Sesame, and Soybean Oils in Aqueous Ethanol. *J. Am. Oil Chem. Soc.* **1955,** 32, (7), 420-423.

11. Hron, R. J.; Koltun, S. P.; Graci, A. V., Biorenewable Solvents for Vegetable Oil Extraction. *J. Am. Oil Chem. Soc.* **1982,** 59, (9), 674-684.

12. Belting, P. C.; Bölts, R.; Rarey, J.; Gmehling, J.; Ceriani, R.; Chiavone-Filho, O.; Meirelles, A. J. A., Excess Enthalpies for Various Binary Mixtures with Vegetable Oil at Temperatures between 298.15 K and 383.15 K. **2013**.

13. Belting, P. C.; Rarey, J.; Gmehling, J.; Ceriani, R.; Chiavone-Filho, O.; Meirelles, A. J. A., Activity Coefficient at Infinite Dilution Measurements for Organic Solutes (polar and nonpolar) in Fatty Compounds: Saturated Fatty Acids. *J. Chem. Thermodyn.* **2012,** 55, 42-49.

14. Belting, P. C.; Rarey, J.; Gmehling, J.; Ceriani, R.; Chiavone-Filho, O.; Meirelles, A. J. A., Measurements of Activity Coefficients at Infinite Dilution in Vegetable Oils and Capric Acid Using the Dilutor Technique. **2013**.

15. Belting, P. C.; Rarey, J.; Gmehling, J.; Ceriani, R.; Chiavone-Filho, O.; Meirelles, A. J. A., Activity coefficient at infinite dilution measurements for organic solutes (polar and non-polar) in fatty compounds – Part II: C18 fatty acids. *J. Chem. Thermodyn.* **2013,** 60, (May), 142–149.

16. Belting, P. C.; Bölts, R.; Rarey, J.; Gmehling, J.; Ceriani, R.; Chiavone-Filho, O.; Meirelles, A. J. A., Measurement, correlation and prediction of isothermal vapor-liquid equilibria of different systems containing vegetable oil. **2013**.

17. AOCS, *Official Methods and recommended Practices of the American Oil Chemists' Society*. 5 th ed.; AOCS Press: Champaign, IL, 2004.

18. Oliveira, H. N. M. Determinação de dados de Equilíbrio Líquido-Vapor para Sistemas Hidrocarbonetos e Desenvolvimento de uma nova Célula Dinâmica. Tese, Universidade Federal de Natal, Natal-RN, 2003.

19. Coelho, R.; Santos, P. G.; Mafra, M. R.; Cardozo-Filho, L.; Corazza, M. L., (Vapor + liquid) equilibrium for the binary systems {water + glycerol} and {ethanol + glycerol, ethyl stearate, and ethyl palmitate} at low pressures. *J. Chem. Thermodyn.* **2011,** 43, 1870-1876.

20. Segalen da Silva, D. I.; Mafra, M. R.; Silva, F. R.; Ndiaye, P. M.; Ramos, L. P.; Cardozo-Filho, L.; Corazza, M. L., Liquid-liquid and vapor-liquid equilibrium data for biodiesel reaction-separation systems. *Fuel* **2013,** 108, 269-276.

21. Othmer, D. F., Composition of Vapors from BOILING BINARY SOLUTIONS. *Ind. Eng. Chem.* **1943,** 35, (5), 614-620.

22. Sandler, S. I., *Chemical, Biochemical, and Engineering Thermodynamics* 4th ed.; John Wiley & Sons, Inc: Oxford, 2006; p 960.

23. Bondi, A., *Physical properties of molecular crystals, liquids, and glasses*. J. Wiley: New York, N.Y., 1968; p 502.

24. Marrero, J.; Gani, R., Group-contribution based estimation of pure component properties. *Fluid Phase Equilib.* **2001,** 183-184, 183–208.

25. Design Institute for Physical Properties Data Bank In AIChE: [2005, 2008, 2009, 2010].

26. Ceriani, R.; Meirelles, A. J. A., Predicting vapor–liquid equilibria of fatty systems. *Fluid Phase Equilibr.* **2004,** 215, 227–236.

27. Kemeny, S.; Manczinger, J.; Skjold-Jørgensen, S.; Toth, K., Reduction of Thermodynamic Data by Means of the Multiresponse Maximum Likelihood Principle. *AIChE J.* **1982,** 28, 20-30.

28. Fredenslund, A.; Gmehling, J.; Rasmussen, P., *Vapor-Liquid Equilibria Using UNIFAC*. Elsevier: Amsterdam, 1977; p 380.

29. Hansen, H. K.; Rasmussen, P.; Fredenslund, A.; Schiller, M.; Gmehling, J., Vapor-Liquid Equilibria by UNIFAC Group Contribution 5. Revision and Extension. *Ind. Eng. Chem. Res.* **1991,** 30, (10), 2352-2355.

30. Weidlich, U.; Gmehling, J., A Modified UNIFAC Model. 1. Prediction of VLE, h_E and γ^{∞} *Ind. Eng. Chem. Res.* **1987,** 26, (7), 1372-1381.

31. Gmehling, J.; Li, J.; Schiller, M., A modified UNIFAC model. 2. Present parameter matrix and results for different thermodynamic properties. *Ind. Eng. Chem. Res.* **1993,** 32, (1), 178-193.

32. Hayden, J. G.; O'Connell, P. O., A Generalized Method for Predicting Second Virial Coefficients. *Ind. Eng. Chem., Process Des. Dev.* **1975,** 14, 209-216.

CAPÍTULO 9: CONSIDERAÇÕES FINAIS E CONCLUSÃO GERAL

O objetivos propostos neste trabalho de doutorado foram atingidos.

A partir dos resultados da primeira parte do trabalho de tese, apresentados nos capítulos 3 e 4 (os coeficientes de atividade à diluição infinita em ácidos graxos), foi possível verificar as interações entre os principais ácidos graxos que compõem a estrutura dos triacilgliceróis (base dos óleos vegetais) e diversos compostos orgânicos, incluindo alcanos, cicloalcanos, alcenos, compostos aromáticos, álcoois, ésteres, cetonas e hidrocarbonetos halogenados. Em relação aos ácidos graxos (solventes), os resultados obtidos permitiram verificar os efeitos do tamanho e do número de insaturações da sua cadeia carbônica no comportamento termodinâmico deste sistema. Em relação aos compostos orgânicos (solutos), foi verificada a influência da polaridade da molécula, da presença de insaturações, do tamanho da cadeia carbônica e de alguns grupos funcionais na interação com ácidos graxos. Além disso, os resultados de coeficiente de atividade à diluição infinita em uma ampla faixa de temperatura permitiram avaliar a influência desta variável na interação solvente-soluto e o cálculo das funções termodinâmicas à diluição infinita. O método utilizado nesta parte do trabalho, cromatografia gás-líquido (GLC), foi bastante conveniente, pois permitiu a obtenção de um grande número de dados a partir de pequenas quantidades de reagente, tornando possível a utilização de ácidos graxos puros, que podem apresentar preços bastante elevados. O número de dados gerados permitiu a

ampliação do banco de dados de propriedades termodinâmicas para compostos graxos puros em uma ampla faixa de temperatura.

Nas determinações de coeficiente de atividade à diluição infinita , γ^{∞}, foi verificado que o desvio em relação ao comportamento ideal é moderado em ácidos graxos saturados; no entanto, o desvio torna-se significativo em ácidos graxos insaturados. Os dados experimentais mostraram que: tanto a presença quanto o número de insaturações na cadeia carbônica do ácido graxo influenciam as interações entre soluto e solvente e, consequentemente, o valor de γ^{∞}. No caso dos ácidos graxos saturados, a combinação entre a longa cadeia de carbonos (variando de 12 a 18) com característica apolar e do grupo funcional carboxílico que apresenta característica fortemente polar, permite que tanto compostos polares quanto apolares se dissolva facilmente em ácidos graxos. Já nos ácidos graxos insaturados, as duplas ligações fazem com que a molécula reduza o caráter apolar da cadeia alquílica.

Altos valores de γ^{∞} indicam pouca interação entre o soluto e o solvente, refletindo em elevada volatilidade do soluto no ácido graxo e, por conseguinte, maior facilidade de separação deste soluto por meio de evaporação. Isso significa que os álcoois de cadeia curta, apesar de apresentarem baixa solubilidade em ácidos graxos saturados, podem ser facilmente separados destes componentes utilizando-se a evaporação. Essa informação é interessante para os processos de extração de óleo, assim como para a recuperação do álcool nos processos de dessolventização do óleo e na produção de biodiesel.

Em relação aos solutos hidrocarbonetos, importantes tendências puderam ser identificadas a partir dos dados experimentais deste trabalho. O γ^{∞} aumenta (ou a

solubilidade diminui) com o aumento da cadeia carbônica do soluto. Além disso, verificou-se que hidrocarbonetos com estrutura cíclica tem maior interação com os ácidos graxos quando comparado aos de estrutura linear com o mesmo número de carbono. Supõe-se que tal fenômeno seja resultado do efeito de empacotameto das moléculas. A presença de insaturações no soluto hidrocarboneto também aumenta a sua interação com os ácidos graxos; dessa forma, compostos aromáticos também apresentaram maior interação com tais componentes.

Os compostos halogenados apresentaram os mais baixos valores de γ^{∞}. Tanto para ácidos graxos saturados quanto insaturados, o clorofórmio foi o soluto que apresentou o menor valor de γ^{∞}. A grande interação de tais compostos com o ácido graxo deve-se, provavemente, ao efeito de fortes interações intermoleculares, resultantes das forças de van der Waals e da polaridade.

Nos ácidos graxos saturados e monoinsaturado, para praticamente todos os solutos testados, observou-se que γ^{∞} diminui com o aumento da temperatura, resultando em valores positivos de entalpia de excesso à diluição infinita, $\Delta H^{E,\infty}$. Tendência contrária foi observada para o ácido graxo linoléico nos casos de diluição infinita de hidrocarbonetos. Os valores negativos de $\Delta H^{E,\infty}$indicam que interações soluto-solvente são maiores que as interações soluto-soluto.

Verificou-se também que, dependendo da polaridade do soluto, o tamanho da cadeia de carbono dos ácidos graxos influencia de maneira diferente os valores de γ^{∞}. No caso de misturas de ácidos graxos saturados e solutos apolares, os valores de γ^{∞} diminuem com o aumento da cadeia alquílica dos ácidos, enquanto que, para misturas com solutos polares,

foi verificado um aumento no valor de γ^{∞}. Tal efeito pode ser resultado da redução da polaridade do solvente devido ao aumento da cadeia de carbono, o que eleva a interação intermolecular dos ácidos graxos com os solventes apolares, e reduz a sua interação com solventes polares, refletindo nos valores de γ^{∞}. Já para os ácidos graxos poli-insaturados, tendência inversa foi verificada à medida que o número de duplas ligações aumentam o carater polar da molécula, indicando, mais uma vez, que a presença e quantidade de insaturações interferem significativamente na interação soluto-solvente.

A segunda parte deste estudo tratou da investigação de soluções contendo óleos vegetais, isto é, de misturas graxas multicomponentes. Para a determinação de coeficientes de atividade à diluição infinita destas misturas houve a necessidade de se utilizar outro método, a técnica do Dilutor ou do gás inerte de arraste. O equipamento Dilutor utilizado neste trabalho apresenta uma célula extra, chamada célula de saturação, que mantem a composição do solvente na célula de equilíbrio constante. Outros métodos, como o GLC, não são adequados para determinações em misturas, pois os diferentes componentes que as constituem apresentam diferentes pressões de vapor; assim, compostos com pressão de vapor mais elevada são removidos mais rapidamente da coluna, de modo que a composição do solvente altera-se com o tempo de análise.

Não foi possível obter uma correlação simples entre os valores de γ^{∞} medidos para os óleos vegetais e os medidos para os ácidos graxos que os compõem. No entanto, foi possível identificar nessas misturas que compostos polares (como álcoois de cadeia curta) e apolares (como o n-hexano) apresentam valores de γ^{∞} com ordem de grandeza diferente, indicando o forte efeito da polaridade do soluto também em sistemas graxos

multicomponentes como os óleos vegetais. A partir dos resultados, obtidos foi possível identificar o efeito da temperatura nos valores de γ^{∞} em óleos vegetais. Assim como na maioria dos ácidos graxos, γ^{∞} diminui com o aumento da temperatura; no entanto, essa tendência é mais pronunciada em solutos polares. Isso pode ser verificado comparando os valores de $\Delta H^{E,\infty}$ do n-hexano e dos álcoois à diluição infinita nos óleos vegetais, $\Delta H^{E,\infty}_{n-hexano}$ é, no mínimo, 6 vezes menor do que o $\Delta H^{E,\infty}_{álcool}$.

Também foi verificado que os modelos de contribuição de grupos UNIFAC original e modificado (Dortmund) não apresentam boa predição dos γ^{∞} para os sistemas com óleo vegetal, provavelmente devido às diferenças entre os tamanhos das moléculas de soluto (n-hexano, metanol e etanol) e solvente (óleos vegetais). Pelos resultados obtidos verificou-se que os modelos assumem que os óleos vegetais são compostos mais polares do que determinado experimentalmente, o que leva a supor que o núcleo polar da molécula de triacilglicerol é blindado pelas longas cadeias de hidrocarbonetos dos ácidos graxos que a compõem, resultando na redução da polaridade da molécula. Além disso, a presença de três grupos éster tão próximos pode resultar na redução do efeito da presença de tal grupo na molécula. A proposta de mudança do modelo UNIFAC modificado (Dortmund) apresentada (a simples redução de um grupo éster) resultou em significantes melhorias na predição de misturas com metanol. Para as misturas com n-hexano e etanol verificou-se apenas uma melhor descrição da variação do γ^{∞} em relação à temperatura.

Os resultados de entalpia de excesso mostraram que as características químicas dos componentes que formam a mistura com o óleo vegetal, como a polaridade, influenciam o comportamento da mistura. As misturas com álcoois apresentaram os maiores desvios em

relação à lei de Raoult, devido ao rompimento das ligações de hidrogênio entre as moléculas de álcool quando misturados com o óleo vegetal. As misturas com n-hexano apresentaram um comportamento entálpico próximo do ideal, sendo que, para todos os óleos e em grande parte da faixa de composição da mistura, um comportamento levemente endotérmico foi medido e, somente na temperatura de 383.15 K e em altas concentrações de n-hexano, foram obtidos valores negativos de H^E.

Os resultados de coeficiente de atividade à diluição infinita e de entalpia de excesso em misturas contendo óleos vegetais, apresentados nos capítulos 5 e 6, respectivamente, mostraram concordância e permitiram um melhor entendimento em termos de interações moleculares entre os compostos graxos e o n-hexano, o etanol e o metanol, substâncias relevantes para os processos nas indústria de óleos vegetais e biodiesel. Além disso, foi possível avaliar o comportamento real destes sistemas graxos complexos em uma ampla faixa de temperatura.

Em relação à determinação de equilíbrio líquido-vapor (ELV) de óleos vegetais, dois métodos foram avaliados: o método estático (dados $P - x$), apresentado no capítulo 7, e o método dinâmico de ebuliometria (dados $PTxy$), apresentado no capítulo 8. No método estático, o ELV é medido controlando-se a temperatura e obtendo os valores de pressão. A vantagem desse último método é que o controle da temperatura permite minimizar a ocorrência de possíveis reações químicas; além disso, a verificação da ocorrência de reação no sistema também é facilitada, já que, neste caso, a pressão do sistema não estabiliza e a sequência de determinação é automaticamente abortada. A limitação deste método é o fato de não permitir a análise da composição das fases. O método dinâmico, por sua vez,

permite a análise da composição das fases. Embora o método analítico utilizado neste trabalho para a determinação da composição das fases (densimetria) não tenha gerado a descrição composicional exata da matéria graxa presente nas fases líquida e vapor, a utilização de um outro método analítico, como a cromatografia gasosa, poderia fornecer a composição exata das mesmas. Neste caso, poderia ser empregada a ideia utilizada na técnica do Dilutor, em que a amostragem seria automática e o cromatógrafo gasoso ficaria dedicado ao equipamento. A limitação do método dinâmico é que, durante o experimento, a medida que o sistema fica mais concentrado em composto graxo, as temperaturas se elevam muito e podem catalisar reações químicas e degradações dos componentes, induzindo a modificação na composição do sistema. Embora tal método, nas medidas de ELV, ainda permita a opção de manter a temperatura constante e variar a pressão do sistema, tal procedimento é muito trabalhoso e susceptível a maiores erros analíticos, já que exige cuidados na elaboração da composição da mistura e a interrupção do sistema a cada ponto determinado para a coleta das fases.

Com base na experiência adquirida neste trabalho, acredita-se que o método estático é o mais indicado para o sistema estudado, tanto em relação à praticidade e rapidez na determinação dos dados, quanto em relação à precisão dos mesmos. Julga-se que as suposições adotadas, como a não volatilidade de compostos graxos nas faixas de temperatura e pressão estudadas, não comprometem os resultados obtidos. Já as elevadas temperaturas utilizadas no método dinâmico e a necessidade de recirculação das fases são considerados fatores limitantes que podem comprometer a qualidade dos dados obtidos.

Os resultados de ELV obtidos pelos dois métodos utilizados neste trabalho foram satisfatoriamente correlacionados pelo modelo UNIQUAC. A abordagem pseudocomponente foi utilizada com sucesso nestes sistemas. Já a predição com os modelos de contribuição de grupos UNIFAC apresentou apenas uma descrição qualitativa dos sistemas estudados, indicando a necessidade do desenvolvimento destes modelos para a aplicação em sistemas graxos. Os sistemas com álcool apresentaram faixas de imiscibilidade. No caso do metanol, a lacuna de miscibilidade foi verificada em todas as misturas com concentração de álcool acima de aproximadamente 0,7 em fração molar a 348,15 K e 0,8 a 373,15 K. Na misturas com etanol, o comportamento heterogêneo foi identificado em composições acima de 0,85 de etanol em fração molar a 348,15 K e apenas a mistura com óleo de canola apresentou lacuna de miscibilidade a 373,15 K ($x_{etanol} > 0{,}9$). Tais resultados confirmam a vantagem já discutida por muito autores, de utilizar o etanol no processo de transesterificação para a produção de biodiesel, devido a sua maior miscibilidade.

Este estudo contribuiu com dados inéditos de coeficientes de atividade à diluição infinita, entalpias de excesso e equilíbrio líquido-vapor de sistemas contendo compostos graxos. Tais dados são úteis para a realização de projeto, otimização e modelagem de processos de separação térmica confiáveis, assim como para a seleção de solventes para processos de extração. A ampliação da base de dados destes compostos é também relevante por permitir o desenvolvimento de novos modelos termodinâmicos e ajuste de parâmetros mais confiáveis necessários para esses sistemas, como verificado neste trabalho.

Abaixo estão relacionadas algumas sugestões para trabalhos futuros:

(i) aplicação dos parâmetros de modelagem termodinâmica obtidos neste trabalho na simulação de processos de extração de oleaginosas, utilizando-se como solvente o etanol e de separação de óleos vegetais e etanol na indústria de óleos vegetais e biodiesel;

(ii) realização de medidas de coeficientes de atividade à diluição infinita, entalpias de excesso e dados de equilíbrio em outros compostos graxos como: ésteres de ácidos graxos (principalmente metílicos e etílicos), acilgliceróis parciais, óleos vegetais de outras fontes e gorduras animais em ampla faixa de temperatura a fim de incrementar o banco de dados destes compostos;

(iii) desenvolvimento de um método de determinação de equilíbrio líquido-vapor (ELV) de sistemas com alta diferença de volatilidade e alta viscosidade, como é o caso de compostos graxos + solvente, que utilize pequenas quantidades de reagentes e que permita a análise da composição exata das fases líquida e vapor, inclusive de traços. Tal método permitiria a descrição mais exata e maior compreensão do comportamento de tais sistemas;

(iv) desenvolvimento de um método de medição de pressão de vapor e constantes críticas de óleos vegetais;

(v) revisão dos parâmetros dos modelos de contribuição de grupos para aplicação em compostos graxos a fim de torná-los mais preditivos.

ANEXOS

Anexo I: Detalhamento da metodologia e equipamento GLC – cromatógrafo gás-líquido

Figure I.1: GLC Oldenburg.

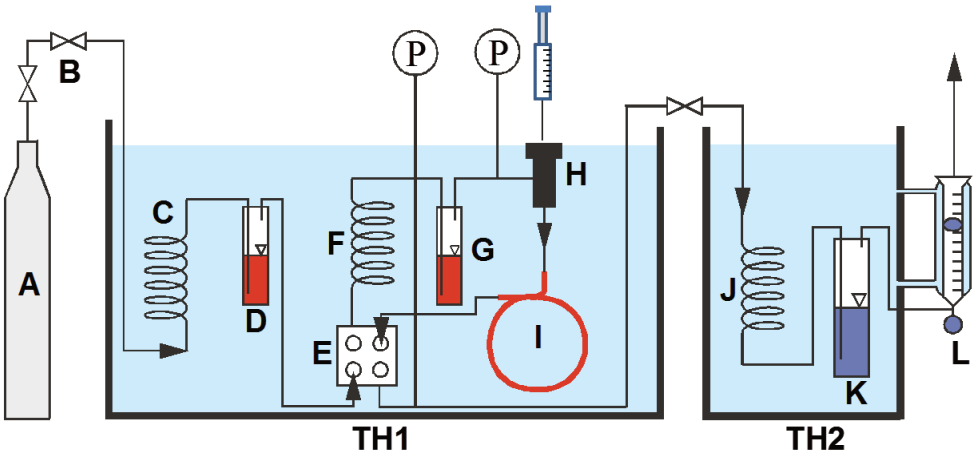

- A – carrier gas reservoir
- B – reduction valve
- C – heating coil
- D, G, K – pre saturators
- E – thermal conductivity detector
- F, J – thermostatting coil
- H – injection block
- I - column
- L – soap bubble flowmeter
- TH1, TH2 - thermostats

Figure I.2: Descriptive scheme of the GLC (KRUMMEN, 2002).

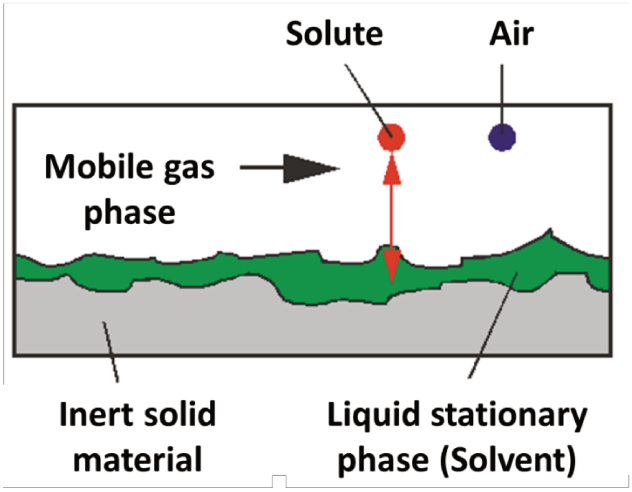

Figure I.3: Simulation of the phenomenon inside the column (KRUMMEN, 2002).

Preparation of the Column – step by step:

Figure I.4: 304 Stainless steel column.

Figure I.5: Suport material: Chromosorb P-AW-DMCS 60/80 Mesh.

Figure I.6: Coating process.

Figure I.7: Coated material after solubilizer evaporation (chromosorb + solvent).

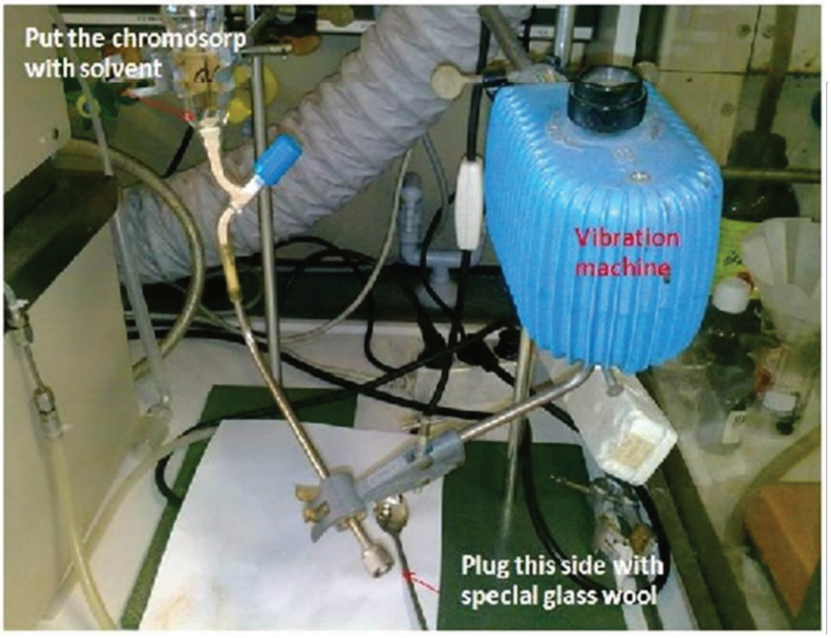

Figure I.8: Filling of the column.

Figure I.9: Installation column in the apparatus.

Figure I.10: Aparattus top view.

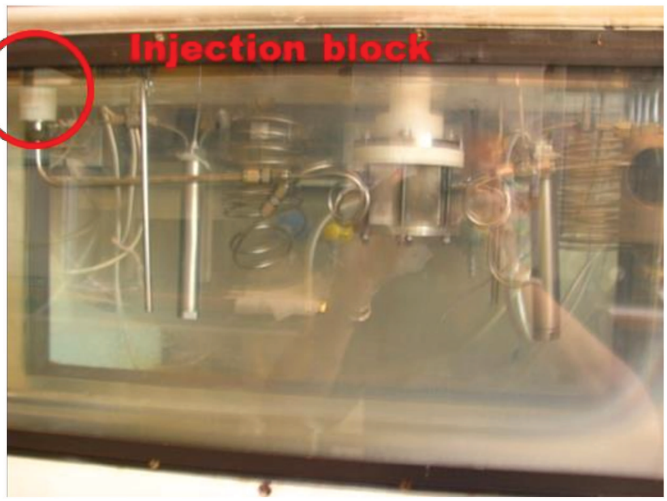

Figure I.11: Thermalbath.

Figure I.12: Integrator HP 3990ª.

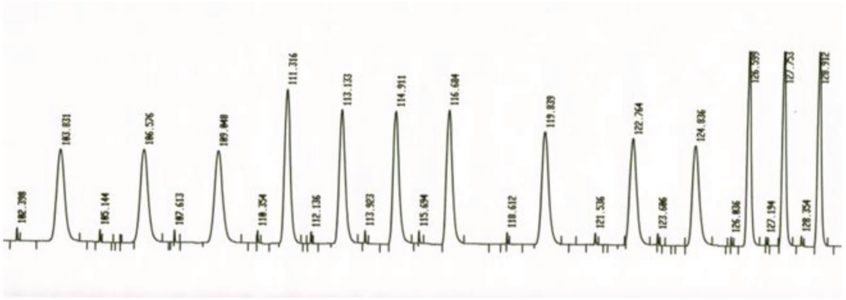

Figure I.13: Chromatogram.

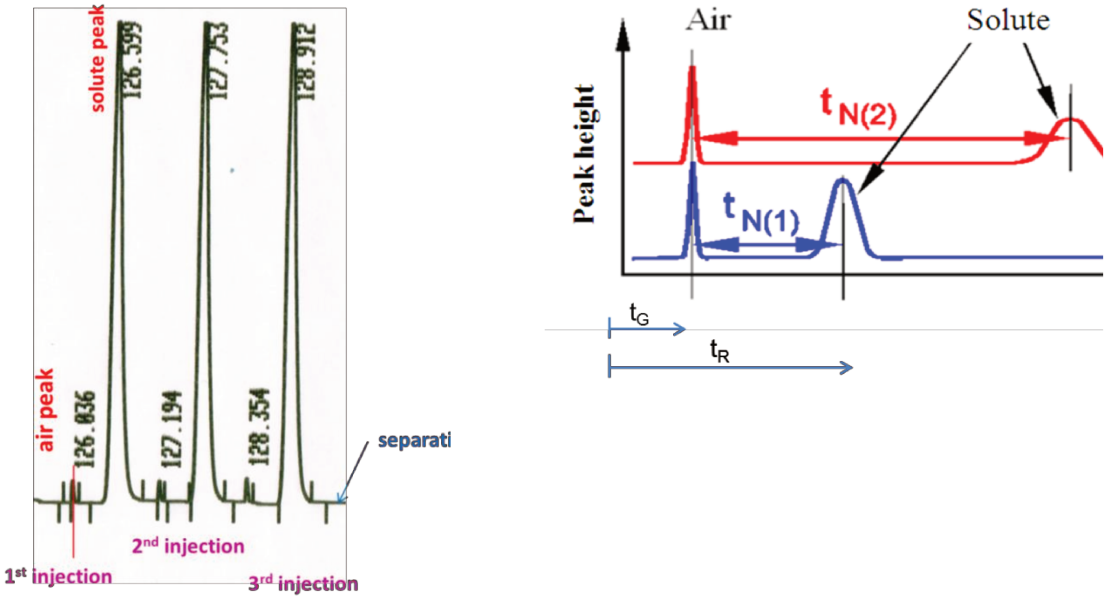

Figure I.14: Chromatogram analysis.

The net retention time ($t_R - t_G$) is obtained by comparison the retention time of the solute and air on the same solvent surface when they are applied at the same time.

Referência Bibliográfica

KRUMMEN, M. **Experimentelle Untersuchung des Aktivitätskoeffizienten bei unendlicher Verdünnung in ausgewählten Lösungsmitteln und Lösungsmittelgemischen als Grundlage für die Synthese thermischer Trennprozesse**. 2002. 198 Thesis (Doktors der Naturwissenschaften). Fachbereich Chemie, Carl von Ossietzky Universität Oldenburg, Oldenburg.

Anexo II – Detalhamento da metodologia e equipamento da técnica do Dilutor

A técnica do dilutor ou o método do arraste (do inglês: *inert gas stripping method* ou *Dilutor Technique*), proposta por LEROI et al. (1977) e aprimorada por RICHON, D., ANTOINE, P. e RENON, H. (1980), consite em um método rápido e preciso para a determinção do coeficiente à diluição infinita. Além disso, apresenta grande vantagem frente aos outros métodos, pois é o único também aplicável para a determinação de γ^{∞} em misturas de solventes, como já realizado com sucesso por LEBERT e RICHON (1984) e SORRENTINO, VOILLEY e RICHON (1986). Outras técnicas, como por exemplo, a cromatografia líquida gasosa (GLC), não são adequadas para a medição do coeficiente de atividade à diluição infinita em misturas de solventes. No caso do GLC, existe uma redução de pressão no decorrer da coluna; desta forma, o componente mais volátil da mistura é removido mais rapidamente, de modo que a composição do solvente altera-se com o tempo (KRUMMEN, M., GRUBER, D. e GMEHLING, J., 2000).

O método é baseado geralmente no seguinte príncipio: a vazão constante de um gás inerte, sob condições isotérmicas, arrasta um componente altamente diluído (soluto) em um solvente (ou, como já falado, uma mistura de solventes) até que se alcance o equilíbrio entre as fases líquida e vapor na célula de medição (ver Figura II.1). O coeficiente de atividade à diluição infinita do soluto pode ser então determinado a partir da medida da composição da fase vapor na célula de medição em função do tempo. O esquema e a foto do dilutor utilizado nos experimentos estão apresentados na Figura II.2.

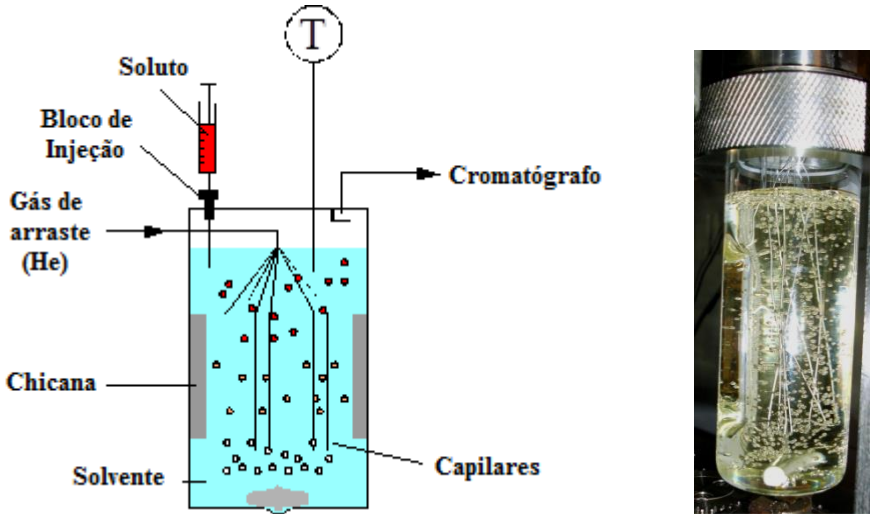

Figura II.1: Célula de medição do Dilutor. (i) esquema da célula (GRUBER, KRUMMEN e GMEHLING, 1999b; KRUMMEN, M., GRUBER, D. e GMEHLING, J., 2000; KRUMMEN, MICHAEL, GRUBER, DETLEF e GMEHLING, JÜRGEN, 2000) (ii) foto da célula.

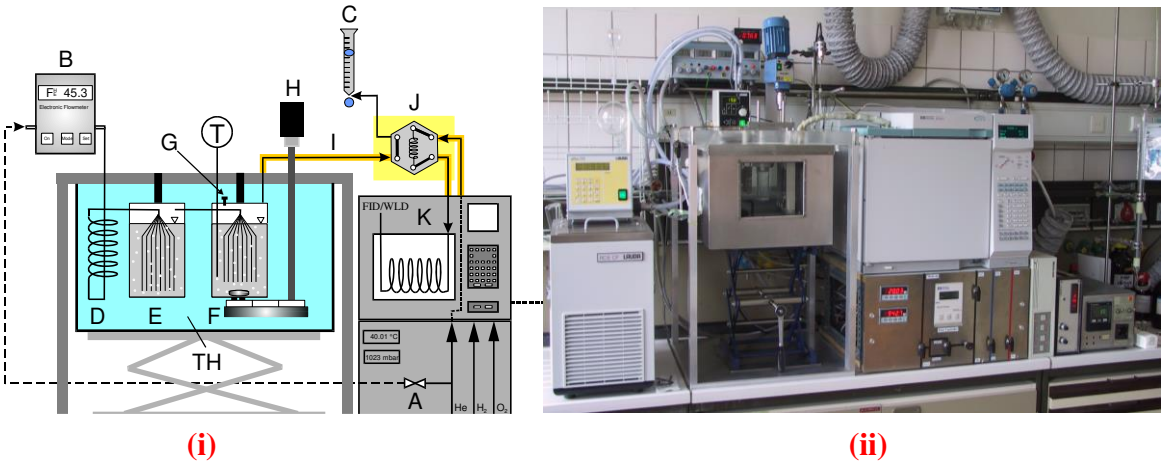

Figura II.2: Equipamento Dilutor. (i) esquema de aparato(GRUBER, KRUMMEN e GMEHLING, 1999b; KRUMMEN, M., GRUBER, D. e GMEHLING, J., 2000) e (ii) foto do equipamento.

A. Medidor e controlador de fluxo mássico digital (DMFC; Bronkhorst Hi-TEC; F-201C-RA-33V); B. Medidor de fluxo eletrônico (Hewlett Packard Nr. 5182-3494); C. Medidor de fluxo tipo bolha de sabão D. Serpentina de aquecimento; E. Célula de saturação; F. Célula de medida; G. Septo; H. Motor do agitador; I. Linha aquecida; J. Válvula de seis vias; K. Cromatógrafo gasoso (CG); L. Computador com *software HP Chemstation*; TH. Termostato (0,01 K).

Para determinar o coeficiente de atividade à diluição infinita, considera-se que as fases vapor e líquida do sistema em questão estão em equilíbrio; portanto, para um composto altamente diluído (soluto i), o equilíbrio de fases para o soluto e para o solvente pode ser descrito pelas equações II.1 e II.2, repectivamente.

$$x_i \gamma_i \varphi_i^s P_i^s Poy_i = y_i \varphi_i^v P \quad \text{(II.1)}$$

$$x_{solv} \gamma_{solv} \varphi_{solv}^s P_{solv}^s Poy_{solv} = y_{solv} \varphi_{solv}^V P \quad \text{(II.2)}$$

Assumindo que:

- o soluto i está presente à diluição infinita, o que significa que para o soluto: $\gamma_i = \gamma_i^\infty$; e para o solvente puro tem-se que: $\gamma_{solv} = 1$ ($x_{solv} \approx 1$);

- o fator de Poynting (Poy_i), que expressa os desvios da fase líquida devido ao efeito da pressão, pode ser, neste caso, negligenciado, já que os experimentos são realizados a pressões ou diferenças de pressão ($P - P_i^s$) baixas. Desta forma, será considerado que $Poy_i \approx 1$;

- a solubilidade do gás de arraste na fase líquida pode ser desprezada;

- o coeficiente de fugacidade do soluto na fase vapor, φ_i^v, pode ser aproximado a 1, já que o gás de arraste utilizado é o hélio (que possui comportamento próximo ao de gás ideal);

- para o solvente puro a seguinte aproximação pode ser realizada:

$$\frac{\varphi_{solv}^s Poy_{solv}}{\varphi_{solv}^V} \approx 1 .$$

A partir desses pressupostos, o equilíbrio de fases para o soluto e para o solvente pode ser reescrito pelas equações II.3 e II.4, respectivamente.

$$x_i \gamma_i^{\infty} \varphi_i^s P_i^s = y_i P \tag{II.3}$$

$$P_{solv}^s = y_{solv} P \tag{4}$$

Como já foi mencionado, o princípio de medição é baseado no arraste do componente altamente diluído pela célula de medição através de um gás de arraste (neste caso hélio). No equipamento em questão, o fluxo de gás de arraste se dá conforme o esquema apresentado na Figura II.3.

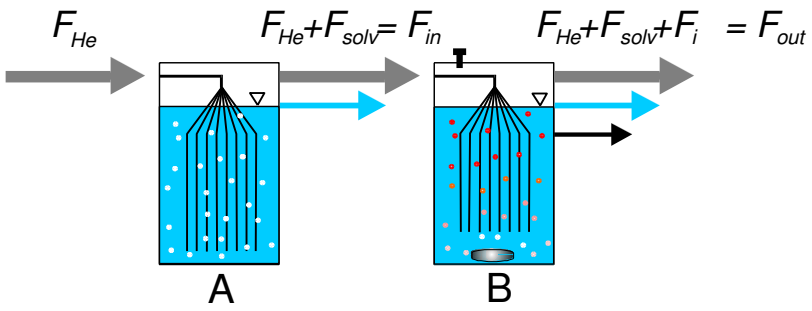

Figura II.3: esquema do fluxo de gás de arraste no equipamento (KRUMMEN, M., GRUBER, D. e GMEHLING, J., 2000).

(A) célula de saturação com solvente (puro ou mistura); (B) célula de medida com solvente (puro ou mistura) e soluto à diluição infinita; F_{He} fluxo do gás de arraste hélio; F_{solv}- fluxo de solvente; F_{in}- fluxo de entrada na célula de medida; F_{out} - fluxo de saída da célula de medida; F_i - fluxo do soluto.

O fluxo do solvente está relacionado com a pressão de vapor de saturação do solvente P_{solv}^s, e é influenciado pela pressão na célula de saturação P e pelo fluxo do gás de arraste hélio, F_{He}, ao longo da célula de saturação através da equação II.5.

$$F_{solv} = F_{He} \frac{P^s_{solv}}{P} \tag{II.5}$$

Substituindo a equação II.5 na expressão do fluxo de entrada na célula de medida, F_{in}, este pode ser representado pela equação II.6.

$$F_{in} = F_{He}\left(1 + \frac{P^s_{solv}}{P}\right) \tag{II.6}$$

Considerando o caso em que a pressão de vapor do solvente não é desprezível ($P^s_{solv} \geq 5\ mbar$), a quantidade de solvente é uma variável importante na medida de γ_i^∞.

A vazão de saída da célula de medida pode ser reescrita como apresentado na equação II.7.

$$F_{out} = F_{in} + F_i \tag{II.7}$$

Assumindo que a lei dos gases ideais é válida para a corrente de soluto, já que esse se apresenta de forma muito diluída, F_{in} pode ser representada pela equação II.8.

$$F_i = -\frac{RT}{P}\frac{dn_i}{dt} \tag{II.8}$$

Combinando as equações II.8 e II.7, tem-se a equação II.9, que representa o fluxo de saída da célula de medida.

$$F_{out} = F_{in} - \frac{RT}{P}\frac{dn_i}{dt} \tag{II.9}$$

A variação da quantidade absoluta de soluto na célula é medida em relação ao tempo, e pode ser representada pela equação II.10.

$$\frac{dn_i}{dt} = -y_i \frac{PF_{out}}{RT} \tag{II.10}$$

Considerando que não existe variação da quantidade absoluta de solvente na célula de medida, já que o fluxo de solvente que sai da célula de medida é igual ao que entra proveniente da célula de saturação, assim $dn_{solv}/_{dt} = 0$.

Substituindo a equação II.10 na equação II.9, tem-se como resultado a equação II.11:

$$F_{in} = F_{out}(1 - y_i) \tag{II.11}$$

Combinando as equações II.3 e II.11 obtem-se a seguinte expressão para F_{out}.

$$F_{out} = \frac{F_{in}}{1 - \frac{x_i \gamma_i^{\infty} \varphi_i^s P_i^s}{P}} \tag{II.12}$$

Se a equação II.12 for substituída na equação II.10, obtem-se a expressão da variação da quantidade de soluto com o tempo, dada pela equação II.13:

$$\frac{dn_i}{dt} = -x_i \gamma_i^{\infty} \varphi_i^s P_i^s \frac{1}{\left(1 - \frac{x_i \gamma_i^{\infty} \varphi_i^s P_i^s}{P}\right)} \frac{F_{in}}{RT} \tag{II.13}$$

Para solutos com alta volatilidade relativa, isto é, com alta pressão de vapor ou grandes valores de γ_i^{∞}., deve constar na definição da fração molar do soluto, x_i, apenas a parte proporcional à fase líquida, sendo descontada a proporção relativa à fase vapor, assim: $n_i = n_i^L + n_i^V = x_i n_{solv} + n_i^V$ (II.14)

A parte do soluto presente na fase vapor pode ser aproximada a um gás ideal, dessa forma:

$$n_i^V = y_i \frac{PV_g}{RT} \tag{II.15}$$

onde: V_g é o volume da fse gasosa na célula de medida.

Ao combinar as equações II.15 e II.3, substituindo na equação II.14 e isolando a variável n_i, tem-se como resultado a equação II.16.

$$x_i = \frac{n_i}{n_{solv}\left(1+\dfrac{\gamma_i^{\infty}\varphi_i^s P_i^s V_g}{n_{solv}RT}\right)} \tag{II.16}$$

Substituindo a equação II.16 na equação II.13, obtem-se a equação II.17 a seguir.

$$\frac{dn_i}{dt} = -\frac{n_i}{n_{solv}\left(1+\dfrac{\gamma_i^{\infty}\varphi_i^s P_i^s V_g}{n_{solv}RT}\right)}\gamma_i^{\infty}\varphi_i^s P_i^s \underbrace{\frac{1}{\left(1-\dfrac{\gamma_i^{\infty}\varphi_i^s P_i^s n_i}{P\,n_{solv}(1+\gamma_i^{\infty}\varphi_i^s P_i^s V_g\,/(n_{solv}RT))}\right)}}_{\text{Termo de correção}}\frac{F_{in}}{RT} \tag{II.17}$$

No decorrer das determinações da concentração de soluto na fase gasosa, ocorre a redução da concentração de soluto no fluxo de gás de saída da célula de medida, no entanto, nas condições utilizadas nos experimentos em relação à velocidade do gás de arraste, essa variação pode ser considerada insignificante. Dessa forma, o termo de correção da equação II.17 tende à unidade e não será considerado na integração desta equação.

A equação II.18 é obtida a partir da integração da equação II.17.

$$\ln\left(\frac{n_i}{n_0}\right) = -\frac{\gamma_i^{\infty}\varphi_i^s P_i^s}{n_{solv}\left(1+\frac{\gamma_i^{\infty}\varphi_i^s P_i^s V_g}{n_{solv}RT}\right)}\frac{F_{in}}{RT}t \tag{II.18}$$

Para evitar os efeitos de condensação no trecho que liga a saída da célula de medida do dilutor até a entrada de injeção do cromatógrafo, esta ligação é aquecida a uma temperatura 40 °C superior à temperatura utilizada na célula. No cromatógrafo é injetada uma quantidade de soluto proporcional à pressão parcial do soluto presente na solução e já que o detector se encontra na faixa linear de diluição (dispensando a necessidade de calibração), a área do pico do soluto é diretamente proporcional à concentração do soluto (de acordo com a equação II.19) e pode ser utilizada para os cálculos.

$$A_i = k\, y_i P \tag{II.19}$$

onde k é o fator de proporcionalidade.

Combinado as equações II.16, II.3 e II.19, obtem-se uma relação entre as áreas de pico do soluto, A_i, e o número de moles do soluto, n_i, de acordo com a equação II.20.

$$A_i = k\underbrace{\frac{n_i\gamma_i^{\infty}\varphi_i^s P_i^s}{n_{solv}\left(1+\frac{\gamma_i^{\infty}\varphi_i^s P_i^s V_g}{n_{solv}\,RT}\right)}}_{\text{Constante}} \tag{II.20}$$

No que o lado direito da equação II.20 só irá alterar quando houver mudança no número de moles do soluto. Substituindo equação II.20 na equação II.18, tem-se que:

$$\frac{\ln\left(A_i/A_0\right)}{t} = -\frac{\gamma_i^{\infty}\varphi_i^s P_i^s}{n_{solv}\left(1+\dfrac{\gamma_i^{\infty}\varphi_i^s P_i^s V_g}{n_{solv}RT}\right)}\frac{\dot{F}_{in}}{RT} = a \qquad \text{(II.21)}$$

A inclinação a apresentada na Figura II.4 pode ser determinada a partir da regressão linear do logarítmo da área do pico versus o tempo.

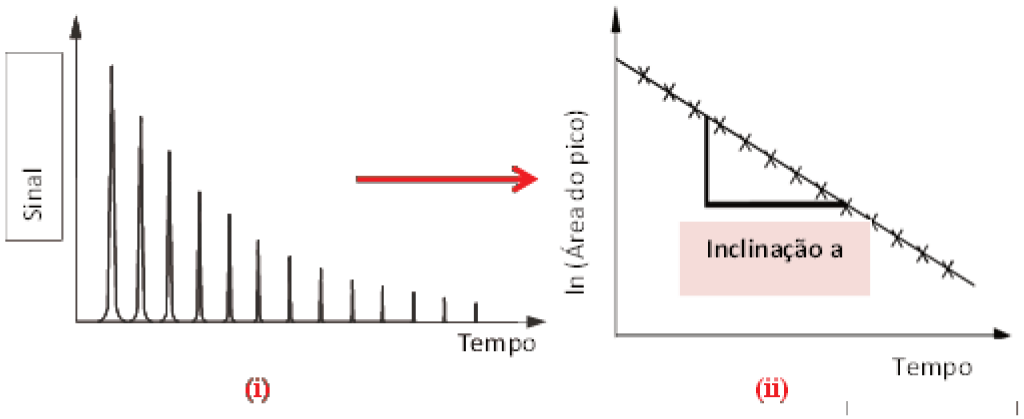

Figura II.4: (i) Gráfico de saída do cromatógrafo gasoso (CG) apresentando os picos do soluto; (ii) gráfico semilogarítmico dos dados obtidos da análise no CG (GRUBER, KRUMMEN e GMEHLING, 1999b; KRUMMEN, M., GRUBER, D. e GMEHLING, J., 2000).

Isolando a propriedade γ_i^{∞} da equação II.21, e substituindo a equação II.6, obtem-se a equação II.22 para o cálculo do coeficiente de atividade à diluição infinita do soluto i.

$$\gamma_i^{\infty} = -\frac{n_{solv}RT}{\varphi_i^s P_i^s\left(\dfrac{F_{He}\left(1+P_{solv}^s/P\right)}{a}+V_g\right)} \qquad \text{(II.22)}$$

Para o caso de mistura de solventes, a soma das pressões parciais dos componentes de mistura é utilizado no lugar da pressão de vapor do solvente na saturação, da mesma forma, é obtido o número de moles da mistura de solvente, através da soma do número de

moles de cada componente presente na mistura, conforme apresentado nas equações II.23 e II.24, respectivamente.

$$P_{solv}^{s} = \sum_{1}^{i} p_{solv(i)} \tag{II.23}$$

$$n_{solv} = \sum_{1}^{i} n_{solv(i)} \tag{II.24}$$

Dessa forma, para a determinação de γ_i^{∞} são necessárias quantidades experimentalmente mensuráveis como: a inclinação a, a pressão e a temperatura; e quantidades preditas como a pressão de vapor dos componentes na saturação e o coeficiente de fugacidade do soluto na saturação. Além disso, é necessário calcular o número de moles do solvente (a partir da massa adicionada na célula de medida e do peso molecular do solvente) e o volume da fase gasosa, V_g (calculado a partir do volume total da célula de medida, da massa e da densidade do solvente na temperatura de análise).

A vazão do gás de arraste é determinada a partir dos dados experimentais obtidos do medidor de fluxo eletrônico através da equação II.25.

$$F_{He} = F_{He}^{\exp} \frac{T}{T_{FM}} \frac{P_{FM}}{P_{cel}} \tag{II.25}$$

onde: F_{He}^{exp} é valor experimental obtido pelo medidor de fluxo eletrônico [$cm^3 \cdot min^{-1}$], T é a temperatura da célula de medida [K], T_{FM} temperatura do medidor de fluxo [K], P_{FM} pressão do medidor de fluxo [Pa] e P_{cel} pressão no interior da célula de medida [Pa].

Referências Bibliográficas

GRUBER, D.; KRUMMEN, M.; GMEHLING, J. The determination of activity coefficients at infinite dilution with the help of the dilutor technique (inert gas stripping). **Chem Eng Technol,** v. 22, n. 10, p. 827-831, 1999.

KRUMMEN, M.; GRUBER, D.; GMEHLING, J. Measurement of activity coefficients at infinite dilution in solvent mixtures using the dilutor technique. **Ind Eng Chem Res,** v. 39, p. 2114-2123, 2000.

LEBERT, A.; RICHON, D. Infinite Dilution Activity Coefficients of n -Alcohols as a Function of Dextrin Concentration in Water-Dextrin Systems. **J. Agric. Food Chem.,** v. 32, n. 5, p. 1156-1161, 1984.

LEROI, J.-C. et al. Accurate Measurement of Activity Coefficients at Infinite Dilution by Inert Gas Stripping and Gas Chromatography. **Ind. Eng. Chem. Proc. DD,** v. 16, n. 1, p. 139-144, 1977.

RICHON, D.; ANTOINE, P.; RENON, H. Infinite Dilution Activity Coefficients of Linear and Branched Alkanes from C, to C9 in n-Hexadecane by Inert Gas Stripping. **Ind. Eng. Chem. Proc. DD,** v. 19, n. 1, p. 144-147, 1980.

SORRENTINO, F.; VOILLEY, A.; RICHON, D. Activity Coefficients of Aroma Compounds in Model Food Systems. **AIChE J.,** v. 32, n. 12, p. 1988-1993, 1986.

Anexo III – Detalhamento da metodologia e equipamento do calorímetro de fluxo para medidas de entalpia de excesso

A entalpia molar de excesso (ou calor de mistura, H^E) foi medida usando um calorímetro de fluxo isotérmico da Hart Scientific (modelo 7501) comercialmente disponível. Detalhes do equipamento e do procedimento de medida foram previamente descritos por Gmehling (GMEHLING, 1993).

No calorímetro duas bombas seringa HPLC (ISCO, modelo LC-2600) fornecem à célula do calorímetro termostatizada um fluxo de composição e temperatura constantes. A célula é equipada com um aquecedor de pulso e um resfriador Peltier, conforme apresentado na Figura III.1.

Todo o conjunto apresentado na Figura III.1 se encontra em um cilindro de aço inoxidável imerso em um banho termostatizado, como apresentado na Figura III.2. A combinação do resfriador Peltier e do aquecedor de pulso permite não só a determinação dos efeitos endotérmicos, mas também dos efeitos exotérmicos da mistura.

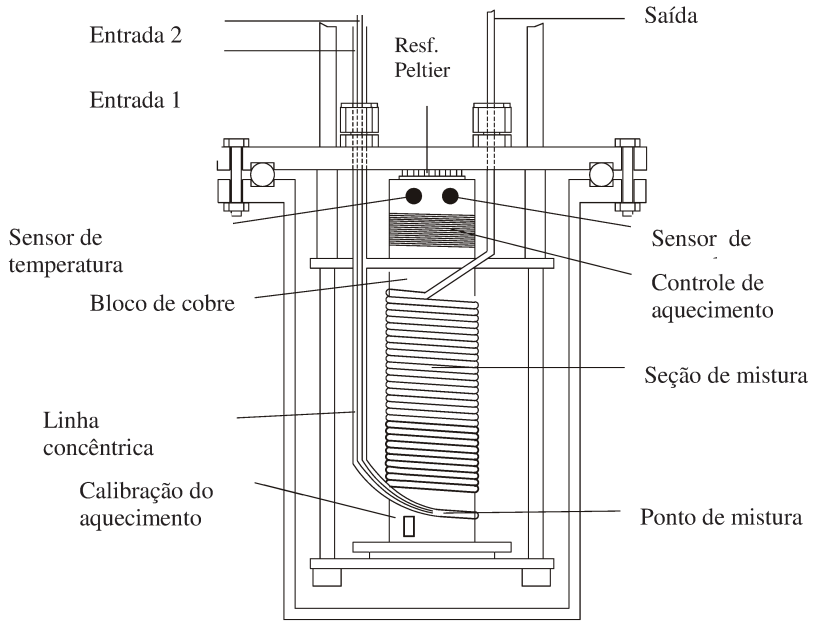

Figura III.1: Esquema da célula de medida do calorímetro (SCHMID, 2011).

O resfriador Peltier trabalha com uma potência constante, produzindo na célula do calorímetro uma perda constante de calor, a qual é compensada pelo aquecedor de pulsos. A frequência requerida dos pulsos é influenciada pelo efeito exotérmico ou endotérmico da mistura. Dessa forma, os calores de mistura podem ser determinados a partir da mudança de frenquência observada entre as linhas base e a medida no momento. Dependendo dos valores de H^E e da taxa de fluxo do sistema a ser medido, a potência por pulso pode variar de (0,05 a 20) μJ. A energia por pulso pode ser obtida por calibração usando a energia dissipada de um resistor preciso fixado no cilindro da célula de fluxo. Óleo de silicone é usado como líquido termostático, dessa forma o equipamento pode ser utilizado em uma

ampla faixa de temperatura (273 K a 453 K), a pressão permanece constante e em um valor de até 140 bar através do uso de um regulador de contrapressão, este mantém a pressão em um nível em que os efeitos de evaporação e de desgaseificação são evitados. As temperaturas das bombas de líquido e do banho termostático são monitoradas através de um termômetro de resistência PT100 Hart Scientific (modelo 1006 Micro-Therm).

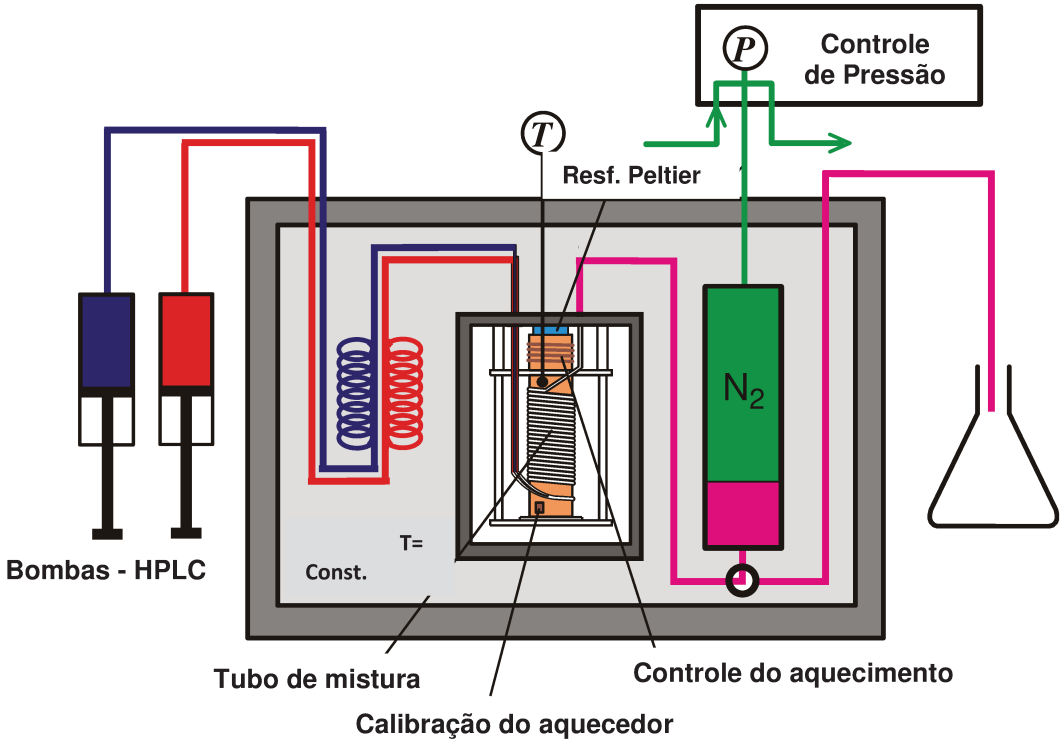

Figura III.2: Esquema do calorímetro de fluxo isotérmico (SCHMID, 2011).

O ajuste da frequência do aquecedor de pulso compensa o resfriamento provocado pelo resfriador Peltier que trabalha a uma potência constante, permitindo, dessa forma, a manutenção da temperatura da célula de fluxo. A frequência requerida dos pulsos é influenciada pelo efeito exotérmico ou endotérmico da mistura. Dessa forma, os calores de

mistura podem ser determinados a partir da mudança de frequência observada entre as linhas base e a medida no momento.

Após a obtenção de uma linha base estável (caracterizada pela frequência constante do aquecedor de pulso), a taxa de fluxo nos experimentos foi controlada por um computador. Durante a medida de uma determinada taxa de fluxo total, a frequência do aquecedor de pulsos foi gravada por aproximadamente 2000 s. Esse procedimento foi seguido para as diferentes taxas de fluxo individual dos compostos até que as bombas de líquido fossem esgotadas. As taxas de fluxo foram selecionadas de tal forma que abrangesse toda a faixa de fração molar. A partir das mudanças de frequência do aquecedor de pulso e das taxas de fluxo gravadas, a entalpia molar foi obtida da energia envolvida por pulso, da densidade dos componentes puros à temperatura da bomba de injeção (em torno de 298,15 K) e das massas molares dos componentes. As incertezas experimentais deste equipamento são as seguintes: $\sigma(T) = \pm$ 0,005 K; $\sigma(x_i) = \pm$ 0,0001; $\sigma(H^E) = \pm$ 1%.

Referência Bibliográfica

GMEHLING, J. Excess Enthalpies for 1, 1, 1 - Trichloroethane with Alkanes, Ketones, and Esters. **J. Chem. Eng. Data,** v. 38, n. 1, p. 143-146, 1993.

SCHMID, B. **Einsatz einer modernen Gruppenbeitragszustandsgleichung für die Synthese thermischer Trennprozesse**. 2011. 143 (Doktors der Naturwissenschaften). Institut für Reine und Angewandte Chemie, Carl von Ossietzky Universität Oldenburg, Oldenburg.

Anexo IV – Detalhamento da metodologia e equipamento utilizado na determinação de dados isotérmios de equilíbrio líquido-vapor

Os dados isotérmicos de ELV, P - x, foram medidos em um equipamento operado automaticamente por computador nas temperaturas de 348,15 K e 373,15 K. O princípio do método (GIBBS, R. E. e VAN NESS, H. C. , 1972), a descrição do equipamento (RAREY e GMEHLING, 1993), e o procedimento de determinação estão apresentado em vários artigos anteriormente publicados (RAREY e GMEHLING, 1993; RAREY, HORSTMANN e GMEHLING, 1999a; NEBIG, BÖLTS e GMEHLING, 2007b). A célula de equilíbrio fabricada em aço inóxidável (Figura IV.1) se encontra imersa em um banho de óleo, que se encontra sobre cuidadosa e constante agitação e termostatização de alta precisão, conforme esquematizado na Figura IV.2. A temperatura da célula é medida usando um termômetro de resistência Pt100 (Modelo 1506, Hart Scientific) com resolução de ± 1 mK. Um sensor de pressão digital Digiquartz (Modelo 245 A, Paroscientific) está conectado à célula de equilíbrio. A pressão do interior da célula é monitorada com a precisão de ± 0,005 % sobre fundo de escala.

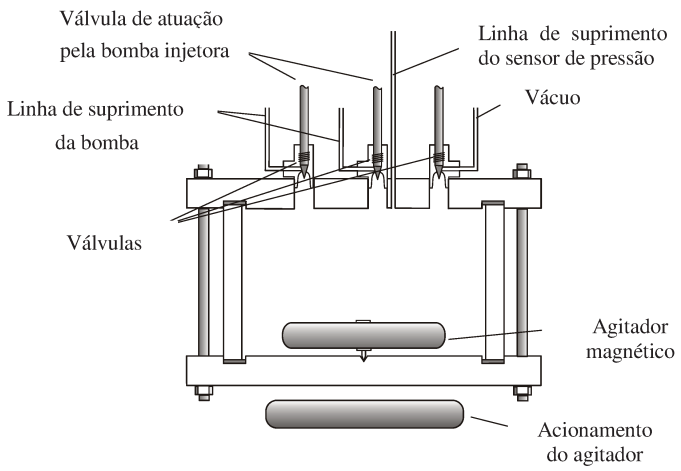

Figura IV.1: Corte longitudinal da célula de equilíbrio (RAREY e GMEHLING, 1993)

A análise inicia com a evacuação da célula de equilíbrio e com o carregamento dos líquidos desgaseificados nas bombas, onde os mesmos são armazenados à sobrepressão (1 MPa) para evitar a contaminação com ar. Após as bombas alcançarem o equilíbrio térmico, ocorre a introdução de uma quantidade desejada de líquido 1 purificado, desgaseificado e termostatizado na célula de equilíbrio (previamente evacuada) via válvulas automáticas com o auxílio de uma bomba pistão injetora de alta precisão ($\pm\ 1\,.\,10^{-6}\ \mathrm{dm}^3$) (*stepping motor driven piston injectors*). Após alcançar o equilíbrio de fases (evidenciado pela temperatura e pressão constantes durante pelo menos 15 minutos) é realizada a leitura da pressão que corresponde à pressão de vapor do componente 1. Então, uma quantidade pequena e previamente determinada do líquido 2, também purificado, desgaseificado e termostatizado é introduzida na célula de equilíbrio. A mistura é submetida à constante agitação, e, novamente, após a obtenção do equilíbrio de fases, é feita a leitura da nova

pressão de equilíbrio. Posteriormente, várias quantidades do segundo componente são injetadas na célula e após o estabelecimento do equilíbrio de fases, a pressão é lida. Na sequência, esse procedimento é repetido iniciando-se as medidas com o líquido 2 puro, obtendo-se a sua pressão de vapor e as pressões de equilíbrio na região do diagrama rico em componente 2.

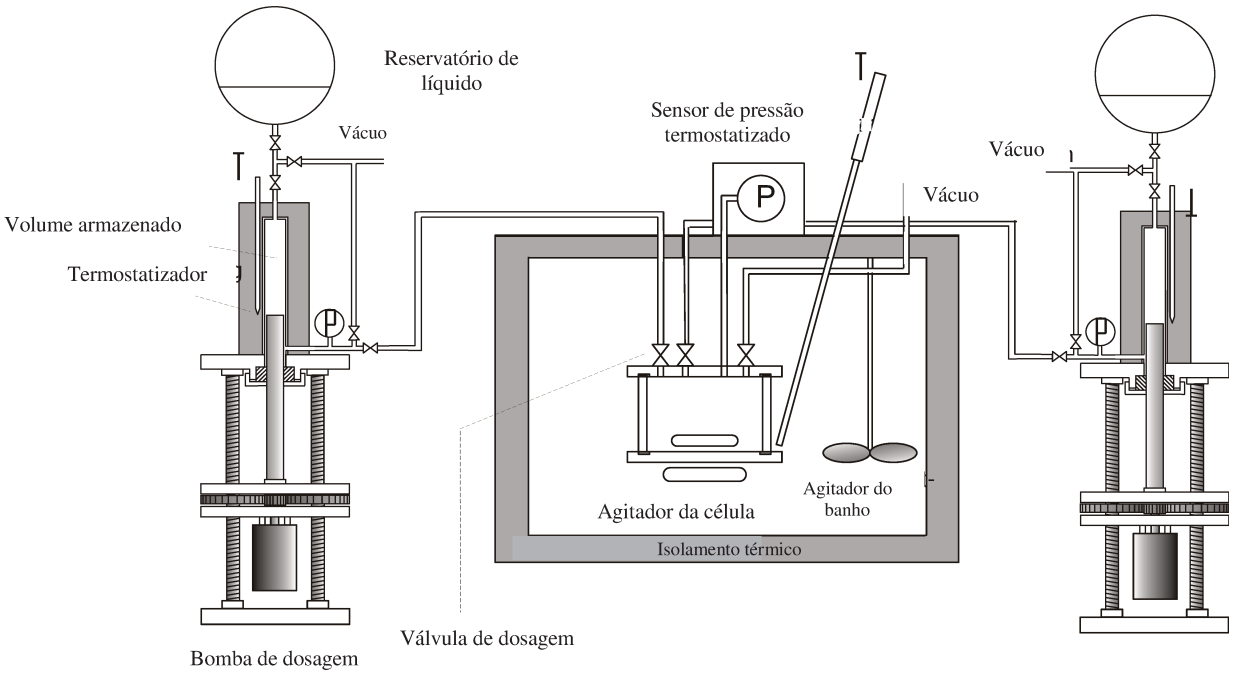

Figura IV.2: Esquema do equipamento utilizado nos experimentos (RAREY e GMEHLING, 1993)

A composição da fase líquida é obtida através da resolução dos balanços de massa e volume, considerando que a mistura se encontra no equilíbrio líquido-vapor. Neste trabalho foram estudados sistemas de baixa pressão, portanto, a composição da fase líquida foi considerada idêntica à composição da alimentação com precisão de ± 0,002 em fração

molar. As incertezas experimentais deste equipamento são as seguintes: $\sigma(T)$= 0,03 K, $\sigma(P)$= 20 Pa + 0,0001 (P/Pa), $\sigma(x_i)$=0,0001.

Fundamentação Teórica

Como apresentado por RAAL e MÜHLBAUER (1998), junto ao método estático outros métodos podem ser utilizados na determinação de dados de ELV a baixas pressões (pressões até 5 bar, de acordo com ABBOTT (1986)), entre eles: o método dinâmico (ou de recirculação ou de fluxo); as técnicas semimicro; as medidas de coeficiente de atividade a diluição infinita ; e os métodos de ponto bolha ou ponto de orvalho.

De acordo com HÁLA et al. (1958), o método estático, por algum tempo, não foi indicado para determinações de ELV a baixas e médias pressões já que a remoção da fase gasosa para análise de composição, mesmo de pequenas alíquotas, poderia afetar o equilíbrio do sistema. Essa restrição foi definitivamente superada quando GIBBS, R. E. e VAN NESS, H. C. (1972) desenvolveram um novo equipamento de determinação de ELV pelo método estático sugerindo o cálculo da composição das fases (líquida e vapor) a partir da composição total precisamente conhecida da célula, dispensando assim a análise da composição das mesmas. O cálculo da fração molar da mistura dosada na célula de equilíbrio requer o conhecimento dos dados de peso molecular e da densidade dos líquidos na temperatura de injeção dos mesmos. No equipamento utilizado neste trabalho, os líquidos injetados são termostatizados na bomba de dosagem por meio de circulação de água proveniente de um banho térmico.

As possíveis fontes de erro deste método foram relacionadas e discutidas por Hála et al. (1958), Gibbs e van Ness (1972) e Rarey e Gmehling (1993), indiscutivelmente, a

principal fonte de erro é a incompleta desgaseificação dos líquidos que provocaria medidas errôneas de pressão.

Seguindo o princípio proposto por Gibbs e van Ness (1972), a configuração típica do procedimento experimental do método estático de determinação de dados de ELV foi descrita por Rarey e Gmehling (1972) da seguinte forma: os volumes precisamente determinados dos componentes cuidadosamente desgaseificados são injetados em uma célula de equilíbrio termostatizada e de volume conhecido, para acelerar a obtenção do equilíbrio termodinâmico, promove-se a agitação da mistura. Após 15 a 60 minutos, dependendo do sistema, uma constante pressão é observada, então a composição é alterada pela injeção de uma quantidade conhecida de um dos componentes. Dessa forma, obtem-se dados de equilíbrio com conhecida temperatura, pressão e composição total. As composições da fase vapor e da fase líquida podem ser calculadas utilizando-se um modelo de g^E flexível ou uma equação de estado. Neste trabalho a energia livre de Gibbs de excesso, g^E, foi descrita por um polinômio de Legendre e as frações molares foram obtidas através de um cálculo iterativo.

As vantagens da determinação de dados de ELV neste equipamento são: a precisão dos dados obtidos (comprovada pelas publicações anteriores), a flexibilidade em relação à temperatura (até 388 K) e pressão (até 355 kPa), consumo relativamente pequeno de substâncias durante a análise (a célula de equilíbrio possui 40 mm de altura e 50 mm de diâmetro interno), o fato de possibilitar o estudo de sistemas especiais como com componentes com grande diferença de volatilidade ou que exibem estabilidade térmica

limitada e a automação do equipamento que simplifica e acelera a obtenção dos dados de equilíbrio.

Referências Bibliográficas

ABBOTT, M. M. LOW-PRESSURE PHASE EOUILIBRIA: MEASUREMENT OF VLE. **Fluid Phase Equilib,** v. 29, p. 193-207, 1986.

GIBBS, R. E.; VAN NESS, H. C. Vapor-Liquid Equilibria from Total-Pressure Measurements. A New Apparatus. **Ind. Eng. Chem. Fundam.,** v. 11, p. 410-413, 1972.

HÁLA, E. et al. **Vapour-Liquid Equilibrium**. New York: Pergamon Press, 1958. 402.

NEBIG, S.; BÖLTS, R.; GMEHLING, J. Measurement of vapor-liquid equilibria (VLE) and excess enthalpies (H^E) of binary systems with 1-alkyl-3-methylimidazolium bis(trifluoromethylsufonyl)imide and prediction of these properties and γ^{∞} using modified UNIFAC (Dortmund). **Fluid Phase Equilib,** v. 258, p. 168-178, 2007.

RAAL, J. D.; MÜHLBAUER, A. L. **Phase equilibria: measurement and computation**. Washington: Taylor & Francis, 1998. 461.

RAREY, J.; GMEHLING, J. Computer-operated Differential Static Apparatus for the Measurement of Vapor-Liquid Equilibrium Data. **Fluid Phase Equilibr.,** v. 83, p. 279-287, 1993.

RAREY, J.; HORSTMANN, S.; GMEHLING, J. Vapor-liquid equilibria and vapor pressure data for systems ethyl *tert*-butyl ether + ethanol and ethyl *tert*-butyl ether + water. **J Chem Eng Data,** v. 44, p. 532-538, 1999.

Anexo V – Detalhamento da metodologia e equipamento utilizado na determinação de dados isobáricos de equilíbrio líquido-vapor

Os dados isobáricos de equilíbrio líquido-vapor (ELV) dos sistemas óleo de algodão + n-hexano a 41,3 kPa, óleo de soja + etanol a 80 kPa e 101,3 kPa e óleo de coco + etanol a 80 kPa e 101,3 kPa foram medidos em um ebuliômetro de Othmer modificado por Oliveira (2003), similar ao utilizado por COELHO et al. (2011) e OLIVEIRA et al. (2003); (OLIVEIRA, NETO e CHIAVONI-FILHO, 2005). O equipamento apresentado na Figura V.1 é construído inteiramente em vidro e possui recirculação apenas da fase vapor. O componente puro ou a mistura dos dois componentes (cerca de 100 mL) é adicionado no balão refervedor do equipamento (1). As temperaturas das fases líquida e vapor são medidas com auxílio de termômetros digitais PT100 (±0,1 K) (2). A redução de pressão é realizada com o auxílio de uma bomba de vácuo (13). A pressão do equipamento é controlada e mantida constante (±0,07 kPa) com o auxílio do sensor de pressão (9), do tanque pulmão (11) e de uma válvula solenóide (12). O aquecimento é realizado por uma resistência em forma de fita (3) que envolve o balão refervedor e a taxa de aquecimento é controlada por meio de um regulador de voltagem (4). A mistura é submetida ao aquecimento até alcançar temperatura suficiente para promover a recirculação da fase vapor à taxa constante, que é observada na taxa de condensado reciclada em cerca de 40 a 60 gotas por minuto. A agitação é realizada através de agitadores magnéticos (5), e é mantida constante, garantindo a homogeneização das fases líquida e vapor condensada, bem como auxiliando a recirculação da fase vapor. Outra observação visual evidenciando a saturação, ou o equilíbrio, é o retorno e a presença de gotas condensado no próprio tubo da célula.

Quando o sistema alcança o regime permanente, detectado pela constância da temperatura e do fluxo de condensado por pelo menos 30 minutos, pode ser considerado que o equilíbrio termodinâmico foi atingido. Nestas condições registra-se a temperatura e pressão de equilíbrio, abre-se o sistema para a atmosfera, e realiza-se a coleta de amostras das fases líquidas e vapor condensada (aproximadamente 6 mL de cada) com auxílio de seringas de vidro que são encaminhadas para análise de composição.

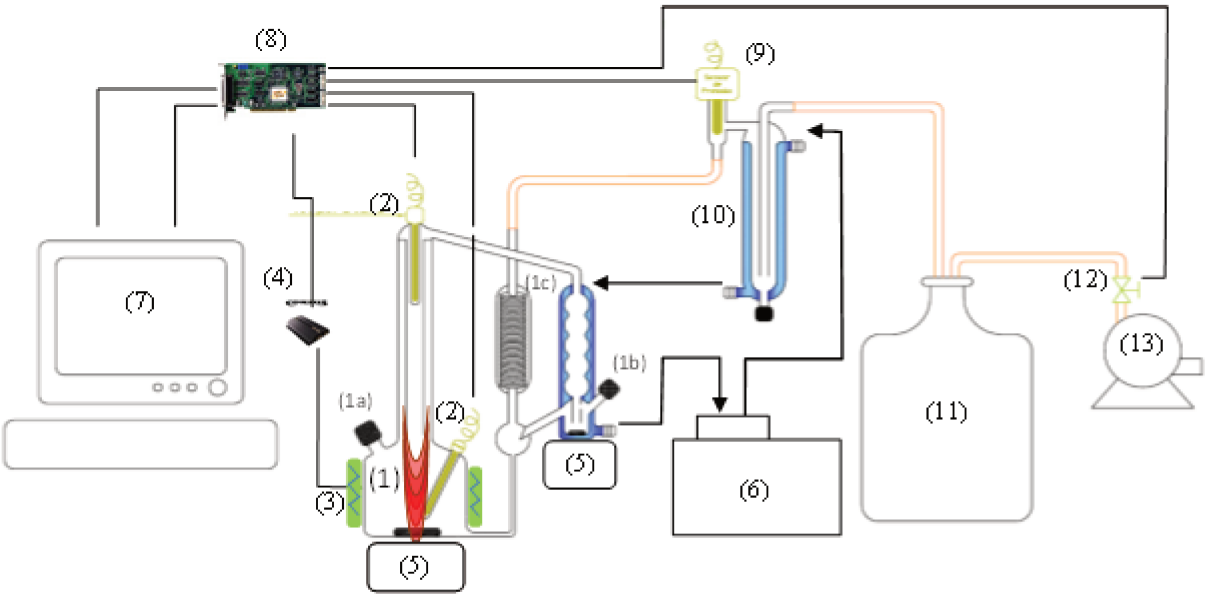

Figura V.1: Esquema do Ebuliômetro de Othmer Modificado (OLIVEIRA, 2003).

(1) Célula de equilíbrio; (1a) bocal para o carregamento e retirada de amostra da fase líquida (1b) bocal para retirada de amostrada fase vapor condensada (1c) condensadores (2) Sensores de temperatura (PT 100); (3) Fita de aquecimento (FISATOM, mod. 5 1600 W); (4) Módulo de potência (regulador de voltagem, taxa de aquecimento contralada pelo computador); (5) Agitadores magnéticos (FISATOM, mod. 752A); (6) Banho termostático circulando água refrigerada a ± 277,15 K; (7) Módulo supervisório instalado em um computador; (8) Placa de aquisição de dados; (9) Sensor de Pressão; (10) Trap; (11) Tanque pulmão, ou buffer (20 L); (12) Válvula solenóide; (13) Bomba de vácuo.

As composições das fases líquida e vapor condensada foram determinadas através de densimetria a 298,15 K ± 0,01 K. Os valores de composição foram determinados com auxílio das curvas de calibração de densidade de misturas com composição conhecida, através de interpolação inversa. As amostras do sistema óleo de algodão + n-hexano foram encaminhadas diretamente ao densimetro. Devido à restrita solubilidade do etanol em óleo, as amostras dos sistemas óleo de soja + etanol e óleo de coco + etanol foram previamente diluídas em quantidade conhecida de n-heptano formando uma mistura homogênea, evitando a sua separação em duas fases na temperatura da análise. A densidade das amostras de cada fase foi determinada em triplicata com o auxílio de um densímetro digital Anton Paar (mod. 4500) com precisão de $\pm$ 5 x 10^{-5} g. cm^{-3}. Para todas as determinações, realizou-se previamente a verificação da limpeza e da calibração do densímetro com ar e água deionizada, respectivamente. A precisão da repetibilidade das densidades dos compostos puros e da temperatura foi de $\pm$ 1 x 10^{-5} g. cm^{-3} e ± 0,01 K, respectivamente.

A composição de óleo vegetal e solvente de cada fase foi determinada através de curva de calibração previamente preparada na temperatura de 298,15 K. As curvas de calibração foram elaboradas através de misturas de composição conhecida de óleo vegetal e solvente (entre frações mássicas de óleo 0,0 a 1,0), no caso das misturas de óleo de soja com etanol, a curva foi realizada acrescentado frações mássicas conhecidas de n-heptano (0,47 a 0,53). Tais misturas foram preparadas gravimetricamente para cada sistema binário (óleo de algodão + n-hexano) e ternário (óleo de soja + etanol + n-heptano e óleo de coco + etanol + n-heptano) utilizando balança analítica Sartorius com precisão de ± 0,00001 g. As composições cobriram toda a faixa de concentração estudada. Os dados obtidos foram

ajustados com um polinônio de terceira ordem. As funções: densidade – composição de óleo e densidade – fração mássica de n-heptano foram ajustadas para determinar as composições desconhecidas de amostras líquidas do ebuliômetro. Estima-se que, com este procedimento, a precisão nas composições seja melhor que 0,0005 em fração molar.

Referências Bibliográficas

COELHO, R. et al. (Vapor + liquid) equilibrium for the binary systems {water + glycerol} and {ethanol + glycerol, ethyl stearate, and ethyl palmitate} at low pressures. **J. Chem. Thermodyn.,** v. 43, p. 1870-1876, 2011.

OLIVEIRA, H. N. M. **Determinação de dados de Equilíbrio Líquido-Vapor para Sistemas Hidrocarbonetos e Desenvolvimento de uma nova Célula Dinâmica**. 2003. 183 Tese (Doctor). Departamento de Engenharia Química, Universidade Federal de Natal, Natal-RN.

OLIVEIRA, H. N. M. et al. **Projeto de Ebuliômetros de Circulação da Fase Vapor e testes com Misturas de Dodecano + Tween 20 e Curva de Destilação de Gasolina**. 2° congresso Brasileiro de Pesquisa e Desenvolvimento em Petróleo e Gás. PETRÓLEO, I.-I. B. D. Rio de Janeiro-RJ, Brazil: IBP - Instituto Brasileiro de Petróleo 2003.

OLIVEIRA, H. N. M.; NETO, A. A. E.; CHIAVONI-FILHO, O. **Densidade e Curva de Destilação de Gasolina com Ebuliômetro de Circulação da Fase vapor**. 3° Congresso Brasileiro de Petróleo e Gás. PETRÓLEO, I.-I. B. D. Salvador-BA, Brazil: IBP - Instituto Brasileiro de Petróleo 2005.

Anexo VI – Dados de equilíbrio líquido-vapor do sistema ácido cáprico + etanol (não publicados)

From: Computer driven static apparatus: VLE (P, x)

Table VI.1 Experimental VLE data for the system Capric Acid + Ethanol at 313.15 K

P (kPa)	$x_{Ethanol}$
0.08	0.0000
2.23	0.0070
4.88	0.0163
6.71	0.0231
10.61	0.0382
13.69	0.0517
18.27	0.0727
22.86	0.0962
27.9	0.1246
33.27	0.1599
40.53	0.2099
49.09	0.2770
58.18	0.3553
67.14	0.4361
76.11	0.5182
84.96	0.5975
93.47	0.6698
101.32	0.7350
108.33	0.7910

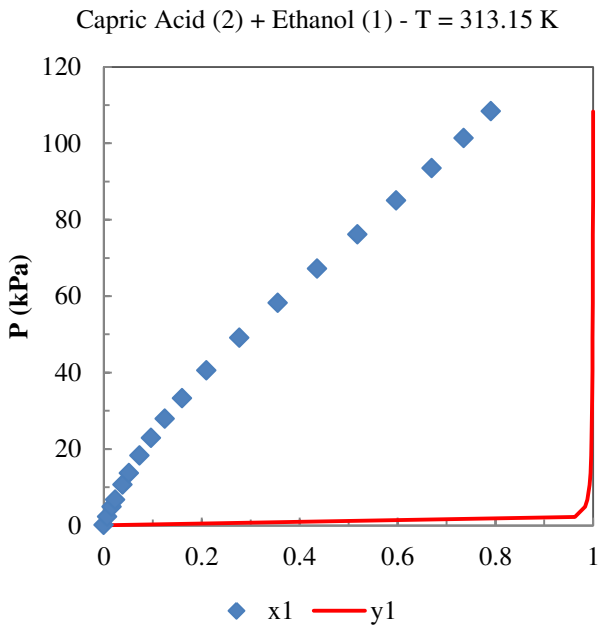

Figure VI.1: VLE data for the system Capric Acid + Ethanol at 313.15 K

Table VI.2. Calculated activity coefficient, Υ, from VLE data for the system Capric Acid + Ethanol at 313.15 K

$x_{Ethanol}$	$\Upsilon_{Ethanol}$	$\Upsilon_{Capric\ Acid}$
0.000E+00	2.297	1.000
7.910E-03	2.243	1.000
1.580E-02	2.191	1.000
2.370E-02	2.143	1.001
3.160E-02	2.096	1.002
3.960E-02	2.051	1.002
4.750E-02	2.009	1.003
5.540E-02	1.968	1.004
6.330E-02	1.930	1.006
7.120E-02	1.893	1.007
7.910E-02	1.857	1.009

8.700E-02	1.823	1.010
9.490E-02	1.791	1.012
0.1028	1.760	1.014
0.1107	1.730	1.016
0.1187	1.702	1.018
0.1266	1.675	1.021
0.1345	1.649	1.023
0.1424	1.624	1.025
0.1503	1.600	1.028
0.1582	1.577	1.031
0.1661	1.555	1.034
0.1740	1.534	1.036
0.1819	1.514	1.039
0.1898	1.494	1.043
0.1978	1.476	1.046
0.2057	1.458	1.049
0.2136	1.441	1.052
0.2215	1.424	1.056
0.2294	1.408	1.059
0.2373	1.393	1.063
0.2452	1.379	1.066
0.2531	1.364	1.070
0.2610	1.351	1.073
0.2689	1.338	1.077
0.2769	1.326	1.081
0.2848	1.314	1.085
0.2927	1.302	1.089
0.3006	1.291	1.093
0.3085	1.280	1.097

0.3164	1.270	1.101
0.3243	1.260	1.105
0.3322	1.251	1.109
0.3401	1.241	1.113
0.3480	1.233	1.117
0.3560	1.224	1.121
0.3639	1.216	1.126
0.3718	1.208	1.130
0.3797	1.200	1.134
0.3876	1.193	1.138
0.3955	1.186	1.143
0.4034	1.179	1.147
0.4113	1.173	1.152
0.4192	1.166	1.156
0.4271	1.160	1.160
0.4351	1.154	1.165
0.4430	1.149	1.169
0.4509	1.143	1.174
0.4588	1.138	1.178
0.4667	1.133	1.183
0.4746	1.128	1.187
0.4825	1.123	1.192
0.4904	1.119	1.197
0.4983	1.114	1.201
0.5063	1.110	1.206
0.5142	1.106	1.211
0.5221	1.102	1.215
0.5300	1.098	1.220
0.5379	1.094	1.225

0.5458	1.091	1.230
0.5537	1.087	1.234
0.5616	1.084	1.239
0.5695	1.081	1.244
0.5774	1.078	1.249
0.5854	1.075	1.254
0.5933	1.072	1.259
0.6012	1.069	1.264
0.6091	1.066	1.269
0.6170	1.063	1.274
0.6249	1.061	1.279
0.6328	1.058	1.284
0.6407	1.056	1.290
0.6486	1.053	1.295
0.6565	1.051	1.300
0.6645	1.049	1.306
0.6724	1.047	1.311
0.6803	1.044	1.317
0.6882	1.042	1.322
0.6961	1.040	1.328
0.7040	1.038	1.334
0.7119	1.036	1.340
0.7198	1.035	1.346
0.7277	1.033	1.352
0.7356	1.031	1.358
0.7436	1.029	1.365
0.7515	1.028	1.371
0.7594	1.026	1.378
0.7673	1.025	1.385

0.7752	1.023	1.391
0.7831	1.022	1.398
0.7910	1.020	1.406

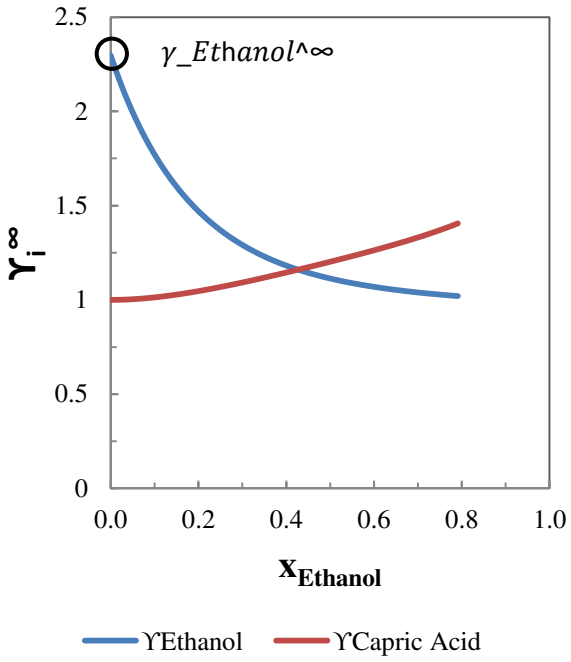

Figure VI.2. Activity coefficient, γ, for the system Capric Acid + Ethanol at 313.15 K

Table VI.3. Comparing activity coefficient at infinite dilution obtained by several method.

Method	T (K)	γ^{∞}Ethanol-CapricAcid
GLC	313.24	2.115
Dilutor	313.13	2.196
VLE	313.15	2.297

Anexo VII – Dados de equilíbrio líquido-vapor do sistema óleo de soja + etanol e óleo de coco + etanol (não publicados)

From: modified Othmer-type ebulliometer: VLE ($PTxy$) and UNIQUAC model

Table VII.1. VLE data for the system Soybean oil + Ethanol at 600 mmHg (80 kPa)

$x_{1\,exp}$	T_{exp}/K	y_{1exp}	P_{exp}/ mmHg	$x_{1\,calc}$	T_{calc}/K	y_{1calc}	P_{calc}/ mmHg
0.00000	345.65	0.00000	600.78	0.00000	346.04	0.00000	600.38
0.00288	345.91	0.00000	601.47	0.00287	346.14	0.00000	601.23
0.00399	345.91	0.00000	601.36	0.00398	346.17	0.00000	601.10
0.00991	345.97	0.00000	600.86	0.00990	346.30	0.00000	600.53
0.02356	346.04	0.00000	601.23	0.02354	346.71	0.00000	600.56
0.01655	346.13	0.00000	600.47	0.01654	346.48	0.00000	600.12
0.00390	346.17	0.00000	601.48	0.00390	346.18	0.00000	601.47
0.01633	346.20	0.00000	601.76	0.01632	346.52	0.00000	601.44
0.02326	346.18	0.00000	601.13	0.02324	346.70	0.00000	600.60
0.03913	346.28	0.00000	600.89	0.03910	347.21	0.00000	599.95
0.04563	346.33	0.00000	601.19	0.04559	347.46	0.00000	600.05
0.03832	346.36	0.00000	601.70	0.03829	347.22	0.00000	600.83
0.03115	346.37	0.00000	601.76	0.03113	346.98	0.00000	601.14
0.04579	346.38	0.00000	601.43	0.04575	347.47	0.00000	600.32
0.03066	346.40	0.00000	601.91	0.03064	346.97	0.00000	601.33
0.06276	346.48	0.00000	599.76	0.06270	348.05	0.00000	598.16
0.05883	346.49	0.00000	599.61	0.05877	347.89	0.00000	598.18
0.07474	346.49	0.00000	599.05	0.07465	348.51	0.00000	596.98
0.07584	346.55	0.00000	599.97	0.07575	348.59	0.00000	597.88
0.05392	346.62	0.00000	600.51	0.05388	347.75	0.00000	599.36

0.06221	346.84	0.00000	599.26	0.06216	348.03	0.00000	598.05
0.13216	346.95	0.00000	599.73	0.13195	351.14	0.00000	595.34
0.18666	347.81	0.00000	601.10	0.18632	353.99	0.00000	594.48
0.22293	349.02	0.00000	600.56	0.22252	355.99	0.00000	592.97
0.27609	351.66	0.00004	601.32	0.27562	359.19	0.00000	592.93
0.39455	362.56	0.00039	600.65	0.39421	367.24	0.00000	595.17
0.47072	367.72	0.00044	601.04	0.47029	373.01	0.00000	594.59
0.50192	372.99	0.00039	601.24	0.50168	375.77	0.00000	597.81
0.51463	373.67	0.00039	600.43	0.51436	376.80	0.00000	596.53
0.57756	379.97	0.00031	600.62	0.57729	382.66	0.00000	597.14
0.65134	396.09	0.00018	598.45	0.65193	391.17	0.00000	605.08
0.66829	401.73	0.00036	600.68	0.66931	393.66	0.00000	611.61

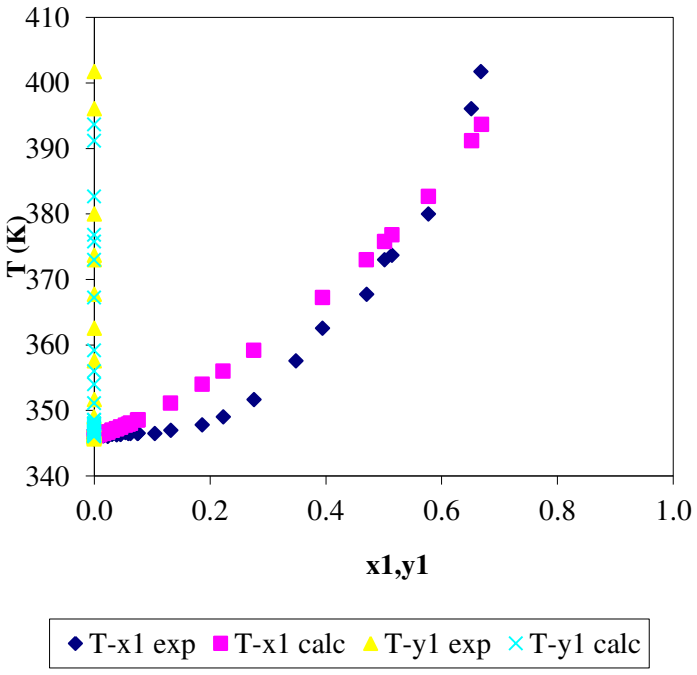

Figure VII.1. VLE data for the system Soybean oil + Ethanol at 80 kPa

From: modified Othmer-type ebulliometer: VLE ($PTxy$) and UNIQUAC model

Table VII.2. VLE data fort he system Coconut oil + Ethanol at 600 mmHg (80 kPa)

$x_{1\,exp}$	T_{exp}/K	y_{1exp}	P_{exp}/ mmHg	$x_{1\,calc}$	T_{calc}/K	y_{1calc}	P_{calc}/ mmHg
0.00000	345.85	0.00000	600.90	0.00000	346.05	0.00000	600.69
0.00000	345.65	0.00000	600.80	0.00000	346.04	0.00000	600.40
0.00774	345.75	0.00000	600.60	0.00774	346.12	0.00000	600.23
0.00812	345.85	0.00027	601.80	0.00812	346.17	0.00000	601.48
0.02090	345.95	0.00025	601.10	0.02090	346.05	0.00000	601.00
0.02285	345.95	0.00023	601.30	0.02285	346.03	0.00000	601.22
0.03876	346.15	0.00006	600.70	0.03876	345.81	0.00000	601.06
0.04264	346.25	0.00008	600.80	0.04263	345.77	0.00000	601.30
0.06377	346.25	0.00049	600.80	0.06377	345.62	0.00000	601.45
0.07202	346.05	0.00024	600.90	0.07202	345.61	0.00000	601.36
0.09168	346.15	0.00035	601.70	0.09168	345.75	0.00000	602.13
0.10351	346.55	0.00035	601.70	0.10352	345.90	0.00000	602.38
0.11455	346.65	0.00040	601.70	0.11456	346.08	0.00000	602.31
0.14848	346.85	0.00032	601.60	0.14848	346.83	0.00000	601.66
0.17838	347.26	0.00039	601.70	0.17836	347.74	0.00000	601.25
0.18623	347.36	0.00049	602.20	0.18621	348.02	0.00000	601.56
0.21948	348.26	0.00049	601.80	0.21944	349.27	0.00000	600.80
0.24305	348.56	0.00081	601.50	0.24298	350.23	0.00000	599.81
0.30325	351.57	0.00017	600.00	0.30683	353.21	0.00000	597.68
0.30694	351.17	0.00075	599.80	0.35045	355.57	0.00000	597.91
0.35063	352.47	0.00076	601.20	0.50635	365.73	0.00001	599.49
0.39367	356.18	0.00024	600.00	0.47697	363.49	0.00001	596.95
0.41586	357.99	0.00124	601.60	0.41576	359.55	0.00001	599.94

0.47724	359.69	0.00181	601.20	0.53610	368.00	0.00001	599.24
0.50647	364.10	0.00081	601.30	0.69559	384.13	0.00003	613.62
0.53621	366.61	0.00127	600.80	0.30317	353.06	0.00000	598.47
0.61783	379.05	0.00012	600.00	0.39355	358.09	0.00001	597.97
0.69434	393.99	0.00120	601.10	0.61820	375.37	0.00002	604.51

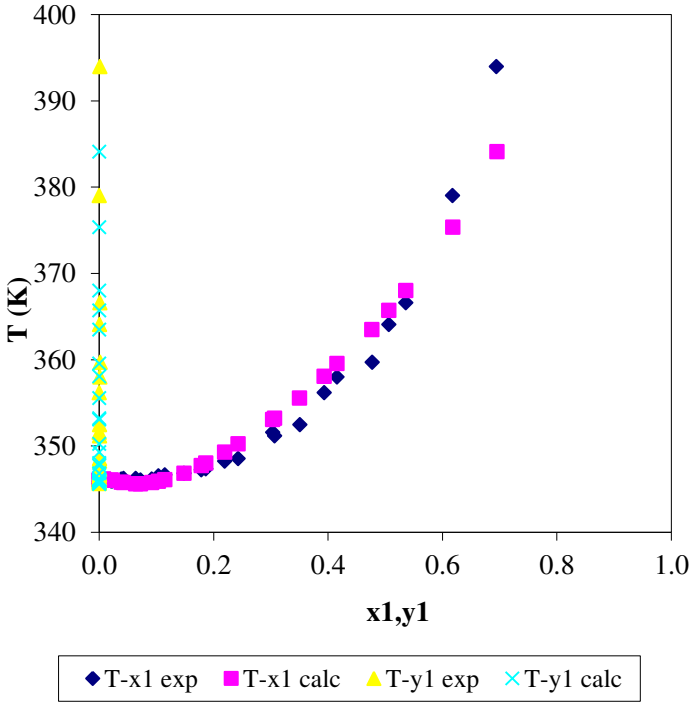

Figure VII.2. VLE data fort he system Coconut oil + Ethanol at 80 kPa.

From: modified Othmer-type ebulliometer: VLE ($PTxy$) and UNIQUAC model

Table VII.3. VLE data fort he system Coconut oil + Ethanol at 760 mmHg (101.3 kPa)

$x_{1\,exp}$	T_{exp}/K	y_{1exp}	P_{exp}/ mmHg	$x_{1\,calc}$	T_{calc}/K	y_{1calc}	P_{calc}/ mmHg
0.00000	351.65	0.00000	753.30	0.00000	351.61	0.00000	753.34
0.00000	351.65	0.00000	754.40	0.00000	351.65	0.00000	754.40
0.00639	351.85	0.00000	754.70	0.00639	351.80	0.00000	754.76
0.00674	351.85	0.00000	754.90	0.00674	351.81	0.00000	754.94
0.01574	352.15	0.00000	757.30	0.01574	352.03	0.00000	757.43
0.01700	352.25	0.00000	757.00	0.01700	352.04	0.00000	757.24
0.02940	352.25	0.00000	757.10	0.02940	352.15	0.00000	757.21
0.03089	352.35	0.00000	756.40	0.03156	352.13	0.00000	756.04
0.03156	352.25	0.00000	755.90	0.03089	352.14	0.00000	756.63
0.03434	352.45	0.00000	756.20	0.04231	352.16	0.00000	755.51
0.04231	352.35	0.00064	755.30	0.04491	352.15	0.00000	754.83
0.04491	352.35	0.00047	754.60	0.06479	352.20	0.00000	754.47
0.05390	352.55	0.00000	755.30	0.03434	352.16	0.00000	756.53
0.05950	352.45	0.00025	754.20	0.06289	352.24	0.00000	755.74
0.06289	352.45	0.00000	755.50	0.05950	352.18	0.00000	754.50
0.06479	352.35	0.00034	754.30	0.05390	352.21	0.00000	755.69
0.09169	352.75	0.00035	756.90	0.09979	352.45	0.00000	757.33
0.09979	352.65	0.00038	757.10	0.09169	352.40	0.00000	757.29
0.13428	353.05	0.00084	756.90	0.13429	352.75	0.00000	757.24
0.15601	353.35	0.00082	756.70	0.15602	353.03	0.00000	757.06
0.16910	353.45	0.00034	755.80	0.16911	353.20	0.00000	756.07
0.18445	353.95	0.00033	755.80	0.18622	353.53	0.00000	756.44
0.18621	353.75	0.00081	756.20	0.18447	353.49	0.00000	756.32

0.20897	355.15	0.00086	755.70	0.21409	354.11	0.00000	755.42
0.21409	354.05	0.00077	755.50	0.27141	355.68	0.00000	754.01
0.26621	355.55	0.00094	756.60	0.20902	354.04	0.00000	756.98
0.27146	354.75	0.00069	755.10	0.26621	355.60	0.00000	756.53
0.30334	356.05	0.00063	756.70	0.30329	356.84	0.00000	755.76
0.35528	358.15	0.00087	756.70	0.35522	358.93	0.00000	755.76
0.38968	359.55	0.00081	756.80	0.43653	362.85	0.00001	753.24
0.43669	361.15	0.00047	755.30	0.38960	360.51	0.00001	755.64
0.50736	365.45	0.00061	755.60	0.50718	367.13	0.00001	753.50
0.55389	369.15	0.00056	754.70	0.55374	370.40	0.00001	753.09
0.60768	373.95	0.00039	756.10	0.60755	374.85	0.00002	754.90
0.63788	379.55	0.00040	755.50	0.63816	377.80	0.00002	757.82
0.64552	380.25	0.00025	756.40	0.64580	378.58	0.00002	758.62
0.74680	392.95	0.00038	754.70	0.74732	390.79	0.00004	757.80

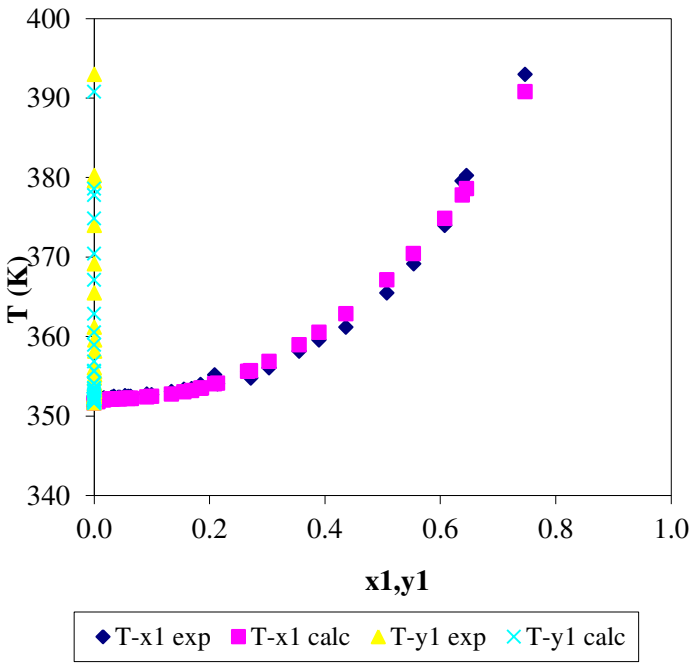

Figure VII.3. VLE data for the system Coconut oil + Ethanol at 101.3 kPa

Anexo VIII – Dados de pressão de vapor dos solventes medidos com ebuliometro de Othmer

Tabela VIII.1: Pressões de Vapor Experimental e da Literatura do solvente n-hexano em função da Temperatura.

n-Hexano					
P_{exp}/ kPa	P_{lit}[a]/ kPa	DR[b] (%)	T_{fase_vapor}/ K	T_{lit}/ K	DR (%)
24,04	24,05	-0,02	303,42	302,27	0,38
32,89	32,97	-0,23	310,63	310,14	0,16
41,50	41,16	0,83	316,50	315,74	0,24
49,00	48,94	0,12	320,77	320,39	0,12
55,98	55,96	0,04	324,22	324,13	0,03
62,93	62,46	0,74	327,23	326,95	0,09
70,90	70,86	0,06	330,72	330,93	-0,06
80,34	80,11	0,28	334,49	334,61	-0,04
87,87	87,73	0,16	336,94	337,38	-0,13
95,79	95,79	0,00	339,64	340,10	-0,14
101,23	101,33	-0,10	341,77	341,70	0,02

[a]Dados da Referência (DDB, 2011); [b] Desvio relativo.

Tabela VIII.2: Pressões de Vapor Experimental e da Literatura do solvente n-heptano em função da Temperatura.

n-Heptano					
P_{exp}/ kPa	P_{lit}[a] / kPa	DR[b] (%)	T_{fase_vapor}/ K	T_{lit}/ K	DR (%)
21,29	21,40	-0,49	327,71	326,36	0,41
31,20	31,15	0,15	336,68	336,00	0,20
38,14	37,90	0,62	341,79	341,30	0,14
46,09	46,02	0,16	346,96	346,79	0,05
54,17	54,13	0,08	351,67	351,30	0,11
62,14	62,50	-0,58	355,56	355,90	-0,09
70,09	70,10	-0,02	359,25	359,75	-0,14
77,93	78,04	-0,14	362,42	362,97	-0,15
85,96	86,30	-0,39	365,37	366,20	-0,23
93,85	94,01	-0,17	368,23	368,94	-0,19
101,45	101,47	-0,01	371,49	371,59	-0,03

[a]Dados da Referência (DDB, 2011) ; [b] Desvio relativo.

Tabela VIII.3: Pressões de Vapor Experimental e da Literatura do solvente etanol em função da Temperatura.

Etanol					
P_{exp}/ kPa	P_{lit}[a] / kPa	DR[b] (%)	T_{fase_vapor}/ K	T_{lit}/ K	DR (%)
25,33	25,33	0,01	320,74	320,25	0,15
30,40	30,35	0,18	324,32	323,75	0,17
35,31	35,20	0,30	327,12	326,93	0,06
40,23	40,29	-0,14	330,03	329,85	0,05
45,21	45,16	0,10	332,86	332,35	0,15
50,31	50,06	0,50	334,85	334,65	0,06
55,35	55,13	0,40	337,05	336,81	0,07
60,17	60,02	0,25	338,80	338,85	-0,01
65,36	65,48	-0,18	339,82	340,82	-0,30
69,92	70,00	-0,12	342,10	342,21	-0,03
75,16	75,15	0,01	343,82	344,00	-0,05
79,79	79,75	0,05	345,90	345,48	0,12
85,13	85,17	-0,05	346,70	347,17	-0,13
90,22	90,20	0,02	348,44	348,45	0,00
95,10	95,06	0,04	349,83	349,95	-0,03
100,48	100,53	-0,05	351,53	351,65	-0,03
101,34	101,38	-0,04	351,51	351,51	0,00

[a]Dados da Referência (DDB, 2011) ; [b] Desvio relativo;

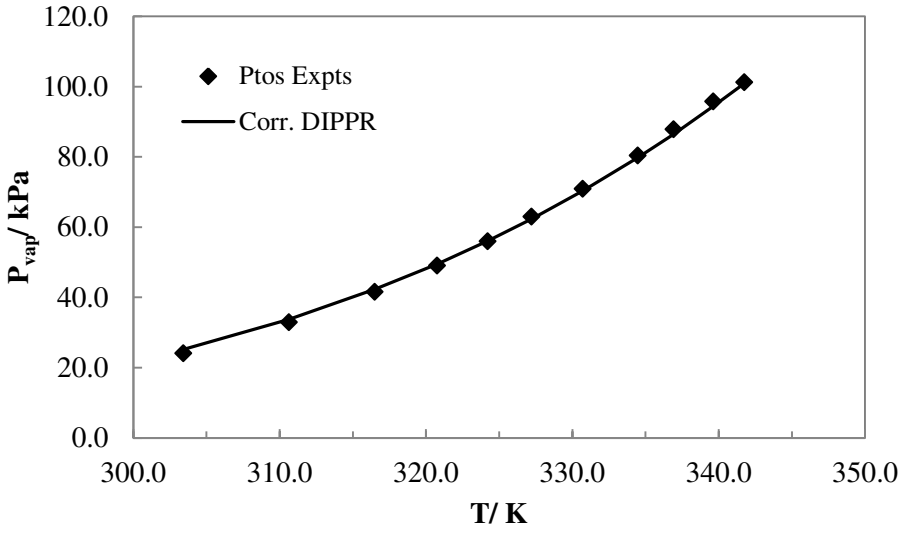

Figura VIII.1: Pressão de vapor do n-hexano obtidos experimentalmente e através da correlação DIPPR.

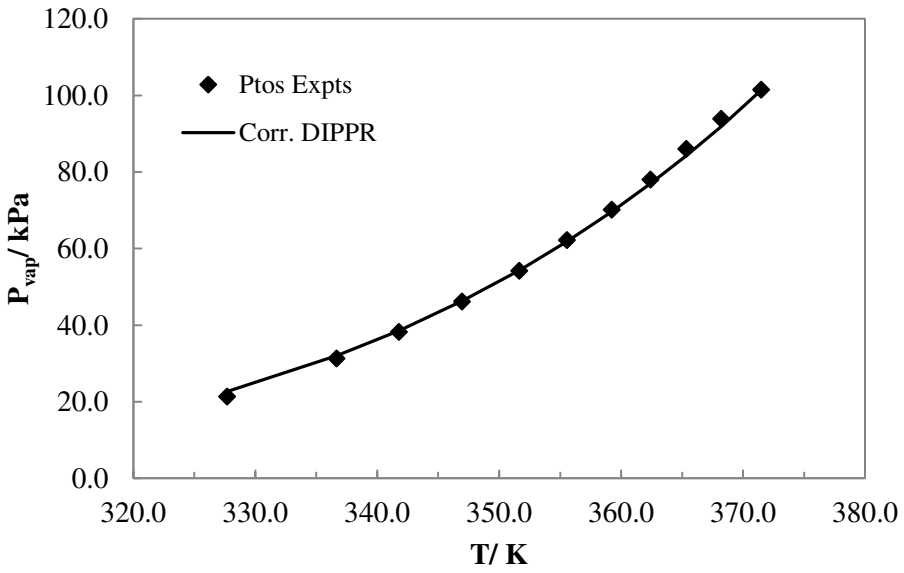

Figura VIII.2: Pressão de vapor do n-heptano obtidos experimentalmente e através da correlação DIPPR.

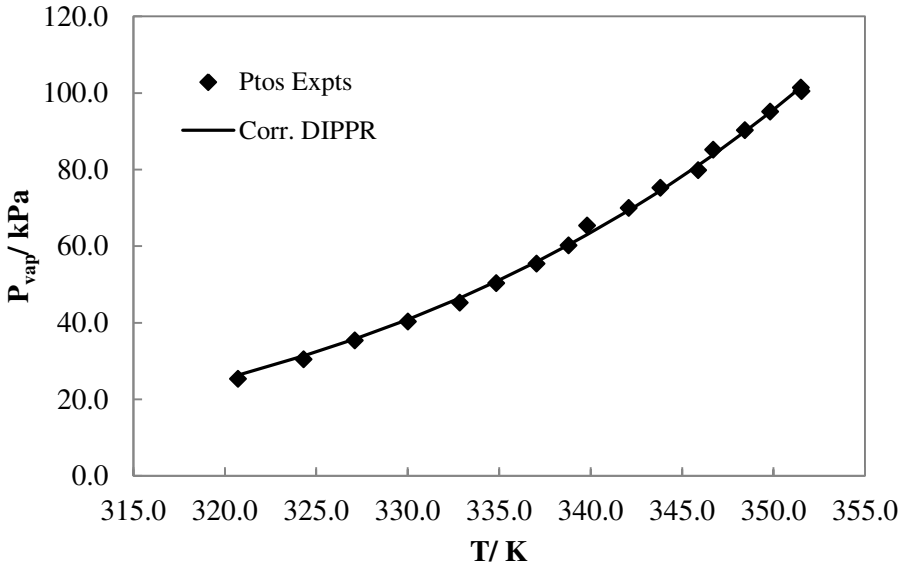

Figura VIII.3: Pressão de vapor do etanol obtidos experimentalmente e através da correlação DIPPR.

Referência Bibliográfica

DDB. Dortmund Data Bank Dortmund Data Bank Software & Separation Technology Oldenburg: DDBST GmbH 2011.

Anexo IX – Calibration curve data

Table IX.1. Calibration curve data of the system ethanol (1) + soybean oil (2)

Oil Concentration											
100% w/w% n-heptane	ρ (g/cm³)	79.999% w/w % n-heptane	ρ (g/cm³)	59.964% w/w % n-heptane	ρ (g/cm³)	40.1669% w/w % n-heptane	ρ (g/cm³)	20.061% w/w % n-heptane	ρ (g/cm³)	0% w/w % n-heptane	ρ (g/cm³)
52.94	0.77835	52.99302	0.76594	53.00012	0.75443	52.98271	0.74374	53.01773	0.73278	52.9997	0.72274
51.96	0.78040	51.99683	0.76791	51.99996	0.75625	52.03538	0.74513	52.00342	0.73405	51.9831	0.72354
51.01	0.78275	51.02411	0.76990	51.00010	0.75804	51.02584	0.74663	51.03917	0.73531	50.9829	0.72467
50.05	0.78482	50.01411	0.77198	50.00000		50.00851	0.74824	50.01771	0.73664	49.9735	0.72568
48.97	0.78710	49.00227	0.77409	48.99978	0.76174	49.01612	0.74986	49.06122	0.73789	48.9923	0.72666
47.84	0.79025	47.99758	0.77623	47.99987	0.76345	48.03467	0.75128	48.07757	0.73920	48.0202	0.72773
46.72	0.79222	47.01299	0.77833	47.00017	0.76542	47.11335	0.75276	46.95873	0.74061	47.0657	0.72865

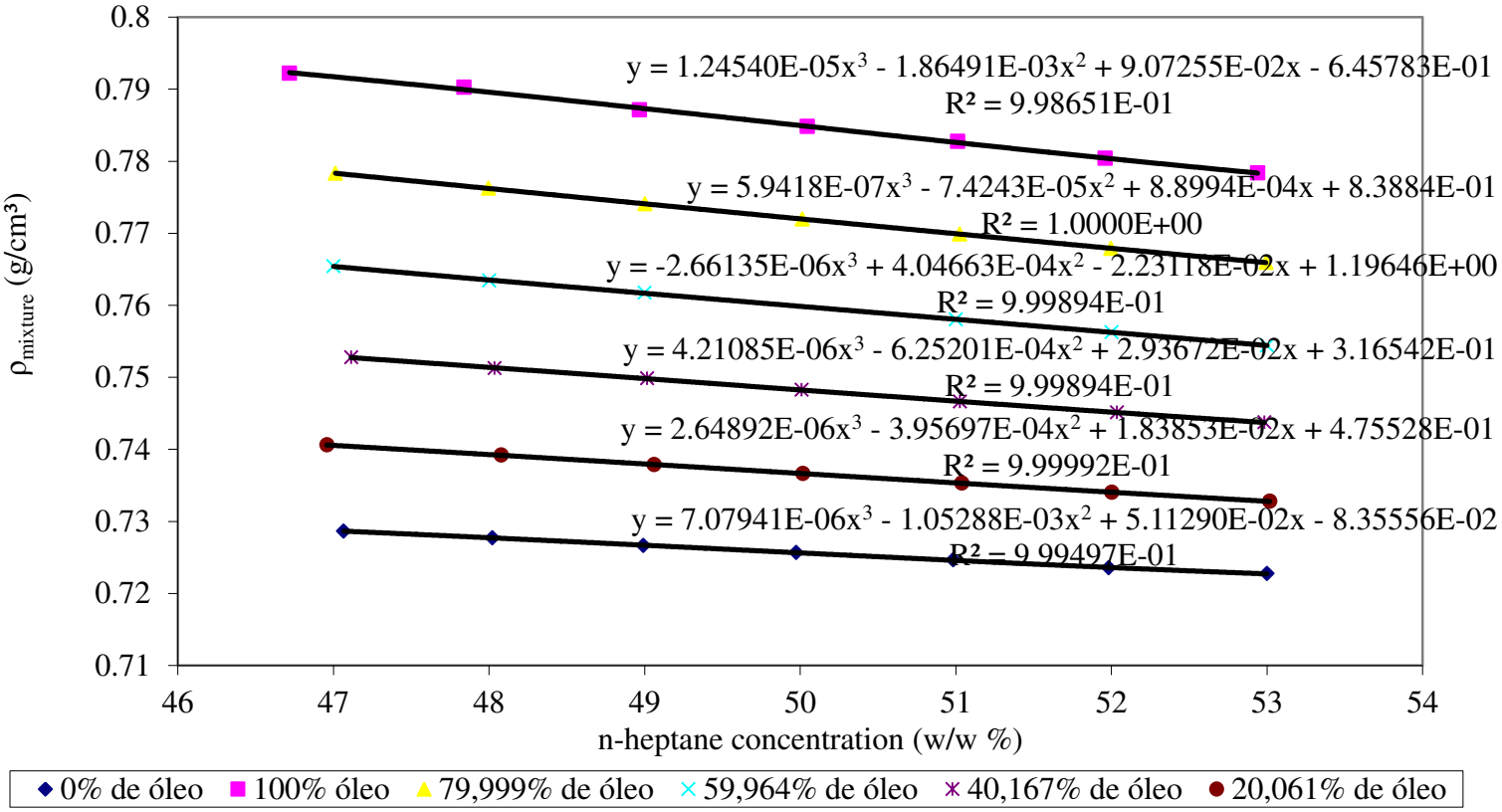

Figure IX.1. Calibration curves of the system ethanol (1) + soybean oil (2)

Table IX.2. Calibration curve of the system ethanol (2) + coconut oil (1)

Oil Concentration											
100% w/w% n-heptane	ρ (g/cm³)	79.996% w/w % n-heptane	ρ (g/cm³)	59.988% w/w % n-heptane	ρ (g/cm³)	39.9919% w/w % n-heptane	ρ (g/cm³)	20.011% w/w % n-heptane	ρ (g/cm³)	0% w/w % n-heptane	ρ (g/cm³)
53.078	0.77718	53.007	0.76537	53.04027	0.75416	53.02271	0.74337	53.087	0.73266	53.000	0.72274
52.154	0.77947	51.973	0.76757	52.04644	0.75606	52.15186	0.74466	51.981	0.73401	51.983	0.72354
51.056	0.78186	51.032	0.76959	51.31413	0.75745	51.03760	0.74638	51.081	0.73520	50.983	0.72467
49.979	0.78460	50.071	0.77160	50.06287	0.75956	50.05901	0.74789	49.992	0.73659	49.974	0.72568
49.058	0.78667	48.959	0.77387	49.08104	0.76135	49.30913	0.74910	49.153	0.73772	48.992	0.72666
47.944	0.78943	47.962	0.77601	48.05021	0.76316	47.90045	0.75138	48.067	0.73911	48.020	0.72773
47.145	0.79123	47.019	0.77787	47.06468	0.76516	45.87438	0.75284	46.822	0.74078	47.066	0.72865

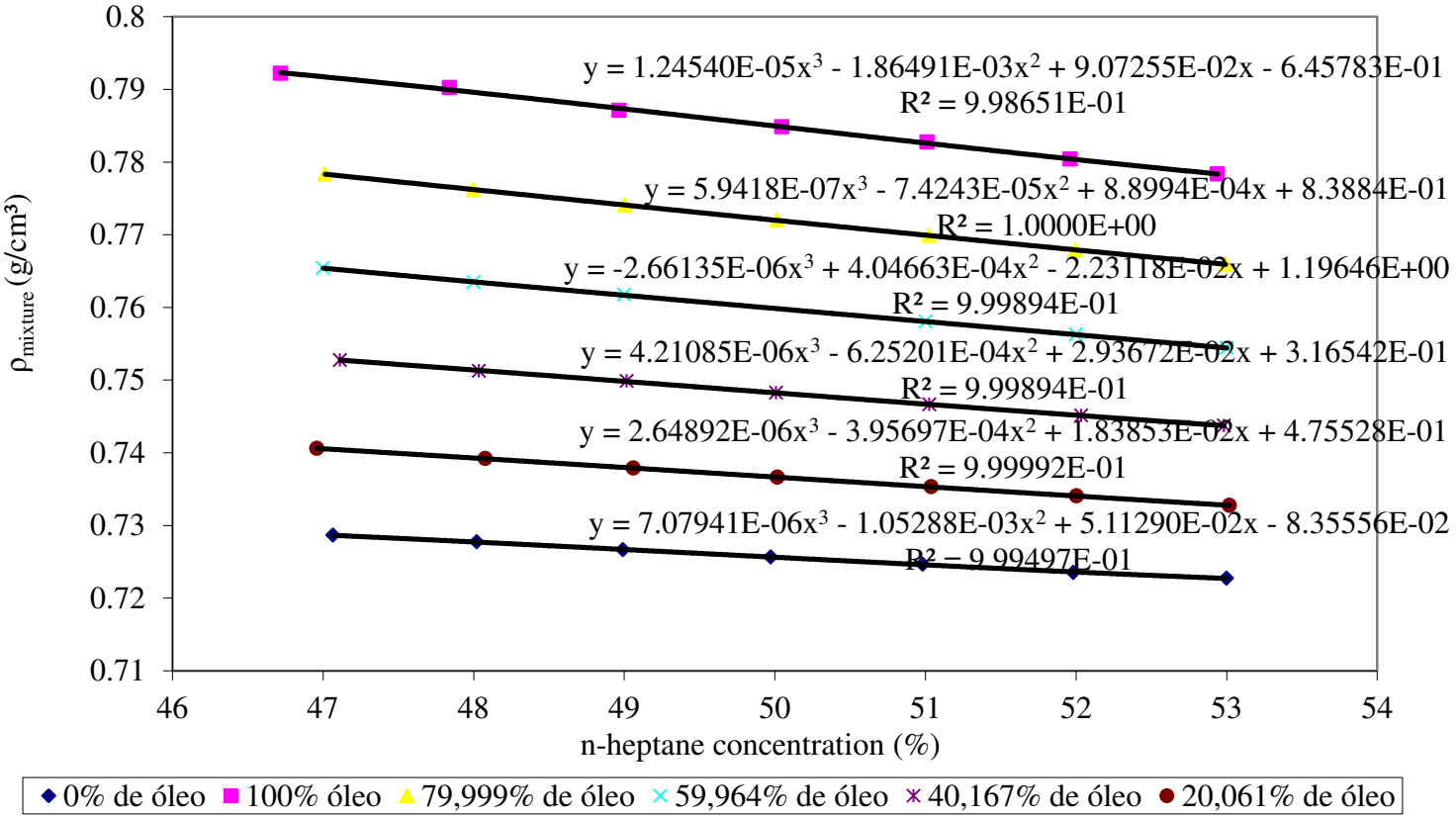

Figure IX.2. Calibration curves of the system ethanol (2) + coconut oil (1)

Anexo X – Figuras de H^E não publicadas

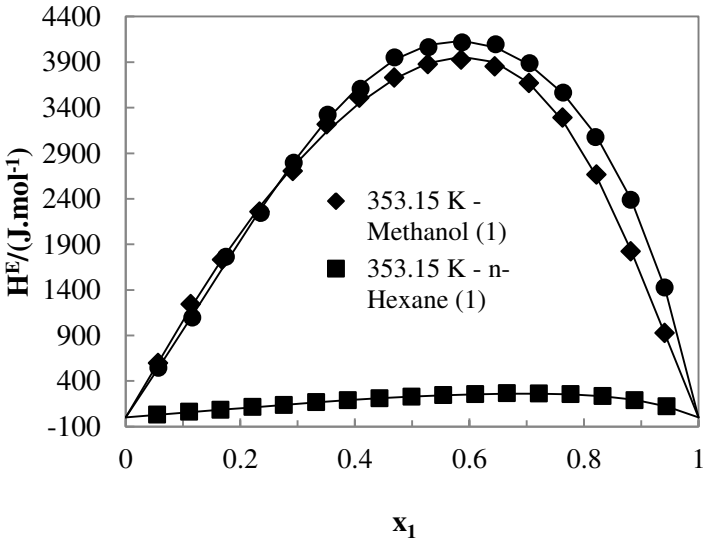

FIGURE X.1. Comparison of the experimental H^E data of mixtures of different solvents (1) with sunflower oil (2) at 353.15 K.

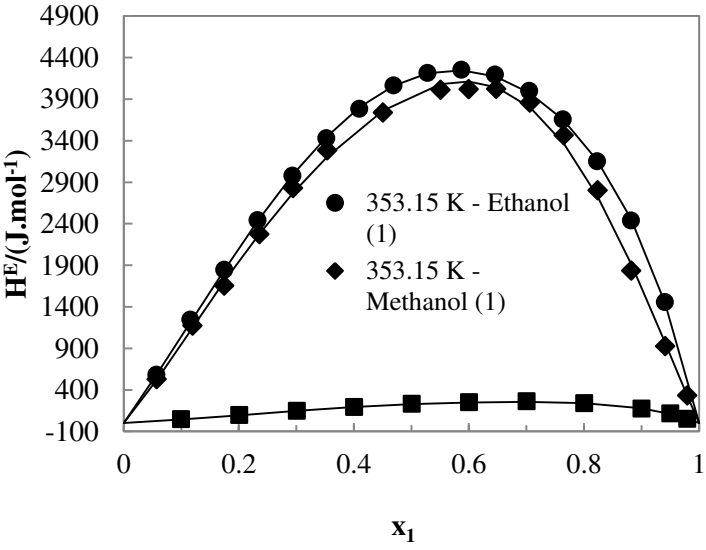

FIGURE X.2. Comparison of the experimental H^E data of mixtures of different solvents (1) with rapeseed oil (2) at 353.15 K.